


Title	An investigation into the role of Bcl-3 in toll-like receptor signalling
Author(s)	Collins, Patricia E.
Publication date	2014
Original citation	Collins, P. E. An investigation into the role of Bcl-3 in toll-like receptor signalling. PhD Thesis, University College Cork.
Type of publication	Doctoral thesis
Rights	© 2014, Patricia E. Collins. http://creativecommons.org/licenses/by-nc-nd/3.0/ 
Item downloaded from	http://hdl.handle.net/10468/1923

Downloaded on 2017-09-05T00:13:35Z



UCC

University College Cork, Ireland
Coláiste na hOllscoile Corcaigh

An Investigation into the Role of Bcl-3 in Toll-Like Receptor Signalling



Submitted to the National University of Ireland, Cork in fulfilment of
the requirement for the degree of Doctor of Philosophy

Patricia E. Collins

February 2014

School of Biochemistry and Cell Biology
National University of Ireland, Cork

Supervisor: Dr. Ruaidhrí J. Carmody
Head of School: Prof. David Sheehan

Contents

DECLARATION	IV
ACKNOWLEDGEMENTS	V
ABSTRACT	VII
LIST OF FIGURES	VIII
LIST OF TABLES	XI
LIST OF ABBREVIATIONS	XII
LIST OF AMINO ACID ABBREVIATIONS	XX

1 GENERAL INTRODUCTION **2**

1.1 MOLECULAR COMPONENTS OF THE NF-KB PATHWAY	3
1.1.1 NF-KB	3
1.1.2 IKB	8
1.1.3 IKK COMPLEX	19
1.2 SIGNALING TO NF-KB	21
1.2.1 TLRs	21
1.2.2 MYD88-DEPENDENT AND INDEPENDENT NF-KB ACTIVATION	26
1.2.3 TLR INDUCED MAPK SIGNALLING	30
1.3 UBIQUITINATION IN NF-KB REGULATION	35
1.3.1 THE UBIQUITIN PROTEASOME SYSTEM	37
1.3.2 STIMULUS INDUCED IKB DEGRADATION	41
1.3.3 PROCESSING OF NF-KB P105 TO P50	42
1.3.4 BCL-3 INHIBITS P50 UBIQUITINATION	43
1.4 THESIS AIMS	46

2 MATERIALS AND METHODS **48**

2.1 MATERIALS	48
2.1.1 ANTIBODIES	48
2.1.2 BCL-3 PEPTIDE SYNTHESIS	49
2.1.3 PLASMID SOURCES	49
2.1.4 DNA SEQUENCING	50

2.1.5	MICE	51
2.1.6	REAGENTS	51
2.1.7	BUFFER COMPOSITION	51
2.2	METHODS	55
2.2.1	CELL CULTURE	55
2.2.2	PROTEIN METHODOLOGIES	57
2.2.3	FUNCTIONAL ASSAYS	59
2.2.4	IMMUNOFLUORESCENCE	62
2.2.5	GST PROTEIN PURIFICATION	63
2.2.6	SPOT SYNTHESIS OF PEPTIDES AND OVERLAY ANALYSIS	64
2.2.7	SITE-DIRECTED MUTAGENESIS	65
2.2.8	MOLECULAR BIOLOGY TECHNIQUES	67
2.2.9	BIOINFORMATIC TOOLS	72
3	<u>INVESTIGATION OF THE MOLECULAR DETERMINANTS OF NF-KB P50 UBIQUITINATION</u>	76
3.1	ABSTRACT	76
3.2	INTRODUCTION	77
3.3	RESULTS	80
3.3.1	IDENTIFICATION OF THE BCL-3 INTERACTING REGIONS OF P50 USING PEPTIDE ARRAYS	80
3.3.2	LYS 249, ARG252 AND MET 253 ARE CRITICAL FOR P50 STABILITY	84
3.3.3	ALANINE SUBSTITUTION ANALYSIS OF BCL-3 BINDING REGION R2	91
3.3.4	REGULATION OF P50 UBIQUITINATION BY TYROSINE 316	97
3.3.5	INHIBITION OF TRANSCRIPTION BY BCL-3 REQUIRES INTERACTION WITH NF-KB P50	102
3.3.6	p105 ^{RKR} EXPRESSION RECAPITULATES <i>Bcl3</i> ^{-/-} PHENOTYPE	115
3.3.7	UBIQUITINATION OF P50 AT LYSINE 128	118
3.4	DISCUSSION	121
4	<u>CHARACTERISATION OF A BCL-3 DERIVED NF-KB INHIBITORY PEPTIDE</u>	128
4.1	ABSTRACT	128
4.2	INTRODUCTION	129
4.3	RESULTS	133
4.3.1	IDENTIFICATION P50 BINDING PEPTIDES	133

4.3.2	BIOINFORMATIC AND STRUCTURAL ANALYSIS OF P50 INTERACTING SITES	138
4.3.3	BCL-3 DERIVED PEPTIDE	142
4.4	DISCUSSION	148
5	<u>IDENTIFICATION OF TPL-2 AS NOVEL BINDING PARTNER OF BCL-3</u>	<u>153</u>
5.1	ABSTRACT	153
5.2	INTRODUCTION	154
5.3	RESULTS	156
5.3.1	BCL-3 NEGATIVELY REGULATES ERK1/2 SIGNALLING	156
5.3.2	TPL-2 INTERACTS WITH BCL-3 INDEPENDENT OF P105	160
5.3.3	BCL-3 NEGATIVELY REGULATES TPL-2	163
5.3.4	ACCUMULATION OF NUCLEAR TPL-2 WITH BCL-3 CO-EXPRESSION	166
5.4	DISCUSSION	168
6	<u>GENERAL DISCUSSION</u>	<u>174</u>
7	<u>APPENDIX</u>	<u>185</u>
7.1	P50 PEPTIDE ARRAY SEQUENCES	185
7.2	P50 ALANINE SUBSTITUTION ARRAY SEQUENCES	188
7.3	P50 ALANINE SUBSTITUTION PEPTIDE ARRAY DATA	200
7.4	ADDITIONAL P50 UBIQUITINATION DATA	207
7.5	BCL-3 PEPTIDE ARRAY SEQUENCES	208
7.6	BCL-3 ALANINE SUBSTITUTION PEPTIDE ARRAY SEQUENCES	211
7.7	BCL-3 ALANINE SUBSTITUTION PEPTIDE ARRAY DATA	218
7.8	MURINE I κ B PROTEIN ALIGNMENT	222
7.9	NETNES PREDICTION RESULTS	224
7.10	NETPHOS PREDICTION RESULTS	225
7.11	BCL-3 DERIVED PEPTIDE <i>IN VIVO</i> TRIAL	226
7.12	SUPPLEMENTARY FIGURES	227
8	<u>REFERENCES</u>	<u>235</u>
9	<u>PUBLICATIONS</u>	<u>258</u>

Declaration

I hereby declare that this thesis is the result of my own work and has not been submitted in whole or in part elsewhere for any award. Any assistance and contribution by others to this work is duly acknowledged within the text.

Patricia E. Collins, BSc.

Acknowledgements

First and foremost I would like to extend my sincere gratitude to my supervisor Dr. Ruaidhrí Carmody for his time, continuous encouragement, guidance and of course and turning me into the kind of person that can't eat pancakes without thinking of NF- κ B. Without his constant enthusiasm for my work and support over the last four years, this thesis would not have been possible.

All of the Keeshmodys past and present but particularly those who participated in the inaugural Lab Olympics of 2011 (Caitriona, Amy, Abrar, Zoe, Fiona, Sarah G and Chris): coming to the lab rarely felt like coming to work and I consider myself very lucky to have been able to do science, eat curry and lose many poker games with my friends over the last four years. I would like to give particular acknowledgment to Dr. Amy Colleran (Nagle) for her invaluable input into this work and more importantly great friendship and Christine, thanks so much for all the help over the years and for actually submitting the beast for me but most importantly, thanks for not eating my submission chocolate. A special mention is due to Zoe, Jen and Caitriona who also bravely doubled up as house and labmates. Caitriona for the seemingly endless supply of Barry's tea, late night who done its, not abandoning me when sleep deprivation made timber a thing and always checking my whereabouts during long lab days, thanks loads.

Thanks to everyone in my new home in Glasgow, office B323, for making me feel welcome, pointing me in the right direction when I was lost and of course, the countless potato jokes that never get old, to be sure. Fabian you found my weakness by rolling M&Ms along the desk until I paid attention, I'm sure I would have finished this thesis earlier if I managed to resist, although the last year would have been a lot less fun! have no doubt one day our dream of a peanut butter peanut M&M hybrid will be a reality. Chris 'wise monkey' Hansel(l), thanks for being my adoptive post doc, colossus and friend over the last year, always having the time and patience to answer the onslaught of questions and to offer genuine encouragement when science was being a beaven. Strokegate 2013 is officially forgotten.

Steven, pilgrim, where would I be without Jackie, our debriefs in the situation room, your killer dinosaur dance moves and the not so red "code reds". The last year probably has been one of the hardest, there were times when we could

only dream of getting out.. getting anywhere.. getting all the way to a p..h..d...but we did and I can't remember a time where I have laughed so much or lost so many valuable possessions, thank you.

A lot of people made a big effort to help me settle in Scotland, in particular I'd like to thank Clare Headquarters Tange for her help with the underground system, a real turning a point in my stay in Glasgow, not to mention introducing me to the official thesis wardrobe of 2013, the onesie. Alison, my first GBRC buddy, thanks for making the move less scary and of course sharing your big day with me! Katie (red ranger), your friendship, inability to order coffee and our many romantic ready meals for 2 have kept a constant smile on my face, couldn't haven't gotten through the last year without you, pal.

I also owe a debt of gratitude to the many people who helped me technically over the course of my studies both in Cork and Glasgow. Fiona thanks for all your help over the past year, Jamie my new NF-κBuddy and Kenny thanks so much for all the help and patience and eventually letting me drive. I would especially like to thank Dr. Pat Kiely for generously providing both technical help and expertise with the peptide arrays which played a big part in this work.

Damien, firstly thank you for telling me all those years ago about a PhD opening with a "this guy" you reckoned I "would get on with", in so many ways this wouldn't have been possible without you. Your patience, understanding and support throughout this process has been immense and I really can't thank you enough.

To my family, thank you for not disowning me after an extended sabbatical from most of my sisterly and daughterly duties. My big brothers Liam and Ed, thanks for always helping me to keep things in perspective, making me laugh and helping me move for the "last time" eight years in a row.

Finally to my parents, I am eternally grateful for your unending support, both financial and emotional, without which I could not have gotten to this stage. Your hard work and dedication will continue to be an inspiration

Abstract

Through the recognition of potentially harmful stimuli, Toll-like receptors (TLRs) initiate the innate immune response and induce the expression of hundreds of immune and pro-inflammatory genes. TLRs are critical in mounting a defence against invading pathogens however, strict control of TLR signalling is vital to prevent host damage from excessive or prolonged immune activation. In this thesis the role of the I κ B protein Bcl (B-cell lymphoma)-3 in the regulation of TLR signalling is investigated. *Bcl3*^{-/-} mice and cells are hyper responsive to TLR stimulation and are defective in LPS tolerance. Bcl-3 interacts with and blocks the ubiquitination of homodimers of the NF- κ B subunit, p50. Through stabilisation of inhibitory p50 homodimers, Bcl-3 negatively regulates NF- κ B dependent inflammatory gene transcription following TLR activation. Firstly, we investigated the nature of the interaction between Bcl-3 and p50 and using peptide array technology. Key amino acids required for the formation of the p50:Bcl-3 immunosuppressor complex were identified. Furthermore, we demonstrate for the first time that interaction between Bcl-3 and p50 is necessary and sufficient for the anti-inflammatory properties of Bcl-3. Using the data generated from peptide array analysis we then generated cell permeable peptides designed to mimic Bcl-3 function and stabilise p50 homodimers. These Bcl-3 derived peptides are potent inhibitors of NF- κ B dependent transcription activity *in vitro* and provide a solid basis for the development of novel gene-specific approaches in the treatment of inflammatory diseases. Secondly, we demonstrate that Bcl-3 mediated regulation of TLR signalling is not limited to NF- κ B and identify the MAK3K Tumour Progression Locus (Tpl)-2 as a new binding partner of Bcl-3. Our data establishes role for Bcl-3 as a negative regulator of the MAPK-ERK pathway.

List of Figures

FIGURE 1.1 MULTIFACETED GENE REGULATION BY NF- κ B.....	2
FIGURE 1.2 NF- κ B FAMILY OF TRANSCRIPTION FACTORS.	5
FIGURE 1.3 POSSIBLE NF- κ B HOMO- AND HETERODIMERS.	6
FIGURE 1.4 ANKYRIN REPEAT CONSENSUS SEQUENCE AND STRUCTURE.	11
FIGURE 1.5 THE FAMILY OF MAMMALIAN I κ B PROTEINS.	12
FIGURE 1.6 INHIBITION OF NF- κ B BY I κ B PROTEINS.	15
FIGURE 1.7 IKK COMPLEX AND B-TRCP DESTRUCTION MOTIF.	20
FIGURE 1.8 CANONICAL AND NON-CANONICAL NF- κ B SIGNALLING.	22
FIGURE 1.9 TLR SIGNALLING	28
FIGURE 1.10 MAPK SIGNALLING CASCADE.	31
FIGURE 1.11 REGULATION OF TPL-2-MEK KINASE ACTIVITY.	34
FIGURE 1.12 POST TRANSLATION MODIFICATION OF THE NF- κ B SUBUNITS.	36
FIGURE 1.13 UBIQUITINATION CASCADE.	38
FIGURE 1.14 UBIQUITIN LINKAGES	40
FIGURE 3.1 SCHEMATIC REPRESENTATION OF PEPTIDE SCANNING USING SPOT SYNTHESIS TECHNOLOGY.	78
FIGURE 3.2 CLONING AND PURIFICATION OF RECOMBINANT BCL-3.	82
FIGURE 3.3 IDENTIFICATION OF BCL-3 INTERACTING REGIONS ON P50 USING PEPTIDE ARRAYS.	83
FIGURE 3.4 ALANINE SUBSTITUTION ANALYSIS OF BCL-3 BINDING REGION R1.	86
FIGURE 3.5 CHARACTERISATION OF P50 ^{KRM}	89
FIGURE 3.6 LYS 249, ARG 252 AND MET 253 ARE CRITICAL FOR P50 STABILITY.	90
FIGURE 3.7 ALANINE SUBSTITUTION ANALYSIS OF BCL-3 BINDING REGION R2.	93
FIGURE 3.8 ASP 297, PHE 298, SER 299, PRO 300 AND THR 301 OF P50 ARE REQUIRED FOR INTERACTION WITH BCL-3.....	94
FIGURE 3.9 P50 ^{DFSP} EMULATES P50 ^{KRM}	95
FIGURE 3.10 POTENTIAL R1/R2 BINDING INTERFACES OF P50 HOMODIMER.	96
FIGURE 3.11 ALANINE SUBSTITUTION ANALYSIS OF BCL-3 BINDING REGION R3.....	99
FIGURE 3.12 P50 LYS 315 AND LYS 317 ARE NOT REQUIRED FOR INTERACTION WITH BCL-3.	100
FIGURE 3.13 KYK MOTIF REGULATES P50 UBIQUITINATION.	101
FIGURE 3.14 ALANINE SUBSTITUTION ANALYSIS OF BCL-3 BINDING REGION R4.....	103
FIGURE 3.15 SURFACE EXPOSURE PREDICTION OF ARG359, LYS360 AND ARG361.....	104
FIGURE 3.16 ARG359, LYS360 AND ARG361 OF P50 ARE ESSENTIAL FOR INTERACTION WITH BCL-3.	107
FIGURE 3.17 MUTATION OF ARG 359, LYS 360 AND ARG 361 DOES NOT AFFECT THE DIMERISATION PROPERTIES OF P50.	108
FIGURE 3.18 P50 ^{RKR} CAN BIND DNA AND TRANSLOCATE TO THE NUCLEUS.....	110
FIGURE 3.19 ARG359, LYS360 AND ARG361 OF P50 ARE CRITICAL FOR PROTEIN STABILITY.	113
FIGURE 3.20 ARG359, LYS360 AND ARG361 OF P50 ARE CRITICAL FOR NEGATIVE REGULATION OF NF- κ B DEPENDENT GENE EXPRESSION.	114

FIGURE 3.21 NORMAL UPSTREAM SIGNALLING AND NF- κ B NUCLEAR TRANSLOCATION OF P105 ^{RKR} MEFs.	116
FIGURE 3.22 P105 ^{RKR} MEFs ARE HYPER-RESPONSIVE TO TNF STIMULATION.	117
FIGURE 3.23 P50 IS UBIQUITINATED AT LYSINE 128.	120
FIGURE 4.1 PROPOSED MECHANISMS OF CELLULAR UPTAKE OF CELL PENETRATING PEPTIDES.	131
FIGURE 4.2 BCL-3 BINDS SPECIFICALLY TO RECOMBINANT GST-P50.	135
FIGURE 4.3 BCL-3 PEPTIDE ARRAY IDENTIFIES P50 INTERACTING PEPTIDES.	136
FIGURE 4.4 ALANINE SUBSTITUTION ANALYSIS OF POSITIVE P50 BINDING BCL-3 PEPTIDES.	137
FIGURE 4.5 STRUCTURAL REPRESENTATIONS OF PUTATIVE P50 INTERACTING RESIDUES.	138
FIGURE 4.6 SCHEMATIC REPRESENTATION OF PUTATIVE P50 INTERACTING RESIDUES DETERMINED BY PEPTIDE ARRAY.	140
FIGURE 4.7 MULTIPLE SEQUENCE ALIGNMENT OF I κ B PROTEINS.	141
FIGURE 4.8 DESIGN OF BCL-3 DERIVED CELL PERMEABLE PEPTIDE.	143
FIGURE 4.9 BDP CAN TRANSLOCATE TO THE NUCLEAS AND INHIBIT IL-23P19 REPORTER ACTIVITY. ...	144
FIGURE 4.10 SEQUENCE OF THE SHORTENED BCL-3 DERIVED CELL PERMEABLE PEPTIDE.	146
FIGURE 4.11 sBDP INHIBITS IL-23P19 LUCIFERASE REPORTER ACTIVITY.	147
FIGURE 4.12 COMPARISON OF BCL-3:P50 COMPLEX WITH COMPLETE P50 STRUCTURE.	149
FIGURE 4.13 STRUCTURAL ANALYSIS OF BCL-3 ANK REPEAT 1.	150
FIGURE 5.1 INCREASED ERK MAPK SIGNALLING IN <i>BCL-3</i> ^{-/-} MACROPHAGE.	157
FIGURE 5.2 INCREASED ERK-DEPENDENT GENE EXPRESSION IN <i>BCL3</i> ^{-/-} MACROPHAGE.	158
FIGURE 5.3 PROTEASOME AND IKK ACTIVITY IS REQUIRED FOR LPS ACTIVATION OF ERK1/2 IN <i>BCL3</i> ^{-/-} MACROPHAGE	159
FIGURE 5.4 BCL-3 INTERACTS WITH TPL-2.	161
FIGURE 5.5 P105 INDEPENDENT BCL-3-TPL-2 INTERACTION.	162
FIGURE 5.6 BCL-3 INHIBITS TPL-2 MEK-KINASE ACTIVITY.	164
FIGURE 5.7 BCL-3 INHIBITS TPL-2 INDUCED AP-1 ACTIVATION.	165
FIGURE 5.8 BCL-3 OVEREXPRESSION INCREASES NUCLEAR TPL-2.	167
FIGURE 5.9 POTENTIAL NUCLEAR EXPORT SEQUENCE IN TPL-2.	172
FIGURE 6.1 SUMMARY OF P50 MUTANTS GENERATED.	176
FIGURE 6.2 SCHEMATIC MODEL OF BCL-3 MEDIATED MAPK REGULATION.	184
FIGURE 7.1 FULL P50 ALANINE SUBSTITUTION PEPTIDE ARRAY.	200
FIGURE 7.2. P50 IS UBIQUITINATED VIA K48 LINKED UBIQUITINATION	207
FIGURE 7.3 FULL BCL-3 ALANINE SUBSTITUTION PEPTIDE ARRAY.	218
FIGURE 7.4 BCL-3 DERIVED PEPTIDE INHIBITS CARRAGEENAN-INDUCED INFLAMMATION.	226
FIGURE 7.5 EMSA.	227
FIGURE 7.6 P50 AND BCL-3 CO-IMMUNOPRECIPITATION.	228
FIGURE 7.7 TPL-2 AND BCL-3 CO-IMMUNOPRECIPITATION.	229

FIGURE 7.8 P50 HOMODIMER CO-IMMUNOPRECIPITATION.....	230
FIGURE 7.9 P50 UBIQUITINATION ASSAY.....	231
FIGURE 7.10 GST PULL DOWN ASSAY.	232
FIGURE 7.11 TNF INDUCED IKA PHOSPHORYLATION IN P105 STABLE CELL LINES.	233
FIGURE 7.12 MEK-KINASE ASSAY.....	234

List of Tables

TABLE 1. KNOCKOUTS OF ATYPICAL I κ B PROTEINS	17
TABLE 2. LIST OF TLR LIGANDS	24
TABLE 3. PRIMARY ANTIBODIES	48
TABLE 4. SECONDARY ANTIBODIES	49
TABLE 5. PEPTIDE SEQUENCES	49
TABLE 6. SEQUENCING PRIMERS	50
TABLE 7. LIST OF BIOCHEMICALS.....	51
TABLE 8. AGAROSE GEL ELECTROPHORESIS BUFFERS	51
TABLE 9. EMSA BUFFERS.....	52
TABLE 10. LUCIFERASE ASSAY BUFFERS.....	52
TABLE 11. LYSIS BUFFERS	52
TABLE 12. GLUTATHIONE S-TRANSFERASES (GST) PROTEIN PURIFICATION.....	53
TABLE 13. COLUMN REGENERATION BUFFERS.....	53
TABLE 14. KINASE ASSAY BUFFER.....	53
TABLE 15. ELECTROPHORESIS BUFFERS FOR WESTERN BLOTTING	53
TABLE 16. SDS PAGE SAMPLE BUFFER.....	54
TABLE 17. TRIS-GLYCINE SDS-POLYACRYLAMIDE GELS	54
TABLE 18. MEDIA.....	54
TABLE 19. P50 SDM OLIGONUCLEOTIDE SEQUENCES	65
TABLE 20. P105 SDM OLIGONUCLEOTIDE SEQUENCES	66
TABLE 21. TRANSFECTION CONDITIONS	69
TABLE 22. ASSAY SPECIFIC TRANSFECTION CONDITIONS	70
TABLE 23. THERMO CYCLING CONDITIONS.....	71
TABLE 24. QUANTITECT PRIMER ASSAYS.....	71
TABLE 25. AMINO ACID HYDROPHOBICITY VALUES	72
TABLE 26. RESIDUE CONSERVATION TABLE	73
TABLE 27. I κ B SEQUENCE IDENTIFIERS	73
TABLE 28. WEB SERVERS FOR STRUCTURE PREDICATION.....	74
TABLE 29. COMPARISON OF HYPOTHETICAL MODELS OF P50:BCL-3 BINDING	122

List of Abbreviations

Abin-2	A20-binding inhibitor of NF- κ B 2
AIP6	Anti-inflammatory peptide-6
AMP	Adenosine monophosphate
ANK	Ankyrin
AP-1	Activator protein 1
ARD	Ankyrin Repeat domain
ASK	Apoptosis signal-regulating kinase
ATP	Adenosine triphosphate
BAFF	B-cell activating factor
Bcl-3	B-cell lymphoma-3
Bcl-XL	B-cell lymphoma-extra large
BCR	B-cell receptor
BCS	Bovine calf serum
BDP	Bcl-3 derived peptide
BMDM	Bone marrow derived macrophage
BSA	Bovine serum albumin
BTrCP	Beta -transducin repeat containing
C/EBP	CCAAT/enhancer-binding protein
CCL	CC chemokine ligand
ChIP	Chormatin Immunoprecipitation
CHX	Cyclohexamide
Class NT	Class Non-tolerisable
Class T	Class Tolerisable

CLL	Chronic lymphocytic leukaemia
Commd1	Copper metabolism mouse U2af1-rs1 region 1-domain-containing protein 1
COT	Cancer Osaka thyroid
COX-2	Cyclo-oxygenase
CPP	Cell permeable peptide
CREB1	cAMP response element-binding protein
CRM1	Chromosome region maintenance 1 protein
CRP	C-reactive protein
C-terminal	Carboxy-terminal
CXCL	chemokine C-X-C motif ligand
DAMP	Danger associated molecular pattern
DLK	Dual leucine zipper kinase
DMEM	Dulbecco's Modified Eagle Medium
DMSO	Dimethyl sulfoxide
dsRNA	Double-stranded RNA
DSS	Dextran sulphate sodium
DTT	Dithiothreitol
DUB	Deubiquitinase
E1	Ubiquitin-activating enzymes
E2	Ubiquitin-conjugating enzymes
E3	Ubiquitin ligases
EGF	Epidermal growth factor
Egr-1	Early growth response 1

ELK1	ETS domain-containing protein
ERK	Extracellular signal-regulated kinases
FBS	Fetal Bovine Serum
Fbw	F-box/WD40 repeat containing
FDA	Food drug authority
Fmoc	N-(9-fluorenylmethoxycarbonyl
FOS	FBJ murine osteosarcoma viral oncogene homolog
FSH	Follicle-stimulating hormone
GMSCF	Granulocyte-macrophage colony-stimulating factor
GRR	Glycine rich region
GSH	Glutathione
GST	Glutathione S-transferases
HDAC	Histone deacetylases
HECT	Homologous to the E6-AP C-Terminal domain
HEK	Human embryonic kidney
HIPK2	Homeodomain-interacting protein kinase
HMGB1	High-mobility group box 1 protein
Hr	Hour
HSP	heat-shock protein
I.p	intraperitoneal
I.v	intravenous
ICAM	Intercellular Adhesion Molecule 1
IEG	Immediate early genes
IFN	Interferon

IGD1	Insulin Growth Factor-1
IκB	Inhibitor of NF-κB
IKK	IκB kinase
IL	Interleukin
IP	Immunoprecipitation
IP-10	Interferon gamma-induced protein 10
IPTG	Isopropyl β-D-1-thiogalactopyranoside
IRAK	Interleukin-1 receptor-associated kinase
IRE	Interferon responsive elements
IRF	Interferon regulatory transcription factor
JNKS	c-Jun N-terminal kinases
LB	Lysogeny broth
LMB	Leptomycin B
LPS	Lipopolysaccharide
LRR	Leucine-rich-repeat
LTA	Lipoteichoic acid
MEK	Mitogen/Extracellular signal-regulated Kinase
MAK3K	Mitogen activated protein kinase kinase kinase (or MEKK)
MAP2K	Mitogen activated protein kinase kinase
MAPK	Mitogen activated protein kinase
MAPKAPK	Mitogen activated protein kinase activated kinases
mBDP	mutant Bcl-3 derived peptide
M-CSF	Macrophage colony-stimulating factor
MDM2	Mouse double minute 2

MEF	Mouse embryonic fibroblast
MEK	mitogen activated protein kinase kinase (or MAP2K or MKK)
MEKK	MAP kinase kinase kinase (or MAP3K)
MHC	major histocompatibility complex
Min	Minute
MK	Map Kinase-Activated Protein Kinase
MKK	Mitogen activated protein kinase kinase (or MAP2K or MEK)
MLK	Mixed-lineage kinase
mM	Mili molar
MNK	MAPK signal-integrating kinase
MSK	Mitogen- and stress-activated kinases
MYD88	Myeloid differentiation primary-response protein 88
NBD	Nemo binding domain
NEM	N-ethylmaleimide
NEMO	NF- κ B essential modulator
NES	Nuclear export signal/sequence
NGF	Nerve growth factor
NIK	NF- κ B-inducing kinase
NLK	Nemo-Like Kinase
NLS	Nuclear localisation
nM	Nano molar
N-terminal	Amino-terminal
NTS	Nuclear translocation signal
PAK1	p21-activated kinase 1

PAMP	pathogen-associated molecular patterns
PBS	Phosphate buffer saline
PBS-T	Phosphate buffer saline-tween
PDB	Protein data bank
PDGF	Platelet-derived growth factor receptors
Pdlim2	PDZ and LIM domain 2
PEST	Proline, glutamic acid , serine , threonine
pl	Isoelectric point
Pin1	Peptidyl-prolyl cis-trans isomerase NIMA-interacting
Ppi	pyrophosphate
PRR	Pathogen recognition receptor
PTD	Protein transduction domain
RAF	Rapidly accelerated fibrosarcoma
RANK	Receptor activator of nuclear factor kappa-B
RANTES	Regulated on Activation Normal T Cell Expressed and Secreted
RHD	Rel homology domain
RHR	Rel homology region
RI	Reliability index
RING	Really Interesting New Gene
RIPA	Radioimmunoprecipitation assay buffer
ROS	Reactive oxygen species
RSK	90 kDa ribosomal S6 kinase
RSV	Respiratory syncytial virus
SARM	Armadillo-motif-containing protein

sBDP	Short Bcl-3 derived protein
SCF	Skp1-Cul1-F-box protein
SD	Standard deviation
SDM	Site-directed mutagenesis
SDS	Sodium dodecyl sulfate
SEM	Standard error of the mean
SOB	Super Optimal Broth
SOC	Super Optimal Broth with catabolite repression
SRD	Signal receiving domain
ssRNA	Single-stranded RNA
TAB	TAK1-binding proteins
TAD	Trans activating domain
TAK1	Transforming growth factor- β -activated kinase-1
TAT	Trans-Activator of Transcription
TBS	Tris buffer saline
TBS-T	Tris buffer saline-Tween
TCR	T-cell receptor
tGP1-mucins	Trypanosoma cruzi glycosylphosphatidylinositol-anchored mucin-like glycoprotein
TIR	Toll/interleukin-1 receptor
TIRAP	TIR -domain-containing adapter protein
TNF	Tumour necrosis factor
TNFR	Tumour necrosis factor receptor
Tpl-2	Tumour Progression Locus 2

TRAF	Tumour necrosis factor receptor-associated factor
TRAM	TRIF-related adaptor molecule
TRIF	TIR-domain-containing adaptor protein inducing IFN beta
TLR	Toll like receptor
TWEAK	Tumour necrosis factor -related weak inducer of apoptosis
Ub	Ubiquitin
uM	Micro molar
Usp	ubiquitin-specific-processing protease
UV	Ultra violet
VCAM	Vascular cell adhesion protein
VSV	Vesicular stomatitis virus
W/V	Weight per volume
WB	Western blot
WT	Wild-type

List of Amino Acid Abbreviations

Alanine	Ala	A
Arginine	Arg	R
Asparagine	Asn	N
Aspartate	Asp	D
Aspartate or Asparagine	Asx	B
Cysteine	Cys	C
Glutamate	Glu	E
Glutamine	Gln	Q
Glutamate or Glutamine	Glx	Z
Glycine	Gly	G
Histidine	His	H
Isoleucine	Ile	I
Leucine	Leu	L
Lysine	Lys	K
Methionine	Met	M
Phenylalanine	Phe	F
Proline	Pro	P
Serine	Ser	S
Threonine	Thr	T
Tryptophan	Trp	W
Tyrosine	Tyr	Y
Valine	Val	V

—— Chapter One ——

1 General Introduction

Nuclear factor (NF)- κ B has evolved as a latent, inducible family of transcription factors, fundamental in the control of a number of important biological processes including cell survival, differentiation and proliferation, in addition to having an essential role in the development and homeostasis of the immune system (Hayden and Ghosh, 2012). Although originally identified as a B-lymphocyte-specific immunoglobulin κ -chain enhancer binding protein, NF- κ B is not limited to B-cells and is activated by a plethora of stimuli, in almost all mammalian cell types (Figure 1.1) (Sen and Baltimore, 1986b, Sen, 2011).

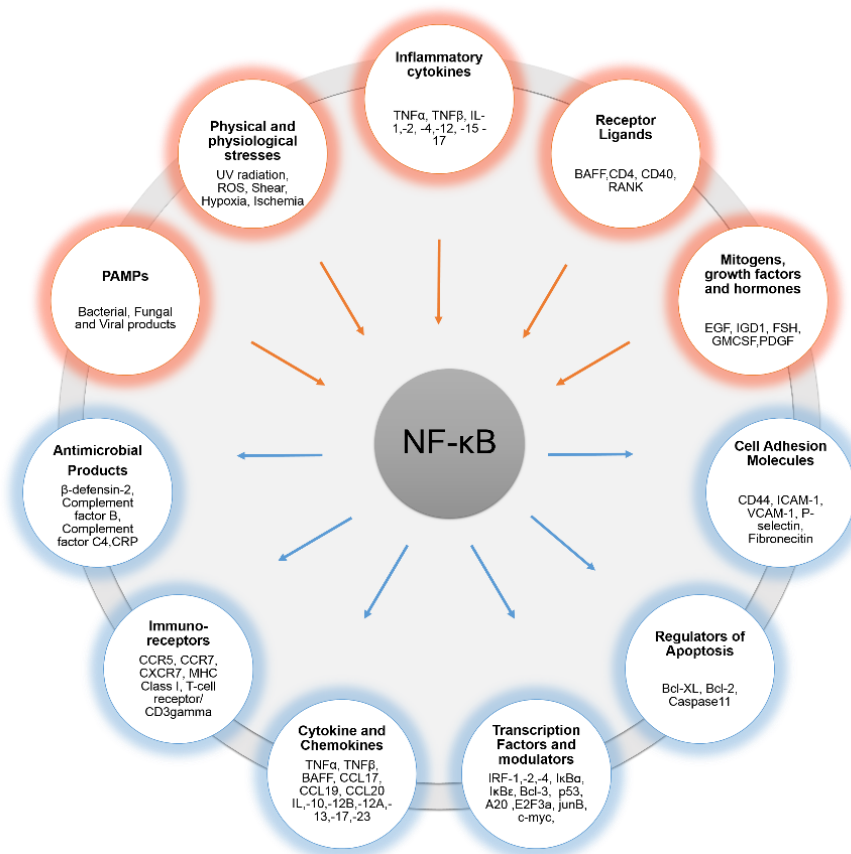


Figure 1.1 Multifaceted gene regulation by NF- κ B.

NF- κ B is activated in response to a wide variety of signals (red circles) which induces the expression of over 500 genes (blue circles) involved in the innate and adaptive immune responses, the regulation of normal developmental processes, cellular growth and apoptosis. (For a full list, see <http://www.bu.edu/nf-kb>)

NF- κ B regulates the inducible transcription of hundreds of genes and as such, aberrant NF- κ B activation is associated with a number of pathological states including but not limited to autoimmunity, cancer and neurodegenerative and cardiovascular diseases (DiDonato et al., 2012, Hayden and Ghosh, 2012). Due to the number and significance of NF- κ B target genes, tight regulation is essential and many mechanisms have evolved to induce specific gene expression patterns in a stimulus- and cell type-specific manner.

1.1 Molecular Components of the NF- κ B pathway

1.1.1 NF- κ B

The mammalian NF- κ B family consists of five members, p65 (RelA), RelB, c-Rel, p50 and p52 (Figure 1.2), which associate to form homo- or heterodimeric complexes. p50 and p52 are synthesised as large precursor proteins, p105 and p100, respectively, that are partially proteolysed by the 26S proteasome. This processing removes the C-terminal halves of p105 and p100 to generate the active p50 and p52 subunits, respectively (discussed in detail in 1.3.3). All NF- κ B subunits are characterised by a conserved N-terminal amino acid sequence termed the Rel homology domain (RHD) or Rel homology region (RHR). The RHD is a 300 amino acid motif identified following the cloning of NF- κ B p50. Sequence analysis revealed homology to the viral oncogene *v-rel* and the *Drosophila* protein dorsal, establishing NF- κ B proteins as members of the larger rel family of transcription factors (Ghosh et al., 1990, Rushlow and Warrior, 1992).

The RHD is responsible for DNA-binding, dimerization, nuclear localisation and interaction with I κ B proteins. The first three-dimensional structure of the RHD was determined by x-ray crystallography of the NF- κ B p50 homodimer bound to DNA (Muller et al., 1995, Ghosh et al., 1995). This structure revealed a symmetrical protein DNA complex described as resembling a butterfly with two protein domain “wings” connected to a cylindrical double-stranded DNA “body” (Figure 1.2) (Ghosh et al., 1995). The RHD consists of two folded domains connected by a short linker, approximately 10 amino acids in length (Figure 1.2). The amino (N)-terminal domain and the shorter carboxyl (C)-terminal domain adopt an immunoglobulin-like fold, which wraps around the major

groove, enclosing the DNA. Unlike DNA binding, dimer contacts are made solely in the C-terminal dimerization domain which consists of a hydrophobic core surrounded by polar residues (Müller and Harrison, 1995). The five NF- κ B proteins assemble to form homo- and hetero-dimers and although in theory 15 combinations are possible, only 12 of these have been identified *in vivo* (Figure 1.3) (Huxford and Ghosh, 2009). The physiological relevance for all dimers has not been fully explored and in addition, some dimers may be limited subsets of cells (Oeckinghaus and Ghosh, 2009). Although the abundance of a particular NF- κ B dimer is dependent on cell type and in some cases is stimulus-specific, in general the p65:p50 heterodimer is the most predominant form of NF- κ B and is expressed in most cell types (Hoffmann et al., 2006, Moorthy et al., 2010).

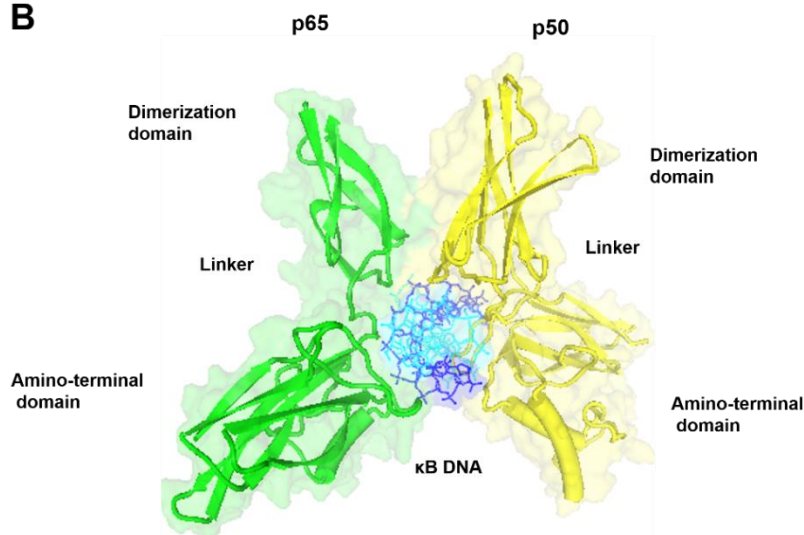
A**B**

Figure 1.2 NF-κB family of transcription factors.

(A) Schematic representation of the NF-κB family members with structural domains indicated. All subunits share a Rel homology domain (RHD) and p65, c-Rel and RelB contain a transactivating domain (TAD). p105 and p100 proteins contain a large C-terminus ankyrin repeat domain and a glycine rich region (GRR) which signal their limited proteasomal processing, generating the p50 and p52 subunits respectively. (B) Crystal structure of the murine p65/p50 heterodimer bound to DNA (PDB: 1VKX). p65 subunit is shaded in green, p50 subunit is shaded in yellow and the dimerization and amino-terminal domains are indicated.

Of the 15 possible NF- κ B dimers, 12 of these can bind DNA to potentially regulate transcription (Hoffmann et al., 2006). As p50 and p52 lack a transactivation domain (TAD) but can still bind DNA, homodimers of these subunits are considered repressors of transcription. It has been proposed that p50 and p52 homodimers compete with TAD-containing NF- κ B dimers for binding to κ B sites thereby negatively regulating NF- κ B dependent transcription. However, studies have also demonstrated that homodimers can enhance the expression of specific genes such as Skp2 and Bcl-2 (Barré and Perkins, 2010, Viatour et al., 2000). Although p50 and p52 lack transactivation capabilities, through dimerization with TAD-containing subunits they can also positively regulate transcription.

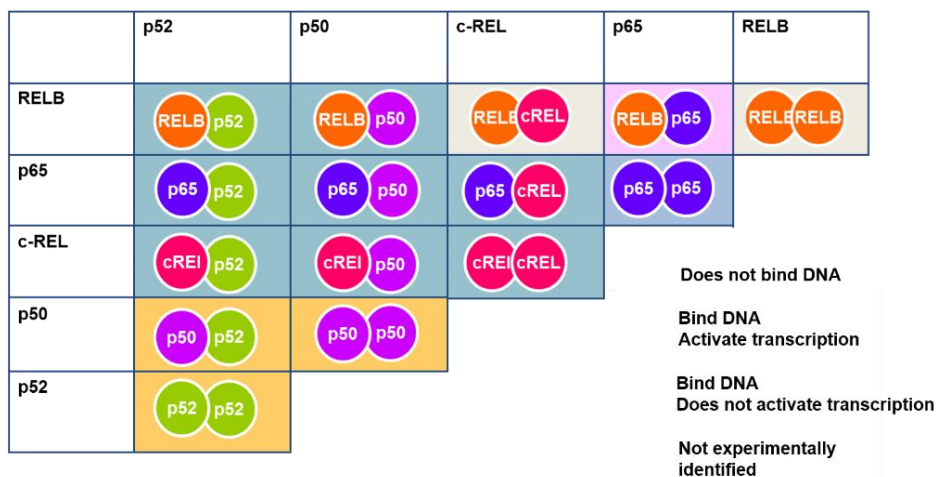


Figure 1.3 Possible NF- κ B homo- and heterodimers.

NF- κ B subunits form 15 possible homo- and hetero-dimers with each other via their RHDs. There are two structural classes of NF- κ B based on the presence of a transactivation domain. p50 and p52 represent one class and do not contain a transactivation domain and therefore homodimers of these subunits cannot activate transcription (orange shading). The second class consists of RelB, p65 and c-Rel which all contain transactivation domains. Dimers containing at least one subunit from this second class have transactivation capabilities (blue shading) with the exception of the RelB:p65 heterodimer which cannot bind DNA (pink shading). Not all possible dimer combinations may exist *in vivo* however, and grey shading represents dimers that have not currently been identified.

NF- κ B dimers bind to 9-11 base pair DNA binding sites (κ B sites), with a loose consensus sequence of G₋₅G₋₄G₋₃R₋₂N₋₁N₀Y₊₁Y₊₂C₊₃C₊₄ (where R represents purine, N represents any nucleotide and Y represents pyrimidine) (Natoli et al., 2005). The list of NF- κ B target genes known to contain a κ B site in the promoter region is currently over five hundred (for up to date list see <http://www.bu.edu/nf-kb>) and contain many immune modulators such as cytokines, chemokines and immunoreceptors. In general most κ B sites show little selectivity for a given NF- κ B dimer, however differences in dimer affinities are possible, ranging from 10-300nM (Udalova et al., 2002, Phelps et al., 2000, Sacconi et al., 2003, Hoffmann et al., 2006). Furthermore, p50 and p52 homodimers preferentially bind 11 bp κ B sites whereas 10 bp sites are preferentially bound by heterodimers of p50 and either p65 or c-Rel (Huang et al., 2001). Some dimers can also selectively regulate target promoters, however there is considerable redundancy in gene activation with most genes induced by more than one NF- κ B dimer (Sacconi et al., 2003). Although different NF- κ B dimers can bind the same κ B site, the transcriptional output following dimer binding is not equivalent (Natoli et al., 2005, Lin et al., 1995). In addition, dimer-specific synergy with other transcription factors and interactions with co-factors can also regulate distinct gene sets following NF- κ B DNA binding (Hoffmann et al., 2003). Moreover, promoter occupancy is a highly dynamic process and it has been suggested that dimer exchange at the same promoter may allow fine tuning of the NF- κ B response over time (Bosisio et al., 2006, Sacconi et al., 2003).

Knockout mouse models for the various NF- κ B family members have provided considerable information in elucidating the distinct and overlapping functions of each NF- κ B subunit, these however, may also be cell type and tissue dependent. For example *RelA*^{-/-} mice are embryonically lethal due to extensive tumour necrosis factor (TNF) α -mediated fetal hepatocyte apoptosis (Beg et al., 1995). Conversely, c-Rel is dispensable for mouse embryonic development and differentiation of hemopoietic precursors, nevertheless, mature lymphocytes and macrophages exhibit a number of activation-associated defects associated with B- and T-cell proliferation (Gerondakis et al., 2000). Knockout mice for more than one NF- κ B subunit such as the *Nfkb1*^{-/-}*RelB*^{-/-}, *Nfkb1*^{-/-}*Nfkb2*^{-/-} *c-Rel*^{-/-}*Nfkb1*^{-/-} and *Rela*^{-/-}*Nfkb1*^{-/-} animals have more severe phenotypes than of those seen in the individual knockouts, suggesting some functional compensation between the NF- κ B subunits (Gerondakis et al., 2000). This was further highlighted in a genetic study using a panel of cell lines deficient in

individual or multiple NF- κ B proteins (Hoffmann et al., 2003). Although a number of NF- κ B dependent genes with distinct subunit requirements were identified, considerable compensation was evident within the family. p50 or p52 deficiency did not have an effect on the TNF-induced expression of a number of genes, however the activation of several genes such as RANTES, IP-10 and M-CSF were defective in cells lacking both subunits. The p50:p65 heterodimer is major NF- κ B dimer present in fibroblasts, however, neither p65^{-/-} or p50^{-/-} cells are deficient in κ B binding activity as p52 and c-Rel compensate in the absence of p50 and p65 respectively (Hoffmann et al., 2003).

1.1.2 I κ B

Shortly after discovering NF- κ B, Baltimore and colleagues described its cytoplasmic localisation in resting cells (Baeuerle and Baltimore, 1988a). This cytoplasmic pool of NF- κ B was found to be inactive, however in the presence of a dissociating agent, cytoplasmic NF- κ B could in fact exhibit DNA binding activity (Baeuerle and Baltimore, 1988b). This suggested that in unstimulated cells, NF- κ B was maintained in an inactive form by reversible association with an inhibitor which they termed I κ B (Baeuerle and Baltimore, 1988a, Baeuerle and Baltimore, 1988b). Upon purification of this inhibitor, two forms of I κ B, I κ B α and I κ B β were identified and subsequently cloned (Zabel and Baeuerle, 1990, Haskill et al., 1991, Thompson et al., 1995). Both I κ B variants bound to a p65 containing NF- κ B heterodimer and exhibited similar inhibitory activity raising the question as to why two biochemically distinct inhibitors were apparently functionally similar. This was the first suggestion that interaction with I κ B proteins may be responsible for the differential regulation of NF- κ B (Zabel and Baeuerle, 1990). A theory that indeed proved correct, with nine mammalian I κ B proteins now described, each differing in NF- κ B dimer affinity, activation kinetics, regulation and function.

Following the initial characterisation of the major I κ B proteins found in mammalian cells, multiple I κ B proteins were identified based on sequence and structural homology to I κ B α and I κ B β . The I κ B family has grown extensively in recent times to include eleven members, (I κ B α , I κ B β , I κ B ϵ , Catcus, p100, p105 Relish, I κ B ζ , I κ B η , I κ BNS and B-cell lymphoma (Bcl)-3). Drosophila proteins, Catcus and Relish however only exist in invertebrates (Basith et al., 2013). In

addition to their inhibitory ability, the defining feature of these I κ B proteins is the presence of multiple copies of ankyrin (ANK) repeats, forming a central ankyrin repeat domain (ARD). The ankyrin repeat is a 33 residue motif first identified in the sequences of yeast Swi6 and Cdc10 and *Drosophila melanogaster* (Breedon and Nasmyth, 1987). It was later named due the presence of twenty four of these repeats in the cytoskeletal protein, Ankyrin (Lux et al., 1990). Ankyrin repeats are present in all three super kingdoms as well as some viral genomes and as of 2013 there were 46,742 ANK domains identified in 25,863 proteins in the non-redundant SMART database (Letunic et al., 2012, Schultz et al., 1998). This huge number of proteins include those involved in cell-cell signalling, cytoskeleton integrity, transcription and cell development and differentiation (Mosavi et al., 2004, Li et al., 2006). The number of repeats per protein can vary from 1 to 33 and function to mediate protein-protein interactions. The high degree of conservation between ankyrin repeats has led to the identification of a consensus sequence and structure. The ARD exhibits a canonical helix-turn-helix conformation in which the two α -helices are arranged in an antiparallel fashion with an almost perpendicular outward projecting β -hairpin loop (Li et al., 2006, Mosavi et al., 2004). The outer helix (helix-2) comprises nine residues, spanning positions 15-24 and is packed against the shorter inner helix (helix-1) positions 5-12. This difference in helix length and packing between helices results in a slight L-shaped curvature (Mosavi et al., 2004). The structures of I κ B proteins I κ B α , I κ B β and Bcl-3 have been resolved and although the ARDs differ in size they retain this characteristic stacked repeat structure with a slight left handed twist (Michel et al., 2001, Jacobs and Harrison, 1998, Huxford et al., 1998, Malek et al., 2003) (Figure 1.4) Insertions in the ARD are not uncommon and are often found in the loop regions, I κ B β for example contains a large 41 residue insertion between ANK 3 and ANK 4 which is responsible for masking the NLS of one of the p65 subunits (Malek et al., 2003). Homology modelling also identified a 20 and 27 residue insertions within ANK4 of I κ BNS and I κ B ζ , respectively (Manavalan et al., 2010).

Although all I κ B proteins contain a ARD, they are distinguished by the number of ANK repeats and also important regulatory sequences contained at their C- and N- termini. Based on phylogenetic and structural analysis, I κ B proteins can be classified into three subfamilies, classical or cytoplasmic I κ B proteins, NF- κ B precursor proteins and atypical or nuclear I κ B proteins (Huxford and Ghosh,

2009, Basith et al., 2013) (Figure 1.5). The classical I κ B proteins, contain six ANK repeats and are flanked at the N -terminus by a signal receiving domain (SRD) which contains sites of IKK phosphorylation, poly ubiquitination and for I κ B α , nuclear export (Huxford and Ghosh, 2009, Huang et al., 2000). At the C-terminus I κ B α , I κ B β but not I κ B ϵ also contain an acidic PEST domain, a region rich in proline, glutamic acid, serine and threonine residues. PEST domains are also common to many other rapidly degraded proteins and are implicated in regulating I κ B protein half-life (Rogers et al., 1986, Rodriguez et al., 1995). The PEST domain is also critical for interaction with NF- κ B (Ernst et al., 1995) and possibly provides a structural mechanism for the divergent functions of I κ B α and I κ B β (Malek et al., 2003).

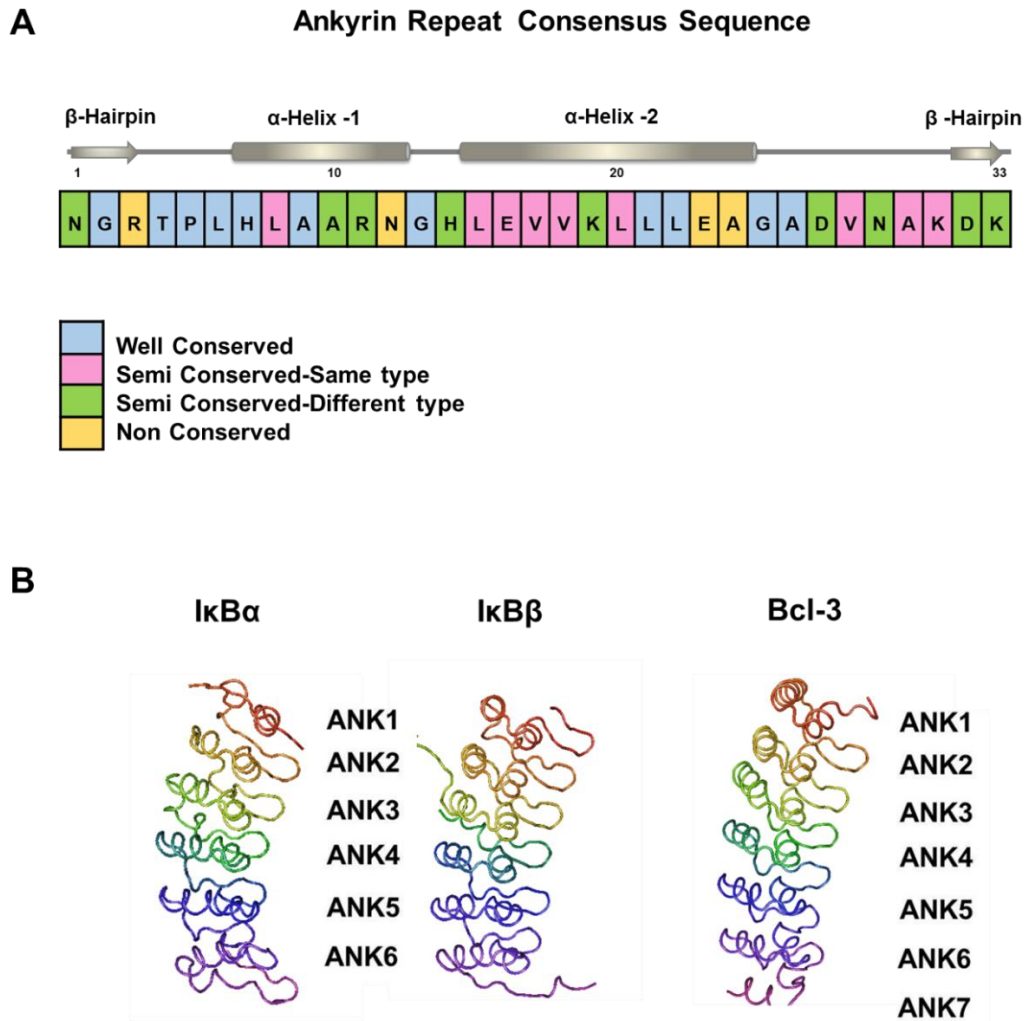
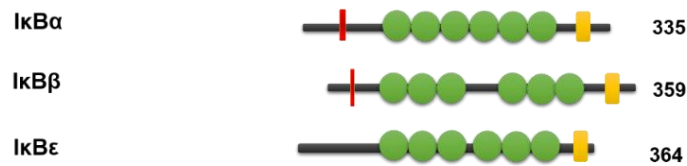


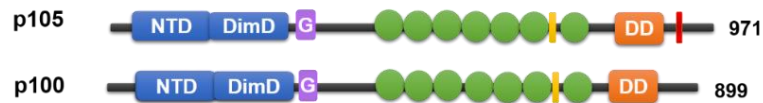
Figure 1.4 Ankyrin repeat consensus sequence and structure.

(A) 33 residue ankyrin repeat consensus sequence with residues 1-33 indicated and positions colour coded according to conservation as described previously (Mosavi et al., 2002). Blue shading represents well-conserved positions where one amino acid was present >50% of the time. Semi conserved (two to four amino acid residues occurred with a higher frequency than any others) positions were subdivided into two categories. Pink denotes high frequency residues had the same biochemical property and green denotes residues belonging to different groups of amino acids. Non-conserved positions were shaded in yellow. (B) Ribbon structures of IκBα from the NF-κB heterodimer: IκBα complex crystal structure (PDB ID: 1K1A), IκBβ from the NF-κB p65 homodimer: IκBβ complex crystal structure (PDB ID: 1K3Z) and Bcl-3 crystal structure (PDB ID: 1K1A) with ankyrin repeats indicated.

Classical



Precursor proteins



Atypical

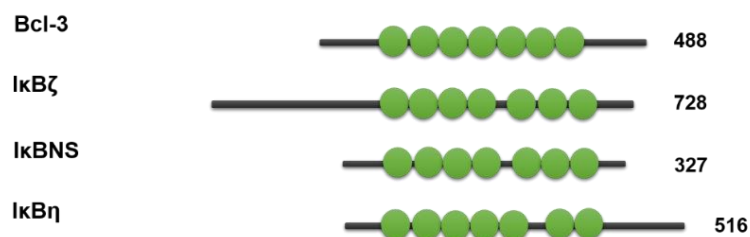


Figure 1.5 The family of mammalian IκB proteins.

Schematic representation of the three groups of IκB proteins: classical, precursor proteins and atypical. Although p105 and p100 are precursors for the NF-κB proteins p50 and p52 respectively, they also function as IκB like molecules via their C-terminal ANK domains. Important structural domains are indicated and residue numbering corresponds to murine IκB sequences.

1.1.2.1 Classical IκB proteins

In most resting cells NF-κB is associated with one of the typical cytoplasmic IκB proteins, IκBα, IκBβ or the lesser described IκBε. They are ubiquitously expressed with higher levels of expression in spleen (IκBα, IκBε), testis (IκBβ, IκBε), thymus (IκBα), and lung (IκBε) (Hinz et al., 2012). IκB proteins exhibit different affinities for NF-κB dimers, with classical IκB proteins preferentially binding dimers containing at least one p65 or c-Rel subunit (Jacobs and Harrison, 1998, Malek et al., 2003, Huxford et al., 1998, Whiteside et al., 1997, Li and Nabel, 1997, Thompson et al., 1995). The first NF-κB:IκB complex to be resolved was that of a p50:p65 heterodimer bound to IκBα and remains the best studied interaction to date (Müller and Harrison, 1995, Ghosh et al., 1995).

When it was observed that nuclear localisation signal (NLS) deficient p65 mutants could no longer interact with IκBα, the first mechanism for NF-κB cytoplasmic retention by IκB proteins was proposed (Beg et al., 1992). IκB proteins were thought to mask the NLS of NF-κB subunits thereby preventing nuclear translocation of NF-κB. Therefore, IκB degradation following a cellular stimulus (discussed in detail in 1.3.2) would allow free NF-κB dimers to translocate from the cytoplasm to the nucleus, supporting the original model of inducible NF-κB regulation (Baeuerle and Baltimore, 1988a, Baeuerle and Baltimore, 1988b). Though still extensively used, the simplicity of this general model of NF-κB regulation by all IκB proteins is inaccurate. Although X-ray crystallography confirmed that indeed IκBα contacts the NLS of p65 in a p65:p50 NF-κB heterodimer, the NLS of p50 remains exposed (Jacobs and Harrison, 1998, Huxford et al., 1998). The nuclear localisation capability of IκBα:p50/p65 complexes was finally shown following the identification of a nuclear export signal (NES) in IκBα. Studies using Leptomycin B (LMB), an inhibitor of chromosome region maintenance 1 protein (CRM1), demonstrated redistribution of NF-κB:IκBα complexes from the cytoplasm to the nucleus (Johnson et al., 1999, Rodriguez et al., 1999, Huang et al., 2000, Tam et al., 2000). These remarkable results suggested that NF-κB:IκBα complexes, previously assumed to be cytoplasmic were in fact constantly shuttling between the cytoplasm and nucleus in resting cells (Huang et al., 2000). The incomplete masking of the p50 NLS is thought to be responsible for the nuclear translocation ability of NF-κB:IκBα complexes (Malek et al., 2001). However, due to dominant IκBα and p65 NESs, the rate of nuclear export exceeds that of nuclear import, the steady

state location for this complex is the cytoplasm (Ghosh and Karin, 2002, Huang et al., 2000).

In contrast, I κ B β lacks an NES and free I κ B β remains cytoplasmic in the presence of LMB (Malek et al., 2001, Chen et al., 2003). Therefore unlike I κ B α , NF- κ B:I κ B β complexes do not undergo nucleo-cytoplasmic shuttling and are retained in the cytoplasm in resting cells. Furthermore, I κ B β masks the NLS on both subunits of a NF- κ B heterodimer explaining the strict cytoplasmic localisation of NF- κ B:I κ B β complexes in resting cells (Malek et al., 2001). Thus it is apparent that even within a subset of I κ B proteins, not all NF- κ B:I κ B interactions are identical. Although I κ B α , I κ B β and I κ B ϵ share many biochemical properties and NF- κ B dimer specificity, the stimulus dependent expression and degradation dynamics of these proteins vary significantly, which are fundamental to their distinct functions (Hinz et al., 2012). Moreover, novel roles of I κ B proteins are only recently emerging although discovered over 25 years ago. A number of studies have identified alternative nuclear functions for members of the classical I κ B proteins (Espinosa et al., 2011, Mulero et al., 2013, Aguilera et al., 2004). Nuclear I κ B α can associate with histone deacetylases (HDAC) -1 and -5 and is recruited to the Notch-target gene, *hes1*, promoter and is associated with transcriptional repression (Rao et al., 2010). I κ B β can also be recruited to the promoters of specific genes such as IL-1 β , forming a complex with p65:c-Rel heterodimers, prolonging the expression of a subset of LPS-induced genes (Scheibel et al., 2010).

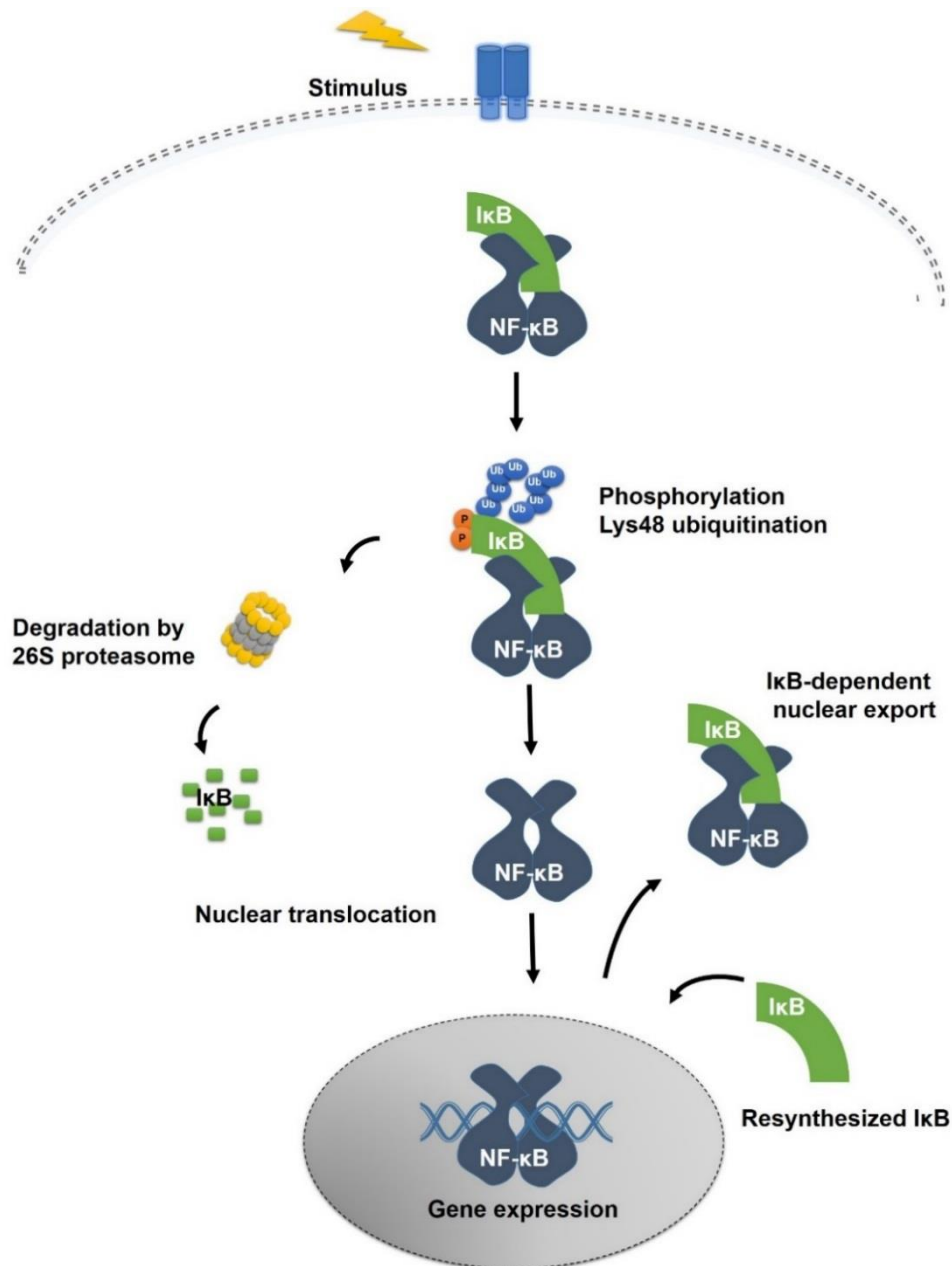


Figure 1.6 Inhibition of NF-κB by IκB proteins.

NF-κB is maintained in an inactive state by association with one of the typical IκB proteins. Multiple stimuli induce the IκB kinase (IKK) mediated phosphorylation (P) and subsequent Lys48-linked polyubiquitination (Ub) of IκBs. IκBs are then targeted to the 26S proteasome for degradation, thereby releasing associated NF-κB dimers. Free NF-κB can translocate to the nucleus and bind to the promoter regions of NF-κB-responsive genes to activate transcription. Newly synthesised IκB enters the nucleus and dissociates DNA bound NF-κB exporting it back to the cytoplasm, terminating the NF-κB response. IκBε shares many biochemical properties and NF-κB dimer specificity, the stimulus dependent expression and degradation dynamics of these proteins vary significantly, which are fundamental to their distinct functions (Hinz et al., 2012).

1.1.2.2 NF- κ B precursors

As previously mentioned the p105 and p100 proteins have dual roles as NF- κ B precursors of p50 and p52 and as inhibitors of NF- κ B (Basak et al., 2007). These precursors are responsible for inhibiting nearly half of NF- κ B in resting cells and as such represent an important second class of I κ B proteins (Huxford and Ghosh, 2009). Cytoplasmic retention of NF- κ B by p105 and p100 can also compensate for the absence of classical I κ Bs (Tergaonkar et al., 2005). However, unlike classical I κ B proteins that form 1:1 complexes with their respective NF- κ B binding partner, NF- κ B precursors form large multiprotein assemblies. p105 and p100 can form high-molecular weight complexes that incorporate multiple NF- κ B subunits which are released in response to specific cellular stimulation (Savinova et al., 2009). The current model of these large multiprotein complexes stems from the unique structure of the precursor proteins having both a RHD and an ANK repeat domain. p105 is thought to be involved in at least three types of interactions: dimerisation of RHDs, binding of preformed RHD dimers to ANK repeat domains of p105 and dimerisation of the α -helical domain in the C-terminal half of p105 (Savinova et al., 2009).

1.1.2.3 Atypical I κ B proteins

Containing seven ANK repeats and the ability to bind NF- κ B dimers, atypical I κ Bs display homology to the cytoplasmic I κ B proteins, however they do not exhibit the properties of these prototypic I κ Bs. In contrast, the atypical I κ Bs, Bcl-3, I κ B ζ , I κ BNS and I κ B η reside predominantly in the nucleus and apart from I κ B η are expressed at low levels in resting cells which increases significantly upon stimulation with NF- κ B inducing agents (Yamamoto et al., 2004, Fiorini et al., 2002, Yamazaki et al., 2001, Ohno et al., 1990, Yamauchi et al., 2010, Hinz et al., 2012). Unlike the typical I κ Bs, they are not degraded upon IKK activation and bind nuclear NF- κ B dimers to modulate gene transcription in response to distinct stimuli. Acting in the nucleus to directly inhibit and in some cases activate NF- κ B, atypical I κ Bs increase the specificity of NF- κ B gene regulation and as revealed by multiple knockout studies (**Table 1**), are critical in mounting an effective immune response.

Table 1. Knockouts of atypical IκB proteins

Knockout	Phenotype
Bcl-3^{-/-}	Defects in splenic and lymph node microarchitecture, reduced Peyer's patches size and number, absent germinal centres. Defects in T-cell differentiation and severe defects in protective humoral immune response Hypersensitivity to endotoxin shock.
IκBζ^{-/-}	Severe atopic dermatitis-like disease with inflammatory cell infiltration. Impaired expression of specific genes activated by TLR/IL-1R signal transduction, e.g. IL-6
IκBNS^{-/-}	High sensitivity to LPS-induced endotoxin shock and intestinal inflammation. Reduced T-cell proliferation and deregulated production of subset of cytokines e.g IL-12p40, IL-6 and IL-18

Adapted from (Hinz et al., 2012, Beinke and Ley, 2004, Franzoso et al., 1997, Schwarz et al., 1997, Paxian* et al., 2002, Pène et al., 2011, Carmody et al., 2007b).

Bcl-3 was the first atypical IκB protein to be described however it was originally identified as a putative proto-oncogene (McKeithan et al., 1987, Kerr et al., 1992, Ohno et al., 1990). *BCL3* was initially cloned from neoplastic cells from patients suffering from B-cell chronic lymphocytic leukaemia (CLL) displaying the t(14;19)(q32;q13.1) translocation (McKeithan et al., 1987). Cloning of the gene located at the break-point junction in this translocation revealed that it encoded a protein of 446 amino acids (Kerr et al., 1992). The amino acid sequence predicted a basic protein with a proline-rich amino terminus, a series of seven tandem ankyrin repeats, and a proline- and serine-rich carboxyl terminus (Kerr et al., 1992). It was subsequently classified as an IκB family member by virtue of these seven ankyrin repeat domains which mediate selective interaction with homodimers of p50 and p52 (Nolan et al., 1993, Wulczyn et al., 1992). Although Bcl-3 is probably the best studied atypical IκB protein, the precise function of Bcl-3 in NF-κB regulation remained unclear for many years. Conflicting early reports suggested that Bcl-3 could both enhance and inhibit p50 homodimer DNA binding and act as both a transcriptional co-activator and repressor of NF-κB gene expression (Franzoso et al., 1992, Fujita et al., 1993, Franzoso, 1993, Caamaño et al., 1996, Bours et al., 1993, Richard et al., 1999). The subsequent development of *Bcl3* knockout mice revealed a

critical role for Bcl-3 in the regulation of the immune response and in central tolerance.

Bcl3^{-/-} mice develop normally however they exhibit severe defects in response to immunogenic challenge from pathogens and display altered microarchitecture of their secondary lymphoid organs including reduced Peyer's patches size and number and lack of germinal centres (Schwarz et al., 1997, Franzoso et al., 1997, Paxian* et al., 2002). Mice deficient in Bcl-3 fail to develop immunologic resistance to *Toxoplasma gondii* and succumb to infection within 3-5 weeks whereas control littermates survived longer than 6 months (Franzoso et al., 1997). *Bcl3*^{-/-} mice are also unable to clear *Listeria monocytogenes* and are more susceptible to infection with *Streptococcus pneumoniae* relative to wild-type mice (Schwarz et al., 1997). Furthermore, *Bcl3* deficiency renders cells and mice hypersensitive to Toll-like receptor (TLR) activation and Lipopolysaccharide (LPS)-induced septic shock (Carmody et al., 2007b). Many defects observed in *Bcl3*^{-/-} mice are very similar to those seen in p52 deficient animals, including loss of B cell follicles within their spleens and lymph nodes and absence of germinal centres. Mice lacking both Bcl-3 and p52 exhibit a more severe phenotype and fail to survive past 4 weeks of birth.

Bcl-3 negatively regulates the expression of a number of cytokines and chemokines following TLR stimulation and plays an essential role in LPS tolerance a process also dependent on p50 homodimers (Riemann et al., 2005, Carmody et al., 2007b) 85]. LPS tolerance is a phenomenon in which cells or organisms exposed to continuous or repeated stimulation with LPS enter into a state altered responsiveness (Biswas and Lopez-Collazo, 2009, Beeson and Roberts, 1947) (Bohuslav et al., 1998). Tolerance is an essential host adaptation, limiting the deleterious consequences of excessive inflammation such as septic shock caused by the overproduction of inflammatory cytokines by monocytes and macrophages. Tolerance was initially viewed as a transient state of hypo responsiveness of macrophages to repeated or prolonged stimulation with LPS (Medvedev et al., 2000). Recent transcriptomic analysis however revealed that, TLR-induced genes can be categorised into two classes, 'toleriseable' (class T), genes that are suppressed during LPS tolerance and 'non-toleriseable' (class NT), genes that are inducible to equal or greater levels in tolerant macrophages. Pro-inflammatory effectors such as TNF and IL-6 belonging to class T genes are rapidly tolerised following prolonged exposure to LPS whereas the expression of

a number anti-microbial peptides, anti-inflammatory and pro-resolution factors are induced. This gene specific regulation is thought to depend on chromatin modifications mediated by primary gene products transcribed during the first stimulation, resulting in the differential regulation of TLR-induced genes with diverse biological functions (Foster et al., 2007). *Bcl3*^{-/-} mice and macrophages are hyper-responsive to TLR stimulation and are defective in LPS tolerance. Bcl-3 stabilises inhibitory p50 homodimers on toleriseable gene promoters thereby preventing further transactivation by c-Rel or p65 containing NF-κB dimers (Carmody et al., 2007b) (Discussed in detail in 1.3.4).

1.1.3 IKK complex

NF-κB signal transduction converges on a core enzymatic complex, the IκB kinase (IKK). The IKK complex is composed of two kinases, IKKα (or IKK-1) and IKKβ (or IKK-2) together with the regulatory subunit, IKKγ also known as NF-κB essential modulator (NEMO). The IKK complex was discovered in 1996 following attempts to identify the serine-kinase responsible for IκB stimulus induced phosphorylation (Mercurio et al., 1997, DiDonato et al., 1997, Rothwarf et al., 1998). The kinase subunits, IKKα and IKKβ are 50% identical and share a similar structure, including an amino-terminal kinase domain, a helix-loop-helix and a leucine zipper domain (Figure 1.7). The leucine zipper domain is responsible for homo- or heterodimerisation of the kinases, which is essential for the formation of active IKK (Israël, 2010). The exact mechanism of IKK activation is not fully understood, however upstream kinases, transforming growth factor-β-activated kinase-1 (TAK1) and NF-κB-inducing kinase (NIK) act as IKK kinases in response to certain stimuli (Israël, 2010). Phosphorylation of IKKα and IKKβ is critical for their kinase activity and essential phosphorylation sites in the kinase domain activation loops have been identified (Delhase et al., 1999). Once activated, the IKK complex is responsible for the phosphorylation of a number of substrates, many of which are involved in the NF-κB pathway. In the case of the IκB proteins, phosphorylation by IKK creates a degron or destruction motif recognised by the ubiquitin ligase complex, Skp1-Cullin1-F-box protein, beta-transducin repeat-containing proteins (SCF β-TrCP). β-TrCP interacts with a substrate via the binding of aspartic acid and phosphorylated serines within the destruction motif (Fuchs et al., 0000, Wu et al., 2003). Polyubiquitinated IκBs

are then rapidly degraded or as in the case for the NF- κ B precursors p105 and p100, partially proteolysed or processed by the 26S proteasome (Discussed in detail 1.3.3).

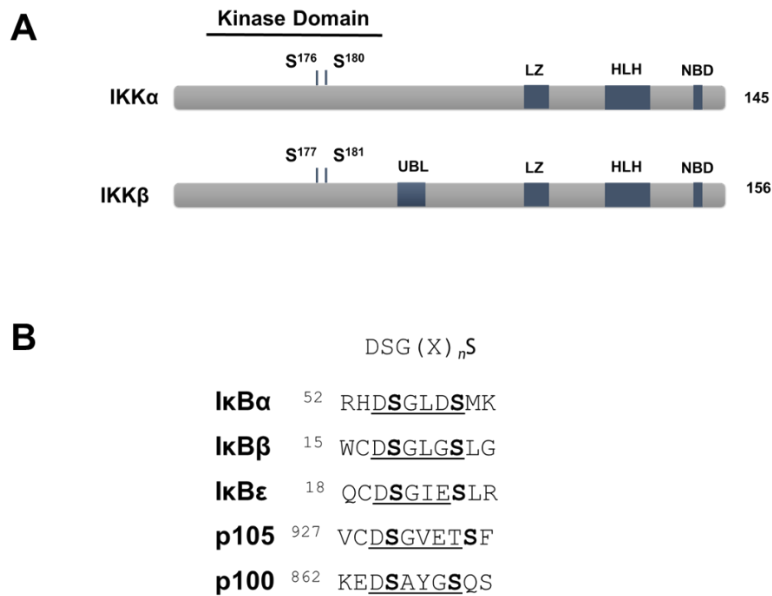


Figure 1.7 IKK complex and β -TrCP destruction motif.

(A) Schematic representation of the catalytic subunits of the IKK complex with structural domains indicated. IKK α and IKK β are 85-kDa and 87 kDa serine/threonine kinases respectively, each containing an amino-terminal kinase domain helix-loop-helix (HLH) and a leucine zipper (LZ). The activation loop is contained within the kinase domain, amino acids 176-180 of IKK α and 177-181 of IKK β . IKK β also contains a ubiquitin-like domain (UBL), the function of which is unknown. (B) NF- κ B-related IKK substrates with β -TrCP destruction/degron motif underlined. X represents any amino acid and n is >2 . Phosphorylated serines are in bold. Numbering corresponding to murine I κ B proteins.

1.2 Signaling to NF- κ B

Several pathways lead to NF- κ B activation, almost all converging on IKK activation and I κ B degradation. Engagement of various receptors, TNF receptor (TNFR), Toll-like receptor (TLR), Interleukin-1 receptor, T-cell receptor (TCR), B-cell receptor (BCR) and receptor activator of nuclear factor kappa-B (RANK) and B-cell activating factor (BAFF) receptor for example, all culminate in the activation of NF- κ B transcriptional activity. Despite significant overlap within these pathways, there are fundamental differences preceding IKK activation, highlighting the specificity of the NF- κ B response. NF- κ B signalling is also considered to occur through either the canonical or non-canonical pathways (Figure 1.8). Non-canonical or alternative NF- κ B activation is triggered by a subset of stimuli including CD40L, lymphotoxin- β and BAFF. Unlike canonical NF- κ B activation which relies on the inducible degradation of classical I κ Bs, non-canonical NF- κ B signalling is dependent on the inducible processing of p100. This pathway activates the RelB/p52 heterodimer and regulates specific biological functions such as lymphoid organogenesis-cell survival and maturation (Sun, 2012).

1.2.1 TLRs

TLRs are an important subset of the pattern-recognition receptor (PRR) family of transmembrane proteins expressed by innate immune cells. TLRs receive their name from similarity to the protein encoded by the *Toll* gene identified in *Drosophila melanogaster* (Chin and Beachy, 1994, Anderson et al., 1985). PRRs are germline encoded and function to recognise conserved molecular motifs associated with microbial pathogens and also cellular stress (Janeway, 1989). These motifs known as pathogen-associated molecular patterns (PAMPs) and danger-associated molecular patterns (DAMPs) are recognised by PRRs, activating the innate immune response to protect the host during infectious and non-infectious inflammatory responses. 13 mammalian TLRs (TLR1 to TLR13) have been identified to date which are activated by a number unrelated ligands of bacterial, viral, parasitic and fungal origin eliciting a specific transcriptional response to the pathogen encountered (Lee et al., 2012). Of these 13, only 10 functional TLRs (TLR1 to TLR10) have been identified in humans, in contrast,

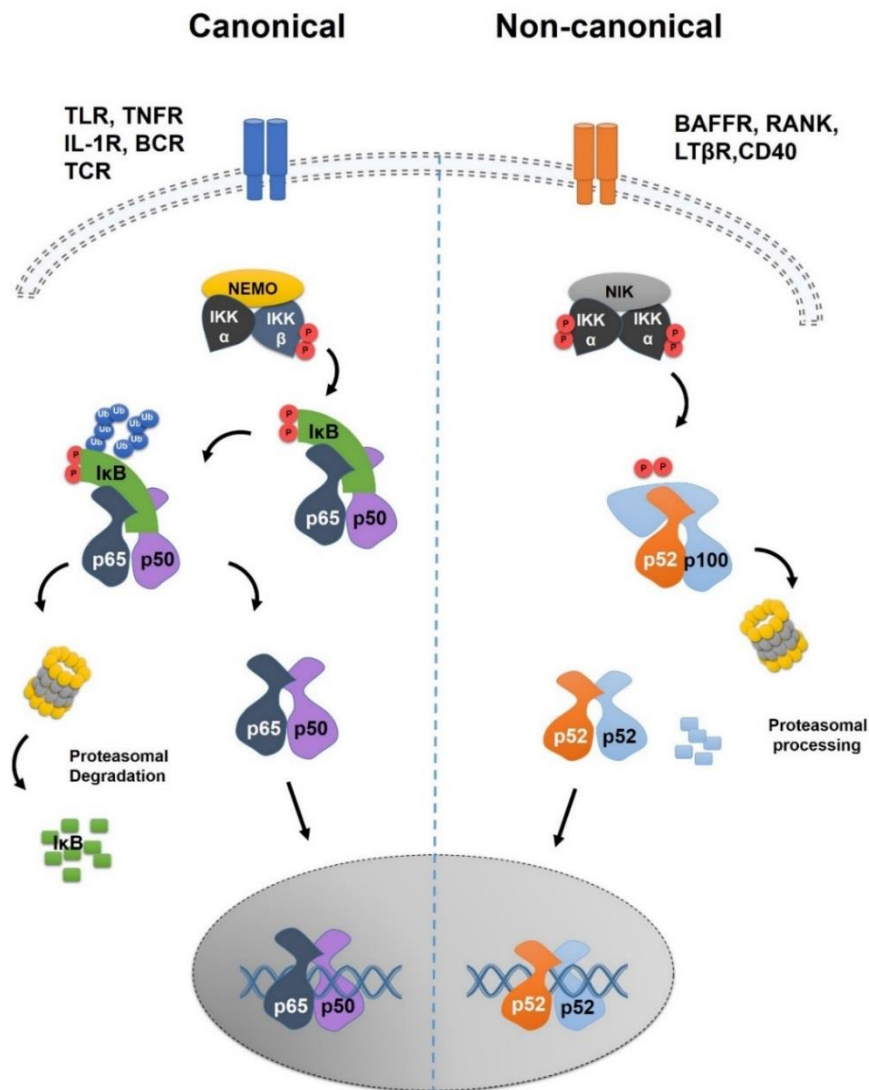


Figure 1.8 Canonical and Non-canonical NF-κB signalling.

In response to diverse stimuli, numerous cellular immune receptors (such as Toll-like receptors (TLRs), interleukin-1 receptors (IL-1Rs), TNF receptors (TNFRs), B-cell receptors and T-cell receptors) activate the canonical NF-κB pathway. Classical or canonical NF-κB signalling is mediated by IKKβ activation by upstream kinases. IKKβ activation results in the induced proteasomal degradation of IκB proteins and subsequent released of NF-κB dimers such as the prototypic p65/p50 heterodimer. Liberated NF-κB translocates to the nucleus modulating the expression of target genes. A subset of TNF family members including CD40, lymphotoxin-β, B cell-activating factor (BAFF), receptor activator of NF-κB ligand (RANKL) and TNF-related weak inducer of apoptosis (TWEAK) activate the alternative or non-canonical NF-κB signalling. Non-canonical NF-κB signalling is dependent on IKKα phosphorylation by NIK. IKKα induces the phosphorylation and proteasomal processing of p100 to p52. Newly formed p52 forms a heterodimer with RelB and translocates to the nucleus.

TLR1 to TLR9 and TLR11 to TLR13 are expressed in mice. TLRs not only differ in ligand specificity but also in subcellular distribution, residing both at the plasma membrane (TLR1, TLR2, TLR4, TLR5, TLR6, TLR11) and intracellularly on the endosome (TLR3, TLR7, TLR8, TLR9) (Lee et al., 2012). Ligands for almost all TLRs have been identified with the exceptions of TLR10, TLR12 and TLR13 (*Table 2*). TLRs are type I integral membrane receptors, characterised by an N-terminal ligand recognition domain, a single transmembrane helix, and a C-terminal cytoplasmic signalling domain (Botos et al., 2011). This signalling domain was found to share homology with the signalling domain of IL-1R family members and so was named the Toll-IL-1 receptor (TIR) domain (Gay and Keith, 1991). The conserved TIR domain is responsible for the recruitment of signalling adaptor molecules to TLR and IL-1 receptors (O'Neill and Bowie, 2007). TIR domains are not restricted to TLRs and IL-1Rs however and have also been found in the plant kingdom in addition to number of TLR related adaptor molecules (Whitham et al., 1994). Myeloid differentiation primary-response protein (MYD88), MYD88-adaptor-like (TIRAP), TIR-domain-containing adaptor protein inducing IFNbeta (TRIF), TRIF-related adaptor molecule (TRAM) and sterile alpha- and armadillo-motif-containing protein (SARM) all contain TIR domains (O'Neill and Bowie, 2007). The N-terminal domain contains tandem copies of a leucine-rich-repeat (LRR), typically a 22-29 residue motif found in many other proteins involved in immune recognition (Botos et al., 2011). TLRs typically contain 1-25 of these repeats which assemble to form the ectodomain responsible for pathogen recognition (Botos et al., 2011).

Table 2. List of TLR Ligands

Receptor	Subcellular localisation	Physiological ligands
TLR1-TLR2	Plasma membrane	Triacylated lipopeptides Peptidoglycan Phospholipomannan tGPI-mucins
TLR2	Plasma membrane	Haemagglutinin Porins Lipoarabinomannan Glucuronoxylomannan HMGB1
TLR2-TLR6	Plasma membrane	Diacylated lipopeptides LTA Zymosan
TLR3	Endosome	dsRNA
TLR4	Plasma membrane	LPS VSV glycoprotein G RSV fusion protein MMTV envelope protein Mannan Glucuronoxylomannan Glycosylinositolphospholipids HSP60 HSP70 Fibrinogen Nickel HMGB1
TLR4-TLR6	Plasma membrane	OxLDL Amyloid- β fibrils
TLR5	Plasma membrane	FLAGellin
TLR7	Endosome	ssRNA
TLR8	Endosome	ssRNA
TLR9	Endosome	DNA Haemozoin

Trypanosoma cruzi glycosylphosphatidylinositol-anchored mucin-like glycoprotein (tGPI-mucins) , high-mobility group box 1 protein (HMGB1), lipoteichoic acid (LTA), double-stranded RNA (dsRNA), vesicular stomatitis virus (VSV), respiratory syncytial virus (RSV), heat-shock protein (HSP), single-stranded RNA (ssRNA). Adapted from (Lee et al., 2012).

1.2.1.1 TLR4

Originally named hToll, TLR4 was one of the first Toll homologues to be identified and cloned (Medzhitov et al., 1997). A year later, four further TLRs were reported however considerable focus remained on the characterisation of TLR4 (Rock et al., 1998). Much like its *Drosophila* equivalent, dToll, TLR4 is a type 1 transmembrane protein and was found to induce transcription of immune response genes (Medzhitov et al., 1997, Hashimoto et al., 1991, Hashimoto et al., 1988). *Drosophila* Toll mediates the nuclear gradient and activity of the Rel homologue, Dorsal, which suggested a potential role for its human counterpart in NF- κ B signal transduction (Steward, 1989, Schneider et al., 1991, Wasserman, 1993). Early studies using a constitutive active mutant of TLR4 induced the transcription of NF- κ B dependent genes IL-1 and IL-8 and also NF- κ B reporter activity (Medzhitov et al., 1997). Subsequent studies using C3H/HeJ mice which contain a missense mutation in *Tlr4* and *Tlr4* deficient mice identified an essential role for TLR4 in LPS signal transduction (Poltorak et al., 1998, Hoshino et al., 1999). LPS is the major component of the outer membrane of Gram-negative bacteria responsible for endotoxin induced sepsis and had previously been shown to induce NF- κ B (Sen and Baltimore, 1986a). Although LPS is the best studied TLR4 ligand, other PAMPs (*Table 2*) can also stimulate signal transduction through TLR4 to induce the expression of proinflammatory cytokines and Type 1 interferons (IFN) (Uematsu and Akira, 2007). TLR signalling has been divided into two pathways based on the requirement of the adaptor protein MYD88 (Figure 1.9) (Medzhitov et al., 1998). TLR4 signals through both the MYD88-dependent and independent pathways to activate canonical NF- κ B signalling. In addition to NF- κ B, members of the mitogen activated protein kinase (MAPK) and interferon regulatory transcription factor (IRF) families are also activated following TLR4 stimulation.

1.2.2 MyD88-dependent and independent NF- κ B activation

All TLRs with the exception of TLR 3 signal through MyD88, however the specific combination of additional adaptors utilised by each TLR may differ (Kawai and Akira, 2007). In addition to MyD88, TLR4 interacts with 3 other adaptor proteins TIRAP, TRIF and TRAM (Yamamoto et al., 2003a, Horng et al., 2001, Fitzgerald et al., 2001, Fitzgerald et al., 2003, Yamamoto et al., 2003b, Oshiumi et al., 2003b). Following ligand binding and receptor dimerisation, MyD88 is recruited to TLRs directly via its TIR domain (TLRs 5, 7, 8, 9) or through the bridging adaptor TIRAP (TLRs 4, 2, 2/1, 2/6). MyD88 then interacts with members of the serine/threonine IL-1 receptor-associated kinase (IRAK) families, including IRAK-1, -2 and -4 via their respective death domains (Meylan and Tschopp, 2008, Kawai and Akira, 2007). Activated IRAK-4 recruits and subsequently phosphorylates IRAK-1. IRAK-1 then auto-phosphorylates, recruiting the ring domain ubiquitin ligase, tumour necrosis factor receptor-associated factor-6 (TRAF6) (Deng et al., 2000). Together with Ubc13/Uev1A, TRAF6 promotes Lys-63 linked polyubiquitination of target proteins including TRAF6 itself and NEMO (Adhikari et al., 2000, Chen et al., 2006). Ubiquitinated TRAF6 recruits a kinase complex involving TAK1 and TAK1 binding proteins (TABs) 2 and 3. This TAK complex activates two major pathways involving NF- κ B and MAPKs, c-Jun amino (N)-terminal kinases (JNKs) and p38 (Wang et al., 2001, Sato et al., 2005, Shim et al., 2005). Recent studies, however, have shown that the role of TAK1 in TLR activation of MAPKs and NF- κ B is cell type-specific. TAK1 is an essential positive regulator of LPS induced IKK, extracellular signal-regulated kinases (ERK)-1/2, p38 and JNK activation in fibroblasts and B cells (Sato et al., 2005). In contrast, TAK1 negatively regulates LPS-induced activation of IKK, p38 and JNK activation in neutrophils and is not required for ERK1/2 activation in macrophage or monocytes (Alagbala Ajibade et al., 2012, Courties et al., 2010, Lee et al., 2000).

Multiple TLRs can also signal independently of MYD88 and although the kinetics of activation are delayed, stimulation of *MyD88*^{-/-} cells with Lipid A, a component of LPS, results in NF- κ B activation (Kawai et al., 1999, Kawai et al., 2001). In the absence of MyD88, the TIR domain-containing adaptor, TRIF mediates NF- κ B signalling. TLR3 exclusively signals through TRIF, which is required for NF- κ B activation and interferon (IFN)- β production following IRF3 induction (Yamamoto et al., 2003a, Oshiumi et al., 2003a). Through association

with the bridging adaptor TRAM, TLR4 also utilises TRIF to signal independently of MyD88 (Yamamoto et al., 2003b). This pathway is activated downstream of endosomal TLR4 mediating the delayed phase of NF- κ B activation and type 1 IFN expression.

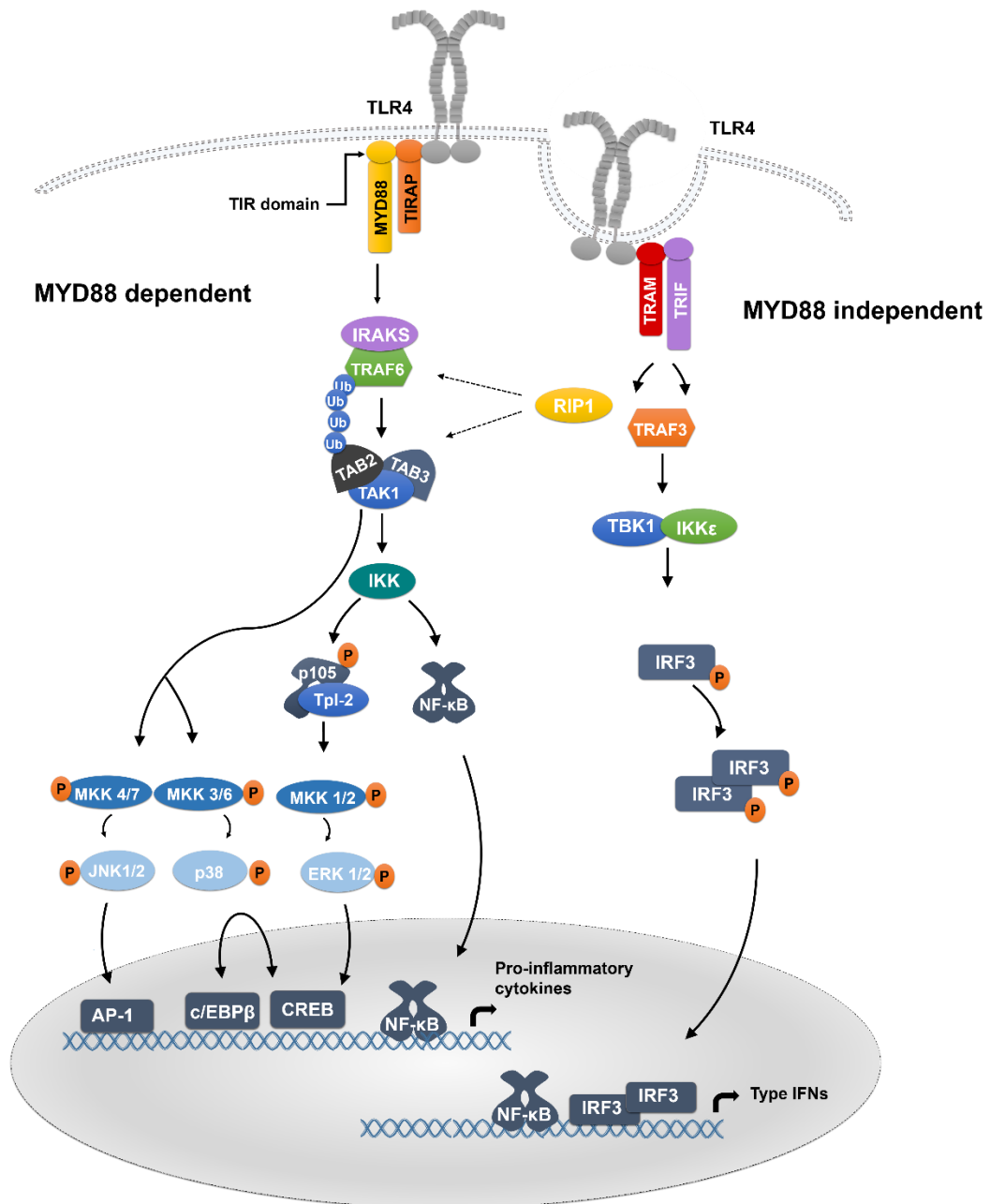


Figure 1.9 TLR signalling

Ligand binding to the TLR4 receptor induces receptor dimerization, activating TLR signalling. TLR4 is localised at the plasma membrane and also in endosomal compartments following endocytosis. The cytoplasmic TIR domain of TLR4 engages the bridging adaptors TIRAP and TRAM. TIRAP and TRAM interact with the TIR domains of MYD88 or TRIF initiating the MYD88-dependent and- independent pathways respectively. MyD88 recruits members of the IRAK family (IRAK1, IRAK2 and IRAK4) and TRAF6. TRAF6 with ubiquitin conjugating enzymes Ubc13 and Uev1A, activates the TAK1 complex (TAK1, TAB2 and TAB3) via K63-linked ubiquitination (Ub) triggering the p38 and JNK MAPK pathways. The regulatory subunit of the IKK complex, NEMO is also recruitment to the TAK complex facilitated by binding Lys63-linked ubiquitin chains. Activated TAK1 phosphorylates IKKβ thus activating the IKK complex and the canonical NF-κB pathway. IKK also phosphorylates p105 at S927 and S932 resulting in induced proteolysis of p105 by the 26S proteasome. The ubiquitin ligase complex SCF B-TrCP facilitates Lys48-linked

ubiquitination of p105 triggering its degradation and subsequent release of Tpl-2. Liberated Tpl-2 phosphorylates MEK1/2 activating downstream ERK signalling. The MyD88 independent (or TRIF dependent) pathway is activated downstream of endosomal TLR4. Through the bridging adaptor TRAM, TRIF recruits TRAF3 and protein kinases TBK1 and IKK ϵ to phosphorylate IRF3. Phosphorylation induces dimerization and nuclear localisation of IRF3 where it activates type 1 interferons. TRIF also recruits the kinase RIP1 which activates the late phase of MAPK and NF- κ B activation, however the exact mechanism is unclear. Adapted from (Botos et al., 2011, Gantke et al., 2011, O'Neill et al., 2013, Carmody and Chen, 2007, Newton and Dixit, 2012).

1.2.3 TLR Induced MAPK Signalling

MAPKs are a family of protein serine/threonine kinases that regulate diverse cellular programs by relaying extracellular signals to intracellular responses (Cargnello and Roux, 2011). Growth factors, hormones, cytokines and environmental stress are among the variety of stimuli that activate MAPK signalling controlling a range biological responses including; gene transcription, cell proliferation, growth survival and cytokine production (Chen et al., 2001). Conventional MAPKs are activated through a three tiered cascade of sequentially acting kinases composed of a MAPK, MAPK kinase (MAP2K) and a MAPK kinase kinase (MAP3K)(Figure 1.10). Although considerable overlap occurs between MAPK cascades, MAPK substrate specificity is determined by a number of factors including, scaffolding interactions, distinct MAPK subcellular localisation, signal intensity and duration (Keshet and Seger, 2010). Signal transduction through several receptor families, (receptor tyrosine kinases (RTK), G- protein-coupled receptors and PRRs), coordinate distinct cellular outcomes via downstream MAPKs, in a cell type- and stimulus- specific manner (Chiariello et al., 2010, Tarcic and Yarden, 2010).

In the innate immune response, ligand binding by most TLRs activates the MAPK pathway, initiated by MAP3K activation. There are over 20 characterised MAP3Ks which provide the specificity for stimulus-dependent activation of MAP2Ks (Craig et al., 2008). Through unique protein-protein interactions and phosphorylation of signalling effectors, MAP3Ks can activate specific MAP2K-MAPK pathways to regulate transcription factors such as cyclic-AMP-responsive-element-binding protein 1 (CREB1), activator protein 1 (AP-1) and ETS domain-containing protein (ELK1). For example, in response to growth factors and mitogens, MAP3Ks Rapidly Accelerated Fibrosarcoma (Raf) and Tat-associated kinase (TAK)-1 play an essential role in cell growth and development through activation of ERK and p38/JNK MAPKs respectively. Conversely, TLR induced activation of these MAPKs is mediated by Tumour Progression Locus 2 (Tpl-2), TAK1, and apoptosis signal-regulating kinase (ASK)-1, promoting the production of pro-inflammatory effectors.

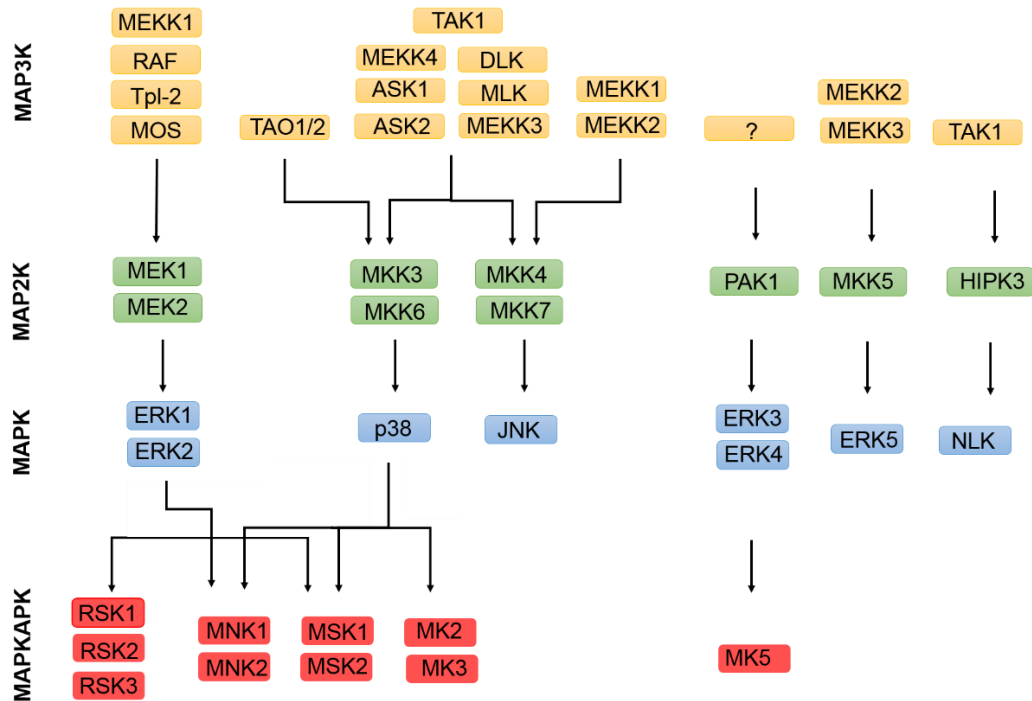


Figure 1.10 MAPK signalling cascade.

To date, 14 mammalian MAPKs have been characterised which can be subdivided based on sequence homology into conventional (extracellular signal-regulated kinases 1/2 (ERK1/2), c-Jun amino (N)-terminal kinases 1/2/3 (JNK1/2/3), p38 isoforms (α , β , γ , and δ), and ERK5) and atypical (ERK3/4, ERK7, and Nemo-like kinase (NLK)) MAPKs. MAPKs are activated through a sequential phosphorylation cascade. An active MAP3K phosphorylates and activates a MAP2K, which in turn activates a MAPK by dual phosphorylation of the Thr-X-Tyr activation motif (where X represents any amino acid). MAPKs can then activate several downstream kinases called MAPK activated kinases (MAPKAPK). MAPK/ERK kinase kinase (MEKK), tumour progression locus 2 (Tpl-2), rapidly accelerated fibrosarcoma (RAF), TGF β -activated kinase 1 (TAK1), apoptosis signal-regulating kinase (ASK), dual leucine zipper kinase (DLK), mixed-lineage kinase (MLK), MAP kinase kinase (MKK), p21-activated kinase 1 (PAK1), homeodomain-interacting protein kinase 2 (HIPK2), Nemo-Like Kinase (NLK), ribosomal protein S6 kinase (RSK), mitogen- and stress-activated kinase (MSK), MAPK signal-integrating kinase (MNK), Map Kinase-Activated Protein Kinase (MK). (Adapted from (Arthur and Ley, 2013) and (Craig et al., 2008)).

1.2.3.1 *Tpl-2*

Tpl-2 (also known as MAP3K8) is a serine/threonine protein kinase first described as a target for provirus integration in Moloney murine leukemia virus-induced T-cell lymphomas (Patriotis et al., 1993). *Cot* (cancer Osaka thyroid), a shortened form of the human *Tpl2* homolog was independently identified as a transforming gene for a human thyroid carcinoma cell line (Miyoshi et al., 1991). *Cot* encodes a protein lacking a complete C-terminus. Full length *Tpl-2* has weak transforming potential and thus the oncogenic transformation of *Tpl-2* is contributed to C-terminal truncation (Ceci et al., 1997). The physiological role of *Tpl-2* as a regulator of MAPK signalling was elucidated from sequence homology comparisons and overexpression studies in COS-7 and MEF cells. Overexpression activates ERK1/2, JNK, p38 γ and ERK5 MAPKs and also phosphorylates MEK1, MKK4, MEK5 and MKK6 *in vitro* (Patriotis et al., 1994, Salmeron et al., 1996, Chiariello et al., 2000). These early results suggested *Tpl-2* acted directly as a MAP3K for a number of substrates however, subsequent *in vivo* studies using *Tpl2*^{-/-} mice revealed the major function of *Tpl-2* is in regulating ERK activation in immune responses. *Tpl2*^{-/-} mice produce low levels of TNF when exposed to LPS and are resistant to LPS/D-Galactosamine-induced endotoxin shock (Dumitru et al., 2000). Furthermore loss of *Tpl-2* also protects from TNF-induced inflammatory bowel disease (IBD) (Kontoyiannis et al., 2002).

Tpl-2 mediates ERK1/2 activation by all TLRs and some members of the TNFR superfamily in primary macrophages (Banerjee et al., 2006, Eliopoulos et al., 2003) and is essential for induction of a number of inflammatory mediators including TNF, IL-1 β , IL-23p19 and cyclo-oxygenase (COX-2) (Dumitru et al., 2000, Mielke et al., 2009, Kakimoto et al., 2010, Eliopoulos et al., 2002) following LPS stimulation. Following LPS induction, *Tpl-2* specifically mediates activation of ERK1/2 in macrophage but not MAPKs, p38 and JNK (Dumitru et al., 2000). *Tpl-2* is also required for optimal TNF production following LPS stimulation in other cell types however, unlike macrophages *Tpl-2* may not be essential for TNF production in these cells. For example, *Tpl-2* also plays a role in TNF induction in dendritic cells however, this is only partially dependent on *Tpl-2* (Mielke et al., 2009). Furthermore, *Tpl-2* is not universally involved in TNF induction, curdlan stimulation of dectin-1, a *Tpl-2* independent ERK activator, also induces TNF (Mielke et al., 2009). *Tpl-2* can also regulate other MAPKs but

in a stimulus- and cell type- dependent manner and it has been suggested that Tpl-2 may not be the sole MAP3K utilised in these cascades (Das et al., 2005).

In resting cells, Tpl-2 exists as part of a cytoplasmic complex with p105 and A20-binding inhibitor of NF- κ B 2 (Abin-2) (Belich et al., 1999, Lang et al., 2004) (Figure 1.11). All detectable Tpl-2 is associated with p105, however the majority of p105 in macrophages is not complexed with Tpl-2 (Beinke et al., 2004). By physically preventing access to MEK1/2, p105 negatively regulates Tpl-2 induced ERK activation (Waterfield et al., 2003, Beinke et al., 2003). p105 and Abin-2 also maintain Tpl-2 stability as free Tpl-2 is very unstable. *Nfkb1*^{-/-} macrophages are therefore defective in LPS induced ERK activation due to the reduced steady state levels of Tpl-2 in these cells (Waterfield et al., 2003, Beinke et al., 2003). Following LPS stimulation, IKK β phosphorylates p105 on S927 and S932, targeting it for proteasomal degradation. IKK induced proteolysis of p105 releases Tpl-2 from inhibition. Abin-2 is also released following p105 degradation and is not associated with the pool of Tpl-2 that can activate MEK. It is yet unclear if Abin-2 has other functions other than stabilising Tpl-2 (Gantke et al., 2012). Liberated Tpl-2 once activated directly phosphorylates MEK1/2 thereby activating downstream ERK signalling (Waterfield et al., 2004, Beinke et al., 2004). Activated ERKs phosphorylate and activate a number of important downstream effectors including the 90kDa ribosomal S6 kinase (RSK) family and mitogen- and stress-activated kinases (MSK) 1 and 2 (Murphy and Blenis, 2006). ERKs and RSKs can translocate to the nucleus immediately following activation where in addition to MSKs they can phosphorylate multiple transcription factors such as Elk-1 and cAMP response element-binding protein (CREB) to induce the transcription of a number of immediate-early (IE) genes including *Fos*, *junB*, *c-Jun* and *Egr1* (Roux and Blenis, 2004).

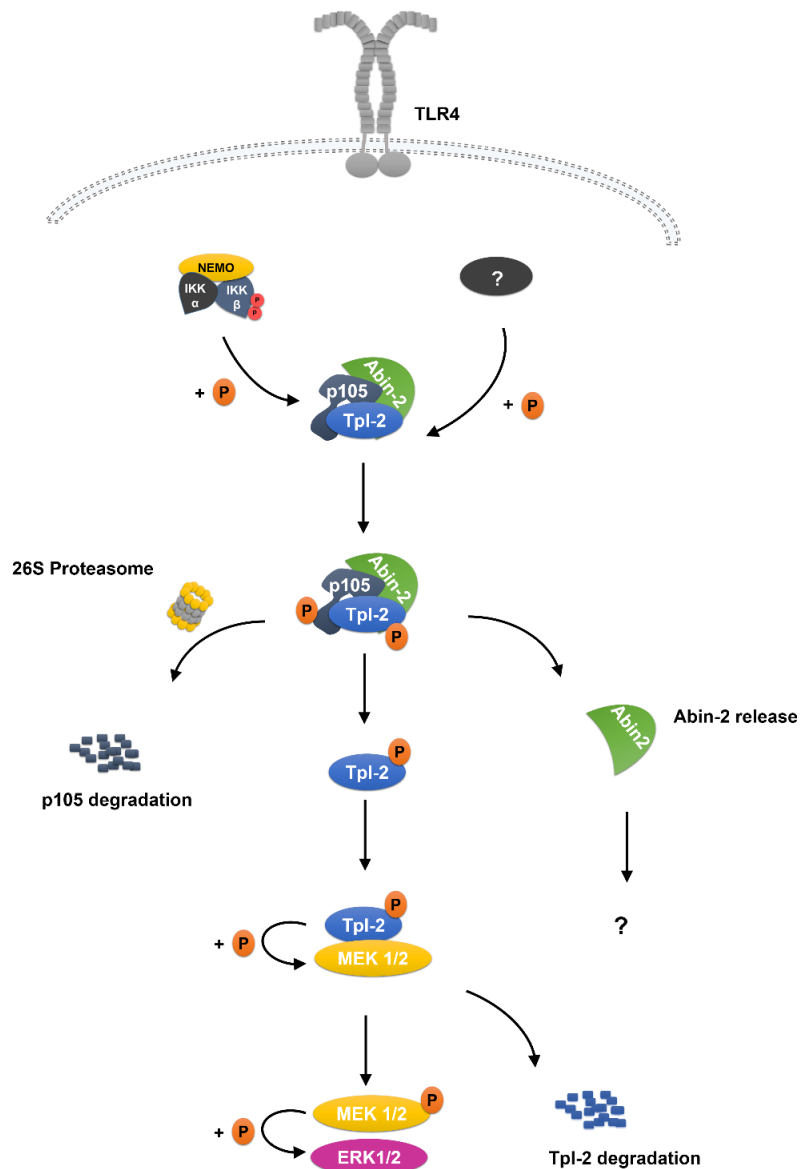


Figure 1.11 Regulation of Tpl-2-MEK kinase activity.

In resting cells, Tpl-2 exists as part of a cytoplasmic complex with p105 and Abin-2. Association with these two proteins is required to maintain the steady state levels of Tpl-2, as free Tpl-2 is unstable. Association with p105 also inhibits the MEK-kinase ability of Tpl-2 by preventing Tpl-2 association with MEK1/2. Agonist stimulation of TLR4 induces IKK β -mediated phosphorylation of p105 at Serines 927 and 932 and triggers complete proteolysis of p105 by the proteasome. Liberated Tpl-2 is then free to bind to its substrate MEK1/2 and facilitate the phosphorylation of serines 217 and 221. Inducible phosphorylation of Tpl-2 at serine 400 by IKK β and by an unknown kinase at threonine 290 is also required for activation of MEK1/2. Activated MEK1/2 then phosphorylates and activates ERK1/2. Abin-2 is also released following p105 degradation but it is unclear if Abin-2 has other downstream targets or functions other than stabilising Tpl-2. Tpl-2 is the sole MAP3K responsible for ERK activation in macrophages following TLR4 engagement and although it is also important in other immune cells, for example dendritic cells, it may not be the sole MAP3K utilised by these cells. Tumour Progression Locus 2 (Tpl-2), A20-binding inhibitor of NF- κ B 2 (Abin-2), mitogen/extracellular signal-regulated kinase (MEK), extracellular signal-regulated kinases (ERK).

1.3 Ubiquitination in NF- κ B Regulation

Independent of the stimulus and pathway engaged, activation and regulation of NF- κ B relies heavily on post-translational modification. The IKKs, the I κ Bs and the NF- κ B subunits themselves are all subjected to a number of regulatory modifications including acetylation, sumolation, nitrosylation, phosphorylation and ubiquitination (Figure 1.12). There are many critical cytoplasmic post-translational modifications required to activate NF- κ B, either directly or through I κ B degradation, however nuclear modifications play an equally important role (Perkins, 2000). Nuclear modifications of NF- κ B are not only necessary for maximal transcriptional activity but are also emerging as a key to signal-specific responses. Stimulus-dependent induction of these modifications can affect the stability and ability of NF- κ B dimers to bind DNA, interact with I κ B proteins and recruit essential co-activators (Guan et al., 2005, Hou et al., 2003, Chen et al., 2002, Kiernan et al., 2003, Hayden and Ghosh, 2004, Ghosh and Hayden, 2008). The “NF- κ B barcode hypothesis” suggests these covalent modifications alone or in combination, generate distinct patterns that function to direct transcription in a target gene-specific fashion (Moreno et al., 2010). Differential phosphorylation of serines 205, 276 and 281 for example, was shown to target p65 to particular gene subsets (Anrather et al., 2005), whereas acetylation of p65 at lysines 122 and 123 inhibited p65 transactivation while the same modification at lysines 218 and 221 enhanced p65 DNA binding (Chen et al., 2002, Kiernan et al., 2003). Although all NF- κ B subunits are subjected to these regulatory modifications, post-translation modification of p65 is the best characterised with other NF- κ B subunits receiving little attention in comparison (Perkins, 2000).

The role of ubiquitination in NF- κ B activation through I κ B degradation and NF- κ B precursor processing pathway has been extensively studied, however ubiquitination is now also emerging as a critical step in the regulation of the NF- κ B transcriptional response (Colleran et al., 2013, Carmody et al., 2007b, Bosisio et al., 2006, Sacconi et al., 2004). The poly-ubiquitination and subsequent proteasomal degradation of nuclear p65 not only regulates its stability, it promotes transcriptional termination by removing promoter bound p65:c-Rel dimers (Sacconi et al., 2004, Geng et al., 2009). A number of key regulators of p65 poly-ubiquitination have been identified, including the deubiquitinase, ubiquitin-specific-processing protease 7 (Usp7), the ubiquitin ligases Pdlim2

(PDZ and LIM domain 2) and copper metabolism mouse U2af1-rs1 region 1-domain-containing protein 1 (Commd1) and peptidyl-prolyl isomerase 1 (Pin1) (Tanaka et al., 2007, Geng et al., 2009, Colleran et al., 2013). p50 homodimers are also subjected to DNA binding-dependent poly-ubiquitination, in contrast to p65 however, relatively little is known about the mechanisms regulating the post-translational modification of p50.

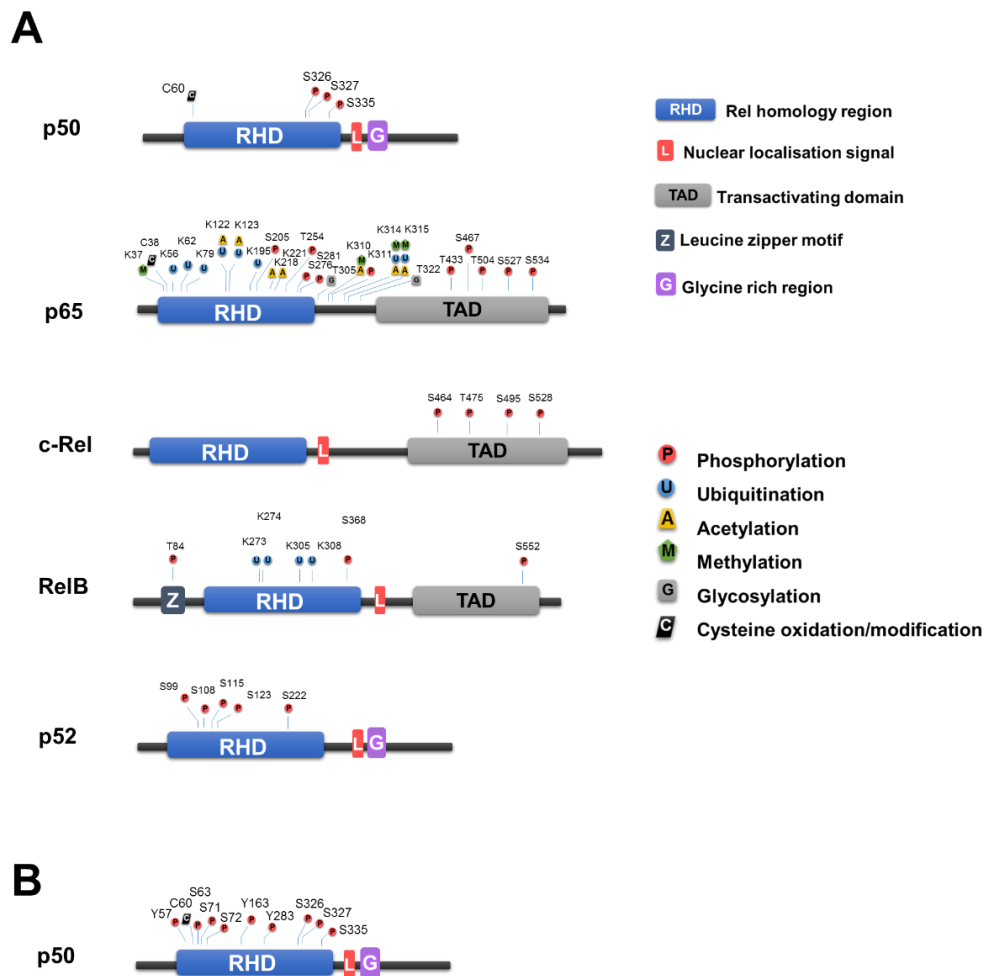


Figure 1.12 Post translation modification of the NF- κ B subunits.

(A) Schematic representation of the structure of the NF- κ B subunits, p50, p65, C-Rel, Relb and p52 with post translational modifications indicated. Experimentally characterised modifications of either human or mouse residues are illustrated with the amino acid numbering corresponding to the murine sequence. (B) Schematic representation of the structure of the NF- κ B subunits p50 with post translational modifications identified only by proteomic discovery mode mass spectrometry illustrated (Hornbeck et al., 2012, Perkins, 2000).

1.3.1 The Ubiquitin Proteasome System

Ubiquitin is a 76-amino-acid protein, that when covalently linked to target proteins may alter their half-life, localization, or function (Wertz and Dixit, 2010). Attachment of a ubiquitin molecule to a substrate protein is achieved by a three component enzymatic system composed of a ubiquitin-activating enzymes (E1s), ubiquitin-conjugating enzyme (E2) and ubiquitin ligase (E3) (Figure 1.13) (Hershko et al., 1983). This sequential process begins with the ATP dependent activation of ubiquitin, in which the C-terminal carboxyl group of ubiquitin becomes linked to the sulfhydryl group of an E1 by a thioester bond. The activated ubiquitin is then transferred to the active site cysteine of one of over 30 E2 enzymes. In the final step, an E3 ligase acts as the substrate recognition molecule, binds to the target protein and catalyses the transfer of ubiquitin from the E2 to a lysine of the substrate protein. There are hundreds of E3 ubiquitin ligases, which along with the E2 confer a great specificity to the ubiquitin system. The process can end after the attachment of a single ubiquitin moiety (mono-ubiquitination) or additional ubiquitin molecules can be added, yielding multi-monoubiquitin or polyubiquitin chains. The outcome of a ubiquitinated protein is largely determined by the type of ubiquitin modification however, a ubiquitinated protein is not always committed to a particular fate. Aptly named, deubiquitinating enzymes (or deubiquitinases) remove ubiquitin from substrate proteins, opposing the ubiquitination process. These are highly specific cysteine proteases that hydrolyse the amide bond between ubiquitin and the substrate protein. Deubiquitination thereby alters the stability of substrate proteins by removing or modifying a potentially degradative signal and also serves to maintain steady state levels of ubiquitin (Komander et al., 2009).

Ubiquitin molecules can be linked through any one of the seven ubiquitin Lys residues (Lys6, Lys11, Lys27, Lys29, Lys33, Lys48 and Lys63) or through the ubiquitin amino terminal Methionine residue (linear) to generate polyubiquitin chains (Figure 1. 14) (Kulathu and Komander, 2012). Although all possible linkages have been detected in cells, studies have largely focused on Lys48- and Lys63- linked homogenous chains and as such the biological significance of other atypical ubiquitin chains (Lys6, Lys11, Lys27, Lys29, Lys33) is less defined (Kulathu and Komander, 2012, Ikeda and Dikic, 2008).

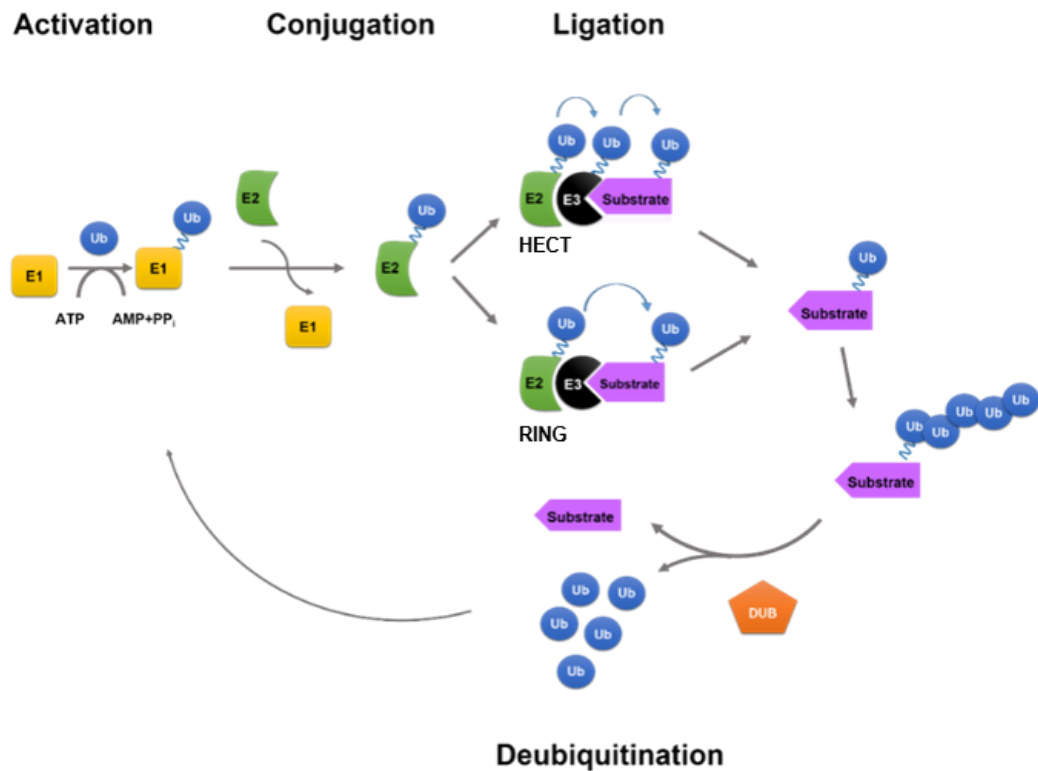


Figure 1.13 Ubiquitination Cascade.

Schematic representation of the ubiquitination process (see text). Ubiquitin-activating enzymes (E1), ubiquitin-conjugating enzymes (E2), ubiquitin ligases (E3), Ubiquitin (Ub), Adenosine triphosphate (ATP), adenosine monophosphate (AMP), pyrophosphates (PP_i), Deubiquitinase (DUB). The two major classes of ubiquitin ligases are depicted, HECT (Homologous to the E6-AP C-Terminal domain) and RING (Really Interesting New Gene). Depending on the type of ubiquitin ligase utilised, activated ubiquitin can be transferred directly to the substrate (RING) or following the formation of an E3-ubiquitin intermediate (HECT).

Lys48-linked ubiquitin chains were the first type of ubiquitin linkage to be identified and remain the best characterised. This form of ubiquitination typically targets the protein for degradation by the 26S proteasome, a large multicatalytic protease that degrades proteins into small peptides in a process known as proteolysis (Glickman and Ciechanover, 2002). The 26S proteasome is a 2.5-MDa molecular machine composed of two sub complexes, a barrel-shaped 20S proteolytic core complex capped at one or both ends by 19S regulatory complexes which recognise the ubiquitinated proteins (Voges et al., 1999). Once delivered to the proteasome, ubiquitinated proteins are then deubiquitinated, unfolded by ATPases in the base and translocated into the 20S complex for degradation (Geng et al., 2012). Within the 20S core, chymotrypsin-like, trypsin-like, and peptidylglutamyl peptide hydrolytic activities are responsible for attacking the target protein and cleaving it into peptide of about 4-25 residues (Voges et al., 1999).

Ubiquitin mediated proteolysis is a critical regulatory mechanism that controls the concentration of a large number intracellular proteins which include cell cycle regulators such as cyclins, cyclin-dependent kinase inhibitors, and proteins, tumour suppressors, transcriptional activators and their inhibitors (Glickman and Ciechanover, 2002). Consequently, this controls a variety of cellular processes involved in cell cycle and division, differentiation and development, DNA repair, transcriptional regulation, transcriptional silencing and regulation of the immune and inflammatory responses (Glickman and Ciechanover, 2002). Lys63-linked ubiquitination in contrast does not label a protein for destruction but rather acts as a scaffold to assemble signalling complexes (Wertz and Dixit, 2010, Ikeda and Dikic, 2008). Lys-63-linked ubiquitination thereby participates in diverse cellular processes from receptor endocytosis and DNA-repair processes to NF- κ B activation (Ikeda and Dikic, 2008, Wertz and Dixit, 2010) .

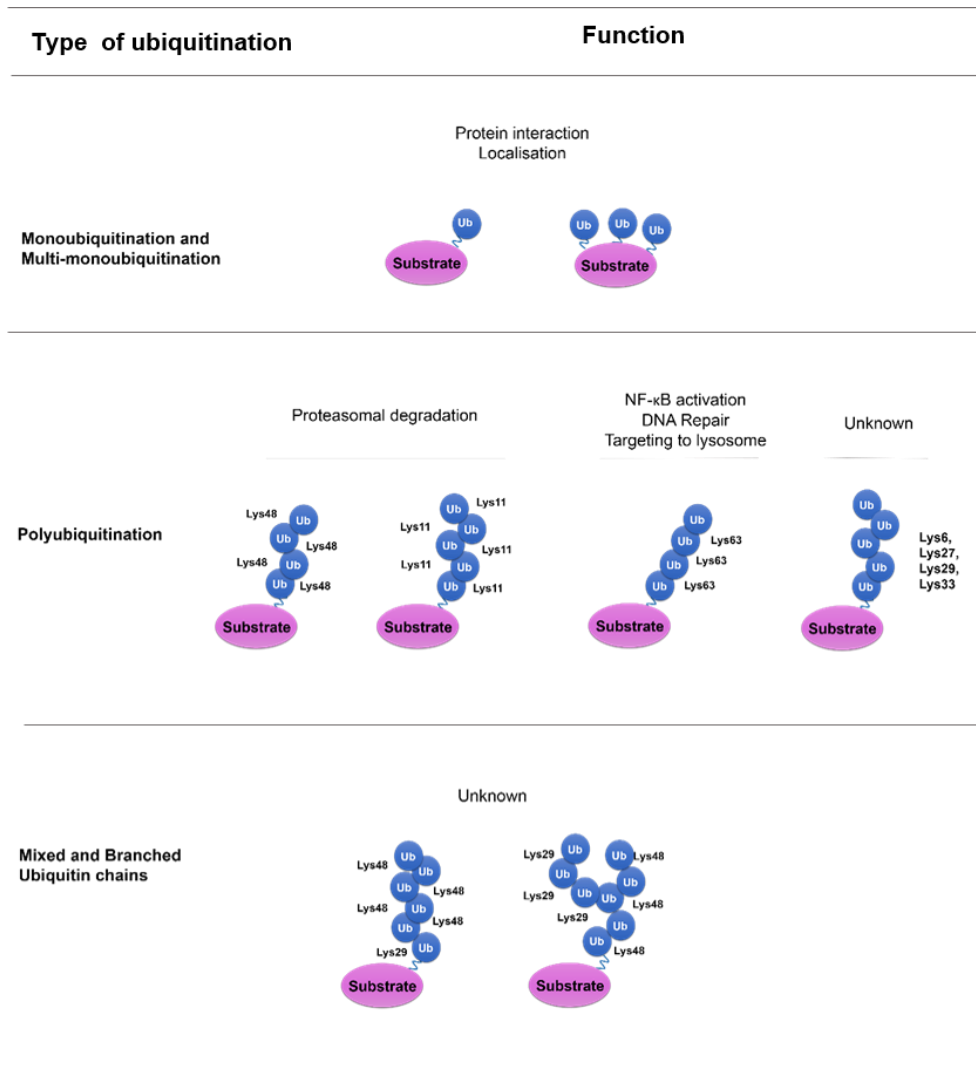


Figure 1. 14 Ubiquitin linkages

A single Ubiquitin (Ub) moiety can be attached to the ϵ -amino group of lysine substrate at one or multiple sites yielding monoubiquitination or multi- monoubiquitination respectively. Ubiquitin also has seven lysine residues (Lys6, Lys11, Lys27, Lys29, Lys33, Lys48 and Lys63) which act as receptors for the conjugation of further ubiquitin moieties in the assembly of polyubiquitin chains. Branched ubiquitin chains can also form when two ubiquitin moieties are attached to different lysine residues of a ubiquitin that is already linked to a substrate protein. Adapted from (Ye and Rape, 2009).

1.3.2 Stimulus Induced I κ B degradation

Following the initial discovery of the I κ Bs, significant interest in elucidating the inhibitory mechanism and function of these proteins ensued. Understanding how NF- κ B was liberated from I κ B association was an obvious goal and an early breakthrough occurred when phosphorylation was identified as a key step in this regulation. Ghosh *et al.* reported that the addition of kinases *in vitro* could dissociate NF- κ B:I κ B complexes (Ghosh and Baltimore, 1990). Subsequent studies demonstrated that a critical step of stimulus-dependent NF- κ B induction *in vivo* involved the phosphorylation of I κ B α and that this was a prerequisite for NF- κ B activation (Brown *et al.*, 1993, Beg *et al.*, 1993, Naumann and Scheidereit, 1994). Serines 32 and 36 of I κ B α were identified as essential phosphorylation sites, later established to be mediated by the IKK complex (Brockman *et al.*, 1995, Brown *et al.*, 1995). Interestingly phosphorylation alone was found to be insufficient for activation and nuclear translocation of NF- κ B (DiDonato *et al.*, 1995, Miyamoto *et al.*, 1994, Alkalay *et al.*, 1995a, Finco *et al.*, 1994). A second step, involving I κ B α stimulus-dependent proteasomal degradation facilitated by β -TrCP, is required for NF- κ B activation (Alkalay *et al.*, 1995b, Chen *et al.*, 1995, Yaron *et al.*, 1998, Winston *et al.*, 1999, Spencer *et al.*, 1999).

β -TrCP is a part of a larger family of F-box/WD40 repeat containing proteins, (Fbw) characterised by the presence of a 42-48 amino-acid F-box motif at the N-terminus and seven WD40 repeats at the C-terminus. These F-box proteins serve as the substrate recognition subunits of a larger SCF ubiquitin ligase complex, a member of the cullin-RING ligases. Substrates recognised by the β -TrCp complex contain a characteristic degron motif in which modification of target serines by phosphorylation serve to rapidly distinguish the inducible degron motif from the non-modified sequence (Figure 1.7) (Kanarek and Ben-Neriah, 2012, Fuchs *et al.*, 0000). Following Lys 48-linked ubiquitination, I κ B α is targeted for degradation by proteasome. Liberated NF- κ B dimers are then free to translocate to the nucleus where they can bind to target promoters and activate transcription.

While I κ B degradation presents a sensitive system for a rapid response to a pathogen or harmful stimuli, prolonged NF- κ B activation is potentially detrimental to the host. The I κ Bs function to not only provide inducibility to NF- κ B activity but also to prevent extended inflammatory gene expression. I κ B α

transcription itself is regulated by NF- κ B and thus is rapidly replenished following degradation. Newly synthesised I κ B α enters the nucleus where it dissociates DNA bound NF- κ B providing an effective negative feedback system to limit NF- κ B dependent gene expression following a stimulus. Like I κ B α , all classical I κ Bs are targeted for ubiquitination by β -TrCP following stimulus-dependent phosphorylation but the kinetics of degradation vary significantly between I κ Bs (Hinz et al., 2012). For example, following LPS stimulation in Jurkat cells, I κ B α is degraded in less than 15 minutes whereas I κ B ϵ degradation takes 60-90 minutes (Kanarek and Ben-Neriah, 2012). In addition to different degradation kinetics, resynthesis of I κ B β and I κ B ϵ is also delayed compared to I κ B α . Combined experimental and computational modelling demonstrated that I κ B α , I κ B β and I κ B ϵ each have distinct roles that coordinate for temporal-regulation of NF- κ B activity (O'Dea and Hoffmann, 2010). Due to stimulus-induced rapid resynthesis, I κ B α provides strong negative feedback of the initial NF- κ B response whereas I κ B β and I κ B ϵ function to control NF- κ B at later time points (Hoffmann et al., 2002).

1.3.3 Processing of NF- κ B p105 to p50

Targeting to the proteasome normally results in complete degradation of a protein but in remarkably rare cases, partial proteolysis by the proteasome can yield biologically active protein fragments (Glickman and Ciechanover, 2002, Rape and Jentsch, 2002). This partial proteolysis or processing is responsible for the generation of the p50 and p52 subunits from the p105 and p100 precursors respectively. Ubiquitination of NF- κ B precursors therefore presents a twofold mode of NF- κ B regulation; complete degradation liberates sequestered NF- κ B dimers from inhibition and processing yields the mature NF- κ B subunits which can homo- or hetero-dimerise with other members of the rel family.

Although several models of this proteasomal protein processing have been suggested, the exact mechanism is still unclear (Rape and Jentsch, 2002, Lin and Ghosh, 1996, Orian et al., 1999). p105 contains a glycine-rich region (GRR) between the RHD and the ankyrin repeats which is essential for constitutive processing of p105 (Figure 1.2) (Lin and Ghosh, 1996). It has been proposed that p105 is degraded from its C-terminal until the proteasome encounters the GRR, which acts as a stop signal preventing p50 degradation (Orian et al., 1999).

Ubiquitination is essential for both proteasomal processing and complete proteolysis of p105 but these may be regulated by independent mechanisms (Orian et al., 1995, Cohen et al., 2004). p105 is constitutively processed to p50 in resting cells however following certain stimuli, p105 can also be targeted for complete degradation by the proteasome (Kanarek et al., 2010). Similar to the classical I κ B proteins, stimulus-induced phosphorylation, targets p105 for ubiquitination via β -TrCp (Cohen et al., 2004). β -TrCp mediated ubiquitination is dependent on IKK phosphorylation on serines 927 and 932 and triggers complete proteolysis of p105 by the proteasome (Figure 1.7) (Lang et al., 2003). In some cases, IKK phosphorylation may also induce the processing of p105 to p50 but this independent of β -TrCp and likely occurs by another currently unidentified ubiquitin ligase (Beinke and Ley, 2004, Orian et al., 2000, Heissmeyer et al., 2001).

In addition to post-translational processing from p105, it has also been proposed that p50 may be generated constitutively by a co-translational mechanism which is also dependent on the proteasome but not on ubiquitination (Lin et al., 1998, Lin et al., 2000). In this mechanism p50 is generated during translation of the *Nfkb1* gene allowing the production of both p50 and p105 from the same mRNA which may be the source of p50 in unstimulated cells (Perkins, 2007, Chen, 2005).

1.3.4 Bcl-3 Inhibits p50 Ubiquitination

Aberrant or deregulated TLR signalling can be detrimental to the host, resulting in inappropriate tissue damage and a variety of pathological conditions including autoimmunity and in severe cases septic shock. Although the rapid induction of NF- κ B target genes is fundamental in mounting an effective innate immune response, NF- κ B activity must be tightly regulated in order to limit the magnitude and duration of TLR-mediated inflammation. In LPS tolerance for example, it has been shown that TLR-induced genes with diverse biological functions can be regulated differently following the same stimulus. NF- κ B dependent pro-inflammatory genes that could cause excessive tissue damage if continually expressed are transiently silenced following repeated LPS

stimulation whereas NF- κ B regulated genes encoding antimicrobial effectors that are essential for the early defence from infection remain inducible (Medvedev et al., 2000).

In addition to gene-specific regulation, NF- κ B activity is also intrinsically regulated with individual subunits having overlapping and distinct biological functions. p50 homodimers lack inherent transactivating potential and their role as transcriptional repressors of pro-inflammatory gene expression has been firmly established. Loss of p105 and consequently p50 impairs innate and adaptive immune function and *Nfkb1*^{-/-} mice exhibit multifocal defects in immune responses (Kastenbauer and Ziegler-Heitbrock, 1999, Dennis et al., 2008, Bohuslav et al., 1998, Wessells et al., 2004, Oakley et al., 2005, Elsharkawy et al., 2010, Panzer et al., 2009, Cao et al., 2006, Sha et al., 1995). Interestingly, a study by Cheng *et.al* demonstrated that a significant number of p50 homodimers are present in the nuclei of unstimulated macrophage, indicating that in addition to regulating inducible transcription, p50 may also play a critical role in controlling the basal expression of NF- κ B target genes. Interestingly, this paper also showed a role for p50 homodimers in regulating IRF mediated transcription by binding to interferon responsive elements (IRE) in interferon inducible gene promoters.

Previous studies have shown that Bcl-3 is an essential regulator of p50 homodimers and is required to limit NF- κ B transcriptional activity in a number of essential immune cells (Carmody et al., 2007b). Bcl-3 inhibits the ubiquitination and degradation of p50 homodimers thereby promoting a stable, p50 homodimer:DNA complex. In the absence of Bcl-3, the half-life and DNA binding of p50 is dramatically reduced. As a result, the promoter occupancy in both resting and stimulated *Bcl3*^{-/-} macrophage is significantly altered. Chromatin immunoprecipitation (ChIP) analysis demonstrated that p50 and not p65 or c-Rel was present on the TNF promoter in unstimulated, wild-type macrophages and upon LPS stimulation p50 was transiently replaced by c-Rel and p65 containing dimers. In contrast, c-Rel and p65 were found to constitutively occupy the TNF and CXCL2 (chemokine C-X-C motif ligand 2) promoters in unstimulated *Bcl3*^{-/-} macrophages. Furthermore, the order of the dimer exchange on both promoters was also disrupted following LPS. Recent studies have shown that NF- κ B chromatin interactions are highly dynamic, occurring in a matter of seconds and exchange of dimers at the same promoter

can regulate NF- κ B dependent transcription. By preventing p50 ubiquitination, Bcl-3 stabilises promoter bound p50 and thus in the absence of Bcl-3, an increased occupancy time of p65 and c-Rel containing dimers results in greater transcriptional output. Consequently, macrophages, dendritic cells and B cells deficient in Bcl-3 are hyper responsive to TLR stimulation and produce significantly more cytokines than wild-type cells.

An essential role for proteasome degradation in the control of NF- κ B dependent gene activity has already been established for p65. p65 polyubiquitination and degradation is required for posttranscriptional repression of the NF- κ B response. A mutant of p65 that exhibits impaired signal-induced proteasomal degradation can reside on the promoters of NF- κ B target genes for a longer period of time than the wild-type protein (Bosisio et al., 2006, Sacconi et al., 2004). Furthermore, inhibiting USP7, a p65 deubiquitinase, inhibits recruitment of p65 to the interleukin (IL)-6 and TNF promoters and consequently cytokine gene expression (Colleran et al., 2013). As with p65, DNA binding also triggers p50 polyubiquitination thereby representing a critical mechanism in controlling nuclear NF- κ B turnover and removal from specific promoters. Unlike p65 however, the mechanisms regulating p50 ubiquitination and its function in TLR signalling are poorly understood and many questions are still outstanding.

1.4 Thesis Aims

The molecular basis for the inhibition of p50 ubiquitination by Bcl-3 is unknown. The exact nature of the interaction between Bcl-3 and p50 has not been experimentally explored and it is not evident whether interaction with p50 is necessary for Bcl-3 mediated inhibition of cytokine expression or if other binding partners of Bcl-3 are also important. In addition to the NF- κ B subunits, Bcl-3 interacts with a number of regulators of transcription including -Jun and c-fos (Na et al., 1999), STAT1 (Jamaluddin et al., 2005), PPAR γ (Yang et al., 2009), CBP/p300 (Na et al., 1999), HDAC-1, -3 and -5 (Viatour et al., 2004), steroid receptor coactivator-1 (Na et al., 1999), TORC3 (Hishiki et al., 2007), retinoic X receptor (RXR) (Na et al., 1998), Fyn (Weyrich et al., 1998) and Lck (Zhao et al., 2005), insulin receptor substrate 3 (IRS3)(Kabuta et al., 2010) and Bag-1 (Southern et al., 2012). To investigate this, we employed an immobilised peptide array approach to identify key regions of p50 critical for interaction with Bcl-3 as illustrated in chapter 3. This allowed us to generate a mutant of p50 incapable of interaction with Bcl-3 thereby enabling us to investigate the role of p50-Bcl-3 interaction in Bcl-3-mediated inhibition of p50 ubiquitination and repression of NF- κ B target gene expression.

As Bcl-3 is a critical negative regulation of TLR and TNFR induced gene expression, the second aim of this thesis was to investigate the potential of Bcl-3 derived peptides as modulators of TLR signalling. We postulated that interaction with p50 mediated Bcl-3's inhibitory activity. In chapter 4, we aimed to identify the minimal regions of Bcl-3 sufficient for interaction with p50 and from this design short peptides capable of mediating Bcl-3 function.

Bcl3^{-/-} mice and cells are hyper responsive to TLR and TNFR stimulation are defective in LPS tolerance. TLR stimulated NF- κ B and MAPK signalling results in the production of IFNs, pro-inflammatory and effector cytokines which activate the innate immune response. As described in chapter 5, the final aim of this thesis, was to further study the role of Bcl-3 in inflammation and explore the possibility of NF- κ B independent functions of Bcl-3 during TLR signalling, specifically investigating MAPK signalling in the absence of *Bcl3*.

—— Chapter Two ——

2 Materials and Methods

2.1 MATERIALS

2.1.1 Antibodies

Table 3. Primary Antibodies

Antibody and clone	Cat #	Supplier
B-Actin(ac-15)	A5441	Sigma Aldrich
Bcl-3	39761	Active Motif
c-Jun(60A8)	9165	Cell Signalling
Phospho-c-Jun (Ser63) II	9261	Cell Signalling
c-Myc (9E10)	sc-40	Santa Cruz
FLAG M2	F1804	Sigma Aldrich
Glutathione-S-Transferase	G7781	Sigma Aldrich
HA (12CA5)	11583816001	Roche
HDAC (H-51)	sc-7872	Santa Cruz
IκBα (44D4)	4812	Cell Signalling
Phospho - IκBα (Ser32/36) (5A5)	9246	Cell Signalling
MEK1/2 (L38C12)	4694	Cell Signalling
Phospho-MEK1/2 (Ser217/221)	9121	Cell Signalling
NF-κB p50 (C-19)	sc-1190	Santa Cruz
NF-κB p50	ADI-KAP-TF112	Enzo
NF-κB p105/p50(phospho S927)	ab60936	Abcam
NF-κB p65 (C-20)	sc-372	Santa Cruz
p38 MAPK Antibody	9212	Cell Signalling
Phospho-p38 MAPK (Thr180/Tyr182)	9211	Cell Signalling
p44/42 MAPK(ERK1/2)	9102	Cell Signalling
Phospho-p44/42 MAPK(ERK1/2) (Thr202/Tyr204)	9101	Cell Signalling
Tpl-2- Cot (M20)	sc-720	Santa Cruz
Ubiquitin	VU-1	Teubu Bio
Xpress(XP)	R910-25	Invitrogen

Table 4. Secondary Antibodies

Antibody and clone	Cat #	Supplier
Anti- mouse IgG HRP	NA931	Amersham
Anti-rabbit IgG HRP	NA934	Amersham
Anti-goat IgG-HRP	sc-2768	Sigma Aldrich
DyLight 680 Conjugates Anti-Mouse IgG	35518	Thermo Scientific
DyLight 800 Conjugates Anti-Mouse IgG	35521	Thermo Scientific
DyLight 680 Conjugates Anti-Rabbit IgG	35568	Thermo Scientific
DyLight 800 Conjugates Anti-Rabbit IgG	35571	Thermo Scientific
Clean-Blot IP Detection Kit (HRP)	21230	Thermo Scientific
Alexa Fluor 488 Dye Chicken Anti-Mouse IgG	A2100	Invitrogen

2.1.2 Bcl-3 Peptide Synthesis

Table 5. Peptide Sequences

Peptide	Sequence	Modification	Supplier
BDP	YGRKKRRQRRHIAVVQNNI AAVYRILSLFKLGSREVDV HN	N-terminal FITC	GL Biochem Ltd. (Shangai)
BDP	YGRKKRRQRRHIAVVQNNI AAVYRILSLFKLGSREVDV HN	None	W.M. Keck Biotechnology Resource Lab (Yale)
sBDP	YGRKKRRQRRAAVYRILSL FKLGSR	None	1.W.M. Keck Biotechnology Resource Lab (Yale) 2.Genscript (Hong Kong)
mBDP	YGRKKRRQRRAAAAAILSL FALGSA	None	1.W.M. Keck Biotechnology Resource Lab (Yale) 2.Genscript (Hong Kong)

2.1.3 Plasmid Sources

pGEX-6P1 was kindly provided from the McCaffrey lab, University College Cork, Cork. pcDNA3-Tpl2 and pcDNA3-Tpl2^{D270A} (Rat) constructs were kindly provided by Steven Ley, National Institute for Medical Research, Mill Hill, London. The

Renella luciferase expression vector pRL-TK was purchased from Promega. The pAP1-luc luciferase expression vector which contains multiple copies of the AP1 enhancer was purchased from Clontech. The pLucp19 luciferase expression vector was described previously (Carmody et al., 2007a) but in summary the *p19* promoter containing the genomic fragment -1180 to +110 of the *p19* gene and three putative NF- κ B binding sites was amplified by PCR from C57BL/6 genomic DNA and cloned into the pGL3-basic vector (Promega). All other plasmids used are listed below were from Carmody lab stocks and were cloned using murine cDNAs.

- pRK5-p50-FLAG
- pEF4a-p50-XPRESS
- pRK5-p105-FLAG
- pEF4a-p105-XPRESS
- pEF4a-p50-MYC
- pcDNA3.1-Bcl-3-MYC
- pRK5-Bcl-3-FLAG
- pRK5-p65-FLAG

2.1.4 DNA Sequencing

Plasmid DNA sequencing following site-directed mutagenesis was carried out by GATC-Biotech Ltd. (Germany), using on site primers or primers generated by Eurofins MWG Operon. Sequencing results were analysed using Vector NTI software (Invitrogen).

Table 6. Sequencing Primers

Vector	Forward	Reverse	Vector	Forward	Reverse
pRK5-FLAG	SP6	SV40	pEF4-Xpress	T7	BGH
pcDNA 3.1-Myc	T7	SP6	pEF4-Myc	T7	BGH

2.1.5 Mice

Bcl3^{-/-} C57BL/6 mice were generated as described previously described (Carmody et al., 2007b). *Bcl3*^{-/-} C57BL/6 male mice were generously provided by Professor Y. Chen (University of Pennsylvania, Philadelphia, Pennsylvania, USA). Wild-type (WT) C57BL/6 mice were purchased from Harlan laboratories, UK at 6 - 8 weeks of age. Establishment of homozygous breeding was carried out by Doctor Christine O'Carroll (University College Cork, Cork, Ireland). Animal husbandry and experimental procedures were approved by the University College Cork Animal Experimentation Ethics Committee (AEEC).

2.1.6 Reagents

All general salts and chemicals were purchased from Sigma Aldrich UK unless otherwise stated. Specific biochemicals and concentrations used are indicated in Table 7 and described in detail in the appropriate figure legends.

Table 7. List of Biochemicals

Biochemical	Concentration used	Supplier
Lipopolysaccharides from Escherichia coli 055:B5	10ng/ml for BMDM 100ng/ml RAW 264.7	Sigma Aldrich
TNF (recombinant mouse)	10-20ng/ml	eBioscience or Miltenyi Biotec
Leptomycin B	20nM	Santa Cruz
MG132 (Z-Leu-Leu-Leu-al)	20µM	Sigma Aldrich
Cyclohexamide	100µg/ml	Sigma Aldrich

2.1.7 Buffer Composition

Table 8. Agarose Gel Electrophoresis Buffers

6X Gel Loading buffer	5xTris/Borate/EDTA (TBE)
0.4% orange G 40% sucrose	450mM Tris-borate 10mM Ethylenediaminetetraacetic acid

Table 9. EMSA Buffers

EMSA buffer	5% Non-denaturing Polyacrylamide Gel
10mM HEPESKOH (pH7.9) 50mM KCl 2.5mM MgCl ₂ 1mM Dithiothreitol (DTT) 10% Ficoll 1.2µg Bovine serum albumin 3.6 µg poly[d(I-C)] (Roche Applied Science)	16.6 ml of 30% polyacrylamide solution 10 ml of 5X TBE 72.3 ml ddH ₂ O 100µl N,N,N',N'-Tetramethylethylene-diamine 1 ml Ammonium persulphate (10%)

Table 10. Luciferase Assay Buffers

Firefly luciferase buffer	Renilla luciferase buffer
25mM Glycylglycine 15mM Dipotassium phosphate pH 8, 4mM Ethylenediaminetetraacetic acid 15mM Magnesium sulphate 75µM Luciferin 1mM Dithiothreitol (DTT) 0.1mM Co-Enzyme A 2mM ATP	1.1M Sodium chloride 2.2mM EDTA 220mM K ₂ PO ₄ pH5.1 0.44mg/ml bovine serum albumin, 1.3mM Sodium Azide 1.43µM Coelenterazine

Table 11. Lysis Buffers

Pull Down Lysis and Binding Buffer	Radioimmunoprecipitation assay (RIPA)
20mM Tris-Cl pH8.0 200mM NaCl 1mM EDTA pH8.0 0.5 % NP-40 1mM PMSF* 2µg/ml aprotinin* 1µg/ml pepstatin*	50mM Tris-HCL pH7.4 1% NP-40 0.25% deoxycholate 150mM NaCl, 1mM EDTA 1mM PMSF* 1mM NaF* 1mM Na ₃ VO ₄ * 2µg/ml aprotinin* 1µg/ml pepstatin* 2µg/ml leupeptin*

Notes: *Proteinase and phosphatase inhibitors added fresh on day of use

Table 12. Glutathione S-transferases (GST) Protein Purification

Lysis/ Binding Buffer	Wash Buffer	Elution Buffer
50mM Tris pH8.5 150mM NaCl 1mM DTT*	50mM Tris pH8.5 500mM NaCl 1mM DTT*	150mM Tris pH8.5 150mM NaCl 10mM Glutathione

*Notes: Lysis/binding buffer adjusted pH to 8.5 and wash buffer to pH 7.5 (dependant on the Isoelectric point (pI) of purified protein - pH cannot be similar to protein pI). Buffers prepared day before use. *DTT added on day of use*

Table 13. Column Regeneration Buffers

Glutathione Regeneration Buffer 1	Glutathione Regeneration Buffer 2
0.1M Tris-HCl 0.5M NaCl Filtered - pH8.5	0.1M Sodium Acetate 0.5M NaCl Filtered - pH4.5

Table 14. Kinase Assay Buffer

MEK Kinase Assay Buffer
50mM Tris pH7.5 150mM NaCl 5mM β -glycerophosphate 2mM DTT 0.1mM Sodium vanadate 10mM $MgCl_2$ 1mM ethylene glycol tetraacetic acid 0.01% Brij-35

Table 15. Electrophoresis Buffers for Western Blotting

1X Tris-glycine Running Buffer	1X Tris-glycine Transfer Buffer
25mM Tris 250mM glycine 0.1% SDS (Electrophoresis grade reagents)	48mM Tris Base 39mM glycine 0.0375% SDS 20% methanol (Electrophoresis grade reagents)

Table 16. SDS PAGE Sample Buffer

2X SDS Sample Buffer
100mM Tris-Cl(pH6.8)
4% (w/v) SDS
0.2% (w/v) bromophenol blue
20% (w/v) glycerol
200mM β -mercaptoethanol

Table 17. Tris-glycine SDS-Polyacrylamide Gels

Gel	5% Stacking	8% Resolving	10% Resolving
Volume	1ml	5ml	5ml
H₂O	0.68	2.3	1.9
30% acrylamide	0.17	1.3	1.7
1.0M Tris(pH6.8)	0.13	-	-
1.5M Tris(pH8.8)	-	1.3	1.3
10%SDS	0.01	0.05	0.05
10% ammoniumpersulfate	0.01	0.05	0.05
TEMED	0.001	0.003	0.002

Table 18. Media

Super optimal broth (SOB) 1L	SOB with catabolite repression (SOC)
20g Tryptone 5g Yeast Extract 0.5g NaCl 10ml 250mM KCl pH 7.0 -Autoclave -Add 5ml sterile 2M MgCl ₂ prior to use	SOC is identical SOB with the addition of 20mM glucose. -Allow autoclaved SOB to cool to 60°C. -Add 20 mL of sterile 1M glucose

2.2 METHODS

2.2.1 Cell Culture

2.2.1.1 Maintenance

Human embryonic kidney 293T (HEK293T) and RAW 264.7 cells were cultured in high glucose Dulbecco's Modified Eagle Medium (DMEM) (Sigma) containing 10% Fetal Bovine Serum (FBS)(Gibco), 2mM glutamine (Sigma), and 100U/ml penicillin/ streptomycin (Sigma). NIH 3T3 and *Nfkb1*^{-/-}MEF cells were cultured in DMEM containing 10% Iron Fortified Bovine Calf Serum (BCS)(Sigma), 2mM glutamine, and 100U/ml penicillin/streptomycin. p105^{WT} and p105^{RKR} MEFs cells were cultured in DMEM containing 10% Iron Fortified Bovine Calf Serum, 2mM glutamine, 100U/ml penicillin/streptomycin and 200µg/ml Zeocin. All cells were maintained at 37°C in a humidified environment with 5% CO₂. Cells were subcultured three times per week following mechanical (RAW 264.7) or enzymatic detachment (HEK293T, NIHMEF, *Nfkb1*^{-/-}MEF, p105^{WT} and p105^{RKR} MEF) with 0.05% Trypsin-EDTA solution (Gibco).

2.2.1.2 Stable Cell Line Generation

2.2.1.2.1 Determining Zeocin sensitivity

The minimal concentration of Zeocin (Invivogen) required to kill the untransfected parental cell line was determined by generating a kill curve. Cells were plated at 25% confluency grown for 24 hours. Media was removed and replaced with fresh media containing varying concentrations of Zeocin from 0µg/ml-1000µg/ml. Selective media was replenished every 3-4 days and the percentage of surviving cells was monitored over time. The concentration of Zeocin that killed all cells within the desired time (1-2 weeks) was determined to be 200µg/ml.

2.2.1.2.2 Stable transfection

7µg of pEF4-p105-XP and pEF4-p105^{RKR}-XP constructs were linearised with PvuI restriction enzyme (New England Biolabs [NEB]). Plasmid were linearised to decrease the likelihood of the vector integrating into the genome in a way that disrupted the gene of interest. DNA was purified with Qiaquick PCR purification

kit and eluted in 30 μ l. *Nfkb1*^{-/-}MEF (7×10^5 /10cm dish) were transfected with purified plasmid (20 μ l) using 15 μ l Attratene (Qiagen) according to manufacturer's instructions. 48 hours post transfection cells were trypsinised, diluted 1/4 in a 10cm dish and subjected to selection pressure with 200 μ g/ml Zeocin. To confirm transient transfection, whole cell lysates were prepared of the remaining cells and analysed by western blot with anti-Xpress for p105^{WT} and p105^{RKR} expression.

Media containing 200 μ g/ml Zeocin (selective media) was replenished every 3-4 days until all negative control cells (untransfected) were dead ~13 days. In order to clonally select stable transfectants, serial dilutions of trypsinised cultures were generated in 96-well plates. Whole cell lysates were prepared of the remaining cells and analysed by western blot with anti-p50 to confirm stable transfection of mixed population. Selective media was replenished every 3-4 days until colonies were visible. As Zeocin is not effective when cells are at confluency, depending on size, single colonies were transferred (following trypsinisation) to a new well of 96- or 24-well plate. Selective media was replenished every 3-4 until cells were near confluency. Negative or low expressing clones were discarded and positive clones were expanded and cryopreserved.

2.2.1.3 Bone Marrow Derived Macrophage

2.2.1.3.1 Bone marrow isolation

Bone marrow was isolated from C57BL6/J mice at 8-12 weeks old for generation of primary bone marrow derived macrophages (BMDM) *in vitro*. Mice were sacrificed by Co2 asphyxiation and cervical dislocation. Hind legs were removed at the hip joint and excess tissue removed from the femur and tibia bones. In sterile culture, bones were cleaned in sterile phosphate buffered saline (PBS) (Gibco) and 70% ethanol. Bones were then cut at each extremity and flushed with cold PBS using a 21 gauge needle and syringe. Isolated bone marrow was collected in sterile PBS and re-suspended to generate a single cell suspension. Debris was removed by passing bone marrow suspension through a 70 μ m cell strainer. The bone marrow suspension was washed twice in BMDM culture media (DMEM, 10% FBS, 1% penicillin/streptomycin, 1% L-Glutamine) and centrifuged

at 4°C at 300 x g for 5 minutes. Bone marrow was typically pooled from three mice.

2.2.1.3.2 BMDM Differentiation and stimulation experiments

Following isolation or recovery from cryopreservation, bone marrow was cultured in BMDM culture media supplemented with 30% L929 conditioned media (BMDM differentiation media) in sterile untreated petri dishes, for seven days. Differentiation media was replaced on day 3 and any non-adherent cells were removed. By day 7 adherent monocytes/macrophage progenitors were differentiated into BMDMs. BMDMs were removed from petri dishes by incubating with 5mM EDTA in sterile PBS at 37°C for 5 minutes. Cells were washed twice in BMDM culture media at 4°C for 5 minutes at 300 x g. Cells were re-suspended in BMDM culture media with no L929 supplement and replated overnight in tissue culture treated dishes for subsequent experiments. For LPS stimulation experiments, LPS was added in a step-wise fashion and all were samples harvested at the same time at the experiment endpoint.

2.2.2 Protein Methodologies

2.2.2.1 Protein Extraction

2.2.2.1.1 Non denaturing whole cell extracts

Cell culture media was aspirated and tissue culture plates gently washed with 4°C PBS. Cells were detached with 4°C PBS Cells and pelleted at 11,000g for 45 seconds. Pellets were re-suspended in 20-200µl radioimmunoprecipitation assay (RIPA) buffer (

Table 11). Re-suspended pellets were incubated on ice for 30 minutes and vortexed every 5 minutes. Lysate was cleared by centrifugation at 16,000g for 10 mins at 4°C. Supernatants were collected and analysed immediately or stored at -20 °C or -80 °C for long term storage.

2.2.2.1.2 Denaturing whole cell extracts

Cells were incubated with 10mM n-ethylmaleimide (NEM) for 30 seconds before cells before harvested. Cell culture media was aspirated and tissue culture plates gently washed with 4°C PBS containing 10mM NEM. Cells were detached

with 4°C PBS containing 10mM NEM and pelleted at 11,000g for 45 seconds. Pellets were re-suspended in 100µl 1%SDS and boiled for 5 minutes at 95°C. Cell pellet was disrupted by sonication for 5-15 seconds (30% amplitude and 50% duty cycle) using a Bandelin SONOPULS ultrasonic homogeniser HD 2070 with the MS 73 microtip. Lysate was cleared by centrifugation at 16,000g for 10 mins at 4°C. Supernatants were collected and analysed immediately or stored at -20 °C or -80 °C.

2.2.2.1.3 Nuclear /Cytoplasmic Extracts

Nuclear and cytoplasmic extractions were carried out using Active Motif nuclear extract kit according to manufacturer's instructions with one deviation. For 10cm dish, cytoplasmic fractions were extracted in 200µl of lysis buffer and nuclear fractions extracted in 20µl of lysis buffer.

2.2.2.2 *Quantification*

Whole cell, cytoplasmic and nuclear protein extracts were quantified by Bradford assay. 1µl of cellular extract was diluted in 1ml 1X Bradford assay reagent (Bio-Rad). Samples were assayed in triplicate using a spectrophotometric 96-well plate reader and absorbance measured at 595nm. A 6 point standard curve between 0-9ug/ml of bovine serum albumin was generated to determine unknown protein concentrations.

2.2.2.3 *Western Blotting*

Protein preparations were separated by denaturing sodium dodecyl sulphate (SDS) polyacrylamide gel electrophoresis (PAGE) using the Mini-PROTEAN Tetra Cell system (Bio-Rad). Cellular extracts diluted in 2X or 5X SDS sample buffer were routinely resolved using 10% acrylamide gels and immunoprecipitated proteins were resolved using 10% acrylamide gels for interaction studies and 8% acrylamide gels for ubiquitination assays (**Table 17**). Gels were run at 100-120V for 90-120 minutes in 1X Tris-glycine Running Buffer (**Table 15**). Resolved proteins were transferred to Amersham Hybond ECL Nitrocellulose Membrane (GE Healthcare) using the Mini Trans-Blot Electrophoretic Transfer system (Bio-Rad) and 1X Tris-glycine Transfer Buffer (**Table 15**). Nitrocellulose membranes

were incubated in a 5% non-fat milk (Marvel)/PBS-T solution to block nonspecific binding to the membrane. For endogenous ubiquitination assays, nitrocellulose membranes were incubated in 0.5% glutaraldehyde/PBS pH 7.0 for 20 min and washed in PBS-T three times prior to blocking.

Nitrocellulose membranes were then probed with primary antibodies in either 5% milk/PBS-T or 5% BSA/PBS-T overnight at 4°C or 1-2 hours at room temperature and secondary antibodies in 5% milk/PBS-T for 1 hour at room temperature. Three 5-minute washes in PBS-T were performed after each antibody incubation.

The method used to detect bound protein was dependent on the type of secondary antibody used (HRP-conjugated or Dylight 680 or 800-conjugated). For HRP-conjugated secondary antibodies, bound protein was detected with SuperSignal West Pico Chemiluminescent Substrate (Thermo Scientific) or WesternBright ECL chemiluminescent HRP substrate (Advansta). Lowly abundant proteins were detected with higher sensitivity ECL substrates, SuperSignal West Femto Chemiluminescent Substrate (Thermo Scientific) or WesternBright Sirius chemiluminescent HRP substrate (Advansta). For Dylight-conjugated secondary antibodies, membranes were scanned using the LI-COR Odyssey infrared scanner.

In the case of multiple antibody reprobes for proteins of similar or identical sizes, membranes were stripped using a commercially available stripping buffer, Restore Western Blot Stripping Buffer (Thermo Scientific) as per instructions. For clarity, Western blots are presented as cropped images throughout this thesis, however an example of a full length Western Blot for individual assays are available in Appendix 7.12.

2.2.3 Functional Assays

2.2.3.1 EMSA

IR-800 dye (DY782) labelled NF- κ B consensus double stranded oligonucleotides 5'AGTTGAGGGGACTTTCCCAGGC-3', 3'TCAACTCCCCTGAAAGGGTCCG5' were purchased from Eurofins MWG Operon. Binding reactions were prepared with EMSA buffer (*Table 9*) containing 5 μ g of nuclear extract and 10ng oligonucleotides in a 30 μ l reaction volume and incubated at room temperature

for 15 mins. Binding reactions were resolved on a 5% non-denaturing polyacrylamide gel (**Table 9**) at 300V at 4°C in 0.5x TBE (**Table 8**). Gels were visualised using LI-COR odyssey. All EMSAs were carried out with nuclear extracts from HEK293T transiently transfected with p50 or p50 mutant expression constructs. As a negative control, a DNA binding defective p50 mutant in which critical residues for DNA binding, Y57 and D60 were mutated to alanine and aspartic acid respectively (p50^{Y57A, D60E}) was included. Cropped EMSAs are presents throughout figures, see Appendix 7, Figure 7.5 for an example of a full EMSA image.

2.2.3.2 GST Pull-down Assay

HEK293T cells were transiently transfected with p50^{WT}- FLAG or p50^{RKR}- FLAG. Whole cells lysates were extracted from cells resuspended in Pull-down lysis and binding buffer. Equal concentrations of lysates were precleared in 1ml of Pull-down lysis and binding buffer (

Table 11) with 50µl GSH-agarose (Sigma) for 2 hours rotating at 4°C. GST or GST-Bcl-3 were incubated with precleared lysates and were affinity purified with 50µl GSH-agarose for 2 hours rotating at 4°C. Following wash steps, pull down complexes were eluted from the beads with 2X SDS sample buffer and analysed by western blot.

2.2.3.3 Immunoprecipitation

Following transient transfection whole cell lystates were prepared as per 2.2.2.1.1 from 6cm or 10cm dishes (see Table 22). Equivalent concentrations of lysates were re-suspended in a total of 1ml of RIPA. Samples were pre-cleared with 20µl of a 50% slurry of protein G agarose/salmon sperm DNA (Millipore) for 30 minutes rotating at 4°C. The pre-cleared lysate was removed from the agarose beads following centrifugation at 14,000g for 2 minutes. 20µl of fresh protein G agarose beads were added to the pre-cleared lysate and immunoprecipitated with 1-5µl primary antibody (anti-FLAG and anti-XPRESS:1µl or anti-MYC:3µl) overnight at 4°C rotating. Beads were pelleted at 11,000g for 10 seconds, the supernatant was discarded and beads were washed in 1ml of RIPA buffer by inverting 10 times. Wash step was repeated twice. To

elute immunoprecipitates, beads were resuspended in 20-40µl 2X SDS sample buffer and boiled for 5 minutes at 95 °C . Samples were vortexed for 10 seconds and eluates removed from the beads following centrifugation at 16,000g for 2 minutes. Eluates were stored short term at -20 °C or analysed immediately by western blot (see section 2.2.2.3). For endogenous immunoprecipitation of p50 from p105 and p105^{RKR} MEFS, assays were carried out as above using 3 x 10cm dishes (1.5x10⁶ cells per dish) per sample using 5ul anti-p50 for immunoprecipitation (Enzo).

2.2.3.4 Dual Luciferase Assay

RAW 264.7 and *Nfkb1*^{-/-} MEF were transiently transfected (see Table 22) with the pLucp19 or pAP1-Luc plasmid for 24 hours . Cotransfection of the *Renella*-luciferase expression vector pRL-TK (Promega) was used as an internal control for all reporter assay. If additional plasmids were required, the total plamid concentration was kept constant between samples with the addition of an empty expression vector. Cells were then cultured with or without 100 ng/ml LPS (Sigma) or 20ng/ml TNF (eBiosciences) for an additional 8 hours before harvest. Cells were washed once with 4 °C PBS and either lysed immediately in 100µl 1x passive lysis buffer (Promega) in the plate or plates were stored at -80 °C following the addition of 100µl 1x passive lysis buffer. 10µl of fresh or thawed lysate was added to 50µl of firefly luciferase assay buffer (**Table 10**) and a 10 second measurement was performed on a GloMax 20/20 luminometer to determine the luciferase activity. 50µl of *Renella* assay buffer (**Table 10**) was added and *Renella* luciferase activity measured as previous. For all samples the firefly luciferase activity was divided by that of the *Renella* luciferase activity to normalise for the transfection efficiency as previously described (Dyer et al., 2000).

2.2.3.5 MEK Kinase Assay

Tpl-2-MYC was immunoprecipitated as described in section 2.2.3.3. Essentially, whole cell lysates were prepared from 293T cells transfected with 1µg pcDNA3-Tpl-2-MYC in the presence or absence of 1µg pRK5-Bcl-3-FLAG. Equivalent concentrations of lysates were re-suspended in a total of 1ml of RIPA. Samples were pre-cleared as in section 2.2.3.3. The pre-cleared lysate was removed

from the agarose beads following centrifugation at 14,000g for 2 minutes. 20µl of fresh protein G agarose beads were added to the pre-cleared lysate and immunoprecipitated with 3µl anti-MYC rotating overnight at 4°C. Beads were pelleted at 11,000g for 10 seconds, the supernatant was discarded and beads were washed in 1ml of RIPA buffer (

Table 11) by inverting 10 times. Wash step was repeated twice. Beads were then washed twice in 1ml MEK kinase assay buffer (*Table 14*). Beads were incubated at 30°C with occasional agitation for 15 minutes in 20µl of MEK kinase assay buffer containing 1µg recombinant inactive MEK1 20µl (Millipore) and 2mM adenosine triphosphate (ATP). Beads were pelleted at 11,000g for 10 seconds and the supernatant was removed, added to 20µl 2X SDS sample buffer and analysed by western blot for phosphorylated MEK. Immunoprecipitates were also eluted from the beads as per section 2.2.3.3 and analysed by western blot.

2.2.3.6 Ubiquitination Assay

Denaturing whole cell lysates were prepared from 6cm or 10cm dishes (see Table 22) as described in section 2.2.2.1.2. Equivalent volumes of lysates were re-suspended in a total of 1ml of RIPA buffer supplemented with 20mM NEM. Samples were pre-cleared and immunoprecipitated overnight as in section 2.2.3.3. Eluates were stored short term at -20°C or analysed immediately by western blot (see section 2.2.2.3). For endogenous p50 ubiquitination assays, assays were carried out as above using 3 x 10cm dishes (1.5×10^6 cells per dish) per sample using 5µl anti-p50 (Enzo). IP samples were resolved by SDS PAGE (8%) and transferred to nitrocellulose membrane. Prior to blocking, nitrocellulose membranes were incubated in 0.5% glutaraldehyde/PBS pH 7.0 solution for 20 min , followed by 3 washes in PBS-T.

2.2.4 Immunofluorescence

NIH3T3 cells were transiently transfected for 24 hours in a 6cm dish (see *Table 22*) before replating 40,000 cells per well in 4-well chamber slide (Lab-Tek, Nunc). 24 hours later, cells were left untreated or treated with 20nM LMB for 2 hours before harvest. Tissue culture media was discarded and slides washed x3 with PST-T. Cells were fixed by the addition of ice cold 1:1 methanol/acetone

solution and incubating at -20°C for 5 minutes. Slides were washed x3 with PST-T. Cells were blocked in 1% BSA/PBS-T for 1 hour. Cells were stained with 1/500 anti-MYC in 1% BSA/PBS-T overnight at 4°C . Slides were washed x5 with PST-T. Cells were stained with 1/800 anti-mouse AF488 secondary antibody 1% BSA/PBS-T at room temperature for 1 hour. Slides were washed x5 with PBS-T. Coverslips were mounted onto slides with vectashield mounting medium with DAPI (Vector Labs).

2.2.5 GST Protein Purification

BL21 Codon Plus cells (provided by McCaffery Lab university College Cork, Cork) were transformed with pGEX6p1, pGEX6p1-p50 or pGEX6p1-Bcl-3 and plated onto LB agar containing $50\mu\text{g/ml}$ ampicillin and chloramphenicol. Plates were incubated overnight at 37°C . A single colony was isolated and incubated overnight in 5ml of L Broth containing $50\mu\text{g/ml}$ ampicillin and chloramphenicol. Cultures were incubated shaking 220-240 rpm at 37°C . 5ml of overnight culture was added to 700ml L Broth containing $50\mu\text{g/ml}$ ampicillin in a Belco flask. Cultures were grown shaking 220-240 rpm at 37°C to an OD_{600} of 1.0-2.0. Before induction, 1ml aliquot was pelleted by centrifugation at 1000g for 5 minutes and resuspended in 1X SDS sample buffer, boiled at 95°C for minutes and stored at -20°C (uninduced). Volume in μl of 1x sample buffer used = $\text{OD}_{600}\times 200$. Cultures were induced with 1mM IPTG (GST, GST-p50) or 0.1mM IPTG (GST-Bcl-3) and incubated overnight shaking 220-240rpm at 20°C . Following induction a 1ml aliquot was prepared as uninduced sample above. Cultures were centrifuged at 4,000g for 15 minutes at 4°C . Pellets were frozen at -20°C .

Pellets were thawed on ice and resuspended in 70ml of cold lysis buffer (**Table 12**) supplemented with two complete, mini, EDTA-free protease inhibitor cocktail tablets (Roche Applied Science). The resuspended pellet was sonicated for 30 minutes with 5 minutes pulses, and 5 minute rest between each pulses (1 hour total run time). Lysates were cleared by centrifugation at 15,000g for 30 minutes at 4°C . $50\mu\text{l}$ of supernatant was added to 50ul 2X SDS sample buffer (**Table 16**) boiled at 95°C for 5 minutes and stored at -20°C (soluble fraction). Pellets were resuspend in 70ml of lysis buffer and an insoluble sample was prepared as soluble fraction above. Subsequent steps were carried out at 4°C . Glutathione agarose (Sigma) in the purification column was equilibrated with

binding buffer (**Table 12**).The cleared supernatant was added to the Glutathione agarose and incubated for 1 hour rocking before passing through the column. Glutathione agarose was washed overnight with 2L of wash buffer adjusted to pH 7.5. Six elutions were performed by incubating the Glutathione agarose with 4ml elution buffer (**Table 12**) and passed through the purification column. Elutions were aliquoted, snap frozen and stored at -80°C. Elutions were analysed by SDS PAGE.

2.2.6 Spot synthesis of Peptides and Overlay Analysis

Spot synthesis of peptides was carried out in collaboration with Dr. Kiely, (University of Limerick, Limerick, Ireland). Peptide libraries of p50 (sequences provided in Appendix 7.1 and 7.2) and Bcl-3 (Appendix 7.5 and 7.6) were generated by automatic SPOT synthesis as previously described (Kramer and Schneider-Mergener, 1998) and synthesised on continuous cellulose membrane supports on Whatman 50 cellulose using Fmoc (N-(9-fluorenylmethoxycarbonyl) chemistry with the AutoSpot-Robot ASS 222 (IntavisBioanalytical Instruments).

Arrays were activated by incubation in 100% Ethanol for 5 minutes, equilibrated in Tris buffered saline (TBS) with 0.05% Tween20 (TBS-T) for 10 minutes and blocked with a 5% non-fat milk (Marvel)/TBS-T solution for 1 hour at room temperature. The interaction of GST and GST-Bcl3 or GST-p50 was investigated by overlaying the cellulose membrane with 10ug/ml of each recombinant protein in 1% Milk/TBS-T overnight at 4°C in. Arrays were washed a total of 3 times for 5 minutes in TBS-T before immunoblotting with anti-GST primary antibody for 2 hours and Anti-rabbit IgG HRP for 1 hour. Arrays were washed as previous following each antibody incubation and bound protein was detected with SuperSignal West Pico Chemiluminescent Substrate (Thermo Scientific). Arrays were incubated in peptide array stripping buffer(2% SDS, 62mM Tris pH6.8, 20mM DTT) for 30 minutes at 70°C and washed twice in TBS-T for 10 minutes to remove bound protein. Specific alanine scanning substitution arrays were generated using the same synthesis procedure. GST and GST-Bcl3 or GST-p50 were incubated with the substitution arrays as previous and immunoblotted with anti-GST and a IR-800 conjugated anti-rabbit secondary. Substitution arrays were scanned on the LI-COR odyssey to detect bound protein.

2.2.7 Site-directed Mutagenesis

Site-directed mutagenesis (SDM) of p50 and p105 was performed using Quick-change I, II and lightning site-directed mutagenesis kits (Stratagene) as per instructions. SDM oligonucleotides were designed using the QuikChange Primer Design online tool:

(<http://www.genomics.agilent.com/primerDesignProgram.jsp>).

HPLC grade oligo-nucleotides were purchased from Eurofins MWG Operon. Concentrations of oligonucleotides and templates as follows: Oligonucleotides 125ng and Template: 100ng.

- SDM for p50^{DFSP} was performed by Aisling McCann (University College Cork).
- SDM for p50^{K315A,K317A} was performed by Jennifer O'Donnell (University College Cork).
- SDM for p50^{K315A,Y316A,K317A} was performed by Diarmuid Glavin (University College Cork).

Table 19. p50 SDM Oligonucleotide Sequences

Mutant	oligonucleotides Sequences 5'-3'
p50 ^{KRM}	5-gccccgaatgcatccaacctggcaatcgtggcagcggacagaaacagcaggatgtgt-3 5-acacatcctgctgttctgtccgctgccacgattgccaggttgatgattcggggc-3 Template: pRK5-p50-FLAG
p50 ^{KRM,DBM}	5-ggatttcgattccgcgctgtgtgacggccatcacacgga-3 5-tccgtgtgatgggccgtcacacacagcgcggaatcgaatcc-3 Template: pRK5-p50 ^{KRM} -FLAG
p50 ^{DFSP}	5-ggagtttgggaaggatttggggcggctccgcccggatgttcatagacagtttc-3 5-gaaactgtctatgaacatccgcgggcagcggcccaaatcctccaaactcc-3 Template: pRK5-p50 ^{KRM} -FLAG
p50 ^{Y316F}	5-cattgtcttcaaacgcaaagttaaggatgtcaacattacaagc-3 5-gctttgtaatgttgacatcctaaactttggcgttttgaagacaatg-3 Template: pRK5-p50-FLAG
p50 ^{RKR}	5- tgaaatcaaagacaaagaggaagtgaagcggcagcccagaagcttatgccgaacttct cgg-3 5-ccgagaagttcggcataagcttctgggctgcccttgacttctctttgtctttgatt

	tca-3 Template: pRK5-p50-FLAG Template: pEF4-p50-MYC
p50 ^{K363A}	5-gtgcaaaggaacgccaggcgcttatgccgaacttctc-3 5-gagaagttcggcataaagcgctggcggttcctttgcac-3 Template: pRK5-p50-FLAG
p50 ^{K128R}	5-gtaacagcaggaccaggacatggtggttg-3 5-caaccacatgtccctgggtcctgctgttac-3 Template: pEF4-p50-XPRESS
p50 ^{Y316A}	5-ccattgtcttcaaacgccaaaggctaaggatgtcaacattacaagc-3 5-gctttgtaatgttgacatccttagcctttggcggtttgaagacaatgg-3 Template: pRK5-p50-FLAG
p50 ^{K315A,Y316A,K317A}	5-tgtcttcaaacgccaggcgctgcggatgtcaacattaca-3 5-tgtaatgttgacatccgcagccgctggcggtttgaagaca-3 Template: pRK5-p50 ^{K315A,K317A} -FLAG
p50 ^{K315A,K317A}	5'cagtttgccattgtcttcaaacgccagcgtatgcggatgtcaacattacaagccagc-3 3 5-gctggctttgtaatgttgacatccgcatacgtggcggtttgaagacaatggcaaactg-3 3 Template: pRK5-p50-FLAG

Table 20. p105 SDM Oligonucleotide Sequences

Mutant	oligonucleotides Sequences 5' -3'
p105 ^{K315A,K317A}	5-cagtttgccattgtcttcaaacgccagcgtatgcggatgtcaacattacaagccagc-3 5-gctggctttgtaatgttgacatccgcatacgtggcggtttgaagacaatggcaaactg-3 Template:pEF4-p105-Xpress
p105 ^{KRM}	5-gccccgaatgcatccaactggcaatcgtggcagcggacagaacagcaggatgtgt-3 5-acacatcctgctgttctgtccgctgccacgattgccaggttgatgattcggggc-3 Template:pEF4-p105-Xpress
p105 ^{RKR}	5-tgaaatcaaagacaagaggaagtgaagcggcagcccagaagcttatgccgaac ttctcg-3 5-ccgagaagttcggcataagcttctgggctgccgcttgcaattcctctttgctttgat ttca-3 Template: pEF4-p105-XPRESS
p105 ^{K128R}	5-gtaacagcaggaccaggacatggtggttg-3 5-caaccacatgtccctgggtcctgctgttac-3

2.2.8 Molecular Biology Techniques

2.2.8.1 Preparation of Chemically Competent Cells

Adapted from (Sambrook and Russell) *Escherichia coli* (*E.coli*) DH5 α were streaked onto LB agar and incubated overnight (16-20 hours). A single colony was isolated and incubated with 100 ml of Lysogeny broth (LB) in a 1L flask at 37°C with agitation. The OD₆₀₀ of the culture was measured every 15-20 minutes and harvested at OD₆₀₀ of 0.35. For efficient transformation it is essential that the number of viable cells not exceed 10⁸ cells/ml which is equivalent to OD₆₀₀ ~ 0.4 for most strains of *E.coli*. Bacterial cells were transferred to 50ml centrifuge tubes and incubated on ice for 10 minutes. Cells were recovered by centrifugation at 2700g for 10 minutes at 4°C. Medium was decanted and tubes inverted for 1 minute to ensure all media was removed. Pellets were resuspended by gentle swirling in 30 ml ice-cold MgCl₂-CaCl₂ solution (80mM MgCl₂, 20mM CaCl₂). Cells were recovered by centrifugation at 2700g for 10 minutes at 4°C. Medium was decanted and tubes inverted for 1 minute to ensure all media was removed. Pellets were resuspended by gentle swirling in 4 ml ice-cold 0.1 M CaCl₂ solution for each 50 ml of original culture.

To prepare frozen stocks of competent cells, 70 μ l of Dimethyl sulfoxide (DMSO) was added per 2ml of resuspended cells and mixed gently. Following 15 minutes incubation on ice, an additional 70 μ l of DMSO was added to each suspension and returned to ice. Cells were quickly dispensed into aliquots into chilled, sterile microfuge tubes and immediately snap-frozen in liquid nitrogen. Competent cells were stored at -80°C.

2.2.8.2 DNA transformation for Routine Plasmid Preparation

10-20 μ l of competent bacteria (as prepared in 2.2.8.1) were thawed on ice. Following the addition of 10ng of plasmid DNA, competent cells were incubated on ice for a further 2 minutes. Bacteria were heat shocked in a 37°C water bath for 1 minute and returned to ice immediately. Cells were recovered in 100 μ l of super optimal broth with catabolite repression (SOC) media (**Table 18**) and

transferred to LB agar containing of 50µg/ml ampicillin. Agar plates were incubated over night at 37°C.

2.2.8.3 Plasmid Extraction

2.2.8.3.1 Midiprep

A single colony was inoculated into 2ml LB containing 50µg/ml ampicillin. Starter cultures were incubated at 37°C shaking for 6-8 hours. 100 ml LB containing 50µg/ml ampicillin was then spiked with 100µl of the starter culture and incubated at 37°C shaking for 16-20 hours. Plasmid DNA was extracted using PureYield Plasmid Midiprep System (Promega) according to manufacturer's instructions. Plasmid concentration and purity was determined using a NanoDrop spectrophotometer.

2.2.8.3.2 Miniprep

5 ml LB containing 50µg/ml ampicillin was inoculated with a single colony and incubated at 37°C shaking for 16-21 hours. Plasmid DNA was extracted using Wizard Plus SV Mini-Prep (Promega) or PureYield Plasmid Miniprep System (Promega) according to manufacturer's instructions.

2.2.8.4 Transfection

Cell lines were transiently transfected as per manufacturer's instructions, cells were transfected for 24 hours for all assays with the exception of immunofluorescence which is described in detail in section 2.2.4. Transfection reagents and ratios of plasmid to transfection reagent used for each cell type are described in Table 21. Assay specific transfection conditions are described in Table 22. Within an experiment total plasmid concentrations were kept constant between samples with the addition of an empty expression vector.

Table 21. Transfection Conditions

Cell line	Transfection Reagent	Supplier	Plasmid(µg): Reagent(µl)
RAW 264.7	X-tremeGENE HP	Roche	1:2
	Attractene	Qiagen	1:3
HEK293T	Turbofect	Fermentas	1:2
	X-tremeGENE HP	Roche	1:3
NIH3T3	Attractene	Qiagen	1:3
<i>Nfkb1</i> ^{-/-} MEF	Attractene	Qiagen	1:3
p105 ^{WT} MEF p105 ^{RKR} MEF	Attractene	Qiagen	1:3

Table 22. Assay Specific Transfection Conditions

Assay Type	Cell Number	Cell Type	Plasmid Concentration
Co-IP	2 x10 ⁶ per 6cm dish	HEK 293T	1ug of each plasmid
	or 5 x10 ⁶ per 10cm dish	HEK 293T	2ug of each plasmid
EMSA	2 x10 ⁶ per 6cm dish	HEK 293T	1ug of each plasmid
Immuno-fluorescence	3.5 x10 ⁵ per 10cm dish	NIH 3T3	1ug of each plasmid
Luciferase assay	1x10 ⁵ per well (24 well plate)	RAW 264.7	100ng of luciferase reporter and 10ng of <i>Renella</i> reporter used per sample. The concentration of additional plasmids were dependent on the individual experiment and are detailed in figure legends.
Luciferase assay	2.5x10 ⁴ per well (24 well plate)	Nfkb1 ^{-/-} MEF	As above
Kinase assay	2 x10 ⁶ per 6cm dish	HEK 293T	1ug of each plasmid
Ubiquitination assay	2 x10 ⁶ per 6cm dish	HEK 293T	1ug of each plasmid
	or 5 x10 ⁶ per 10cm dish	HEK 293T	2ug of each plasmid

2.2.8.5 Sub cloning

To generate GST expression vectors. Murine Bcl-3 and p50 cDNAs were subcloned from pRK5-Bcl-3-FLAG and pRK5-p50-FLAG vectors respectively into pGEX-6p1. NEB supplied all restriction enzymes. 20µl restriction digests were performed with 1µg plasmid DNA and 10 units of *Bam*H1 and *Sal*1 as per manufacturer's instructions. DNA fragments were resolved on 1% agarose gel, excised and purified with Wizard SV Gel and PCR Clean-Up System (Promega). Ligation reactions were performed with T4 DNA ligase (NEB) using a 1:6 molar ratio of vector to insert in 10µl, overnight at 16°C. 1µl of ligation reaction was transformed into NovaBlue Singles Competent Cells (Novagen) as per manufacturer's instructions.

2.2.8.6 Gene expression analysis

For real-time PCR, total RNA was isolated using RNeasy kits (Qiagen) and reversely transcribed using cDyNAmo cDNA synthesis kit (Thermo scientific) or NanoScript reverse transcription kit (Primer Design) as per manufacturer's instructions. Real-time PCR was performed with SensiMix SYBR master mix or PerfeCTa SYBR Green SuperMix with ROX using QuantiTect Primer Assays (Qiagen). Data were normalised to 18s Gene expression changes calculated using the $2^{-\Delta\Delta CT}$ method.

Table 23. Thermo cycling conditions

	Cycle	Temperature	Time
SensiMix SYBR master mix	1	95° C	10 minutes
Roche lightcycler 480 384well format	40-45	95° C	15 seconds
		60° C	30 seconds
		72° C	15 seconds
PerfeCTa SYBR Green SuperMix	1	95° C	20 seconds
Applied Biosystems 7500 Fast Real-Time PCR System 96 well format	40	95° C	3 seconds
		60° C	30 seconds

Table 24. QuantiTect Primer Assays

Gene	Product Number	Gene	Product Number
<i>Ccl2</i>	QT00167832	<i>IL6</i>	QT01048355
<i>cFos</i>	QT00147308	<i>IL6</i>	QT00098875
<i>Cxcl2</i>	QT00113253	<i>IκBa</i>	QT00134421
<i>Egr1</i>	QT00265846	<i>Ptgs2</i>	QT00165347
<i>IL10</i>	QT00106169	<i>Tnf</i>	QT00104006
<i>IL12b</i>	QT00153643	<i>Ccl2</i>	QT00167832

2.2.9 Bioinformatic tools

2.2.9.1 Hydrophobicity analysis

Hydrophobicity analysis was performed on the murine p50 protein sequence using the Cowan and Whittaker Hydrophobicity scale (Cowan and Whittaker, 1990) and BioAnnotator (Vector NTI, Invitrogen).

Table 25. Amino Acid Hydrophobicity Values

Amino Acid Hydrophobicity Values			
Ala:0.420	Gln:-0.960	Leu: 1.800	Ser:-0.640
Arg:-1.560	Glu:-0.370	Lys:-2.030	Thr:-0.260
Asn:-1.030	Gly: 0.000	Met: 1.180	Trp: 1.460
Asp:-0.510	His:-2.280	Phe: 1.740	Tyr: 0.510
Cys: 0.840	Ile: 1.810	Pro: 0.860	Val: 1.340

2.2.9.2 Crystal structure analysis

Protein crystal structures were analysed with 3D Molecule Viewer (Vector NTI, Invitrogen). p50 crystal structure with predicted C-and N-terminal domains was modelled using Phyre² (Structural Bioinformatics Group, Imperial College London) (Kelley and Sternberg, 2009). Confidence in the model: 332 residues (83%) modelled at >90% accuracy.

Protein data bank (PDB) structures used:

- Structure of NF-kappa b p50 homodimer bound to a kappa b site (Ghosh et al., 1995)
- Crystal Structure Of The Ankyrin Repeat Domain Of Bcl-3: A Unique Member Of The Ikappa b Protein Family (Michel et al., 2001).

2.2.9.3 Similarity index

Similarity index of the ARD of murine I κ B family members was determined with AlignX software (Vector NTI, Invitrogen) following multiple sequence alignment. Residues are scored based on the similarity value. Identical residues =1, similar residues = 0.5 and weakly similar residues = 0.2.

Table 26. Residue conservation table

Residue	Strong Similarity	Weak Similarity	Residue	Strong Similarity	Weak Similarity
A	GS	CTV	M	ILV	F
B			N	Q	DEGHKRST
C		AS	P		ST
D	E	GHKNQRS	Q	N	DEHKRS
E	D	HKNQRS	R	K	DEHNQ
F	WY	HILM	S	AT	CDEGKNPQ
G	A	DNS	T	S	AKNPV
H	Y	DEFKNQR	V	ILM	AT
I	LMV	F	W	FY	
K	R	DEHNQST	Y	FHW	
L	IMV	F	Z		

2.2.9.4 Multiple sequence alignment

Multiple sequence alignment of the ANK repeat domains of murine I κ B family members was performed using AlignX software (Vector NTI, Invitrogen) and gaps manually adjusted based on secondary structure as per (Basith et al., 2013).

Table 27. I κ B sequence Identifiers

Protein	Reference Sequence ID	Protein	Reference Sequence ID
Bcl-3	NP_291079.2	I κ B ζ	NP_001152866.1
I κ B α	EDL36726.1	I κ BNS	NP_742154.1
I κ B β	NP_035038.2	p100	NP_001170840.1
I κ B ϵ	NP_032716.2	p105	NP_032715.2

2.2.9.5 Protein structure prediction software

A number of web based protein prediction software tools were utilised in this study and are summarised in Table 28.

Table 28. Web servers for structure prediction

Prediction Tool	Server name	Server location and web address	Reference
3D structure	Phyre2	Structural Bioinformatics Group, Imperial College, London. http://www.sbg.bio.ic.ac.uk/phyre2	(Kelley and Sternberg, 2009)
Surface accessibility and secondary structure	Predictprotein	Rost Lab, Bioinformatics and Computational Biology Department, Technical University of Munich. https://www.predictprotein.org/	(Rost et al., 2004)
	NetSurfP	Centre for Biological Sequence Analysis, CBS, Department of Systems Biology. The Technical University of Denmark. http://www.cbs.dtu.dk/services/NetSurfP	(Petersen et al., 2009)

— Chapter Three —

3 Investigation of the molecular determinants of NF- κ B p50 ubiquitination

3.1 ABSTRACT

Bcl-3 is an essential negative regulator of NF- κ B during TLR and TNF Receptor signalling. Bcl-3 interacts with a number of transcriptional regulators including homodimers of the NF- κ B p50 subunit. Deletion of Bcl-3 results in increased NF- κ B p50 ubiquitination and increased inflammatory gene expression. We employed immobilised peptide array technology to define a region of p50 required for the formation of a Bcl-3:p50 homodimer immunosuppressor complex. Key amino acids of p50 critical for interaction with Bcl-3 and are essential for Bcl-3 mediated inhibition of inflammatory gene expression were identified. Bcl-3 is unable to interact with p50 when these amino acids are mutated, rendering it incapable of inhibiting the transcriptional activity of NF- κ B. *Nfkb1*^{-/-} cells reconstituted with mutated p50 precursor, p105, recapitulate the *Bcl3*^{-/-} phenotype and are hyper-responsive to TNF stimulation as measured by inflammatory gene expression. Our study demonstrates that interaction with p50 essential for the anti-inflammatory properties of Bcl-3 and further highlights the importance of p50 homodimer stability in the control of NF- κ B target gene expression.

3.2 INTRODUCTION

Bcl-3 is a critical regulator of NF- κ B during TLR-induced gene expression and recent work has shown that Bcl-3 mediated stabilisation of p50 is required for limiting NF- κ B transcriptional activity (Carmody et al., 2007b). Supported by increased levels of p50 ubiquitination in *Bcl3*^{-/-} macrophages, Bcl-3 over expression blocks p50 homodimer ubiquitination and subsequent degradation (Carmody et al., 2007b). This inhibition of ubiquitination extends the half-life of p50 thereby stabilising a DNA bound p50 homodimer complex. DNA binding triggers p50 ubiquitination, thus in the absence of Bcl-3 this p50:DNA complex is short lived, permitting an increase in promoter occupancy of active NF- κ B dimers. In unstimulated macrophage, p50 homodimers occupy the promoters of *Tnf* and *Cxcl2* genes, however in *Bcl3*^{-/-} cells, these promoters are bound by cRel and p65 (Carmody et al., 2007b). This altered dimer equilibrium results in increased NF- κ B transcriptional activity and proinflammatory gene expression (Carmody et al., 2007b). p50 ubiquitination is therefore a critical regulatory step of NF- κ B gene expression following TLR activation. The precise mechanism of p50 ubiquitination following TLR signalling and its role in innate immunity is however yet to be elucidated.

In 1995, the structure of murine and human NF- κ B p50 homodimer bound to DNA was determined independently by two groups (Ghosh et al., 1995, Müller et al., 1995). Although the orientation of the N-terminal domains varied slightly due to different half site spacing, both structures show identical protein folds (Müller and Harrison, 1995). Not surprisingly the structure of I κ B α :NF- κ B heterodimer complex quickly followed but remains the only resolved structure of an I κ B protein bound to NF- κ B p50 complex to date (Huxford et al., 1998, Jacobs and Harrison, 1998). Due to the homologous nature of I κ B proteins, this complex provided a template for the available models of a DNA bound Bcl-3:p50 homodimer complex (Michel et al., 2001, Manavalan et al., 2010). Michel *et al.* superimposed the crystal structures of Bcl-3 and a p50 homodimer onto the I κ B α :NF- κ B complex (Michel et al., 2001), whereas Manavalan *et al.* performed a molecular docking approach (Manavalan et al., 2010). While *in silico* methods provide an excellent basis to study protein-protein interactions these approaches have significant limitations. Unlike the predicted Bcl-3:p50 homodimer complex, the solved I κ B α :NF- κ B structure is not a DNA bound complex and DNA binding can directly alter p50 conformation (Müller et al.,

1996). Docking models also predict complexes based on individual structures and may not account for conformational changes of bound and unbound proteins. Both approaches predicted specific p50:Bcl-3 interacting residues but neither were confirmed experimentally.

Peptide arrays provide an excellent tool to aid in the investigation of protein interaction domains through epitope mapping (Geysen et al., 1987, Frank and Overwin, 1996). This strategy involves synthesising a library of overlapping peptides that span the entire protein of interest. There are many methods available to prepare peptides arrays but one of the most common technique used for synthesising peptides directly on a solid support is the SPOT-synthesis technique. The SPOT method allows simultaneous multiple short peptides to be synthesised on a variety of solid supports (Frank, 1992). Ronald Frank developed the system in 1990 based on Merrifield's solid phase peptide chemistry and earlier work by Frank *et al.* describing parallel synthesis of large numbers of oligonucleotides on cellulose filter disks (Frank et al., 1983). Originally developed as a manual method, the SPOT-synthesis technique has been commercially adapted allowing reliable high throughput automatic synthesis of peptide arrays. The range of applications are growing (reviewed in (Reineke et al., 2001, Frank, 2002)) but peptide arrays are commonly used to map B and T cell epitopes, characterise enzyme substrates and study protein-protein interactions.

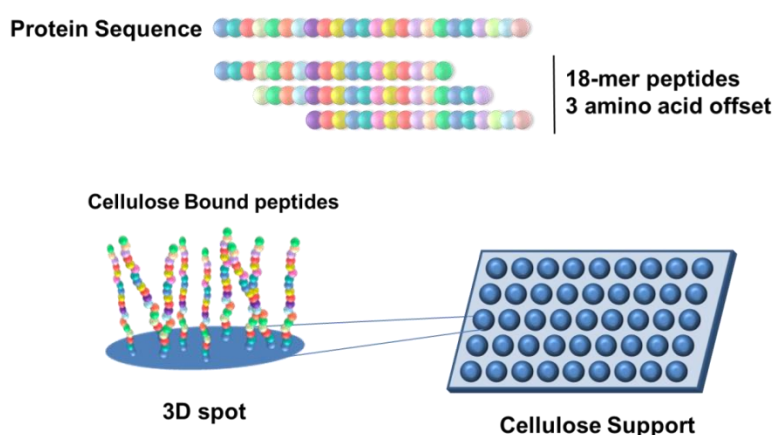


Figure 3.1 Schematic representation of peptide scanning using SPOT synthesis technology

Peptides are synthesised on cellulose membranes in a cyclic procedure where essentially during each cycle, a single 9-Fluorenylmethoxycarbonyl (Fmoc)-protected (Carpino and Han, 1972) amino acid is coupled to a growing peptide chain bound to the solid support. Following Fmoc deprotection and dimethylformamide and ethanol wash steps, the process is repeated until the entire peptide is assembled. Peptide length and offset number are determined by the user but ideally longer peptides with a short offset will yield a greater chance of epitope hits. This approach is ideally suited for continuous epitope regions, mapping of partial discontinuous binding sites although limited, is possible. Following synthesis the peptide array is then incubated with a binding partner for example cell extract or recombinant protein. Detection of the peptide-protein complex can be performed by a number of methods, dependent on the specific assay. Typically, an antibody based approach is used in which a primary antibody against the partner protein or fused tag coupled with a secondary antibody is used (Kiely et al., 2009, Collieran et al., 2013).

In this chapter, we investigated the mechanisms through which Bcl-3 inhibits p50 ubiquitination specifically aiming to determine if interaction with p50 is necessary for Bcl-3 mediated inhibition of p50 ubiquitination and repression of NF- κ B transcriptional activity. A peptide array approach was utilised to identify key regions of p50 required for interaction with Bcl-3. Using site-directed mutagenesis, we generated a p50 mutant incapable of interaction with Bcl-3. Our data demonstrates that interaction between Bcl-3 and p50 is required for Bcl-3-mediated inhibition of p50 ubiquitination and the anti-inflammatory properties of Bcl-3. During this study, we also identified a number of residues of p50 critical in regulating p50 ubiquitination.

3.3 RESULTS

3.3.1 Identification of the Bcl-3 Interacting Regions of p50 Using Peptide Arrays

3.3.1.1 Expression and Purification of Recombinant Bcl-3

Recombinant Bcl-3 was constructed by inserting murine Bcl-3 cDNA into the multiple cloning site of pGEX6p1 (Figure 3.2 A). The pGEX vector series allows inducible expression of GST fusion proteins in *E.coli*. Expression of the fusion protein is under the control of the *tac* promoter, which is induced by addition of IPTG. *E.coli* BL21 CodonPlus were transformed with pGEX-6p1 or pGEX-6p1-Bcl-3. GST proteins were induced overnight at 20°C with optimised concentrations of IPTG 1.0mM or 0.1mM for GST or GST-Bcl-3, respectively. The lower concentration of IPTG resulted in a reduced yield of Bcl-3 fusion protein but was required to express a soluble intact protein as higher IPTG concentrations induced expression of an insoluble form of Bcl-3. Recombinant proteins were then affinity-purified against GSH-agarose and eluted with glutathione over a number of elutions (Figure 3.2 B). The suitability of GST-Bcl-3 for use as a p50 peptide library probe was established using a GST pull-down assay. GST or GST-Bcl-3 were incubated with a whole cell lysate overexpressing FLAG tagged p50 and affinity purified with GSH agarose. p50-FLAG bound specifically to purified GST-Bcl-3, but not GST indicating a functional Bcl-3 fusion protein. (Figure 3.2 C).

3.3.1.2 Bcl-3 Binds to Distinct Peptides on a p50 Peptide Array

The crystal structures of Bcl-3 and p50 homodimers have been resolved independently and computational modelling of a Bcl-3:p50 homodimer complex indicates that Bcl-3 makes a number of contacts with amino acids in both subunits of a p50 homodimer (Michel et al., 2001, Manavalan et al., 2010). In order to experimentally identify the regions of p50 mediating interaction with Bcl-3, an immobilised peptide array based technique using recombinant GST-Bcl-3 protein as a probe was employed. Specifically, a library of overlapping peptides 18 amino acids in length, each shifted by 3 amino acids and encompassing the entire sequence of p50, was SPOT-synthesised on

nitrocellulose membranes to generate p50 peptide arrays (see Appendix 7.1 for peptide library). p50 peptide arrays were then probed with either GST or GST-Bcl-3 and bound protein was detected by immunoblotting with anti-GST antibody (Figure 3.3A). GST-Bcl-3 bound specifically to a number of peptides on the p50 peptide array suggesting that Bcl-3 probably makes a substantial number of contacts with p50. This is not surprising as it is likely Bcl-3 will make unique contacts on both p50 subunits (Michel et al., 2001, Manavalan et al., 2010). These stretches of peptides were examined further and using the available crystal structure of a p50 homodimer bound to DNA, many peptides were excluded from additional analysis. Protein-protein interactions are dependent on exposed residues to create a binding interface, many of the positive Bcl-3 peptides identified from the peptide array however did not appear to be exposed and therefore were unlikely to be available for binding with Bcl-3. Furthermore, peptides that contained residues involved in DNA binding were also excluded as mutation of these amino acids would likely result in substantial changes in the properties of p50, for example peptides 12-17 contain several p50 amino acids that make direct contacts with DNA (Muller et al., 1995). The full p50 peptide array and alanine scanning data is available in Appendixes 7.1-7.3.

Four regions of positive Bcl-3 binding were however considered to be of particular interest (Figure 3.3 B). Regions R1-R3 are highlighted on the crystal structure of p50 (Figure 3.3 C). R1 spans both the DNA binding and dimerisation domains of the RHD whereas R2 and R3 are contained within the dimerisation domain of p50. Residues from region R4 lie in extreme C-terminus of the RHD and are not represented in the currently available structures of p50.

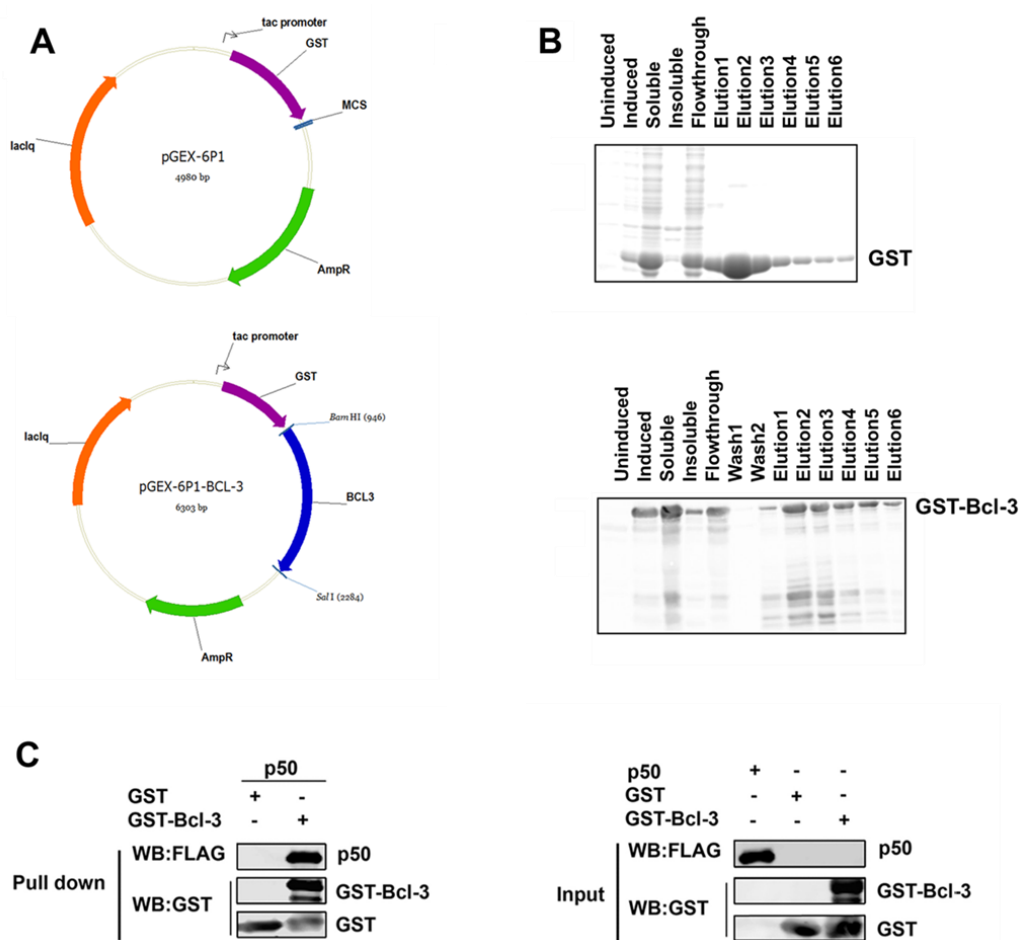


Figure 3.2 Cloning and purification of recombinant Bcl-3.

(A) Murine Bcl-3 was ligated via *Bam*H1 and *Sal*1 restriction sites into pGEX6p1 to produce a GST-Bcl-3 expression vector. (B) *Escherichia coli* BL21 CodonPlus were transformed with pGEX-6p1 or pGEX-6p1-Bcl-3. GST and GST-Bcl-3 were induced with the addition of IPTG. Recombinant proteins were affinity-purified against GSH-agarose and eluted with glutathione. (C) p50 binds specifically to GST-Bcl3 in a GST pull down assay. Purified bacterial recombinant GST or GST-Bcl-3 was incubated with a HEK293 whole cell lysate overexpressing FLAG-p50 and were affinity purified with GSH agarose. Pull down complexes were immunoblotted with anti-FLAG and anti-GST .

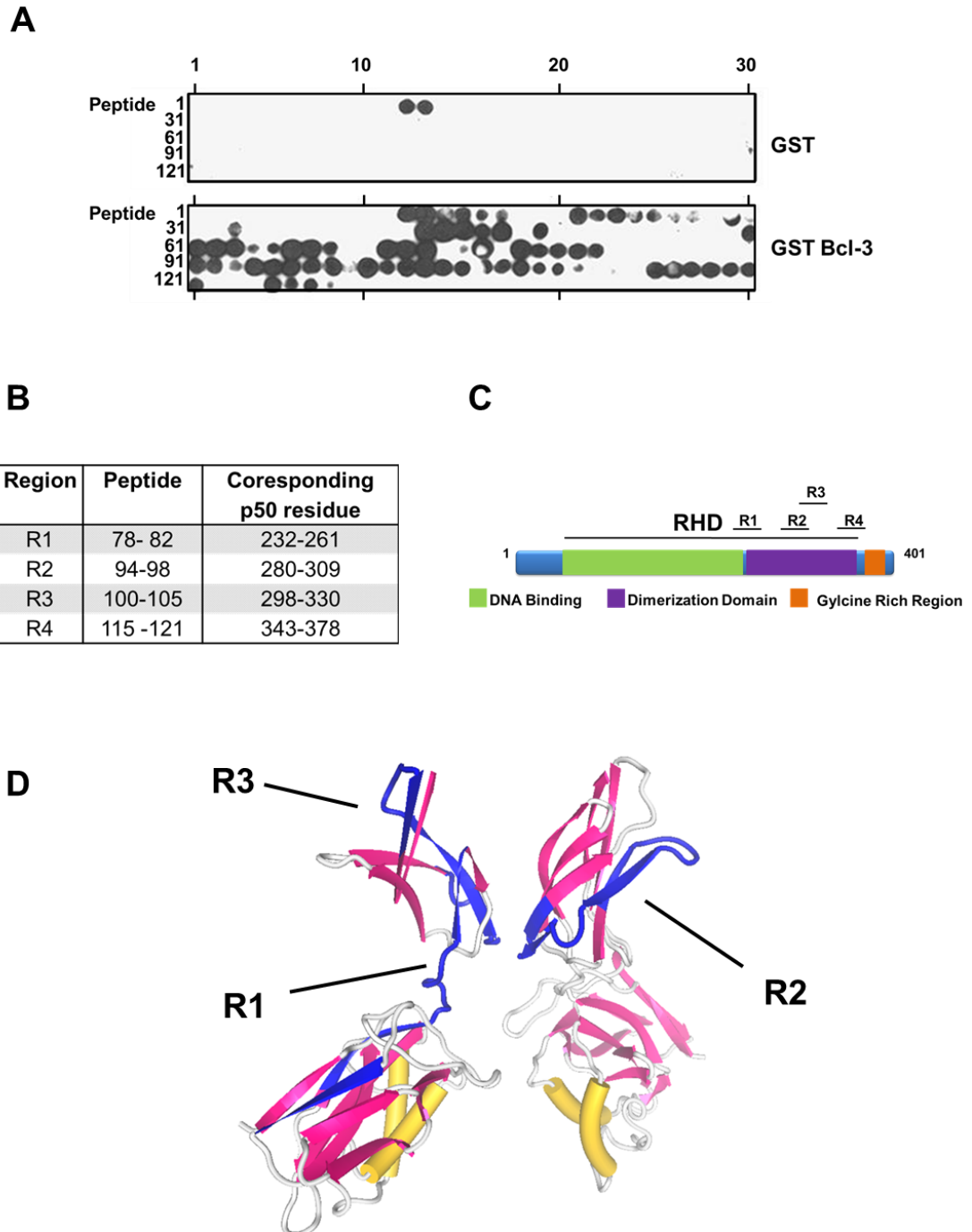


Figure 3.3 Identification of Bcl-3 interacting regions on p50 using peptide arrays.

(A) Peptide arrays of immobilised overlapping 18-mer peptides, each shifted to the right by 3 amino acids encompassing the entire p50 sequence were generated. Arrays were probed with GST or GST-Bcl-3 and detected by immunoblotting with anti-GST antibody. GST-Bcl-3 binding to p50 peptides is shown and is representative of duplicate arrays. (B) Table indicating GST- Bcl-3 positive binding regions of interest with corresponding p50 amino acids. (C) Schematic representation of GST-Bcl-3 binding regions R1-R4 on p50. (D) p50 homodimer crystal structure with R1-R3 shaded in blue. For clarity, each region is highlighted on only one subunit. Murine p50 amino acid numbering (B-D).

3.3.1.3 Alanine Substitution Arrays Identify Key Interacting Residues on p50

In order to identify individual amino acids within these regions of p50 that are essential for Bcl-3 binding a series of alanine-scanning arrays were generated. Alanine scanning arrays were derived from the positive 18-mer parent peptides of region R1-R4. For each parent peptide, 18 new peptides were generated. Each peptide contained a single successive alanine substitution of the original peptide (see Appendix 7.2 for alanine substitution library). The alanine scanning array was again incubated with GST-Bcl-3 prior to staining with anti-GST antibody. Detection of GST-Bcl-3 binding was then performed using near infra-red IR-Dye-conjugated secondary antibody to facilitate quantification of GST-Bcl-3 binding to specific peptides using an infra-red scanner. In each case the binding of GST-Bcl-3 to the substituted peptide was calculated with respect to the parent peptide contained on the same array. Substitution of amino acids that resulted in significantly decreased Bcl-3 binding i.e. less than 50% binding of the parent peptide were considered to be strong candidates for interaction. These data indicated a number of key residues in each of the four regions R1 - R4 which were subsequently mutated through site-directed mutagenesis (SDM) of full length p50.

3.3.2 Lys 249, Arg252 and Met 253 are Critical for p50 Stability

3.3.2.1 Alanine Substitution Analysis of Bcl-3 Binding Region R1

The first region of the p50 array to be investigated was R1, a 30 residue stretch corresponding to amino acids 232-261 of p50 (Figure 3.4 A). An alanine scanning approach was then employed to identify the specific amino acids within R1 that may be required for interaction with Bcl-3. The 18 amino acids of p50-derived peptides 78, 80 and 82 were sequentially substituted with alanine and probed with GST-Bcl-3. Bcl-3 binding was detected by immunoblotting and quantified by densitometry and represented as a percentage binding of the control parent peptide (Figure 3.4 B). These data demonstrate that alanine substitutions at Lys 249, Arg252 and Met 253 significantly decreased GST-Bcl-3 binding when compared to the parent p50 peptide. Direct interaction with Bcl-3 requires contributing amino acids to be present on the outer surface of p50. Examination

of the crystal structure of p50 homodimer bound to DNA reveals that indeed Lys 249, Arg252 and Met 253 are surfaced exposed and available for binding (Figure 3.4 C).

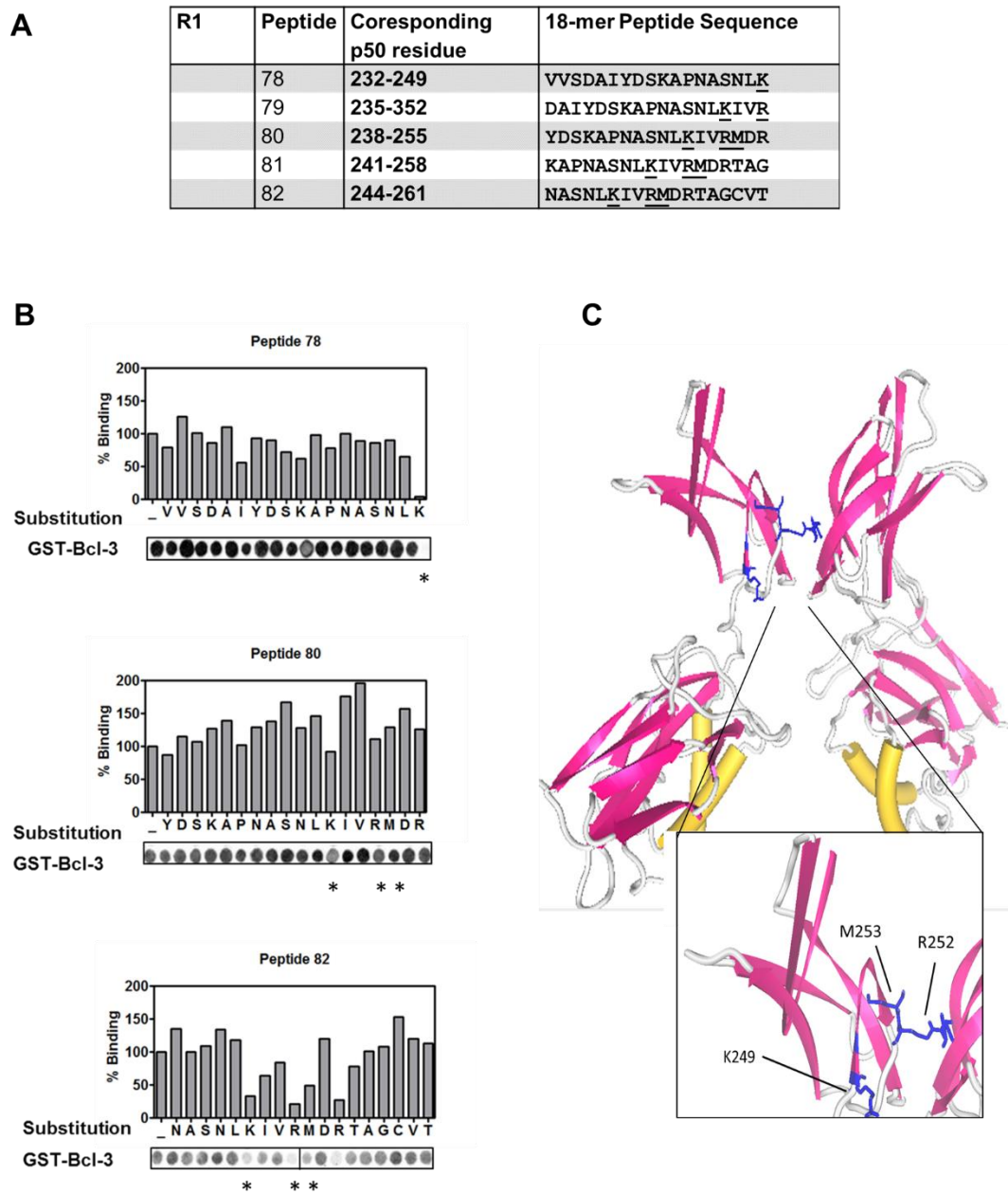


Figure 3.4 Alanine substitution analysis of Bcl-3 binding Region R1.

(A) Sequences of peptides 78-82 of region 1 are shown with Lys249, Arg252 and Met253 underlined. (B) The 18 amino acids of p50-derived peptides 78, 80 and 82 were sequentially substituted with alanine and probed with GST-Bcl-3. Bcl-3 binding was quantified by densitometry and represented as a percentage binding of the control parent peptide. Substitution of amino acids Lys249, Arg252 and Met253 (denoted with *) resulted in a decrease of $\geq 50\%$ in Bcl-3 binding and are represented on p50 crystal structure in (C). Murine p50 amino acid numbering (A-C).

3.3.2.2 Characterisation of p50^{KRM}

In order to evaluate the contribution of residues Lys 249, Arg252 and Met 253 of p50 to interaction with Bcl-3, a p50 mutant in which Lys 249, Arg252 and Met 253 were mutated to alanine (p50^{KRM}) was generated. The interaction of this p50^{KRM} mutant with Bcl-3 was then assessed by co-transfection in 293T cells (Figure 3.5 A). Bcl-3 was weakly detectable in immunoprecipitates of p50^{KRM} but was significantly decreased compared to levels purifying with p50, suggesting that Lys 249, Arg 252 and Met 253 promote p50 interaction with Bcl-3. Bcl-3 is a predominantly nuclear protein and thus changes in the subcellular localisation of p50 can in directly affect the ability of Bcl-3 to bind p50. Therefore nuclear and cytoplasmic fractions of cells transfected with p50 or p50^{KRM} were generated and protein levels analysed by immunoblot. As demonstrated in Figure 3.5 B, subcellular fractionation revealed that p50^{KRM} localised to the nucleus to similar levels as p50, indicating that the mutation of the amino acids Lys 249, Arg 252 and Met 253 to alanine does not disrupt the nuclear localisation of p50. These data was supported by an analysis of the DNA binding activity of p50^{KRM} using EMSA which incorporated a double stranded oligonucleotide probe containing the NF- κ B consensus DNA binding sequence and nuclear extracts from 293T cells transfected with expression vectors for p50 or p50^{KRM}. No significant differences were seen in the DNA binding activity of p50^{KRM} compared to wild type p50 (Figure 3.5 C). Together these data demonstrate that reduced binding of p50^{KRM} to Bcl-3 is not due to a change in nuclear localisation or DNA binding properties resulting from the mutation.

3.3.2.3 Mutation of Lys 249, Arg 252 and Met 253 Disrupt p50 Stability

Previous studies indicated that Bcl-3 negatively regulates NF- κ B through inhibition of p50 homodimer ubiquitination and subsequent proteasome degradation (Carmody et al., 2007b). We next wanted to determine whether Lys 249, Arg252 and Met 253 are important for Bcl-3 mediated inhibition of p50 ubiquitination. A ubiquitination assay in 293T cells transfected with HA-tagged ubiquitin, p50 or p50^{KRM}, with or without Bcl-3 was performed. Following denaturing lysis, p50 was immunoprecipitated with anti-FLAG and immunoblotted with anti-HA antibody. Strikingly this analysis revealed a huge increase in the ubiquitination of p50^{KRM} relative to wild type p50 (Figure 3.6 A).

Overexpression of Bcl-3 effectively blocked p50 ubiquitination and although the levels of ubiquitination of p50^{KRM} were substantially increased Bcl-3 was also able to inhibit p50^{KRM} ubiquitination, as evident upon lighter exposure of the Western blot.

Ubiquitination of p50 is closely linked to its degradation indicating that a hyper ubiquitinated form of p50 would have reduced stability and function. To investigate this, a luciferase reporter assay incorporating the Bcl-3 regulated NF- κ B-dependent IL-23p19 gene promoter was employed (Carmody et al., 2007a). p50 homodimers are generally considered repressors of NF- κ B transcription. Dose-dependent analysis of p50 and p50^{KRM} expression on IL-23p19 reporter activity was performed by transfecting low but increasing amounts of p50 or p50^{KRM} expression vectors in RAW 264.7 cells. Total plasmid was kept constant by including appropriate amounts of an empty plasmid expression vector. Following LPS stimulation, a dose dependent inhibition of reporter activity following transfection with p50 but not with p50^{KRM} was observed (Figure 3.6 B). Furthermore mutation of these residues in p105, the p50 precursor, produced a very unstable form of p50 as p50 processed from mutated p105 (p105^{KRM}) was almost undetectable by immunoblot (Figure 3.6 C). Together these data demonstrate that although important, Lys 249, Arg252 and Met253 of p50 are not essential for Bcl-3 binding. The hyper-ubiquitination and instability of p50 generated from p105 suggest that these residues may be critical in regulating p50 stability independently of Bcl-3.

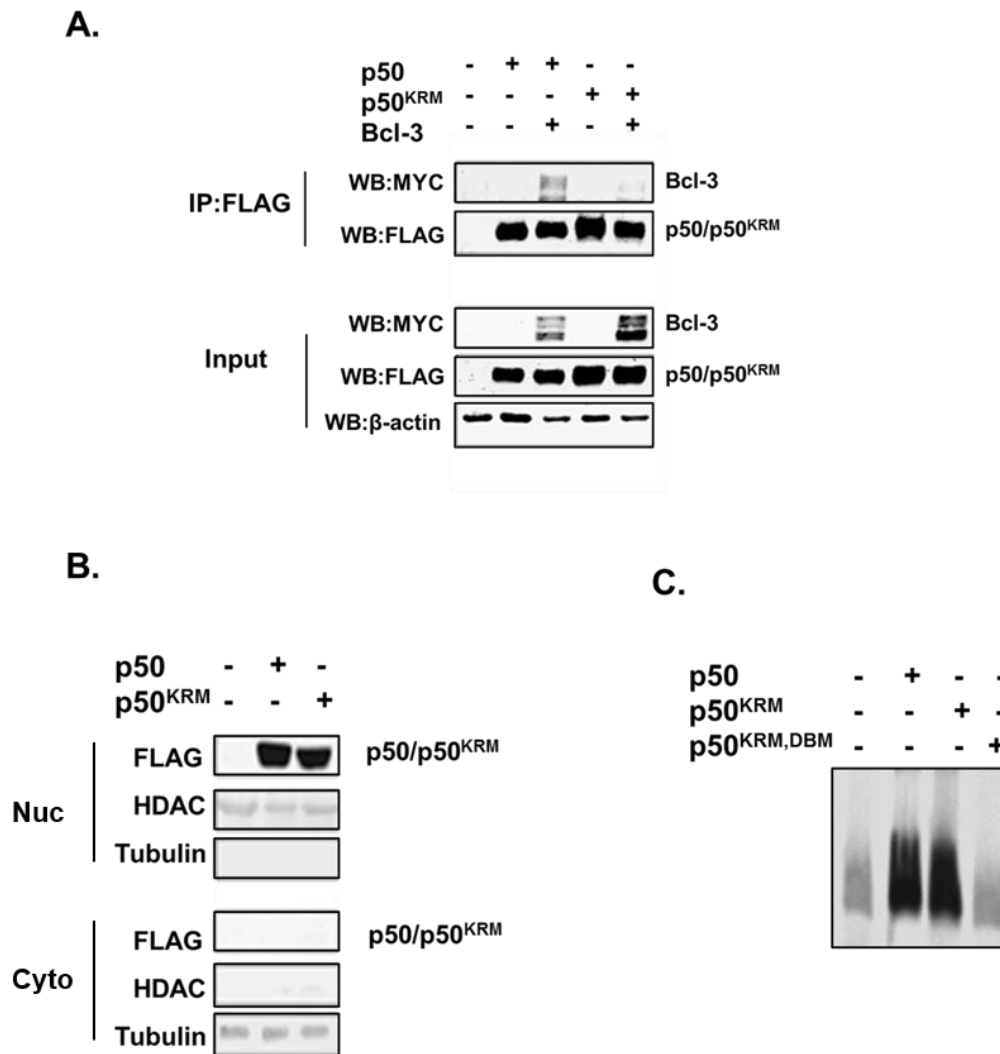
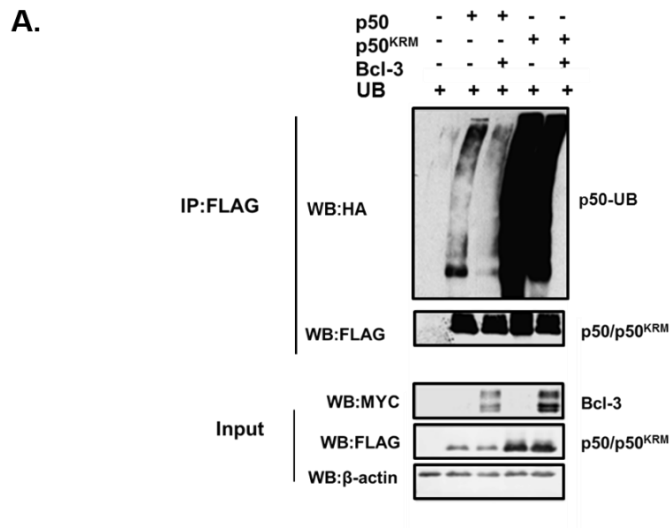
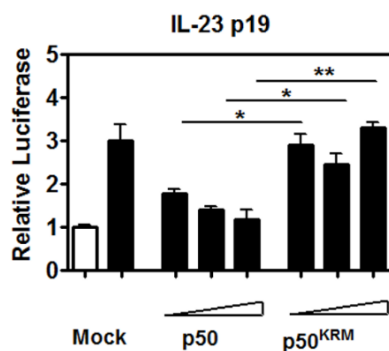


Figure 3.5 Characterisation of p50^{KRM}.

(A) HEK293T cells were transfected with pRK5-p50-FLAG(p50) or pRK5-p50-FLAG in which Lys249, Arg252 and Met253 of p50 are mutated to alanine (p50^{KRM}) with or without pcDNA3.1-Bcl-3-MYC (Bcl-3). Whole cell lysates were immunoprecipitated (IP) with anti-FLAG and analysed by western blot (WB) with the indicated antibodies. Immunoblotting with anti-β-actin was used as a loading control. (B) Nuclear (Nuc) and cytoplasmic (Cyto) extracts were prepared from HEK293T cells transfected with expression plasmids as indicated. p50 and p50^{KRM} subcellular localisation were analysed by WB with anti-FLAG. (C) HEK293T cells were transfected with expression plasmids as indicated. Nuclear extracts were prepared from the transfected cells and tested in an Electrophoretic Mobility Shift Assay (EMSA) using the consensus NF-κB binding nucleotide. As a negative control, in addition to the KRM mutation, residues critical for DNA binding, Y57 and D60 were mutated to alanine and aspartic acid respectively (p50^{KRM,DBM}). DNA binding mutant (DBM).



B.



C.

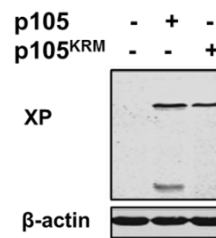


Figure 3.6 Lys 249, Arg 252 and Met 253 are critical for p50 stability.

(A) HEK293T cells were transfected as indicated with pRK5-p50-FLAG(p50) or pRK5-p50-FLAG in which Lys249, Arg252 and Met253 of p50 are mutated to alanine (p50^{KRM}) with or without pcDNA3.1-Bcl-3-MYC (Bcl-3). p50/p50^{KRM} ubiquitination was determined by IP from whole cell lysates with anti-FLAG and WB with anti-HA for HA-ubiquitin. Bcl-3 can inhibit p50^{KRM} ubiquitination (Lower Exposure). (B) RAW 264.7 cells were transiently transfected with the pLucp19 plasmid expression vector with increasing amounts (1.25, 2.5 and 5ng) of p50 or p50^{KRM} for 24 hours and cultured with or without 100 ng/ml LPS for an additional 8 hours before luciferase activity was measured. The total amount of plasmid was constant across all samples by adjusting the amount of empty vector. The *Renella* luciferase expression vector pRL-TK was used as an internal control to normalise the transfection efficiency across all samples. IL23 p19 reporter activity is represented as fold increase over untreated (UNT) cells transfected with pLucp19 plasmid and empty vector expression (mock). Transfections were performed in triplicate per experiment and data shown are means + SEM and are representative of independent experiments. Statistical significance between corresponding p50 and p50^{KRM} mutant reporter activities was determined by Student's t test; P<0.05 (*), P<0.01 (**), P<0.001(***)). (C) HEK293T cells were transfected with p105 or p105 in which Lys 249, Arg 252 and Met 253 were mutated to alanine and analysed by western blot.

3.3.3 Alanine Substitution Analysis of Bcl-3 Binding Region R2

A similar approach was carried out to analyse Bcl-3 binding region R2 of p50. Alanine scanning arrays of spots 91-97 were generated as in Figure 3.5. Bcl-3 binding was detected by immunoblotting and represented as a percentage binding of the control parent peptide (Figure 3.7 B). The alanine substitution array identified a number of amino acids that when mutated to alanine significantly reduced Bcl-3 binding (Figure 3.7 B). Specifically a stretch of 5 amino acids of p50 DFSP^T 297-301 were considered to be of particular interest as, equivalent amino acids in p65 make contact with I κ B α as part of a p50 heterodimer (Huxford et al., 1998, Jacobs and Harrison, 1998). These amino acids are surface exposed and available for binding (Figure 3.7 C).

3.3.3.1 p50^{DFSP^T} Emulates p50^{KRM} Phenotype

When Asp297, Phe298, Ser299, Pro300 and Thr301 were mutated to alanine (p50^{DFSP^T}), Bcl-3 binding was drastically reduced. The interaction of p50^{DFSP^T} and Bcl-3 was assessed by co-transfection in 293T cells. Bcl-3 was readily detectable in p50 immunoprecipitates in contrast to almost undetectable levels with p50^{DFSP^T} (Figure 3.8 A). These mutations did not affect the nuclear localisation or DNA binding activity of p50^{DFSP^T} compared to wild type p50 (Figure 3.8 B). Interestingly, these mutations also lead to a hyper ubiquitinated phenotype similar to that seen for p50^{KRM}, which was also sensitive to inhibition by Bcl-3 (Figure 3.9 A). As with p50^{KRM}, p50^{DFSP^T} was next tested in an IL-23p19 luciferase reporter assay. Following LPS stimulation a dose dependent inhibition of reporter activity following transfection with p50 but not with p50^{DFSP^T} was observed (Figure 3.9 B).

3.3.3.2 Potential R1/R2 Binding Interface

As both p50^{KRM} and p50^{DFSP^T} mutants displayed apparent identical phenotypes, the crystal structure of these regions was further analysed. The amino acid sequence information of a protein determines its three-dimensional structure, however due to complex folding mechanisms; distinct regions of a protein's one-dimensional sequence can be adjacent on the crystal structure. The p50 RHD

folds into two domains and although Lys 249, Arg252 and Met 253 and Asp297-Thr 301 are both in the C terminus they are located at opposite sides of the three-dimensional p50 structure (Figure 3.10 B). p50 is stable only as part of an NF- κ B dimer and two p50 subunits bind asymmetrically to produce a p50 homodimer (Figure 3.10 A). When visualised as part of the complete structure, it is evident that these regions on opposite subunits complement each other to produce an interface on each side of the p50 homodimer (Figure 3.10 E). This suggests that this region may be critical in the stability/ubiquitination of p50 independent of Bcl-3.

A

R2	Peptide	Corresponding p50 residue	18-mer Peptide Sequence
	94	280-297	IRFYEEEENGGVWEGFG <u>D</u>
	95	283-300	YEEEENGGVWEGFG <u>D</u> FSP
	96	286-303	EENGGVWEGFG <u>D</u> FSP <u>T</u> DV
	97	289-306	GGVWEGFG <u>D</u> FSP <u>T</u> DVHRQ
	98	294-309	WEGFG <u>D</u> FSP <u>T</u> DVHRQFAI

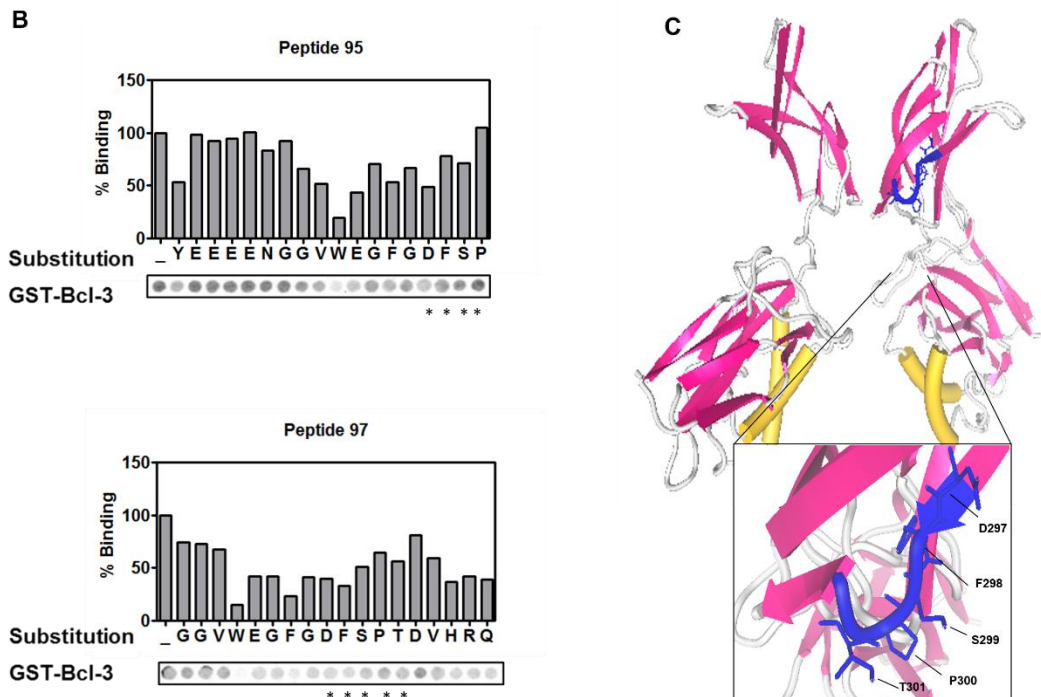
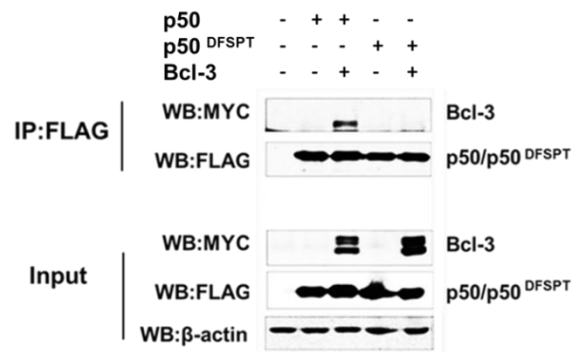


Figure 3.7 Alanine substitution analysis of Bcl-3 binding Region R2.

(A) Sequences of peptides 94-98 of p50 region 2 are shown with amino acids Asp297, Phe298, Ser299, Pro300 and Thr301 underlined. (B) The 18 amino acids of p50-derived peptides 95 and 97 were sequentially substituted with alanine and probed with GST-Bcl-3. Bcl-3 binding was quantified by densitometry and represented as a percentage binding of the control parent peptide. Substitution of amino acids Asp297, Phe298, Ser299, Pro300 and Thr301 (denoted with *) resulted in a decrease of $\geq 50\%$ in Bcl-3 binding and are represented on the p50 crystal structure in (C). Murine p50 amino acid numbering (A-C).

A



B

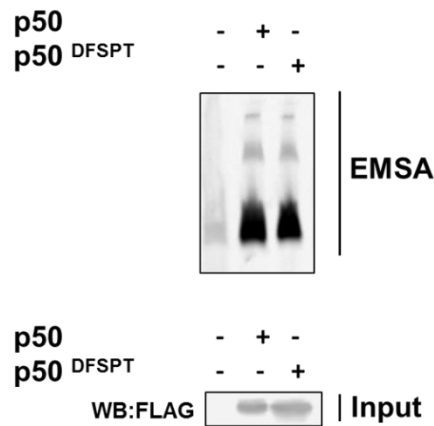


Figure 3.8 Asp 297, Phe 298, Ser 299, Pro 300 and Thr 301 of p50 are required for interaction with Bcl-3.

(A) HEK293T cells were transfected as indicated with pRK5-p50-FLAG(p50) or pRK5-p50-FLAG in which Asp 297, Phe 298, Ser 299, Pro 300 and Thr 301 of p50 are mutated to alanine (p50^{DFSP}) with or without pcDNA3.1-Bcl-3-MYC (Bcl-3). Whole cell lysates were immunoprecipitated (IP) with anti-FLAG and analysed by western blot (WB) with the indicated antibodies. Immunoblotting with anti-β-actin was used as a loading control. (B) HEK293T cells were transfected with expression plasmids as indicated. Nuclear extracts were prepared from the transfected cells and tested in an Electrophoretic Mobility Shift Assay (EMSA) using the consensus NF-κB binding nucleotide. Nuclear inputs were analysed by WB with anti-FLAG.

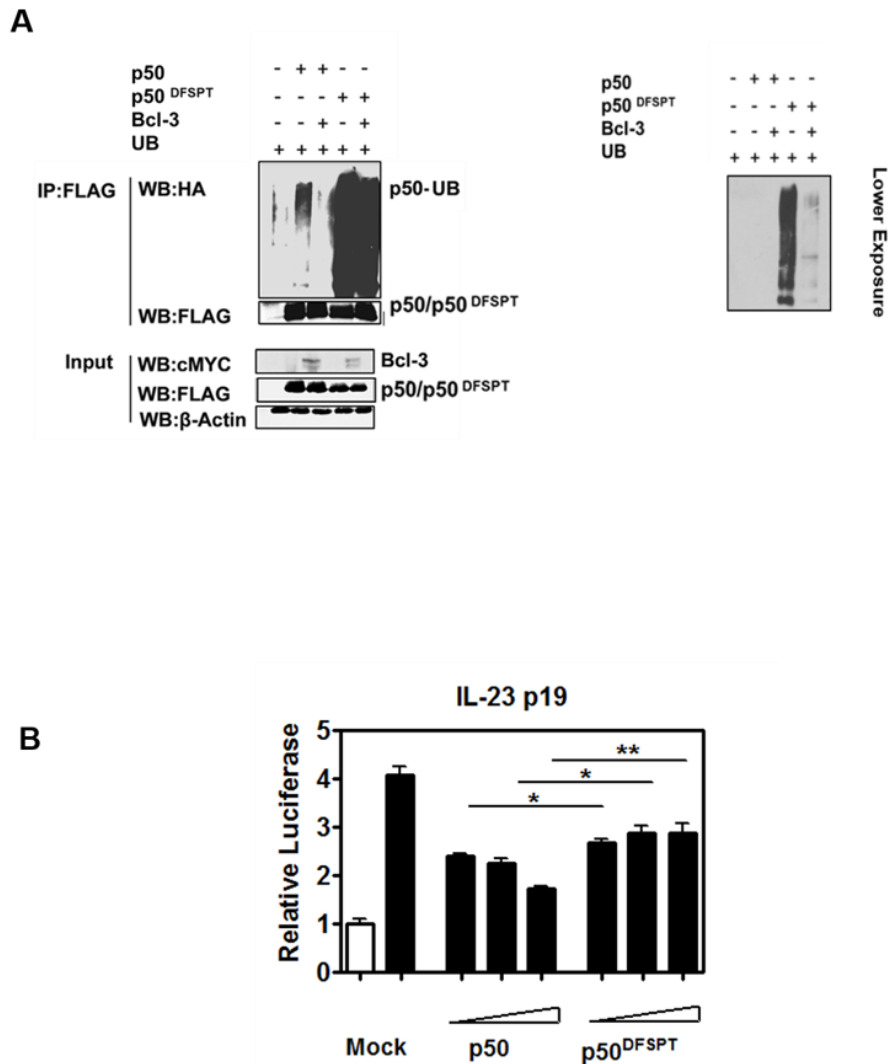


Figure 3.9 p50^{DFSP} emulates p50^{KRM}.

(A) HEK293T cells were transfected as indicated with pRK5-p50-FLAG(p50) or pRK5-p50-FLAG in which Asp 297, Phe 298, Ser 299, Pro 300 and Thr 301 of p50 are mutated to alanine (p50^{DFSP}) with or without pcDNA3.1-Bcl-3-MYC (Bcl-3). p50/p50^{DFSP} ubiquitination was determined by IP from whole cell lysates with anti-FLAG and WB with anti-HA for HA-ubiquitin. (B) RAW 264.7 cells were transiently transfected with the pLucp19 plasmid and with empty expression vector or expression vectors containing increasing amounts (1.25, 2.5 and 5ng) of p50 or p50^{DFSP} for 24 hours and cultured with or without 100 ng/ml LPS for an additional 8 hours before luciferase activity was measured. IL23 p19 reporter activity was determined as in Figure 3.6. Transfections were performed in triplicate and data shown are means + SEM and are representative of independent experiments. Statistical significance between corresponding p50 and p50^{DFSP} mutant reporter activities was determined by Student's t test; P<0.05 (*), P<0.01 (**), P<0.001(***)

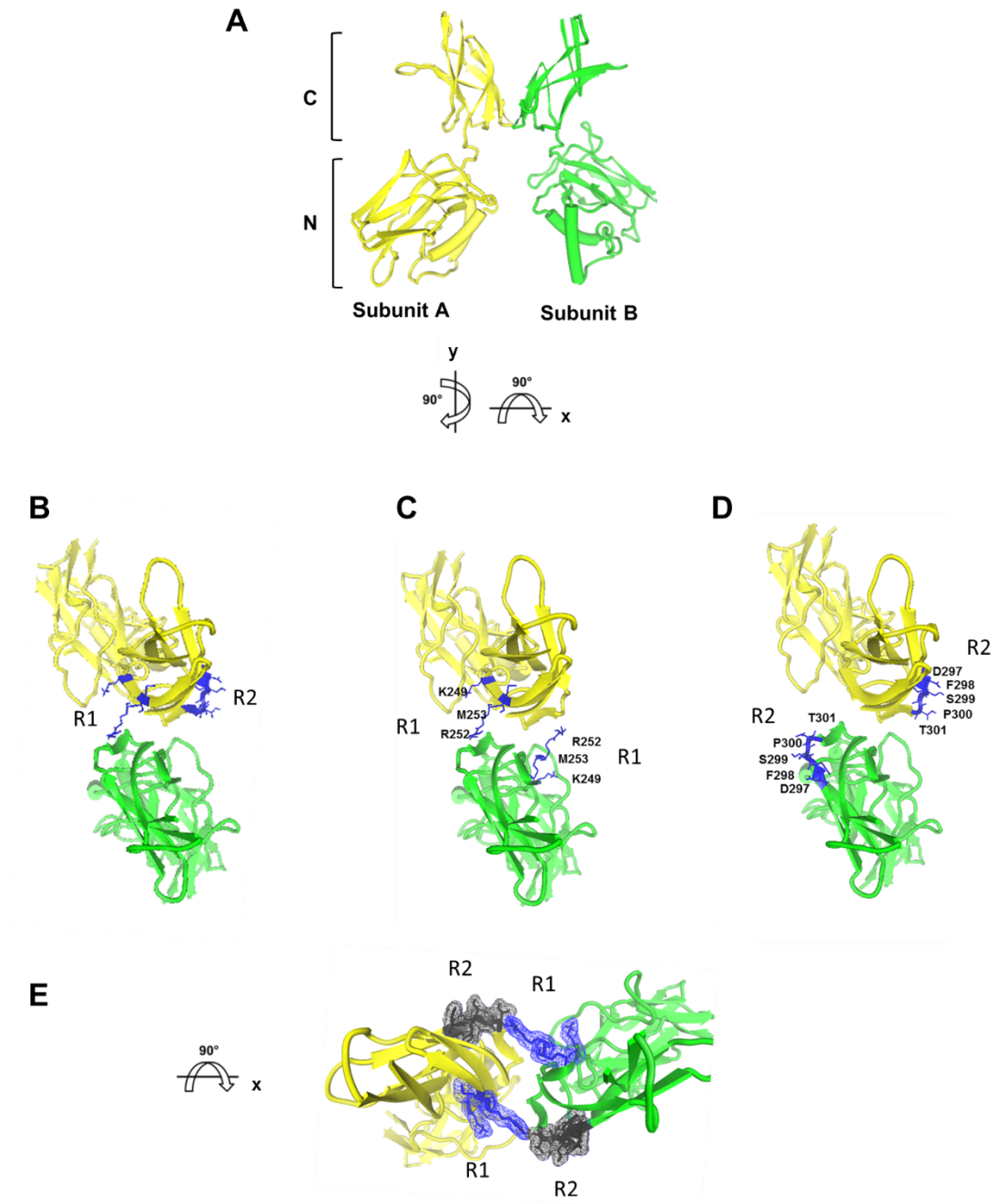


Figure 3.10 Potential R1/R2 binding interfaces of p50 homodimer.

(A) Amino (N)- and Carboxyl (C)- termini of subunit A (yellow) and B (green) of the p50 homodimer (murine). (B-D) Top view of dimer rotated 90° on its y- axis. (B) Region R1 and R2 of subunit A shaded in blue. (C) Amino acids of region R1 indicated on both subunits A and B. (D) Amino acids of region R2 indicated on both subunits A and B. (E) Detailed top view of R1/R2 interface.

3.3.4 Regulation of p50 Ubiquitination by Tyrosine 316

Based on the alanine scanning arrays of peptides 103 and 105 a three amino acid motif, KYK in loop 5 of p50 appeared to be a potential Bcl-3 binding region. Individual mutation of Lys315 and Lys317 to alanine in the substitution array reduced Bcl-3 binding by at least 50% (Figure 3.11 B). A number of mutants (p50^{K315A,K317A}, p50^{Y316A} and p50^{Y316F}) of this region were made with various phenotypes each characterised below.

3.3.4.1 *p50 Lys 315 and Lys 317 are not essential for interaction with Bcl-3*

A mutant of p50 in which Lys 315 and Lys 317 were mutated to alanine (p50^{K315A,K317A}) retained the ability to interact with Bcl-3. Reduced levels of Bcl-3 immunoprecipitated with p50^{K315A,K317A} however this correlates with decreased expression of Bcl-3 when co-transfected with this mutant. Co-immunoprecipitation with increasing levels of Bcl-3 demonstrated that p50^{K315A,K317A} interacted dose dependently with Bcl-3 similar to wild type p50 (Figure 3.12 A). Although this mutation had no effect on Bcl-3 binding, the ubiquitination of this mutant was significantly reduced (Figure 3.12 B). This reduction of ubiquitination was not due to a defect in DNA binding as p50^{K315A,K317A} bound to an NF- κ B probe with similar levels to wild type p50 (Figure 3.12 C). Previous data generated in the lab in which Lys 315 and Lys 317 were mutated to arginine, another positively charged, polar, amino acid showed no reduction in ubiquitination. This suggested that neither lysine was directly ubiquitinated or that this defect was due to a possible structural change or alternation in the interaction with the ubiquitination machinery.

3.3.4.2 *Tyr 316 is critical for negative regulation of p50 ubiquitination*

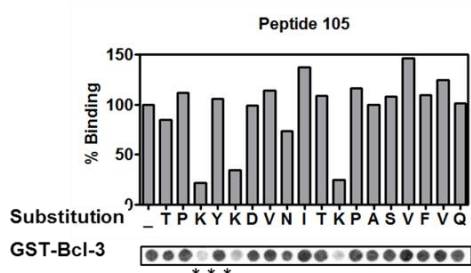
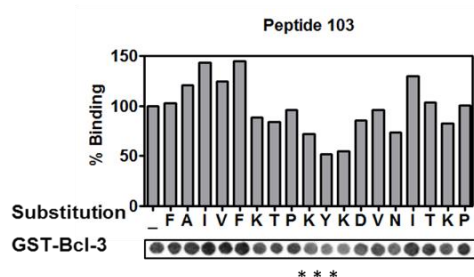
To further elucidate the role of this region in regulating p50 ubiquitination Tyr 316 was mutated to alanine (p50^{Y316A}). Surprisingly p50^{Y316A} was ubiquitinated to an even greater extent than wild type p50 as opposed to a reduction as seen again with p50^{K315A,K317A} (Figure 3.13 A). Tyrosine contains a bulky aromatic side chain which is completely absent in alanine, therefore a second Tyr 316 mutant

in which tyrosine was mutated to phenylalanine p50^{Y316F} was made. As with tyrosine, phenylalanine contains a large benzyl side chain, but it does not contain a hydroxyl group, essentially a non phosphorylatable tyrosine. This version of p50 was also hyper-ubiquitinated compared to wild type p50 (Figure 3.13 B). A double mutant, p50^{K315A,Y316A,K317A} was also hyper ubiquitinated and was unable to inhibit LPS induced IL23p19 reporter activity as effectively wild type p50 (Figure 3.13 C). Collectively these data suggest that Tyr 316 is essential for negatively regulating p50 ubiquitination. As the tyrosine to phenylalanine mutation (p50^{Y316F}) did not rescue the hyper-ubiquitination phenotype of p50^{Y316A}, this suggests that phosphorylation at Tyr 316 may play a role in blocking ubiquitination of p50.

A

R3	Peptide	Coresponding p50 residue	18-mer Peptide Sequence
	100	298-315	<u>FS</u> PTDVHRQFAIVFK <u>TPK</u>
	101	301-318	TDVHRQFAIVFK <u>TPKYK</u>
	102	304-321	HRQFAIVFKTPKYK <u>DVNI</u>
	103	307-324	FAIVFKTPKYK <u>DVNITKP</u>
	104	311-327	VFKTPKYK <u>DVNITKPASV</u>
	105	314-330	TPKYK <u>DVNITKPASVFVQ</u>

B



C

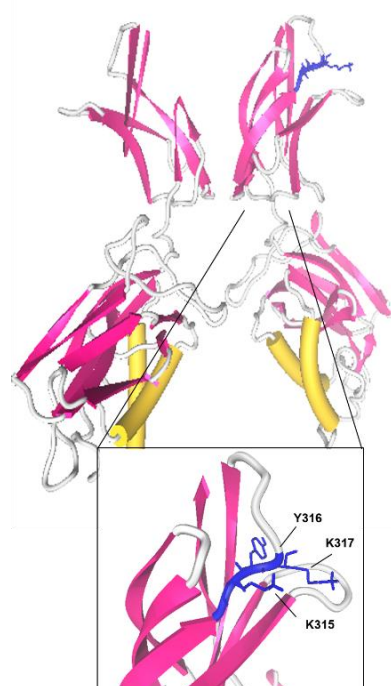


Figure 3.11 Alanine substitution analysis of Bcl-3 binding Region R3.

(A) Sequences of peptides 100-105 of region R3 are shown and Lys315, Tyr316 and Lys137 underlined. (B) The 18 amino acids of p50-derived peptides 103 and 105 were sequentially substituted with alanine and probed with GST-Bcl-3. Bcl-3 binding was quantified by densitometry and represented as a percentage binding of the control parent peptide. Substitution of amino acids Lys315, Tyr316 and Lys137 (denoted with *) resulted in a decrease of $\geq 50\%$ of Bcl-3 in Bcl-3 binding and are represented on p50 crystal structure in (C). Murine amino acid numbering (A-C).

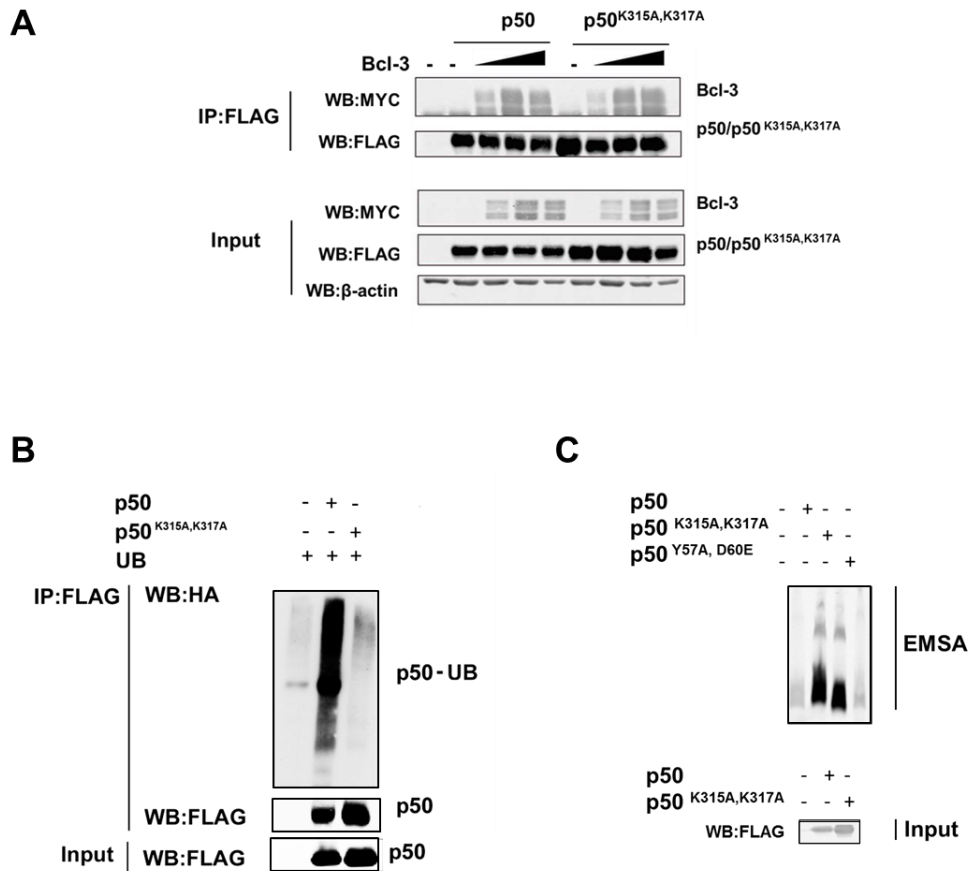


Figure 3.12 p50 Lys 315 and Lys 317 are not required for interaction with Bcl-3.

(A) HEK293T cells were transfected as indicated with pRK5-p50-FLAG(p50) or pRK5-p50-FLAG in which in which Lys 315 and 317 were mutated to alanine (p50^{K315A,K317A}) with or without increasing concentrations of pcDNA3.1-Bcl-3-MYC (Bcl-3). The total amount of plasmid was constant across all samples by adjusting the amount of empty vector. (B) p50/p50^{K315A,K317A} ubiquitination was determined by IP from whole cell lysates with anti-FLAG and WB with anti-HA for HA-ubiquitin. (C) HEK293T cells were transfected as indicated with p50, p50^{K315A,K317A} or p50 in which in which Tyr 57 and Asp 60 were mutated to alanine and glutamic acid respectively (p50^{Y57A,D60E}). Nuclear extracts were prepared from the transfected cells and tested in an Electrophoretic Mobility Shift Assay (EMSA) using the consensus NF-κB binding nucleotide. Nuclear inputs were analysed by WB with anti-FLAG.

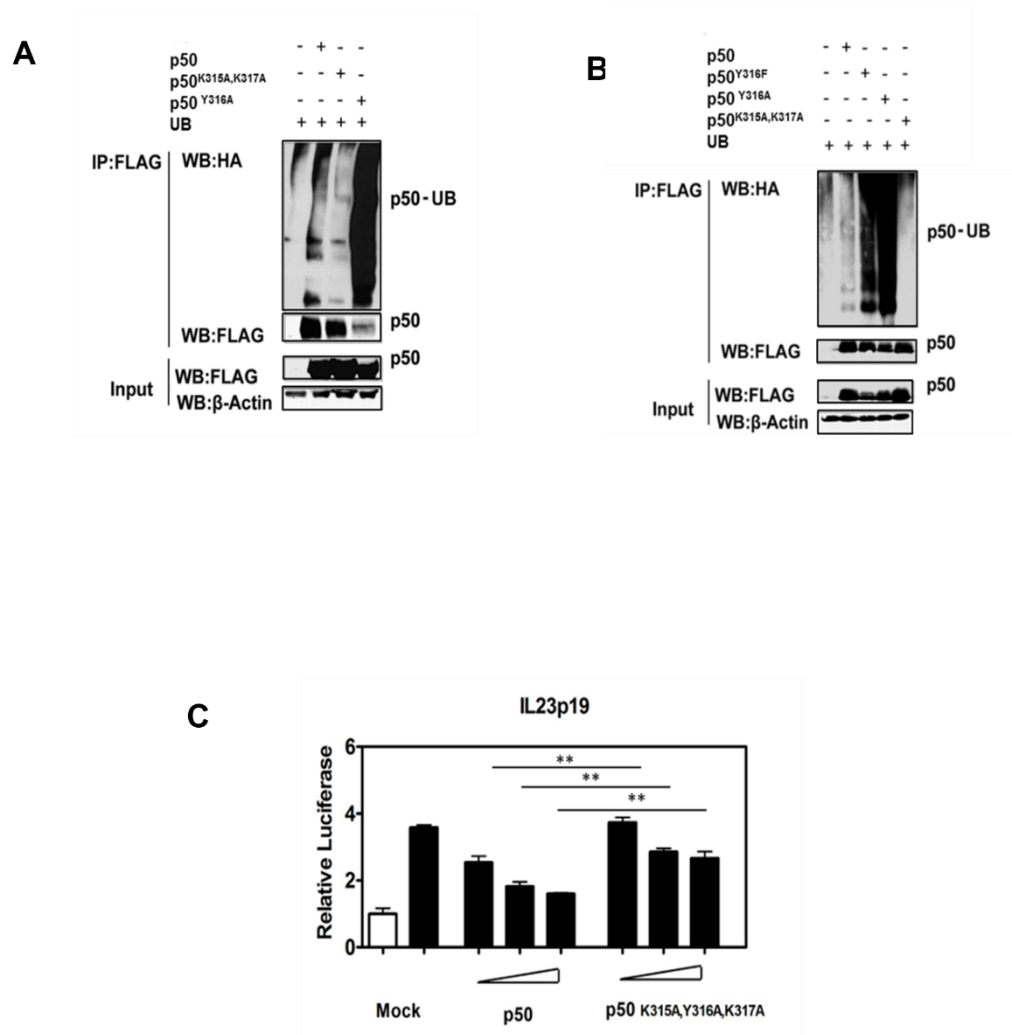


Figure 3.13 KYK motif regulates p50 ubiquitination.

(A,B) HEK293T cells were transfected as indicated with pRK5-p50-FLAG(p50) or pRK5-p50-FLAG in which Tyr 316 was mutated to alanine (p50^{Y316A}) or phenylalanine (p50^{Y316F}). p50^{Y316A} and p50^{Y316F} ubiquitination was determined by IP from whole cell lysates with anti-FLAG and WB with anti-HA for HA-ubiquitin. (C) RAW 264.7 cells were transiently transfected with the pLucp19 plasmid and with empty expression vector or expression vectors containing increasing amounts (1.25,2.5 and 5ng) of p50, p50^{K315A,K317A} or p50^{K315A,Y316A,K317A} for 24 hours and cultured with or without 100 ng/ml LPS for an additional 8 hours before luciferase activity was measured. IL23p19 reporter activity was determined as in Figure 3.6. Transfections were performed in triplicate and data shown are means + SEM and are representative of independent experiments. Statistical significance between corresponding p50 and p50^{K315A,Y316A,K317A} mutant reporter activities was determined by Student's t test; P<0.05 (*), P<0.01 (**), P<0.001(***)).

3.3.5 Inhibition of transcription by Bcl-3 Requires Interaction with NF- κ B p50

3.3.5.1 Alanine substitution analysis of Bcl-3 binding Region R4

Alanine scanning arrays of spots 115, 117, 119 and 121 were generated as in figure 3.5. Bcl-3 binding was detected by immunoblotting and represented as a percentage binding of the control parent peptide (Figure 3.14 B). Substitution of Arg359, Lys360 and Arg361 resulted in a large decrease of at least 50% in Bcl-3 binding, confirmed by independent arrays.

3.3.5.2 Surface exposure prediction of Arg359, Lys360, Arg361

The identified residues lie in the extreme C-terminal region of the RHD of p50 and are not represented in the currently available structures of p50. However, hydrophobicity analysis of the primary structure of p50 indicated that these residues are in a region of low hydrophobicity (Cowan and Whittaker, 1990) (Figure 3.15 A). Hydrophobicity of an amino acid is correlated with its average surface exposure and typically polar residues tend to occur at the surface of a folded protein. The solvent accessibility of this region was also analysed using Predictprotein (Rost et al., 2004) a profile based neural network secondary structure prediction programme. This method predicted that Arg359, Lys360, Arg361 are exposed residues, exposed Arg359 and Lys360 was also confirmed by NetSurfP (Petersen et al., 2009) an independent prediction programme (Figure 3.15 B). Using Phyre2 (Kelley and Sternberg, 2009) homology modelling, a predicted three-dimensional structure of the entire p50 protein was generated (Figure 3.15 C). Together with the hydrophobicity index, these prediction tools suggest that residues Arg359, Lys360, Arg361 are exposed and likely to be available for interaction with Bcl-3.

A

R4	Peptide	Corresponding p50 residue	18-mer Peptide Sequence
	115	337-354	<u>K</u> PFLYYPEIKDKEEVQRK
	116	343-360	LYYPEIKDKEEVQR <u>K</u> RQK
	117	349-366	PEIKDKEEVQR <u>K</u> RQKLMP
	118	352-369	KDKEEVQR <u>K</u> RQKLMPNFS
	119	355-372	EEVQR <u>K</u> RQKLMPNFSDF
	120	358-375	QR <u>K</u> RQKLMPNFSDFGGG
	121	361-378	RQKLMPNFSDFGGG <u>S</u> GA

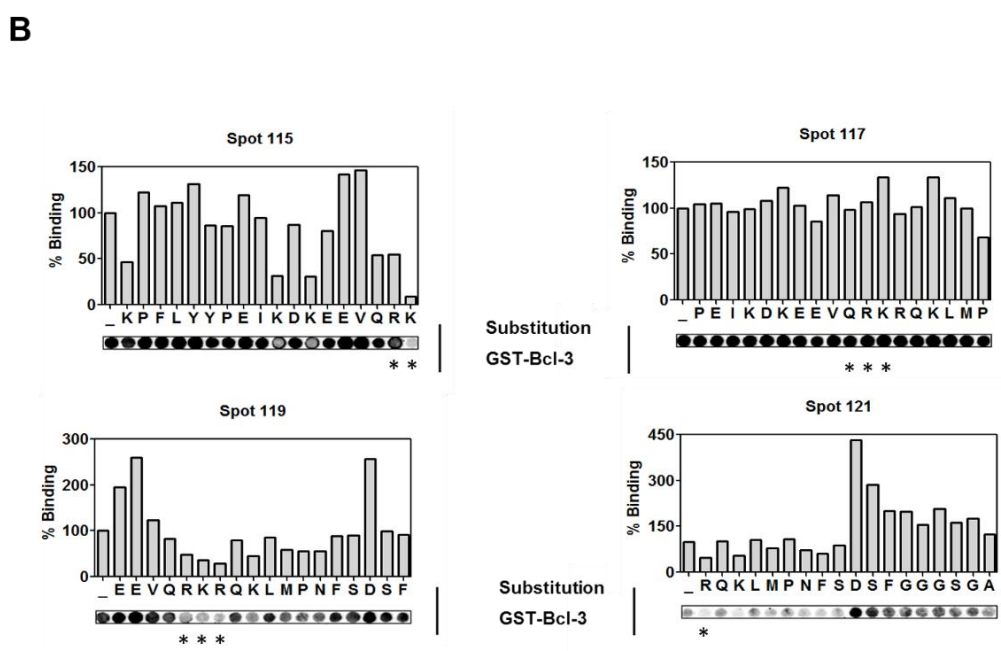


Figure 3.14 Alanine substitution analysis of Bcl-3 binding Region R4.

(A) Sequences of peptides 113-121 of R4 are shown and Arg359, Lys360 and Arg361 underlined. (B) The 18 amino acids of p50-derived peptides 115,117,119 and 121 were sequentially substituted with alanine and a peptide arrays probed with GST-Bcl-3. Bcl-3 binding was quantified by densitometry and represented as a percentage binding of the control parent peptide. Substitution of amino acids Arg359, Lys360 and Arg361 with alanine (*) resulted in a decrease of $\geq 50\%$ of Bcl-3 binding. Murine amino acid numbering (A-B).

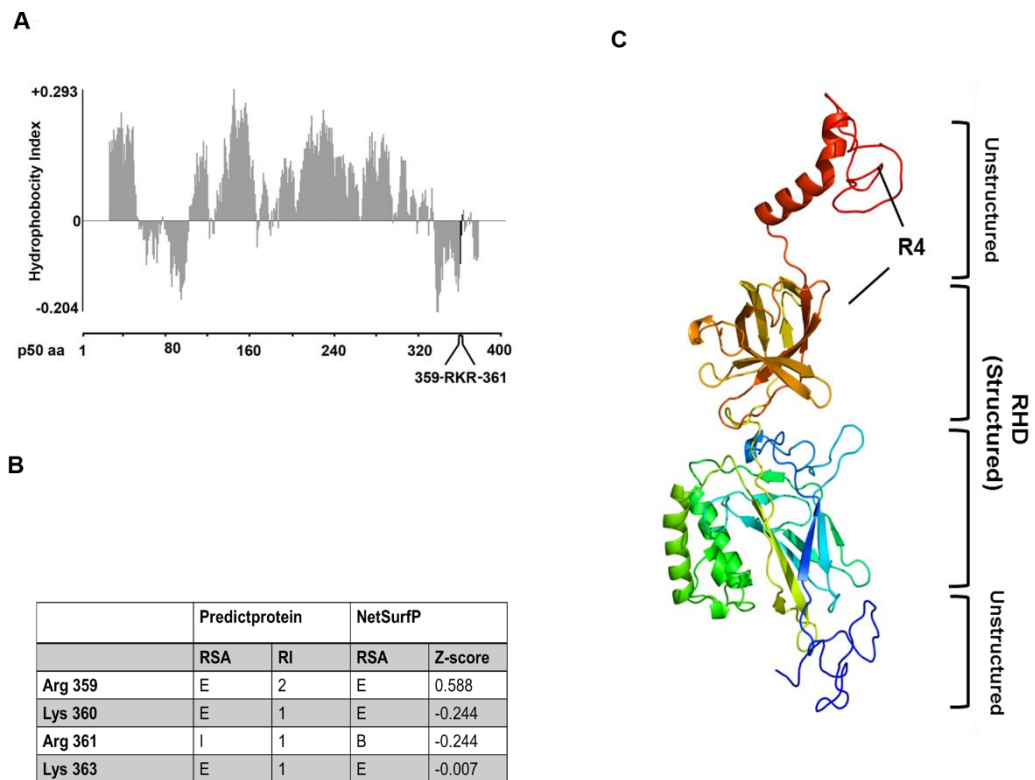


Figure 3.15 Surface Exposure prediction of Arg359, Lys360 and Arg361.

(A) Hydrophobicity analysis of p50 using Cowan and Whittaker Hydrophobicity scale (Cowan and Whittaker, 1990), positive values are hydrophobic. Amino acids 359-361 highlighted. (B) Solvent accessibility analysis of amino acids 359-361. Predictprotein (Rost et al., 2004) relative solvent accessibility (RSA) in 3 states: B=Buried 0-9%, I = intermediate 9-36%, and E=exposed 36-100% exposure. Reliability index (RI) for RSA prediction (0=low to 9=high). NetSurfP (Petersen et al., 2009) RSA in 2 states B=buried < 25% and E=exposed >25% exposure. Z-fit score for RSA prediction.(C) Hypothetical model of the entire p50 subunit using Phyre2 (Kelley and Sternberg, 2009) with R4 indicated. Murine amino acid numbering (A-C).

3.3.5.3 Arg359, Lys360 and Arg361 are essential for interaction with Bcl-3

We next generated a mutant of p50 in which Arg359, Lys360 and Arg361 were mutated to alanine (p50^{RKR}) and assessed the contribution of these residues to Bcl-3 interaction by co transfection in 293T cells. Bcl-3 was undetectable in immunoprecipitates of p50^{RKR} while Bcl-3 was readily detectable in immunoprecipitates of wild type p50 (Figure 3.16 A). Additionally the binding of p50^{RKR} mutant with purified GST-Bcl-3 was evaluated in a GST-pull down assay. As expected, GST-Bcl-3 pull-down readily purified p50, however, p50^{RKR} protein was not detectable following GST-Bcl-3 pull-down from p50^{RKR} containing lysates (Figure 3.16 B).

3.3.5.4 p50RKR retains p50WT properties of nuclear translocation, dimerisation and DNA binding

In order to rule out an indirect effect of Arg359, Lys360 and Arg361 mutation on the ability of the p50^{RKR} mutant to interact with Bcl-3 additional characterisation of p50^{RKR} mutant protein were out. Homodimerisation of p50^{RKR} was assessed by co-transfection of 293T cells with FLAG-tagged and Myc-tagged p50^{RKR} or FLAG-tagged and MYC tagged p50. Lysates were immunoprecipitated using anti-FLAG antibody and immunoblotted with anti-MYC antibody. This analysis demonstrated no significant differences in the formation of homodimers by p50^{RKR} when compared to wild type p50 protein (Figure 3.17A).

We next assessed the heterodimerisation of p50^{RKR} using a similar approach. MYC- tagged p50 or p50^{RKR} was co-expressed with FLAG-tagged NF- κ B p65 and lysates immunoprecipitated using anti-FLAG antibody. Immunoblot analysis of FLAG-p65 immunoprecipitates demonstrated no differences in the levels of p50^{RKR} co-immunoprecipitating with p65 relative to p50 indicating that the p50^{RKR} mutation has no effect on heterodimerisation with p65 (Figure 3.17 B). I κ B α has a high affinity for p65:p50 heterodimers and so the levels of endogenous I κ B α in p65 immunoprecipitates from cells expressing p50 or p50^{RKR} were also assessed. No significant differences in the amount of I κ B α co-immunoprecipitating with p65 was found between cells expressing p50 or p50^{RKR} (Figure 3.17 B). Similarly, no difference in the levels of p50^{RKR} interacting with p105 relative to p50 in cells co-transfected with p105 and p50 WT or p50^{RKR} were observed, as assessed by immunoprecipitation (Figure 3.17 C). Together these

data demonstrate that the p50^{RKR} mutation does not alter p50 dimerisation or interaction with IκBα or p105 proteins.

The amino acids 359 to 361 of p50 have previously been indicated to function in the nuclear translocation of p50 (Latimer et al., 1998). Since Bcl-3 is predominant nuclear in localisation it was important to rule out that lack of nuclear p50^{RKR} prevented the interaction with Bcl-3 in co-transfected cells. To address this, nuclear and cytoplasmic fractions of cells transfected with p50^{RKR} or p50 were generated and analysed protein levels by immunoblot. As demonstrated in Figure 3.18 A, subcellular fractionation revealed that p50^{RKR} translocated to the nucleus to similar levels as wild type p50, indicating that the mutation of the amino acids 359-361 to alanine does not disrupt the nuclear localisation of p50. This data was supported by an analysis of the DNA binding activity of p50^{RKR} in which no significant differences between wild type p50 and p50^{RKR} DNA binding tested by EMSA (Figure 3.18 B). Taken together, these data reveal that the p50^{RKR} mutant is defective in binding to Bcl-3 but retains the p50 WT properties of nuclear translocation, dimerisation and DNA binding.

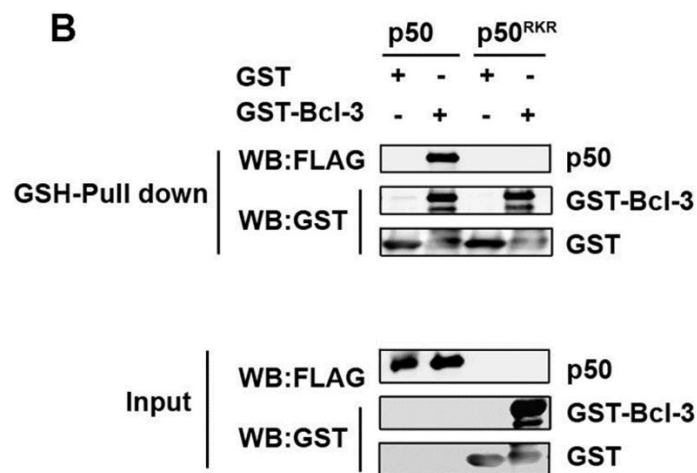
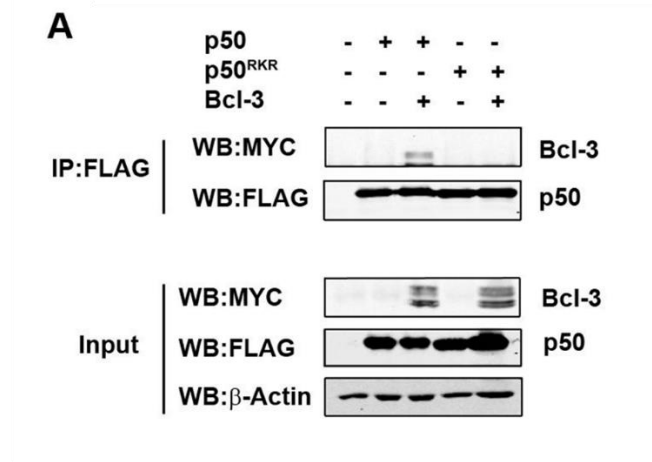


Figure 3.16 Arg359, Lys360 and Arg361 of p50 are essential for interaction with Bcl-3.

(A) HEK293T cells were transfected as indicated with pRK5-p50-FLAG (p50) or pRK5-p50-FLAG in which Arg359, Lys360 and Arg361 were mutated to alanine (p50^{RKR}) with or without pcDNA3.1-Bcl-3-MYC (Bcl-3). Whole cell lysates were immunoprecipitated (IP) with anti-FLAG and analysed by western blot (WB) with the indicated antibodies. Immunoblotting with anti-β-actin was used as a loading control. (B) Purified bacterial recombinant GST or GST-Bcl3 was incubated with a whole cell lysate overexpressing p50 or p50^{RKR} and were affinity purified with GSH agarose. Pull down complexes were analysed by western blot with anti-FLAG and anti-GST antibodies.

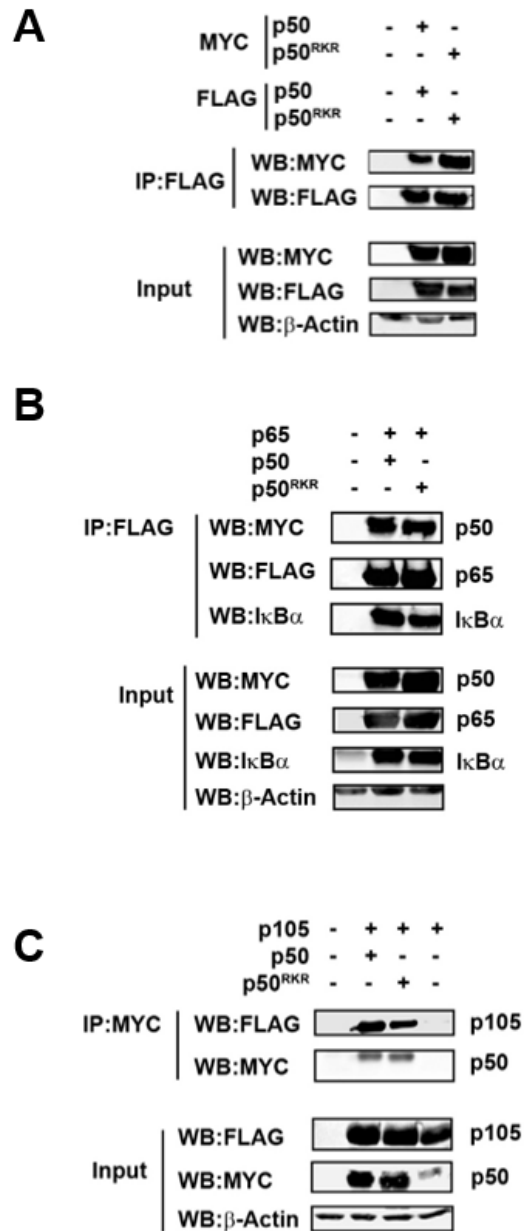


Figure 3.17 Mutation of Arg 359, Lys 360 and Arg 361 does not affect the dimerisation properties of p50.

p50^{RKR} can form homodimers and heterodimers with p65 and p105. (A) HEK293T cells were transfected as indicated with pRK5-p50-FLAG and pEF4a-p50-MYC (p50) or pRK5-p50-FLAG and pEF4a-p50-MYC in which Arg359, Lys360 and Arg361 of p50 were mutated to alanine (p50^{RKR}). FLAG-p50 or FLAG-p50^{RKR} were immunoprecipitated (IP) from whole cell lysates with anti-FLAG and analysed by western blot (WB) with anti-MYC for MYC-p50 and p50^{RKR}. (B) HEK293T cells were transfected as indicated with pRK5-p65-FLAG (p65) and pEF4a-p50-MYC (p50) or pEF4a-p50^{RKR}-MYC (p50^{RKR}). FLAG-p65 was immunoprecipitated (IP) from whole cell lysates with anti-FLAG and analysed by western blot (WB) with anti-MYC for MYC-p50 and p50^{RKR}. (C) HEK293T cells were transfected as indicated with pRK5-p105-FLAG (p105) and pEF4a-p50-MYC (p50) or pEF4a-p50-pEF4a-p50^{RKR}-MYC (p50^{RKR}). FLAG-p50 or FLAG-p50^{RKR} were immunoprecipitated (IP) from

whole cell lysates with anti-MYC and analysed by western blot (WB) with anti-FLAG for p105.

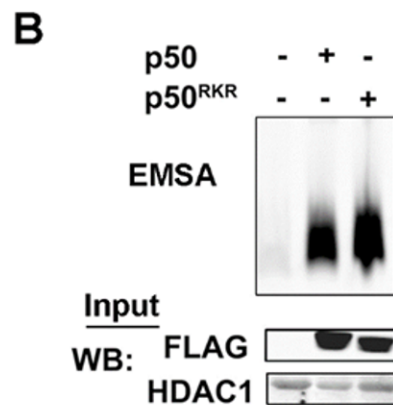
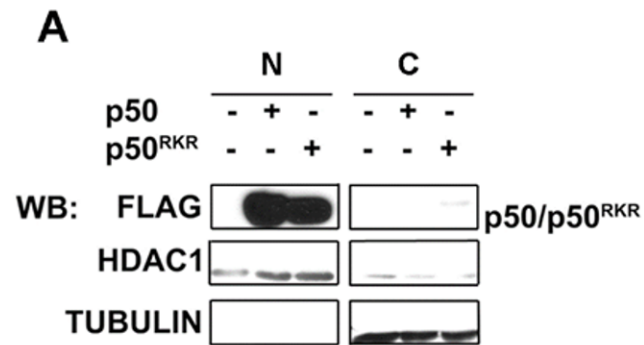


Figure 3.18 p50^{RKR} can bind DNA and translocate to the nucleus.

(A) HEK293T cells were transfected as indicated with pRK5-p50-FLAG or pRK5-p50-FLAG in which Arg359, Lys360 and Arg361 of p50 were mutated to alanine (p50^{RKR}). Nuclear (N) and cytoplasmic (C) extracts were prepared and fractions were analysed by Western blot (WB) with anti-FLAG for p50 and p50^{RKR}. (B) HEK293T cells were transfected as indicated with p50 or p50^{RKR}. Nuclear extracts were prepared and tested in an Electrophoretic Mobility Shift Assay (EMSA) using the consensus NF- κ B binding nucleotide.

3.3.5.5 *Bcl-3 inhibits ubiquitination through interaction with p50*

The ubiquitination of p50 is significantly increased in *Bcl3*^{-/-} cells and overexpression of Bcl-3 inhibits p50 ubiquitination (Carmody et al., 2007b). To establish whether the inhibition of p50 ubiquitination by Bcl-3 requires interaction with p50, a ubiquitination assay was performed in 293T cells transfected with HA-tagged ubiquitin, p50 or p50^{RKR}, with or without Bcl-3. In contrast to the complete inhibition of p50 ubiquitination by Bcl-3, the expression of Bcl-3 failed to inhibit the ubiquitination of p50^{RKR} (Figure 3.19 A). These data demonstrate that the interaction of Bcl-3 with p50 is required for Bcl-3 mediated inhibition of p50 ubiquitination. p50 ubiquitination leads to degradation by the proteasome and thereby controlling p50 protein stability. Next, the stability of p50^{RKR} was assessed by treating p50 or p50^{RKR} expressing cells with the protein synthesis inhibitor cyclohexamide and monitoring protein levels over a short time period by immunoblotting. This analysis demonstrated that p50^{RKR} is significantly less stable than p50 and has a half-life less than 50% that of wild type p50 (Figure 3.19 B). These data demonstrate that interaction with Bcl-3 is critical for the regulation of p50 ubiquitination and protein stability.

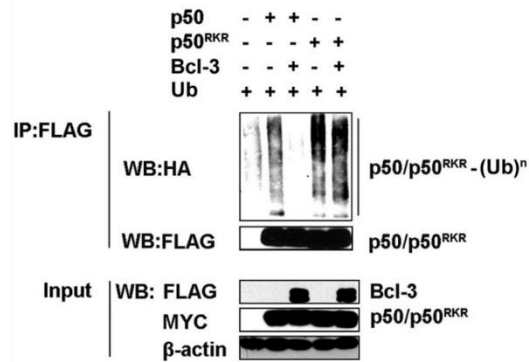
3.3.5.6 *Arg359, Lys360 and Arg361 of p50 are critical for negative regulation of NF-κB dependent gene expression*

It has been proposed that Bcl-3 regulates NF-κB mediated transcription through inhibition of p50 homodimer ubiquitination and proteasomal degradation. However, additional p50-independent functions of Bcl-3 in regulating transcription can not be ruled out in studies employing *Bcl3*^{-/-} cells. Our findings that interaction with Bcl-3 is important for the regulation of p50 ubiquitination and stability led us to examine the regulation of gene transcription by p50^{RKR}.

To investigate this, a luciferase reporter assay incorporating the NF-κB-dependent IL-23p19 gene promoter was employed (Carmody et al., 2007a). In agreement with previous reports (Muhlbauer et al., 2008), Bcl-3 expression inhibited the reporter activity in RAW 264.7 macrophage cells following stimulation with LPS. Similarly, overexpression of both p50 and p50^{RKR} inhibited LPS-induced reporter activity. However, whereas co-expression of p50 with Bcl-3 completely abolished LPS-induced reporter activity, the co-expression of

p50^{RKR} with Bcl-3 failed to inhibit reporter activity below the level seen when either are expressed alone (Figure 3.20 A). Next, dose-dependent analysis of p50 and p50^{RKR} expression on IL-23p19 reporter activity was performed by transfecting increasing, but low amounts of p50 or p50^{RKR} expression vector in *Nfkb1*^{-/-} mouse embryonic fibroblast cells (MEFs). Here a dose dependent inhibition of reporter activity following transfection with p50 but not with p50^{RKR} was observed (Figure 3.20 B). Similar results were obtained when *Nfkb1*^{-/-} MEFs were transfected with an expression vector for wild type p105 or p105 containing alanine substitutions at position 359-361 (p105^{RKR}) (Figure 3.20 C). Together these data demonstrate that the interaction between Bcl-3 and p50 is critical for the negative regulation of NF-κB target genes by both of these factors.

A



B

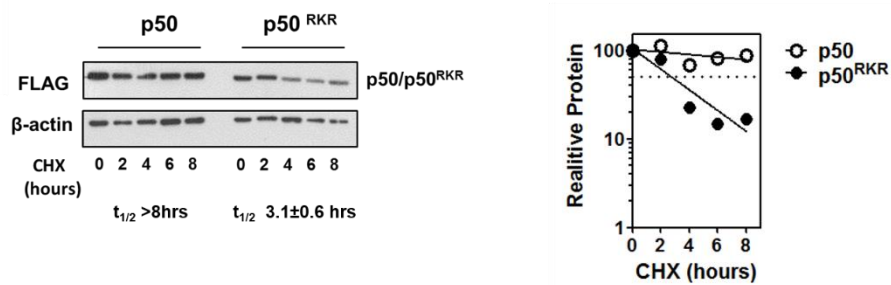


Figure 3.19 Arg359, Lys360 and Arg361 of p50 are critical for protein stability.

(A) Bcl-3 cannot block p50^{RKR} ubiquitination. HEK293T cells were transfected as indicated with pRK5-p50-FLAG or pRK5-p50-FLAG in which Arg359, Lys360 and Arg361 of p50 were mutated to alanine (p50^{RKR}). p50/ p50^{RKR} ubiquitination was determined by IP from whole cell lysates with anti-FLAG and WB with anti-HA for HA-ubiquitin. (B) Reduced half-life of p50^{RKR}. HEK293T cells were transfected with p50 or p50^{RKR}. Following 24 hours transfection cells were treated with 100ug/ml cyclohexamide (CHX) and harvested at the indicated times following treatment. For each sample p50 protein levels were quantified by densitometry and normalised with β-actin. Graph represents western blot shown. The half-life ($t_{1/2}$) of p50 and p50^{RKR} was calculated from three independent experiments and is presented as ± SD.

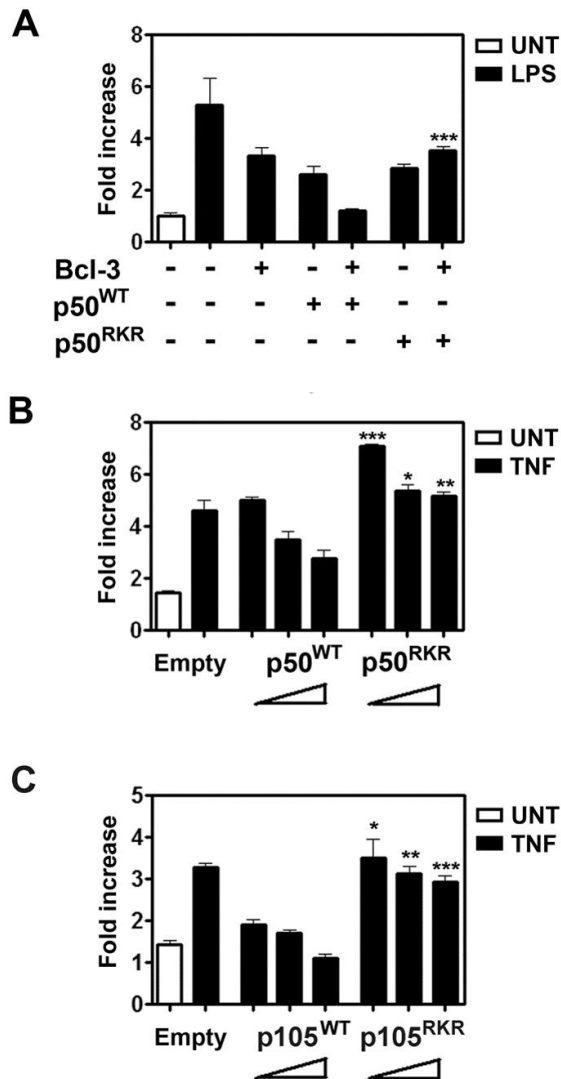


Figure 3.20 Arg359, Lys360 and Arg361 of p50 are critical for negative regulation of NF- κ B dependent gene expression.

(A) Bcl-3 is unable to synergise with p50^{RKR} to inhibit LPS induced activation of IL23 p19 reporter activity. RAW 264.7 cells were transiently transfected with the pLucp19 plasmid and with empty expression vector or pRK5-p50-FLAG or pRK5-p50-FLAG in which Arg359, Lys360 and Arg361 of p50 were mutated to alanine (p50^{RKR}) (5ng) and pcDNA3.1-Bcl3-MYC (Bcl-3) (2.5ng). Following 24 hours transfection cells were cultured with or without 100 ng/ml LPS for an additional 8 hours before luciferase activity was measured. (B,C) *Nfkb1*^{-/-} MEFs cells were transiently transfected with the pLucp19 plasmid and increasing amount of expression vectors containing p50 or p50^{RKR} (1.25,2.5 and 5ng) (B) or pEF4a-p105-Xpress or pEF4a-p105-Xpress in which Arg359, Lys360 and Arg361 of 105 were mutated to alanine p105^{RKR} (200,300 and 400ng) (C). The total amount of plasmid was constant across all samples by adjusting the amount of empty vector used. Cells were transfected for 24 hours and cultured with or without 20 ng/ml TNF for an additional 8 hours before luciferase activity were measured. IL23p19 reporter activity was determined as in Figure 3.6. Transfections were performed in triplicate and data shown are means + SEM and are representative of independent experiments Statistical significance between corresponding p50 and p50^{DFSP} mutant reporter activities was determined by Student's t test; P<0.05 (*), P<0.01 (**), P<0.001(***).

3.3.6 p105^{RKR} Expression Recapitulates *Bcl3*^{-/-} Phenotype

In order to further analyse the lack of p50:Bcl-3 complex formation in the context of an inflammatory signal, *Nfkb1*^{-/-} MEFs were reconstituted with expression vectors for p105 or p105^{RKR}. Stably transfected cells were clonally selected for equivalent expression of p105 and p105^{RKR} (Figure 3.21 A). No differences in the activation of the NF-κB pathway by TNF between p105 and p105^{RKR} cells were found as determined by IκBα phosphorylation and degradation (Figure 3.21 B). TNF-induced nuclear localisation of p50 and p65 was not significantly altered in p105^{RKR} cells relative to p105 wild type cells. However, p105^{RKR} cells had significantly reduced p50 protein levels compared to p105 cells (Figure 3.21 C), reflecting the reduced stability of p50^{RKR} (Figure 3.19 B). In agreement with over expression analysis (Figure 3.16), endogenous Bcl-3 failed to co-immunoprecipitate with p50^{RKR} in TNF stimulated cells, whereas TNF-inducible interaction with wild-type p50 was readily detectable (Figure 3.22 A). Consequently, endogenous ubiquitination of p50^{RKR} in both untreated and TNF-stimulated cells was elevated relative to p50^{WT} (Figure 3.21 B). Realtime-PCR analysis of TNF-induced gene expression revealed that p105^{RKR} cells express significantly higher levels of the NF-κB target genes *Tnf*, *IL6*, *Ccl2* and *Cxcl2* when compared to p105 wild type cells (Figure 3.21 C). This hyper-responsiveness towards TNF stimulation in p105^{RKR} cells correlates with the increased ubiquitination and reduced half-life of the p50^{RKR} protein and importantly recapitulates the hyper-responsiveness of *Bcl3*^{-/-} cells. Together these data demonstrate that interaction with Bcl-3 is essential for p50 homodimer repressor function and suggests that repression of transcription by Bcl-3 is dependent on interaction with p50 homodimers.

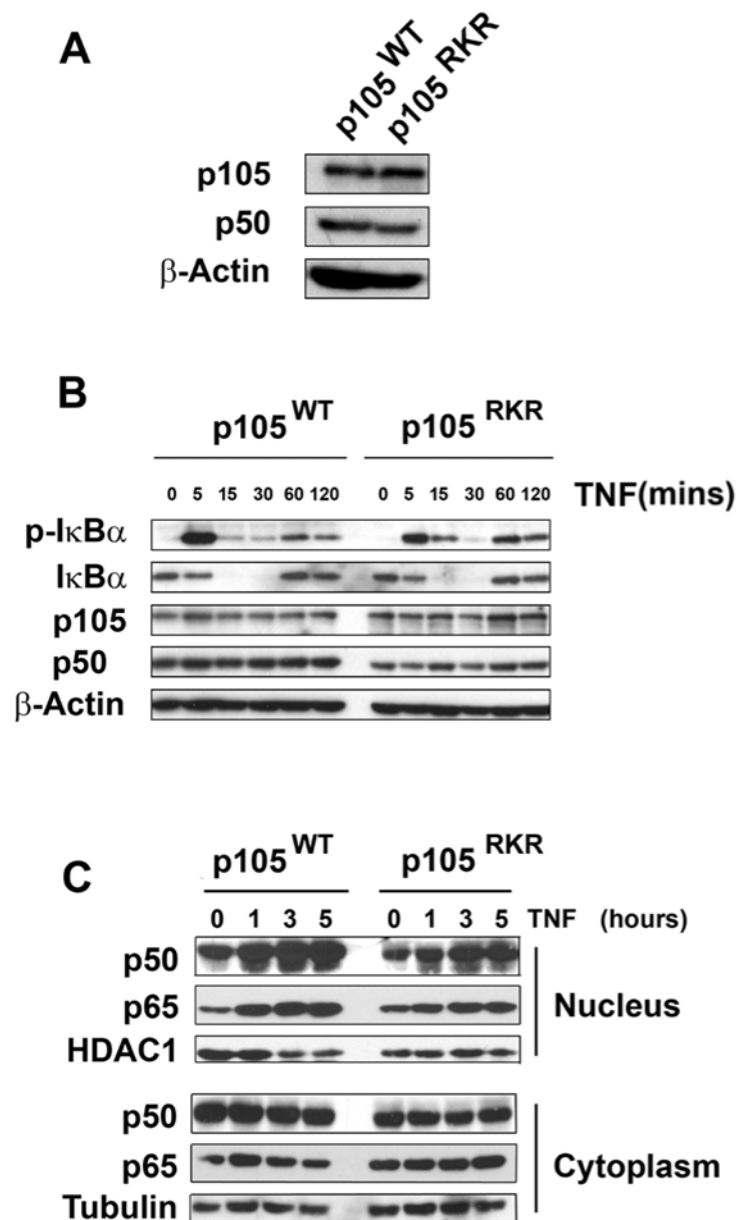


Figure 3.21 Normal upstream signalling and NF-κB nuclear translocation of p105^{RKR} MEFs.

(A) *Nfkb1*^{-/-} MEF cells were stably transfected with expression vectors encoding p105^{WT} or p105^{RKR}. (B) p105^{WT} or p105^{RKR} MEFs were stimulated with 20ng/ml TNF for the indicated times prior to lysis. Whole cell extracts were analysed by western blotting for phosphorylated IκBα and total IκBα. (C) p105^{WT} or p105^{RKR} MEFs were stimulated with 20ng/ml TNF for the indicated times prior to lysis. Nuclear and cytoplasmic extracts were prepared and analysed for p50 and p65 proteins by western blot.

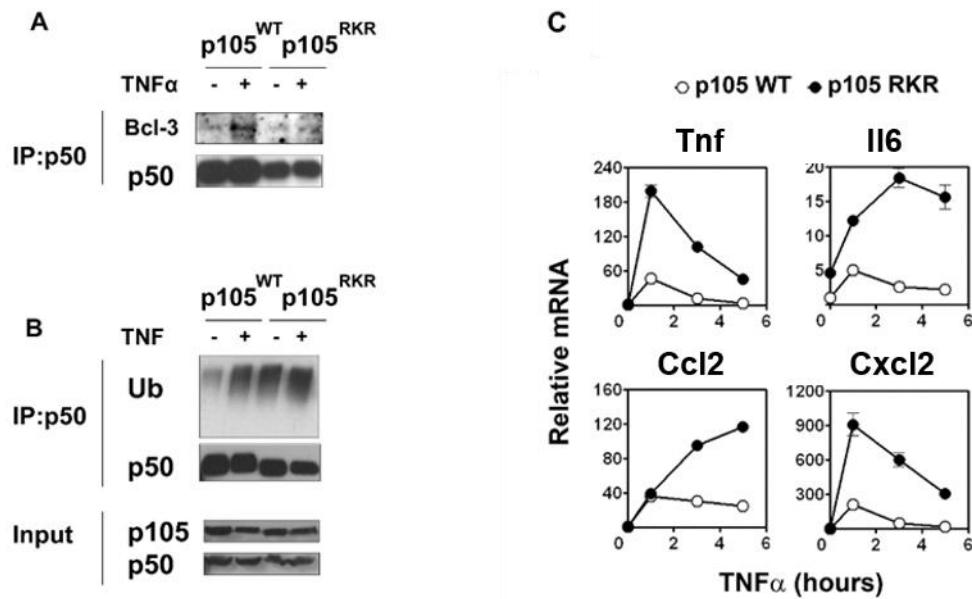


Figure 3.22 p105^{RKR} MEFs are hyper-responsive to TNF stimulation.

(A) p105^{WT} or p105^{RKR} MEFs were left untreated (-) or stimulated with 10ng/ml TNF (+) for 1 hour. Following stimulation cells were pre-treated with 20μM MG132 for 30 minutes prior to harvest. p50^{WT} and p50^{RKR} were immunoprecipitated (IP) from whole cell lysates and analysed by western blot (WB) with anti-Bcl-3 antibody for endogenous Bcl-3. (B) Endogenous ubiquitination assay. p105^{WT} or p105^{RKR} MEFs were treated as in (A). p50^{WT} and p50^{RKR} were immunoprecipitated (IP) from whole cell lysates and ubiquitination was determined by western blot (WB) with anti-ubiquitin (Ub). (C) p105^{WT} or p105^{RKR} MEFs were stimulated with 20ng/ml TNF. Gene expression levels were determined by real-time PCR. Data shown are means ± SEM of replicate samples and are representative of three independent experiments.

3.3.7 Ubiquitination of p50 at Lysine 128

p50 homodimer binding to DNA is a critical step which triggers its ubiquitination, leading to its subsequent degradation (Carmody et al., 2007b). TLR4 activation triggers p50 ubiquitination and we hypothesise that this ubiquitination is required for NF- κ B mediated expression of inflammatory genes following TLR stimulation (Carmody et al., 2007b). Ubiquitination of p65 has previously been shown to play an essential role in the regulation of NF- κ B dependent gene activity and post-transcriptional repression of the NF- κ B response (Bosisio et al., 2006, Sacconi et al., 2004). Ubiquitination resistant p65 resides on the promoters of NF- κ B target genes longer than the wild-type protein (Bosisio et al., 2006, Sacconi et al., 2004). Little is known about the mechanisms regulating p50 ubiquitination, for example a ubiquitin ligase for p50 has not been identified, whereas three ubiquitin ligases have been reported for p65 thus far (Maine et al., 2007, Tanaka et al., 2007, Ryo et al., 2003). As shown in the previous section, Bcl-3 prevents p50 ubiquitination and this action is dependent on interaction with p50. p50 which cannot interact with is hyper-ubiquitinated and has a significantly reduced half-life relative to wild type p50. p105^{RKR} MEFS are hyper responsive to stimulation with TNF, further highlighting the significance of p50 homodimer stability in the control of NF- κ B target gene expression. In order to further investigate the role of p50 ubiquitination in TLR signalling we aimed to identify the lysine(s) required for ubiquitination with the goal of generating a ubiquitination resistant version of p50 which should have profound effects TLR activation and NF- κ B-mediated inflammatory responses.

A target protein can be mono or poly-ubiquitinated and attachment of ubiquitin can occur at a single or multiple lysine residues. p50 is ubiquitinated via lysine 48-mediated poly-ubiquitination (Carmody et al., 2007b) (Appendix 7.4). Preliminary data previously generated in the lab suggested that this ubiquitination occurs at a single lysine substrate as ubiquitination assays carried out with a ubiquitin mutant incapable of forming K48-linked polyubiquitin chains produced a single ubiquitination band corresponding to 58 kDA, p50 modified with one ubiquitin. In order to identify the specific lysine modified during p50 ubiquitination, a series of lysine to arginine mutants were generated and tested in the p50 ubiquitination assay as previously outlined. Mutation of lysine to arginine, another positively charged, polar amino acid, conserves some of the

biochemical properties of the amino acid, but unlike lysine, ubiquitin can not be conjugated to an arginine.

Mutation of lysine 128 of p50 to arginine (p50^{K128R}) dramatically reduced p50 ubiquitination suggesting that this lysine may be the target of ubiquitination on p50. (Figure 3.23 A). To investigate the effect of this mutation on the regulation of transcription, a IL23p19 reporter assay was employed as previous. Dose-dependent analysis of p105 and p105 in which Lys128 was mutated to arginine (p105^{K128R}) expression on IL-23p19 reporter activity was performed by transfecting increasing, but low amounts of these expression vectors in *Nfkb1*^{-/-} MEFs (Figure 3.23 B). At lower concentrations, p105^{K128R} was significantly more effective than wild type p105 at reducing TNF simulated reporter activity. Crystal structure analysis revealed Lys128 is surface exposed and likely accessible for binding by ubiquitin machinery (Figure 3.23 C), furthermore Lys128 is also highly conserved among a number of species (Figure 3.23 D). Taken together, these data suggest that Lys128 is the major ubiquitinated lysine in p50 and in keeping with our hypothesis, a ubiquitin-resistant p50 mutant may be a stronger repressor of NF-κB dependent transcription.

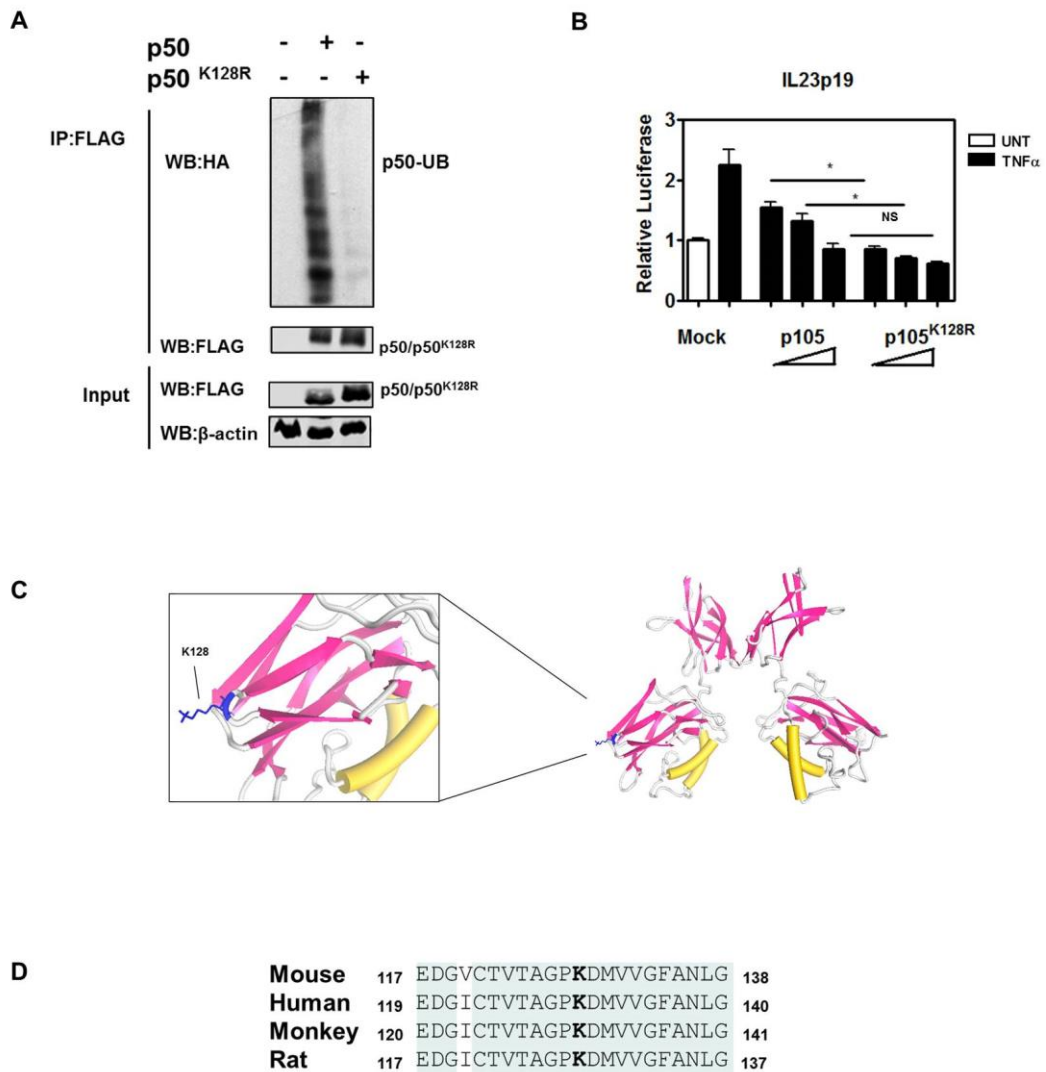


Figure 3.23 p50 is ubiquitinated at Lysine 128.

(A) HEK293T cells were transfected with pEF4a-p50-Xpress or pEF4a-p50-Xpress in which Lys 128 of p50 was mutated to arginine (p50^{K128R}). All cells were also transfected with ubiquitin-HA expression vector. p50 or p50^{K128R} ubiquitination was determined by immunoprecipitation (IP) from whole cell lysates with anti-Xpress (XP) and WB with anti-HA for HA tagged ubiquitin. (B) NF- κ B1^{-/-} MEFs cells were transiently transfected with the pLucp19 plasmid and increasing amount (200,300 and 400ng) of pEF4a-p105-Xpress or pEF4a-p105-Xpress in which Lys 128 of p105 was mutated to arginine p105^{K128R}. The total amount of plasmid was constant across all samples by adjusting the amount of empty vector used. Cells were transfected for 24 hours and cultured with or without 20 ng/ml TNF for an additional 8 hours before luciferase activity were measured. IL23p19 reporter activity was determined as in Figure 3.6. (C) Crystal structure of p50 homodimer with Lys 128 highlighted in blue. (D) Lysine 128 (bold) in p50 is highly conserved across species, identical residues are shaded in green. Murine amino acids numbering used (A-D).

3.4 DISCUSSION

Bcl-3 is an I κ B protein that regulates NF- κ B-dependent gene expression through interaction with NF- κ B p50 and p52 homodimers. Bcl-3 also interacts with a number of non NF- κ B subunits that regulate transcription (Zhao et al., 2005, Yang et al., 2009, Weyrich et al., 1998, Viatour et al., 2004, Southern et al., 2012, Na et al., 1999, Na et al., 1998, Kabuta et al., 2010, Jamaluddin et al., 2005, Hishiki et al., 2007). The contribution of these factors to immune regulation by Bcl-3 has not been determined. Previous studies have demonstrated that Bcl-3 regulates p50 homodimer stability through the inhibition of ubiquitination and subsequent proteasomal mediated degradation (Carmody et al., 2007b). However, studies employing *Bcl3*^{-/-} cells and mice do not exclude the possibility that Bcl-3 may also function through p50-independent mechanisms to regulate gene expression. This study describes the experimental characterisation of the interaction between p50 and Bcl-3 and demonstrates for the first time that interaction between Bcl-3 and p50 is required for the stability of p50 homodimers and is necessary for the anti-inflammatory function of Bcl-3.

A peptide array approach was employed to identify residues of p50 necessary for interaction with Bcl-3. Peptide arrays provide an efficient tool to map protein interaction domains of known binding partners. A large library of immobilised peptides can be screened simultaneously on a single array, rapidly reducing the vast number of potential binding sites within a complex. This approach is also advantageous over traditional deletional mutagenic approaches where significant portions of a protein are disrupted. Mutations in the p50 RHD for example, could affect DNA binding and dimerisation, artefactually inhibiting a p50-Bcl-3 complex (Ghosh et al., 1995, Sengchanthalangsy et al., 1999). In this study, a series of overlapping peptides with high affinity for purified recombinant Bcl-3 were identified. Four regions R1-R4, located in the C terminus of p50, were considered to be strong candidates for interaction with Bcl-3. To further increase the resolution of these potential binding sites, a series of alanine substitution arrays were generated. These arrays identified a number of potentially key amino acids, subsequently mutated in full length p50, in order to verify their contribution to Bcl-3 binding.

Although mutation of Lys249, Arg253 and M253 to alanine (p50^{KRM}) did not completely inhibit interaction, Bcl-3 binding affinity was significantly reduced. The hypothetical model of Manavalan *et al.* published after this data was generated, further supports the role of these amino acids in Bcl-3 binding (Manavalan *et al.*, 2010) (**Table 29**). Using a molecular docking approach based on the available crystal structure of IκBα bound to an NF-κB heterodimer, they predicted residues 249-257 of p50 to be directly involved in Bcl-3 interaction. Nevertheless, Bcl-3 overexpression was able to inhibit p50^{KRM} ubiquitination, however the huge increase in ubiquitination of this mutant relative to wild-type p50 was unexpected. Not surprisingly, p50^{KRM} processed from p105 in which these residues were mutated, was inherently unstable. Moreover p50^{KRM} failed to inhibit IL-23p19 reporter activity following LPS stimulation. Based on the solved crystal structure Lys249, Arg253 and M253 of p50 also contribute to IκBα binding part of a p65 heterodimer (Jacobs and Harrison, 1998). Reconstitution of *Nfkb1*^{-/-} cells with p105^{KRM} would therefore result in disrupted p50:Bcl-3 and p50/p65:IκBα complexes, the effects of which, would be indistinguishable from one another. Thus, further characterisation of this mutant in was not performed.

Table 29. Comparison of Hypothetical Models of p50:Bcl-3 binding

Model	p50 Subunit	Interacting Residues
Manavalan Complex A	Subunit A	Lys74, <u>Lys249</u> , Ile250, Val251, <u>Arg252</u> , <u>Met253</u> , Asp254, Arg255, Thr256, Ala257, Pro324, Ser326, Val327, Phe328, Glu341, Pro342, Pro344, Phe345, Leu346, Tyr348
	Subunit B	Arg255, Cys259, Thr261, Gly262, Gly263, Glu264, Glu265, Tyr267, <u>Ser299</u> , <u>Thr301</u> , <u>Asp302</u> , Val310, Lys312, Glu350
Manavalan Complex B	Subunit A	Glu73, Lys 74, Tyr248, <u>Lys 249</u> , Val251, <u>Arg252</u> , <u>Met 253</u> , Asp254, Thr256, Pro324, Ser326, Lys343, Pro344, Phe345, Leu346, Tyr348,
	Subunit B	Gly263, Glu254, Glu265, Tyr26, <u>Asp297</u> , <u>Ser299</u> , <u>Thr301</u> , Lys312, Thr313
Michel		Tyr263, <u>Asp297</u> , <u>Pro300</u> , <u>Thr301</u> , Lys315

Table comparing the hypothetical models of p50 and Bcl-3 interaction. There are three predicted models of interaction, Manavalan complex A and B (Manavalan *et al.*, 2010) and Michel (Michel *et al.*, 2001). Putative Bcl-3 interacting residues of p50 identified by peptide array are underlined.

Interestingly, the p50^{DFSPT} mutant had an almost identical phenotype to p50^{KRM}. Despite very reduced levels of Bcl-3 binding, overexpression of Bcl-3 was still partially capable of inhibiting p50^{DFSPT} ubiquitination. Although Lys249, Arg253 and M253 (R1) and Asp297, Phe 298, Ser 299, Pro300 and Thr 301(R2) reside on opposite sides of a p50 subunit, they form a potential interface on each side of a p50 homodimer. While differing in the precise amino acids, both computational models of a p50:Bcl-3 complex predicted amino acids within this DFSPT region to be important for interaction with Bcl-3. Furthermore Manavalan *et al* predicted these amino acids were also important for interaction with IκBNS, another nuclear IκB protein. The structures of the IκB proteins are very homologous (Figure 1.4), Bcl-3 and IκBα for example, share 35% sequence identity within the ARD (Michel et al., 2001). These data suggests that regions R1 and R2 provide an important binding interface for multiple IκB protein, mutation of which severely disrupts p50 stability and function.

Another region important in regulating p50 ubiquitination identified from the peptide array was a three amino acid stretch, Lys315, Tyr316 and Lys317. Mutation of lysines 315 and 317 to alanine in full length p50 did not have a significant effect on Bcl-3 binding. This suggests that these amino acids are not essential for interaction with Bcl-3 but does not rule out the contribution of this region to Bcl-3 binding. Recombinant Bcl-3 bound to a number of peptides representing amino acids 298-330 (R3). It is possible that these peptides represent artificial binding sites not represented in full-length p50. However, as Lys312, Thr313 and Lys315 were predicted to contact Bcl-3 in Manavalan *et al.* (Manavalan et al., 2010) and Michel *et al* (Michel et al., 2001) models, it is likely that Bcl-3 makes contacts in this region.

Unlike immobilised peptides on an array, binding sites are not static and are considerably flexible. Critical amino acids tightly packed within protein-protein interfaces are considered *hot spots* (Clackson T, 1995) and these *hot spots* cluster within a *hot region*, contributing cooperatively to the stability of a complex (Keskin et al., 2005). Thus, Lys 315 and Lys 317 could be just two of a number of contacting amino acids within this potential hot region, mutation of which is insufficient to disrupt Bcl-3 binding. A recent Study (Moreira et al., 2007) of the Alanine Scanning Energetics database (ASEdb) (Thorn and Bogan, 2001) estimated that only 9.5% of interfacial residues to be hot spots. Therefore, it is also possible that Lys 315 and Lys 317 are contained within a hot

region but under physiological conditions are not the critical contacting amino acids.

Although mutation of Lys 315 and Lys317 had no effect on Bcl-3 binding, these mutations did alter the ubiquitination status of p50. p50^{K315A,K317A} ubiquitination was significantly reduced when compared to wild type p50. Previous work in the lab in which Lys 315 and Lys 317 were mutated to arginine, showed no reduction in ubiquitination. This suggested that p50 was not ubiquitinated on Lys315 or Lys317 but rather this defect was due to a structural change in this region. Tyr316 is flanked by these two lysines and when mutated to alanine, also increases the ubiquitination of p50. Tyrosine is a polar amino acid with a bulky benzyl side chain and substitution with alanine, a much smaller amino acid could create a significant hole and alter protein confirmation. Mutation to phenylalanine however also resulted in a similar hyper-ubiquitinated phenotype.

Post-translational modification of tyrosine is a widely established mechanism for regulating signal transduction and cellular processes such as proliferation and differentiation. Within the NF- κ B pathway, I κ B α and p65 are phosphorylated and nitrated on tyrosine residues respectively (Imbert et al., 1996, Park et al., 2005) but no known tyrosine modifications on p50 have been established to date. Collectively these data suggest an essential role for Tyr316 in negatively regulating p50 ubiquitination, either through post-translational modification or interaction with an unknown binding partner. Lysines 315 and 317 may act to hinder binding to Tyr316 and when mutated to alanine actually increase binding affinity, resulting in decreased ubiquitination. This mechanism of attenuation by neighbouring residues in a hot spot has previously been reported for the human growth factor receptor complex (Keskin et al., 2005). Further investigation into the possible posttranslational modification of Tyr316 and its role in regulating p50 ubiquitination need to be investigated.

The final region identified by the peptide array to contribute to Bcl-3 binding was peptides 115-121, corresponding to amino acids 337 to 378 at the extreme C-terminal region of p50. The serial substitution of amino acids 355 to 372 with alanine as immobilised peptide identified Arg359, Lys360 and Arg361 as essential residues for interaction with Bcl-3. Subsequently, the mutation of Arg359, Lys360 and Arg361 to alanine in full length p50 blocked the interaction with purified, recombinant Bcl-3. The region of p50 containing Arg359, Lys360

and Arg361 is C terminal to previously identified ankyrin repeat domain interaction sites determined from the crystal structure of a p65:p50 heterodimer complexed with I κ B α (Jacobs and Harrison, 1998). Unfortunately, the amino acids 359 to 361 are not represented on the crystal structures of p50 containing complexes and so no structural data is available. However, a hydrophobicity plot reveals that these amino acids lie in a region of low hydrophobicity and thus are expected to be available for interaction with Bcl-3.

Importantly, mutation of these amino acids does not alter the hetero- or homodimer formation properties of p50, or interfere with DNA binding of p50. This allows us to rule out the loss of repressor function of p50^{RKR} homodimers due to lack of dimerisation or DNA binding. Moreover, despite being located in a region previously reported to be important for nuclear localisation (Latimer et al., 1998), the mutation of Arg359, Lys360 and Arg361 to alanine had no effect on the nuclear localisation of p50 as monitored by sub-cellular fractionation analysis and DNA binding assays. Our data suggests that additional sequences of p50 are important in its nuclear translocation. The mutation of Arg359, Lys360 and Arg361 in p50 (p50^{RKR}) functionally recapitulates the previously described phenotype of *Bcl3*^{-/-} cells. Thus, p50^{RKR} undergoes increased ubiquitination corresponding to a reduced half-life and cells expressing p50^{RKR} display increased NF- κ B transcriptional activity relative to wild type p50. Critically, Bcl-3 is unable to rescue the increased NF- κ B activity in p50^{RKR} expressing cells. NF- κ B transactivation is not inhibited by overexpression of Bcl-3 in cells expressing p50^{RKR} and Bcl-3 is unable to inhibit p50^{RKR} ubiquitination. Recent studies have highlighted the role of p50 in regulating transcriptional programmes during inflammation during TLR and interferon-induced responses (Yan et al., 2012, Cheng et al., 2011). Our data further highlights the importance of Bcl-3 and p50 interaction in the regulation of the inflammatory response, which is independent of Bcl-3 interaction with other transcriptional regulators.

TLR activation triggers p50 homodimer ubiquitination however the precise sequences involved in regulation its ubiquitination and degradation are unknown. p50 Lys128 is highly conserved across species and mutation to arginine dramatically reduced p50 ubiquitination. Arginine, like lysine is a positive polar amino acid but cannot be modified with ubiquitin. This suggests a critical role

for Lys128 in p50 homodimer ubiquitination. Ubiquitination removes inhibitory homodimers from target promoters allowing activation of NF- κ B target genes, a critical step in the regulation of TLR activation. Expression of a ubiquitination-resistant p50 mutant should therefore result in reduced inflammatory response. Initial studies over expressing p105^{K128R} in a luciferase IL-23p19 gene promoter assay supports this theory as p105^{K128R} was significantly more effective than wild type p105 at inhibiting reporter activation following TNF stimulation. *Nfkb1*^{-/-} MEFS stably expressing either p105 or p105^{K128R} have also been generated and these will provide an excellent tool in determining the role of p50 ubiquitination in innate immunity. Gene expression analysis and chromatin immunoprecipitation studies in these cells will provide a further insight into the mechanism of p50 ubiquitination in TLR signalling.

—— Chapter Four ——

4 Characterisation of a Bcl-3 derived NF- κ B inhibitory peptide

4.1 ABSTRACT

Bcl-3 regulates NF- κ B dependent transcription through interaction with homodimers of NF- κ B subunits, p50 and p52. Bcl-3 inhibits p50 ubiquitination and subsequent degradation, stabilises inhibitory p50 homodimers and negatively regulates TLR-induced NF- κ B-dependent inflammatory gene expression. Bcl-3 interaction with p50 is necessary for the inhibition of ubiquitination and the negative regulation of pro-inflammatory gene expression. Immobilised peptide arrays were employed to experimentally characterise the interaction between Bcl-3 and p50. A number of short peptides derived from Bcl-3 capable of binding to p50 with high affinity were identified. We generated a cell permeable peptide representing the outer helix and linker domains of Bcl-3 ANK1, a region poorly conserved among I κ B proteins. The Bcl-3 derived peptide (BDP) effectively inhibited LPS induced NF- κ B activity *in vitro*. This inhibitory activity was significantly reduced when key amino acids required for p50 interaction were mutated. This study provides a basis for the development of Bcl-3 derived therapies for the treatment of inflammatory diseases.

4.2 INTRODUCTION

NF- κ B controls the transcription of hundreds of genes critical for the inflammatory response, aberrant activity of which underlies the pathophysiology of a number of human diseases. Ubiquitination and proteasomal degradation of NF- κ B represents a major limiting factor in the control of the NF- κ B transcriptional response (Bosisio et al., 2006, Saccani et al., 2004, Carmody et al., 2007b, Wertz and Dixit, 2010, Colleran et al., 2013). Thus, ubiquitin based drug discovery presents a promising field for the development of novel therapies for the treatment of many immunological diseases and cancers. However when compared to inhibitors of kinases for example, the limited success of such drugs is apparent. To date the proteasome inhibitor bortezomib (Velcade, Millenium Pharmaceuticals) is the only FDA approved drug targeting the ubiquitin system, while currently there are 24 small molecule kinase inhibitors approved by the FDA, with hundreds in clinical trials.

The complexity of the ubiquitination system is such that establishment of selective inhibitors of the ubiquitin pathway for clinical use is challenging. Many experimental inhibitors of the ubiquitin/proteasome pathway are available and include inhibitors of specific E1, E2, E3 and DUP enzymes which provide valuable tools to study the ubiquitin system (Brownell et al., 2010, Ceccarelli et al., 2011, Yang et al., 2007, Issaeva et al., 2004, Michel Espinoza-Fonseca, 2005, Colland et al., 2009). Due to the broad specificity of the enzymes involved in conjugating ubiquitin to a substrate, inhibition of enzyme activity is likely to affect a number of cellular proteins. For example, the ubiquitin E3 ligase β -TrCP mediates the degradation of I κ B α (Suzuki et al., 1999) and the proteasome dependent processing of p105 (Orian et al., 2000), thereby activating the NF- κ B pathway. However β -TrCP can also inhibit the Wnt pathway through association with β -catenin (Latres et al., 1999). As a consequence much work has focused on inhibiting E3 substrate binding for specific E3 substrate pairs (Cohen and Tcherpakov, 2010). Inhibitors of the interaction between p53 and two of its E3 ligases COP1 (Yamada et al., 2013) and MDM2 (Vassilev et al., 2004) have already been developed with the latter currently in clinical trials for the treatment leukaemia and retinoblastoma.

A current exciting strategy in the intracellular delivery of bioactive material is through a process called peptide transduction. This involves the covalent or non

covalent conjugation of molecular 'cargoes' (peptides, proteins, DNA, siRNA (Sterghios Moschos, 2006)) to small peptides that can translocate the plasma membrane (Järver and Langel, 2006). These natural and synthetic cell-penetrating peptides (CPP), also called protein transduction domains (PTD) are relatively short peptides, 5-40 amino acids in length, with the ability to gain access to the cell interior (Langel, 2006). CPPs vary in size, sequence, charge and origin but can be classified by physical-chemical properties into 3 main groups; cationic, amphiphilic and hydrophobic (Milletti, 2012). Cationic and amphiphilic CPPs have been utilised extensively in the development of inhibitors of NF- κ B signalling and have been used effectively *in vitro* and some *in vivo* models (Orange and May, 2008). The NEMO binding domain (NBD) peptide (May et al., 2000) is probably the most widely studied NF- κ B CPP inhibitor to date and has been used successfully to inhibit inflammation in a wide range of models including, dextran sulphate sodium (DSS) induced colitis, arthritis, and in models of lung inflammation (Orange and May, 2008). This peptide blocks the association of NEMO with the IKK complex thereby inhibiting cytokine-induced NF- κ B activation and NF- κ B-dependent gene expression (May et al., 2000).

The first CPP discovered was derived from the human immunodeficiency virus (HIV)-1 TAT protein, a 86 amino acid protein which can translocate through the plasma membrane and transactivate the viral genome (Frankel and Pabo, 1988). Further studies identified the minimal domain required for this translocation activity to a cluster of basic amino acids 47-57, YGYKKRRQRR (Vivès et al., 1997). Early work by Fawell et al. (Fawell et al., 1994) illustrated the huge potential of the TAT peptide in conferring cell penetrating properties to an attached cargo. They demonstrated delivery of a TAT (37-72)- β -galactosidase conjugate to a number of tissues including the heart, liver and spleen following intravenous (i.v) injection. More recent work investigating the kinetics of a TAT fusion into the mouse, detailed distribution in all tissues following portal vein (i.v.), intraperitoneal (i.p.) and oral administration (Cai et al., 2006). The exact mechanism of cellular uptake utilised by CPPs has not been fully elucidated but reports suggest that a number of mechanisms (extensively reviewed in (Madani et al., 2011)) may be involved which are dependent on the class and concentration of the CPP and the attached molecular cargo (Tünnemann et al., 2006). Initial studies proposed an energy independent mechanism of internalisation by the TAT peptide however it is now clear endocytosis is involved (Richard et al., 2003, Tünnemann et al., 2006, Vendeville et al., 2004).

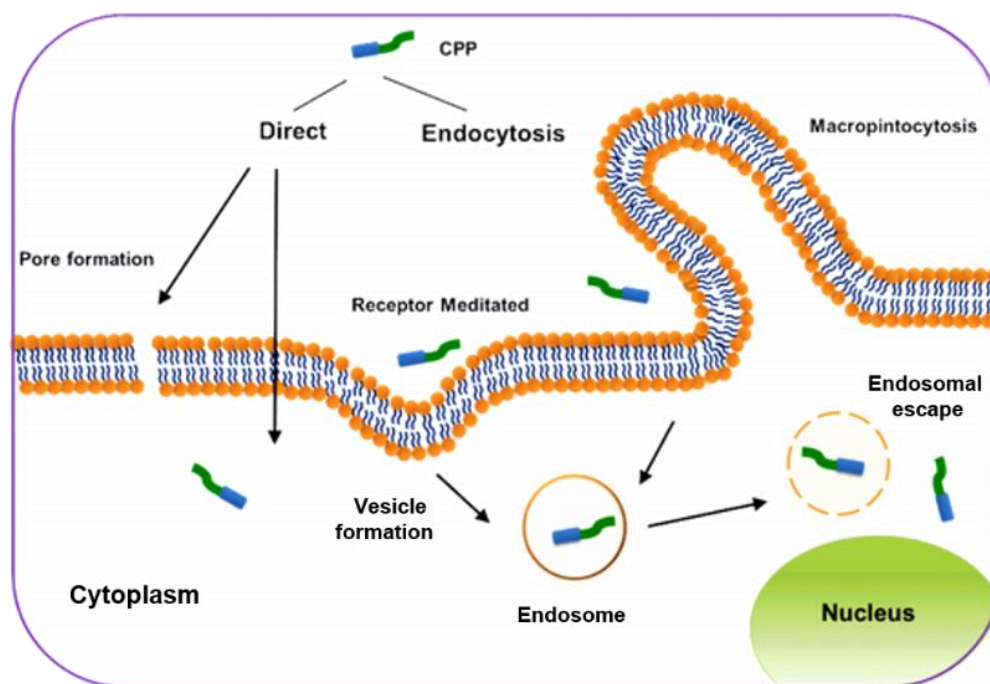


Figure 4.1 Proposed mechanisms of cellular uptake of cell penetrating peptides.

The exact mechanism of cellular uptake of cell penetrating peptides (CPP) is currently unknown however a number of mechanisms have been proposed. Peptides are thought to transverse the plasma membrane through energy independent (direct translocation or through pore formation) and energy dependent (clathrin or caveolae mediated endocytosis and macropinocytosis).

The NF- κ B transcriptional response is tightly regulated by a number of processes including the phosphorylation, ubiquitination and subsequent proteasomal degradation of NF- κ B. Through inhibition of p50 ubiquitination, Bcl-3 stabilises a p50 homodimer:DNA complex that suppresses inflammatory gene expression (Carmody et al., 2007b). This complex prevents the binding of the transcriptionally active NF- κ B subunits on the promoters of NF- κ B target genes, however the precise mechanism of Bcl-3 mediated regulation of p50 homodimer ubiquitination is unknown. As shown in chapter 3, Bcl-3 interaction with p50 is critical step. *Nfkb1*^{-/-} MEFs reconstituted with a version of p50 that can no longer bind Bcl-3 are hyper responsive to TNF stimulation, further highlighting the importance of Bcl-3-p50 interaction in the control NF- κ B-associated inflammation. p50 homodimer ubiquitination thus signifies a critical step in the regulation of TLR signalling and presents novel therapeutic targets in the

control of NF- κ B mediated gene expression. Interaction with p50 is essential for Bcl-3 mediated inhibition of p50 ubiquitination and thus the anti-inflammatory properties of Bcl-3. In this chapter, we identified the regions of Bcl-3 that are necessary and sufficient to bind p50 and from this designed short mimetic peptides capable of mediating Bcl-3 function i.e. inhibiting NF- κ B mediated inflammatory gene expression.

4.3 RESULTS

4.3.1 Identification p50 Binding Peptides

4.3.1.1 Cloning and Purification of Recombinant p50

To experimentally identify the minimum regions of Bcl-3 sufficient to bind p50, a peptide array based technique using recombinant GST-p50 protein as a probe was employed. Recombinant p50 was constructed by inserting murine p50 cDNA into the multiple cloning site of pGEX6p1. (Figure 4.2 A) *E. coli* BL21 CodonPlus were transformed with either pGEX-6p1 or pGEX-6p1-p50 and GST fusion proteins were induced overnight at 20°C with 1.0mM IPTG. Recombinant proteins were then affinity-purified using GSH-agarose and eluted with Glutathione over a number of elutions. (Figure 4.2 B). The suitability of GST-p50 for use as a Bcl-3 peptide library probe was established using a GST pulldown assay. GST or GST-p50 was incubated with a whole cell lysate overexpressing Bcl-3 and affinity purified with GSH agarose. Bcl-3 bound specifically to purified GST-p50, but not GST indicating a functional p50 fusion protein. (Figure 4.2 C).

4.3.1.2 Bcl-3 Peptide Array

A library of overlapping peptides 18 amino acids in length, each shifted by 4 amino acids and encompassing the entire sequence of Bcl-3, was Spot-synthesised on a cellulose membrane to generate the Bcl-3 peptide array (see Appendix 7.5 for Bcl-3 peptide library). Arrays were probed with either GST as a control or GST-p50, positive binding was detected by immunoblotting with anti-GST antibody (Figure 4.3 A). GST-p50 bound specifically to a number of Bcl-3 peptides representing the N terminus and ANK repeats 1, 6 and 7 of Bcl-3 (Figure 4.3 C). In order to identify amino acids within these peptides essential for binding to p50, a series of alanine scanning arrays were generated. Arrays were derived from the positive 18-mer parent peptide of interest and 18 new peptides containing a single successive alanine substitution were generated (see Appendix 7.6 for alanine substitution library). The alanine scanning array was again incubated with GST-p50 prior to immunoblotting with anti-GST antibody. Detection of GST-p50 binding was then performed using near infra red IR-Dye-conjugated secondary antibody to facilitate quantification of GST-p50 binding to specific peptides using an infra red scanner (Figure 4.4). The binding of GST-

p50 to the substituted peptide was calculated and represented as a percentage binding of the control parent peptide contained on the same array (see Appendix 7.7 for full alanine substitution binding data). Substitution of amino acids that resulted in significantly decreased Bcl-3 binding i.e. less than 50% binding, are underlined.

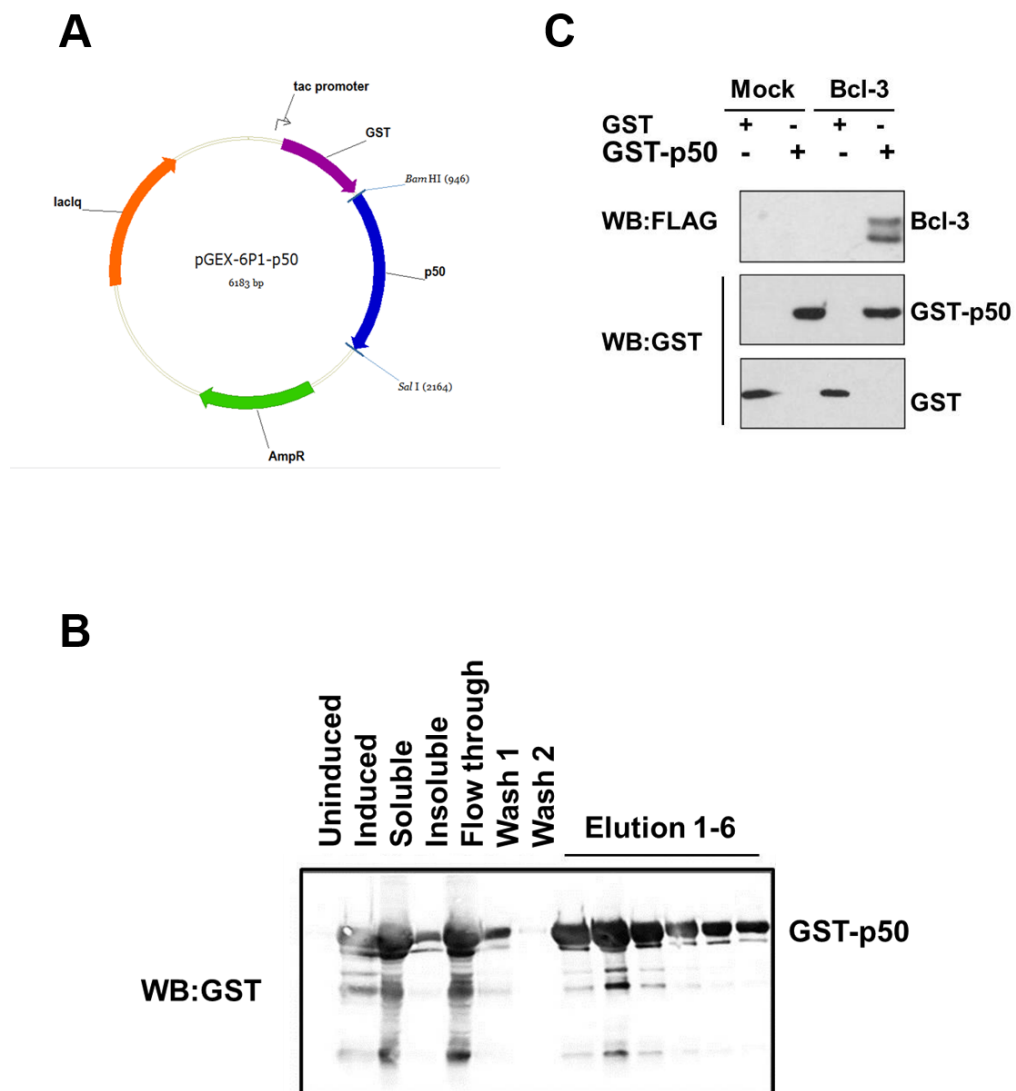
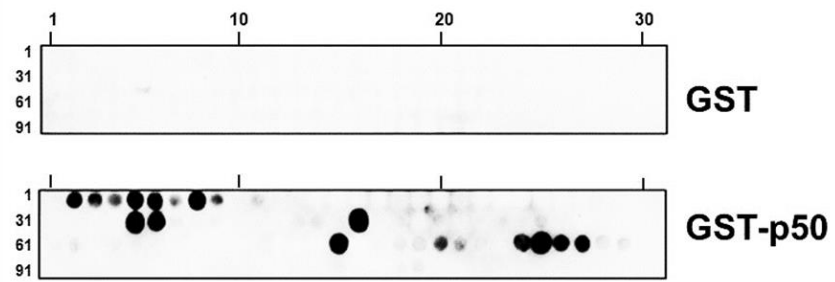


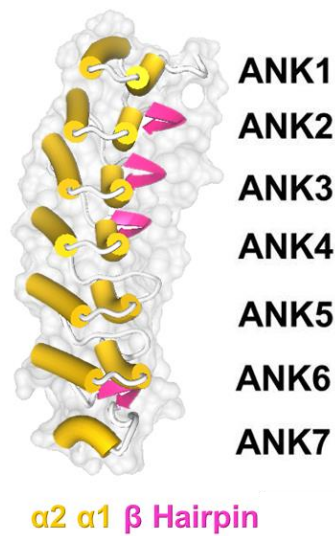
Figure 4.2 Bcl-3 binds specifically to recombinant GST-p50.

(A) Murine p50 cDNA was ligated via *Bam*H1 and *Sal*1 restriction sites into pGEX6p1 to produce a GST-p50 expression vector. (B) *Escherichia coli* BL21 CodonPlus were transformed with pGEX-6p1-p50 and expression of GST-p50 was induced with the addition of IPTG. Recombinant proteins were affinity-purified against GSH-agarose and eluted with glutathione. (C) Bcl-3 binds specifically to GST-p50 in a GST pull down assay. Purified bacterial recombinant GST or GST-p50 was incubated with a whole cell lysate from HEK293 cells transfected with empty vector (Mock) or FLAG-Bcl-3 (Bcl-3) and affinity purified with GSH agarose. Pull down complexes were immunoblotted with anti-FLAG and anti-GST antibodies.

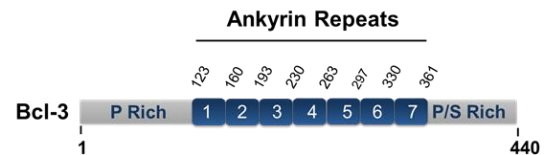
A



B



C



Peptides	Bcl-3 Region
1-10	N terminus
11-20	N terminus
21-30	N terminus -ANK1
31-40	ANK1-ANK2
41-50	ANK2-ANK3
51-60	ANK3-ANK4
61-70	ANK4-ANK5
71-80	ANK5-ANK7
81-90	ANK6-ANK7
91-100	C terminus
101-109	C terminus

Figure 4.3 Bcl-3 peptide array identifies p50 interacting peptides.

(A) Peptide arrays of immobilised overlapping 18-mer peptides, each shifted to the right by 3 amino acids encompassing the entire Bcl-3 sequence were generated. Arrays were probed with GST or GST-p50 and detected by immunoblotting with anti-GST antibody. GST-p50 binding to Bcl-3 peptides is shown (black spots) and is representative of duplicate arrays. (B) Crystal structure of human Bcl-3 ankyrin repeat domain with beta (β)- hairpin and inner ($\alpha 1$) and outer alpha helices indicated. (C) Schematic representation of murine Bcl-3 with ANK repeats 1-7 indicated and table of Bcl-3 peptides 1-109 with corresponding Bcl-3 structural region.

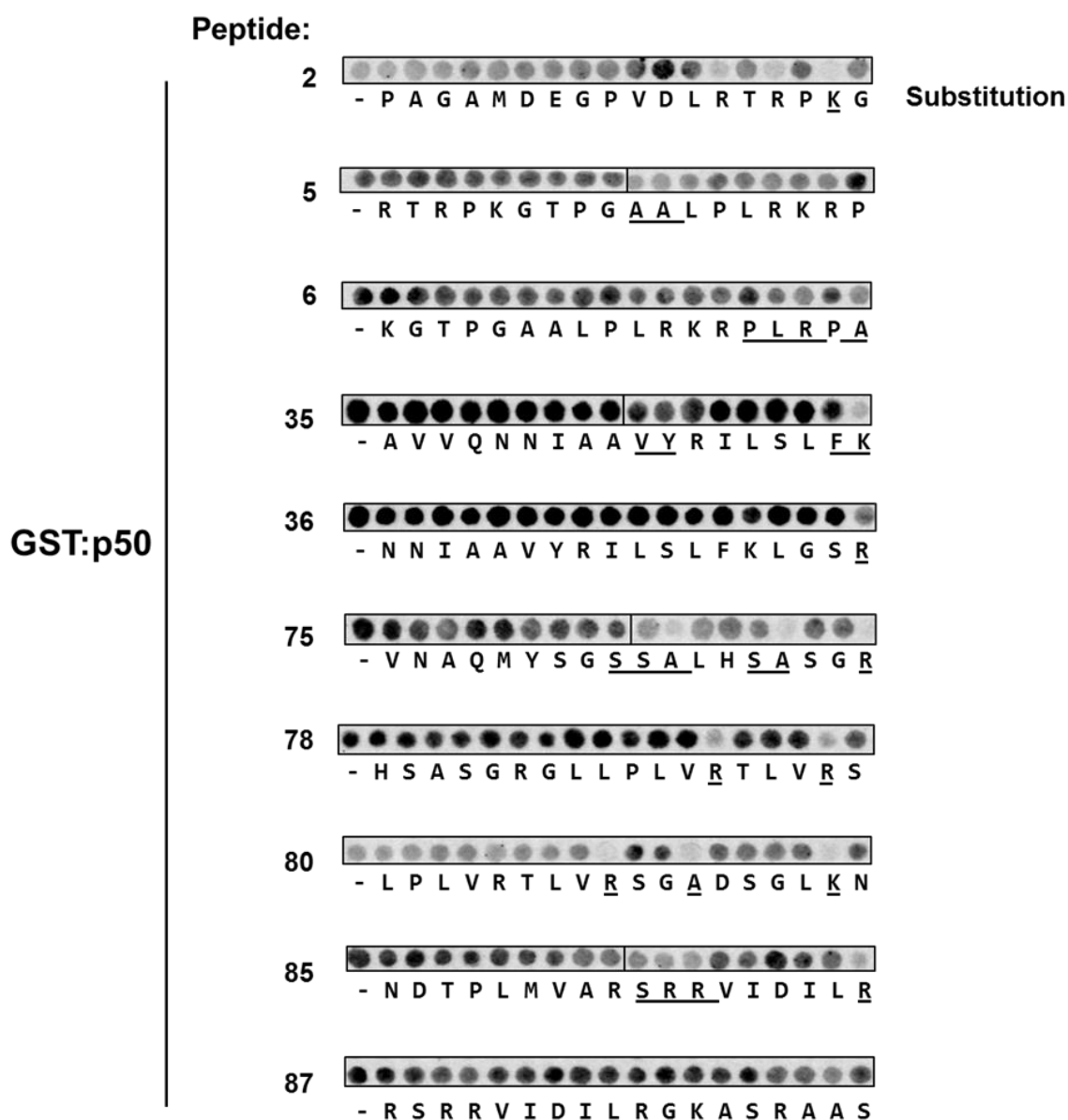


Figure 4.4 Alanine substitution analysis of positive p50 binding Bcl-3 peptides.

(A) The 18 amino acids of Bcl-3-derived peptides of interest were sequentially substituted with alanine and probed with GST-p50 and detected by immunoblotting with anti-GST antibody. p50 binding was quantified by densitometry and calculated as a percentage binding of the parent unsubstituted peptide on the same array. The full substitution peptide array data is available Appendix 7.7. Alanine substitution of an amino acid that significantly decreased ($\leq 50\%$ of parent peptide) p50 binding is underlined.

4.3.2 Bioinformatic and Structural Analysis of p50 Interacting Sites

As there is no available crystal structure for a p50:Bcl-3 complex, previous studies have used *in silico* modelling and molecular docking techniques based on the solved NF- κ B heterodimer:I κ B α complex to predict sites of p50 and Bcl-3 interaction (Manavalan et al., 2010, Michel et al., 2001). As detailed in chapter 3, these methods are limited by the available, incomplete Bcl-3 and p50 crystal structures. To determine the correlation of these methods with sites experimentally determined in this study, we aligned the putative interacting amino acids determined by peptide array and computational modelling. The peptide array detected two unique potential binding regions not identified by the three available computational models, representing residues in ANK1 and the unstructured N-terminus (Figure 4.5 and Figure 4.6). Considerable overlap between all methods occurred in ANK6 and ANK7, further validating the use of peptide arrays to investigate Bcl-3-p50 binding.

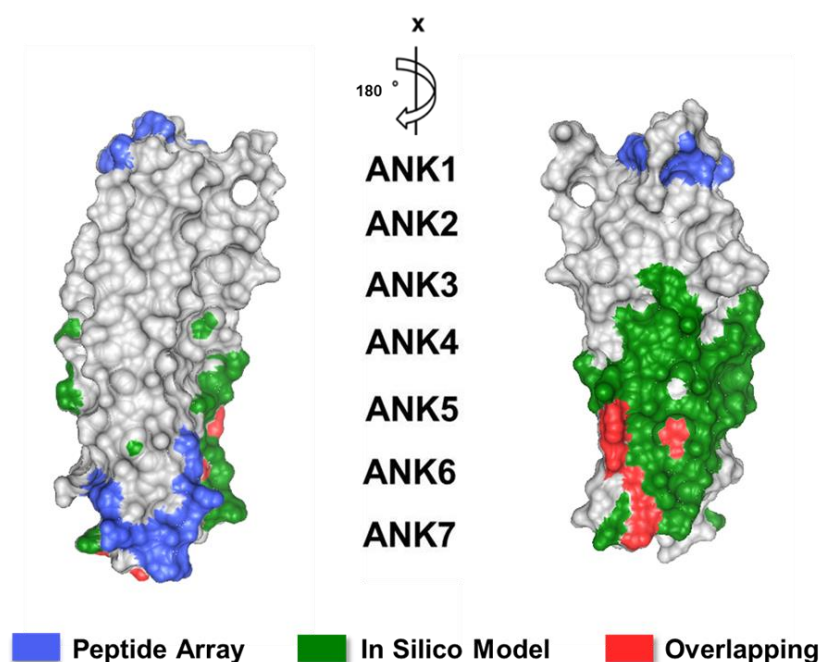


Figure 4.5 Structural representations of putative p50 interacting residues.

Human Bcl-3 crystal structure with unique p50 interacting residues determined by peptide array in blue, those predicted by combined *in silico* models (Manavalan complex A, complex B) (Manavalan et al., 2010) and Michel (Michel et al., 2001) in green and overlapping residues identified by both methods in red. As the murine Bcl-3 structure is unsolved, corresponding human residues are indicated.

A

1 MDEGPVDLRTRPKGTPG **AALPLRKRPLRPA** SPEPATRSPAGPLDALRSGCDVPVVGPPH
 CVARPEALYYQGPLMPIYSTPTMAPHFLLNLPTHYPYSMICPMEHPLSADIAM 122

B



Array	ANK1	123	ATRVEDED-GDTPHLHIAVVQNNIA AAVYRILSLFKLGSRE
Manavalan^A	ANK1	120	ATRADED-GDTPHLHIAVVQGNLPAVHRLVNL FQQGGRE
Manavalan^B	ANK1	120	ATRADED-GDTPHLHIAVVQGNLPAVHRLVNL FQQGGRE
Michel	ANK1	120	ATRADED-GDTPHLHIAVVQGNLPAVHRLVNL FQQGGRE
Array	ANK2	160	VDVHNN-LRQTPLHLAVITTL PDMVRL LVTAGAS
Manavalan^A	ANK2	157	LDIYNN-LRQTPLHLAVITTL PSVRL LVTAGAS
Manavalan^B	ANK2	157	LDIYNN-LRQTPLHLAVITTL PSVRL LVTAGAS
Michel	ANK2	157	LDIYNN-LRQTPLHLAVITTL PSVRL LVTAGAS
Array	ANK3	193	PMALDR-HGQTAIHLACEHRSP SLQAL LDSATSGSVD
Manavalan^A	ANK3	190	PMALDR -HGQTAHLACEHR SPTCLRAL LDSAAP GTLD
Manavalan^B	ANK3	190	PMALDR -HGQTAHLACEHR SPTCLRAL LDSAAP GTLD
Michel	ANK3	190	PMALDR -HGQTAHLACEHR SPTCLRAL LDSAAP GTLD
Array	ANK4	230	LEVRNY-EGLTALHVA VNTGCQEAV LLLL LERGAD
Manavalan^A	ANK4	227	LEARNY -DGLTALHVA NTECQETVQ LLLL LERGAD
Manavalan^B	ANK4	227	LEARNY -DGLTALHVA NTECQETVQ LLLL LERGAD
Michel	ANK4	227	LEARNY -DGLTALHVA NTECQETVQ LLLL LERGAD
Array	ANK5	263	IDAVDIKSGRSPLIHAVENNSL NMVQ LLLL LHGAN
Manavalan^A	ANK5	260	IDAVDIKSGRSPLIHAVENNSL SMVQ LLLL LQHGAN
Manavalan^B	ANK5	260	IDAVDIKSGRSPLIHAVENNSL SMVQ LLLL LQHGAN
Michel	ANK5	260	IDAVDIKSGRSPLIHAVENNSL SMVQ LLLL LQHGAN
Array	ANK6	297	VNAQMY-SGSSALHSASGRGLLPLV RTLVR SGAD
Manavalan^A	ANK6	294	VNAQMY -SGSSALHSASGRGLLPLV RTLVR SGAD
Manavalan^B	ANK6	294	VNAQMY -SGSSALHSASGRGLLPLV RTLVR SGAD
Michel	ANK6	294	VNAQMY -SGSSALHSASGRGLLPLV RTLVR SGAD
Array	ANK7	330	SGL KNC -HNDT PLMVAR ---SRRVIDI LRGKASRAAS
Manavalan^A	ANK7	327	SSLKNC -HNDT PLMVAR ---SRRVIDI LRGKATRPAS
Manavalan^B	ANK7	327	SSLKNC -HNDT PLMVAR ---SRRVIDI LRGKATRPAS
Michel	ANK7	327	SSLKNC -HNDT PLMVAR ---SRRVIDI LRGKATRPAS

Figure 4.6 Schematic representation of putative p50 interacting residues determined by peptide array.

(A) For Bcl-3 alanine scanning array, p50 binding was quantified by densitometry and calculated as a percentage binding of the parent unsubstituted peptide, full alanine scanning peptide data is available in Appendix 7.7. The unstructured extreme N-terminal of murine Bcl-3 is presented and alanine substitution of amino acids that decreased p50 binding by $\geq 50\%$ are shaded in yellow and $\geq 40\%$ shaded in grey. (B) Alignment of the seven ANK repeats of Bcl-3 with a schematic indicating the conserved structural features of the each ANK repeat within the ANK repeat domain. Putative p50 binding residues of Bcl-3 were identified as in A and compared with the interacting residues predicted by the three currently available *in silico* models (shaded in yellow), Manavalan complex A (ManavalanA), complex B (ManavalanB) (Manavalan et al., 2010) and Michel (Michel et al., 2001). Human Bcl-3 amino acid numbering was used for Manavalan complex A and B and Michel *in silico* models and murine Bcl-3 amino acid numbering for Bcl-3 array.

In order to identify Bcl-3 specific sequences, the protein sequences of a number of IκB proteins were analysed. Multiple sequence alignment of Bcl-3 homologs was performed and gaps were manually adjusted based on secondary structure elements (see Appendix 7.8 for full alignment). The ARD of IκB proteins is highly conserved and this analysis identified a consensus residue at almost 80% of all positions within this domain however, the potential p50 binding region identified by the Bcl-3 peptide array encompassing Bcl-3 amino acids 144-158, is within an area of low similarity to other IκB proteins (Figure 4.7 A). While no identical residues occur across all six proteins in this region, a consensus sequence can be calculated (Figure 4.7 B). Bcl-3 however shows little similarity to this motif, with only two identical residues shared with the consensus sequence. These data indicate that this short putative p50 binding region is specific to Bcl-3 and not conserved among other IκB family members.

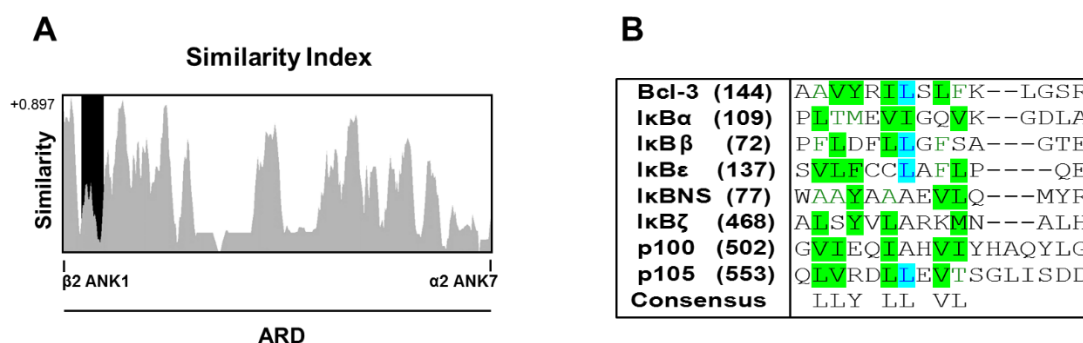


Figure 4.7 Multiple sequence alignment of IκB proteins.

(A) Similarity index of ANK1-ANK7 of the ARD of murine IκB family members, Bcl-3, IκBα, IκBβ, IκBε, IκBNS, p100 and p105. Similarity scoring: identical amino acids=1, similar residues=0.5 and weakly similar residues =0.2 (**Table 26**). Bcl-3 144-158 shaded in black. (B) Section of multiple sequence alignment of murine IκB family members, Bcl-3, IκBα, IκBβ, IκBε, IκBNS, p100 and p105 (see Appendix 7.8 for full alignment). Colour coding: non similar amino acids black on white background, conservative amino acids black on green background, block of similar amino acids dark blue on blue background and weakly similar amino acids green on white background. Only identical and similar amino acids were used in consensus calculation.

4.3.3 Bcl-3 Derived Peptide

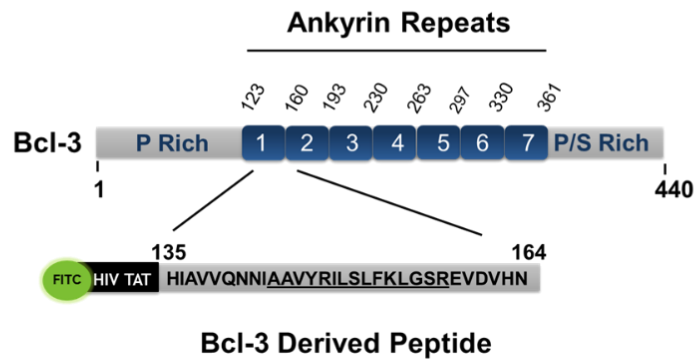
4.3.3.1 Design and synthesis

A short Bcl-3 derived peptide (BDP) was designed to span both α -helices of ANK1 and the first β -sheet of ANK2 (Figure 4.8 B), incorporating the putative p50 binding region identified by the peptide array (Figure 4.8 C). The derived peptide consisted of the region H135-N164 of Bcl-3 fused with the cell permeable HIV-TAT peptide to mediate cellular uptake without transfection (Figure 4.8 A). A Fluorescein isothiocyanate (FITC) tag was also conjugated to the N-terminus to visualise peptide internalisation by the cell.

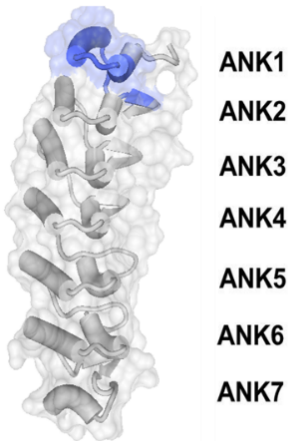
4.3.3.2 Peptide characterisation

As the BDP was labelled with a C-terminal FITC tag, peptide uptake was easily assessed by immunofluorescence and flow cytometry analysis. Following 2 hours of peptide treatment, 98% of cells were FITC positive by flow cytometry analysis (Figure 4.9 A) and the peptide predominantly localised to the nucleus (Figure 4.9 B). These data indicate that the BDP is effectively internalised by cells and can translocate to the nucleus, where Bcl-3 is localised. To investigate the potential of this peptide to regulate TLR function *in vitro*, a luciferase reporter assay incorporating the Bcl-3 regulated NF- κ B-dependent IL-23p19 gene promoter was employed (Carmody et al., 2007a, Muhlbauer et al., 2008). RAW 264.7 cells were cotransfected with firefly IL-23p19 and *Renella* luciferase expression vectors, with or without Bcl-3. Following 24 hours transfection, cells were pre-treated with BDP before stimulation with LPS for 8 hours (Figure 4.9 C). To exclude any nonspecific effects due to peptide transduction, cells were also pre-treated with a mutant NEMO binding domain peptide (mNBD) as an additional control. The mNBD peptide contains mutations of two critical IKK β interacting amino acids within in the NEMO binding domain necessary for inhibition of NF- κ B activation (Tas et al., 2005). In agreement with previous reports (Muhlbauer et al., 2008), Bcl-3 expression inhibited IL-23p19 reporter activity in RAW 264.7 cells following stimulation with LPS. As expected the mNBD peptide had no significant effect on reporter activity while the BDP inhibited reporter activity to equivalent levels as seen with over expressed Bcl-3.

A



B



C

Peptide	Sequence	Coressponding Bcl-3 Residue
33	DGDTPLHIAVVQNNIAAV	129-146
34	PLHIAVVQNNIAAVYRIL	133-150
35*	<u>AVVQNNIAAVYRILSLFK</u>	137-154
36*	<u>NNIAAVYRILSLFKLGS</u>	141-158
37	<u>AVYRILSLFKLGSREVDV</u>	145-162
38	<u>ILSLFKLGSREVDVHNNL</u>	159-166
39	<u>FKLGSREVDVHNNLRQTP</u>	153-170
40	<u>SREVDVHNNLRQTPLHLA</u>	157-174

Figure 4.8 Design of Bcl-3 derived cell permeable peptide.

(A) Schematic representation of murine Bcl-3 with the Bcl-3 derived peptide corresponding to Bcl-3 amino acids 135-164 indicated. Sequence of peptide 35 and 36 (144-158) identified as positive p50 binding peptides in Figure 4.3 are underlined. (B) Bcl-3 crystal structure with residues corresponding to the BDP shaded in blue. (C) Sequences of Bcl-3 peptides 33-40 from Bcl-3 peptide array with corresponding Bcl-3 amino acids indicated. * denotes positive p50 binding peptides identified in Figure 4.3. Sequence of BDP underlined with 144-158 in italics.

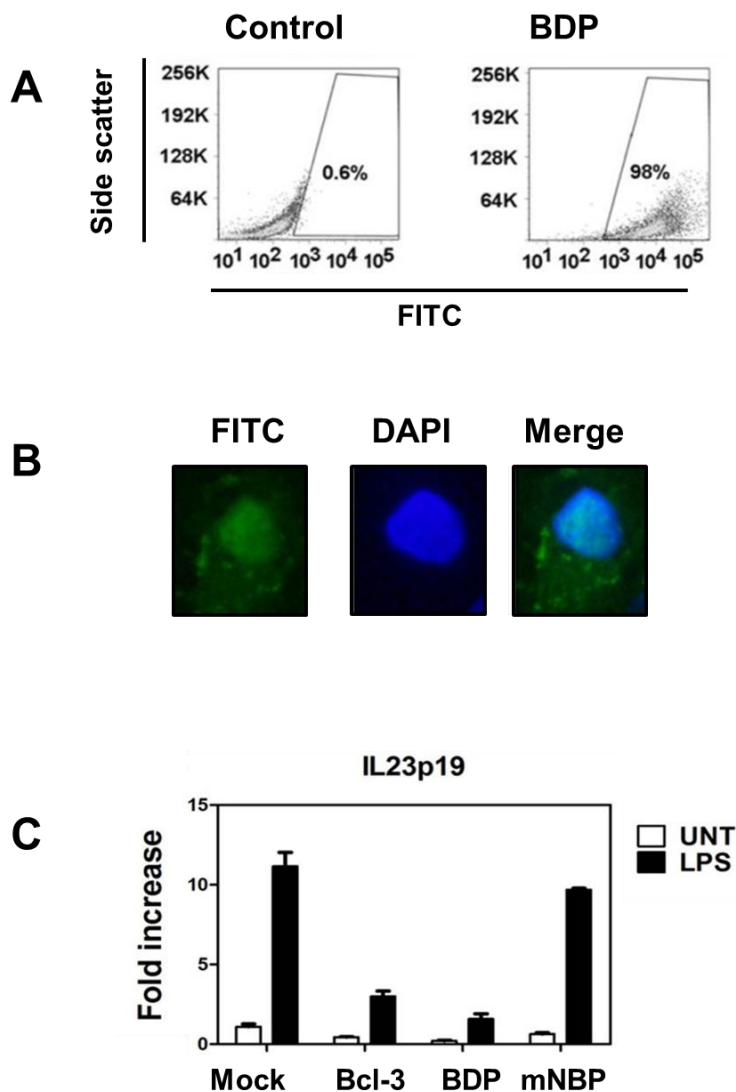


Figure 4.9 BDP can translocate to the nucleus and inhibit IL-23p19 reporter activity.

Work carried out by Dr Amy Collieran (University College Cork, Cork, Ireland) (A) Flow cytometry analysis of RAW 264.7 following treatment with 2 μ M FITC labelled BDP or DMSO control for 2 hours. (B) Immunofluorescence analysis of HeLa cells treated with 20 μ M FITC labelled BDP for 2.5 hours. (C) RAW 264.7 cells were transiently transfected with the pLucp19 plasmid and Bcl-3 expression vector (Bcl-3) or with empty vector (Mock, BDP, mNBP) for 24 hours. Cells were left untreated (Mock, Bcl-3) or pre-treated with 20 μ M peptide as indicated for 1.5 hours before stimulation with 100ng/ml LPS. Cells were cultured for an additional 8 hours before luciferase activity was measured. The *Renella* luciferase expression vector pRL-TK was used as an internal control to normalise the transfection efficiency across all samples. IL-23p19 reporter activity is represented as fold increase over untreated (UNT) cells transfected with pLucp19 plasmid and empty vector expression (Mock). Transfections were performed in triplicate per experiment and data shown are means + SEM and are representative of independent experiments. Statistical significance was determined by Student's t test; $P < 0.05$ (*), $P < 0.01$ (**), $P < 0.001$ (***)

4.3.3.3 Peptide optimization

Preliminary characterisation of the BDP in the RAW 264.7 cell line identified a novel peptide with the ability mimic Bcl-3 *in vitro*. Cargo size can effect uptake and cell toxicity of a peptide (Tünnemann et al., 2006) . Thus, the initial BDP sequence was refined to produce a more effective peptide for *in vivo* use to study Bcl-3 function and regulation of TLR activation (Figure 4.10A). The new short Bcl-3 derived peptide (sBDP) consisted of only Bcl-3 amino acids 144-158 (corresponding to peptides 35 and 36) fused with the HIV TAT CPP. The sBDP represents the outer helix and linker domains of Bcl-3 ANK1 (Figure 4.10 B). A mutant sBDP was also designed to establish an additional control for peptide transduction. The mutant peptide was identical to the wild type sequence apart from alanine substitutions of essential p50 interacting amino acids determined by the alanine scanning array (Figure 4.11 A and B). The mutated amino acids are highlighted on the human Bcl-3 structure which are identical or highly conserved in the murine sequence (Figure 4.11 B). The sBDP and mBDP were tested as before in the IL-23p19 luciferase reporter assay. RAW 264.7 cells were either pre-treated with sBDP or mBDP before stimulation with LPS. Expression of Bcl-3 and transduction with sBDP inhibited IL-23p19 reporter activity while the mutant peptide had no effect on reporter activity (Figure 4.11D). These data demonstrates that the inhibitory activity of BDP is contained within the 144-158 region and that this activity is dependent on the key amino acids required for peptide interaction with p50.

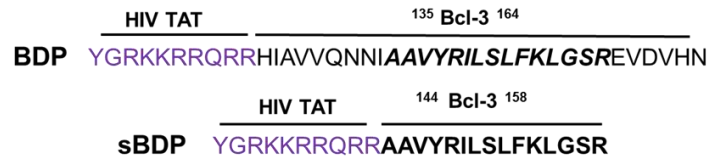
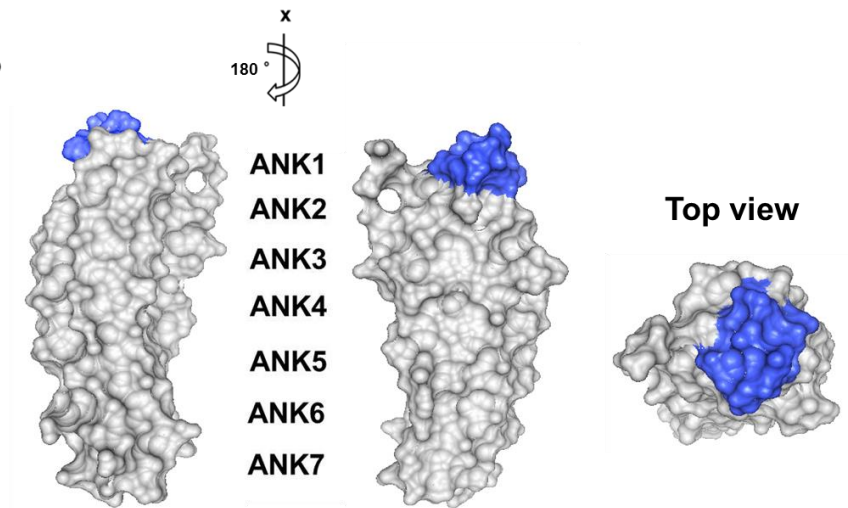
A**B**

Figure 4.10 Sequence of the shortened Bcl-3 derived cell permeable peptide.

(A) Schematic representation of the full length (BDP) and shortened (sBDP) Bcl-3 derived peptide sequences with corresponding murine Bcl-3 amino acids indicated. The N-terminal HIV TAT sequence is coloured in purple. (B) Human Bcl-3 crystal structure with residues 144-158 corresponding to the sBDP sequence are in shaded blue.

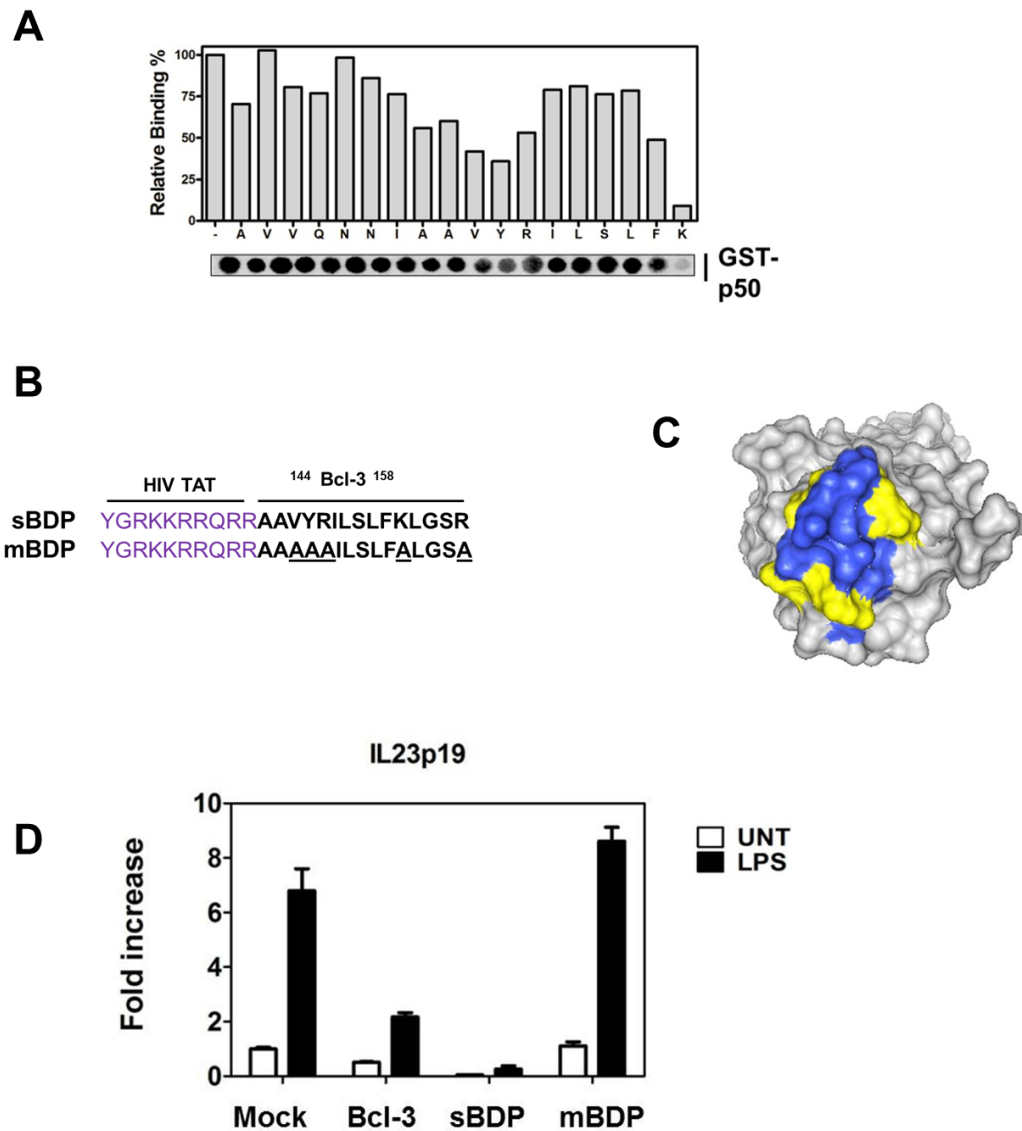


Figure 4.11 sBDP inhibits IL-23p19 luciferase reporter activity.

(A) Alanine substitution analysis of positive peptide p50 binding Bcl-3 peptide 35, identified in Figure 4.3. The 18 amino acids of Bcl-3-derived peptide 35 were sequentially substituted with alanine and probed with GST-p50 and detected by immunoblotting with anti-GST antibody. p50 binding was quantified by densitometry and calculated as a percentage binding of the parent unsubstituted peptide on the same array. (B) Sequences of short BDP (sBDP) and mutated short BDP (mBDP) with alanine substitutions underlined. (C) Top view of human Bcl-3 crystal structure with residues corresponding sBDP shaded in blue and residues mutated in mBDP shaded in yellow. (D) RAW 264.7 cells were transiently transfected with the pLucp19 plasmid and Bcl-3 expression vector (Bcl-3) or with empty vector (Mock, sBDP, mBDP) for 24 hours. Cells were left untreated (Mock, Bcl-3) or pre-treated with 20 μ M peptide as indicated for 2 hours before stimulation with 100ng/ml LPS for an additional 18 hours. Transfections were performed in triplicate per experiment and data shown are means + SEM and are representative of independent experiments. IL-23p19 reporter activity was determined as in Figure 4.9. Statistical significance was determined by Student's t test; P<0.05 (*), P<0.01 (**), P<0.001(***)

4.4 DISCUSSION

Bcl-3 mediated inhibition of p50 homodimer ubiquitination results in a stable p50:Bcl-3 repressor complex bound to the promoters of NF- κ B target genes. Interaction with p50 is necessary and sufficient for this anti-inflammatory function of Bcl-3. In order to further investigate the role of this complex in the regulation of NF- κ B mediated gene transcription, a Bcl-3 peptomimetic strategy was employed. A peptide array approach was utilised to identify short peptides of Bcl-3 capable of binding p50. A number of positive interactions between recombinant p50 and Bcl-3 peptides representing the N terminus, ANK1, ANK6 and ANK7 were observed. Following alanine substitution analysis, critical residues within these peptides were identified. Considerable overlap between interacting residues determined by peptide array and those predicted from computation modelling occurred in ANK6 and ANK7, further supporting peptide array as a method to identify critical p50 binding regions.

As the Bcl-3 p50 crystal structure is unsolved, *in silico* models are developed based on the p50/p65:I κ B α complex. These computational complexes are limited by the available crystal structure of a p50 homodimer bound to DNA and the ARD of Bcl-3. The extreme N- and C-terminal domains of both p50 and Bcl-3 are not represented in the current resolved structures and thus the predicted complexes do not account for interactions in these domains. This may explain the differences observed between interacting amino acids predicted by *in silico* modelling and those determined by peptide array. Comparison of the predicted structure of a complete p50 subunit to Manavlan *et al.* modelled Bcl-3:p50 complex, it is likely the N-terminal domain of Bcl-3 makes additional contacts with the extreme C terminus of p50, previously determined to be important for binding in chapter1 (Figure 4.12).

Residues 144-158 of Bcl-3, comprising the outer alpha helix and linker region of ANK1 were considered to contain a putative p50 binding domain. The ARD of the I κ B proteins are highly conserved, for instance Bcl-3 and I κ B α share almost 34% sequence identity between ANK1-6. However, multiple sequence alignment of this region of Bcl-3 (144-158) illustrates an area of low similarity between all I κ B proteins. The most significant structural differences between nuclear and cytoplasmic I κ B proteins occur in the N- and C-termini (Basith *et al.*, 2013, Manavalan *et al.*, 2010, Michel *et al.*, 2001). Although the ARDs of I κ B proteins

typically represent a series of conserved ANK repeats, ANK1 deviates from the other ANK repeats of Bcl-3. Compared to the consensus sequence, the outer alpha helix of ANK 1 is extended by four amino acids, three of which (GSR) contribute to the polarity of this region (Michel et al., 2001) and A145 and R148 replace the hydrophobic residues observed at these positions in other repeats. Analysis of the ARD of multiple I κ B family members by Basith *et al.* and Manavalan *et al.* identified residues contained within ANK1 involved in flexibility and functional divergence (Figure 4. 13) (Basith et al., 2013, Manavalan et al., 2010, Michel et al., 2001). ANK1 of Bcl-3 has also been implicated in the survival of activated T and B cells (Mitchell et al., 2002). Taken together, these data suggested this region of ANK1 would be an ideal candidate in developing a Bcl-3 specific mimetic peptide as it represents a structurally unique, flexible domain capable of binding p50.

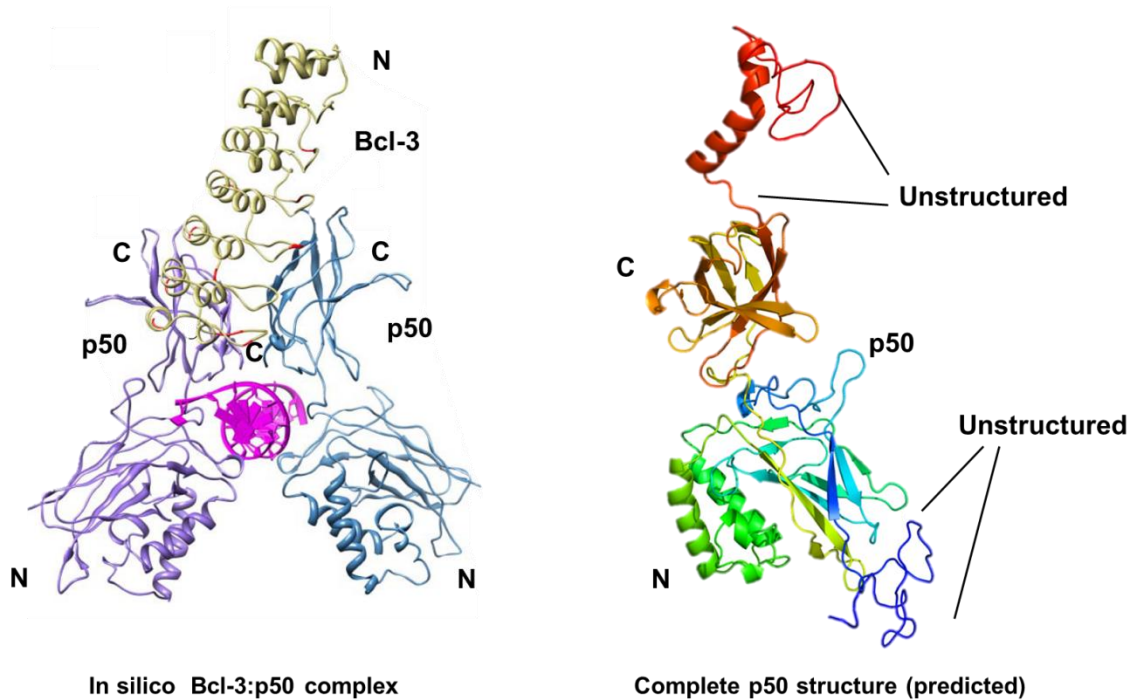


Figure 4.12 Comparison of Bcl-3:p50 complex with complete p50 structure.

In silico model of a predicted of a DNA bound Bcl-3:p50 homodimer complex (Manavalan et al., 2010) and the predicted structure of a complete p50 subunit including the unstructured extreme N- and C-terminal domains (N and C respectively) determined by homology modelling with Phyre 2.

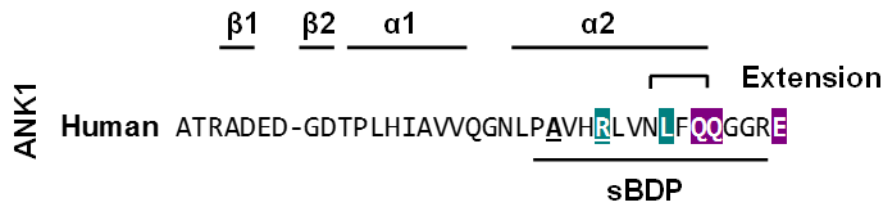


Figure 4. 13 Structural analysis of Bcl-3 ANK repeat 1.

Teal shading represent flexible residues (Manavalan et al., 2010), purple shading represent residues involved in type II divergence (radical biochemical changes between the I κ B subfamilies) (Basith et al., 2013) and underlined amino acids are replaced by hydrophobic residues in all other ANK repeats. The extension of the outer α -helix is indicated. The corresponding murine sequence representing sBDP is underlined.

The initial Bcl-3 derived peptide consisted of a HIV-TAT CPP fused to 30 derived amino acids (135-164) of Bcl-3, encompassing the putative p50 binding domain (144-158) with 6-9 N- and C-terminal flanking residues. The N-terminal FITC tag allowed visualisation of peptide uptake and consistent with previous reports for HIV-TAT conjugated peptides, the BDP translocated to the nucleus, the site of Bcl-3:p50 interaction. In an *in vitro* luciferase reporter assay, the peptide inhibited expression of the pro-inflammatory cytokine IL-23p19 to equivalent levels as that seen with Bcl-3 overexpression. These results provide proof of principle for Bcl-3 mimetic peptides as regulators of NF- κ B. The BDP was further reduced in size to contain only 15 Bcl-3 amino acids (144-158) fused with the HIV-TAT CPP. A mutant version of this short peptide was also designed, where critical p50 binding residues determined by alanine substitution peptide array analysis were mutated to alanine. This short peptide retained the functional properties of the parent BDP however the mutant peptide had no significant effect on IL-23p19 reporter activity. These data further support the importance of Bcl-3:p50 interaction for Bcl-3 mediated inhibition NF- κ B activity and inflammatory gene expression.

NF- κ B regulates the transcription of a number of genes critical for the inflammatory response and is considered a potential therapeutic target in a range of human diseases where inflammation plays a role. Hundreds inhibitors of NF- κ B activation have been described (Gilmore and Herscovitch, 0000) but are limited by broad specificity. Inhibition of NF- κ B mediated transcription may represent a more specific strategy in the control of NF- κ B signalling. For example, anti-inflammatory peptide-6 (AIP6), a peptide designed to bind p65

and inhibit DNA binding, was shown to inhibit the transcriptional activity of p65 and production of proinflammatory mediators including TNF while having no effect I κ B α phosphorylation or nuclear localisation of p65 (Wang et al., 2011). The peptides described here were designed to mimic Bcl-3 function, by suppressing NF- κ B regulated transcription, thus representing a potential gene specific inhibitor of inflammation. These mimetic peptides can modulate TLR mediated function *in vitro* however; their potential *in vivo* is yet to be established. The ability of these peptides to rescue the phenotype of *Bcl3*^{-/-} cells and as possible inhibitors of NF- κ B in models of LPS induced septic shock should next be determined. Bcl-3 derived peptides provide a valuable tool for further analysis of Bcl-3 function and the development of Bcl-3 based therapeutic agents for inflammatory disease.

—— Chapter Five ——

5 Identification of Tpl-2 as novel binding partner of Bcl-3

5.1 ABSTRACT

The I κ B protein, Bcl-3 is an essential negative regulator of NF- κ B during TLR and TNFR signalling. Here we report a novel role for Bcl-3 as an inhibitor of MAPK signalling. MAP kinases are serine/threonine-specific protein kinases activated by a three tiered protein kinase pathway. The best characterised of these MAP kinases, ERK1/2 regulate a number of cellular processes such as differentiation, proliferation and inflammatory gene expression. The MAP kinase kinase kinase, Tpl-2, mediates ERK1/2 activation during innate immune responses triggered by TLRs and TNF. We have identified Bcl-3 as a novel regulator of Tpl-2 mediated activation of ERK1/2. Following LPS stimulation, Bcl-3 deficient macrophages demonstrate increased phosphorylation of ERK1/2 and increased expression of a number of ERK dependent genes. Furthermore, Bcl-3 overexpression inhibits TPL-2 MEK-kinase activity and Tpl-2 mediated ERK1/2 activation, supporting the role of Bcl-3 as a negative regulator of MAPK signalling. Bcl-3 interacts with TPL-2 independently of p105, an essential regulator of TPL-2 activation. Our data establishes Bcl-3 as a critical regulator of both MAPK and NF- κ B activity following TLR activation. We identify Bcl-3 as a unique member of the I κ B family which co-ordinates MAPK and NF- κ B activity in the innate immune response.

5.2 INTRODUCTION

Engagement of all TLRs activate a common pathway culminating in the activation of NF- κ B and MAPKs p38, JNK and ERK1/2 (Figure 1.9) (Barton and Medzhitov, 2003). ERK1 (or MAPK3), the first MAPK to be discovered, was identified over 20 years ago as a 43 kDa protein kinase characterised by its ability to phosphorylate microtubule-associated protein-2 (MAP2) (Boulton et al., 1990). Shortly after, a 41 kDa ERK-related protein/serine kinase sharing 90% sequence identity to ERK1 was described and named ERK2 (or MAPK1) (Boulton et al., 1991, Keshet and Seger, 2010). ERK1/2 are ubiquitously expressed and over one hundred nuclear and cytoplasmic ERK substrates have now been identified, regulating cellular processes such as proliferation, differentiation and cell cycle progression. ERK1/2 are activated following stepwise phosphorylation of two sites, threonine and tyrosine by the dual-specificity MAP2Ks, MEK1 and MEK2 (Ferrell and Bhatt, 1997). A number of MAP3Ks can initiate MAPK signalling by activating MEK1 and MEK 2 however, the specific MAP3K utilised, is cell type- and stimulus-dependent. For example, the ERK cascade is primarily initiated by the MAP3K, RAF however, in innate responses, Tpl-2 plays a dominant role. Tpl-2 mediates ERK1/2 activation by all TLRs and some members of the TNFR superfamily in primary macrophages (Banerjee et al., 2006, Eliopoulos et al., 2003). In macrophages, Tpl-2 specifically mediates activation of ERK1/2 but not MAPKs, p38 and JNK following LPS induction (Dumitru et al., 2000). Although Tpl-2 is the sole MAP3K responsible for ERK1/2 activation in macrophages, the mechanisms involved in Tpl-2 regulation are still poorly understood.

Activation and function of Tpl-2 requires at least two regulatory steps, phosphorylation of Thr 290 in the activation loop of its kinase domain and also at Ser 400 in its C-terminus (Gantke et al., 2011). Different kinases have been reported to be responsible for these phosphorylation steps but this may be dependent on the different experimental systems utilised. Stafford *et al.* and Lucian *et al.* suggest that Tpl-2 autophosphorylates on Thr 270 in 293T cells, whereas Cho *et al.* report this phosphorylation is controlled by IKK β in RAW264.7 macrophages (Stafford et al., 2006, Luciano et al., 2004, Cho et al., 2005). Recently Roget et al. demonstrated that Tpl-2 Ser 400 phosphorylation is mediated by IKK β in macrophages (Roget et al., 2012). These phosphorylation steps are thought activate Tpl-2-MEK kinase activity by inducing conformational

changes in the inhibitory C-terminal domain, which facilitate MEK binding and phosphorylation (Gantke et al., 2012). Phosphorylation at Ser 400 is also required for association of 14-3-3 with the Tpl-2 C terminus which increases the efficiency of MEK-1 phosphorylation, potentially by altering the inhibitory interaction between the Tpl-2 C terminus and kinase domain (Ben-Addi et al., 2014).

Although p105 maintains Tpl-2 in an inactive state in the cytoplasm of resting cells, p105 does not directly regulate Tpl-2 kinase activity (Figure 1.11). p105 inhibits Tpl-2 dependent MEK phosphorylation by preventing Tpl-2/MEK interaction and as Tpl-2 catalytic activity is not inhibited by p105, it is thought that Tpl-2 may have other substrates other than MEK. In support of this, recent work has implicated Tpl-2 in the phosphorylation of histone H3 and was shown to be recruited to the *c-fos* promoter directly activating AP-1 transcription (Choi et al., 2008). Steady state levels of Tpl-2 are regulated by interaction with p105, however following stimulus-induced liberation from p105, Tpl-2 is rapidly degraded (Waterfield et al., 2003). Very little is known about the mechanisms governing this degradation or negative regulators of Tpl-2 following activation.

In this chapter we further investigated the regulation of TLR signalling by Bcl-3, specifically exploring the role of Bcl-3 in the MAPK pathway. Using macrophages derived from *Bcl3*^{-/-} mice we analysed LPS-induced MAPK activation and MAPK dependent gene expression. ERK1/2 was found to be phosphorylated to a much greater extent in *Bcl3* deficient cells, correlating with increased expression of ERK dependent genes *Fos* and *Egr1*. To delineate the function of Bcl-3 in ERK activation we examined the MAPK ERK cascade and identified Tpl-2 as a new interacting partner of Bcl-3. This chapter illustrates a novel role for Bcl-3 in TLR signalling and as a potential negative regulator of the MAPK pathway.

5.3 RESULTS

5.3.1 Bcl-3 Negatively Regulates ERK1/2 Signalling

To search for novel functions of Bcl-3, the effect of *Bcl3* deficiency on the activation of MAPK signalling pathways was investigated. The MAPK signalling cascade is one of the key downstream targets following LPS activation in macrophage. Bone marrow derived macrophages (BMDM) prepared from either wild-type or *Bcl3*^{-/-} mice were stimulated with LPS and analysed by immunoblot and qPCR. Bcl-3 deficiency resulted in increased ERK1/2 phosphorylation (Figure 5.1 A and B) and ERK-dependent gene expression following LPS stimulation (Figure 5.2). In addition to NF- κ B dependent genes, *Tnf* and *Il6*, early growth response 1 (*Egr1*), a zinc finger transcription factor (Guha et al., 2001, Waterfield et al., 2003, Robinson et al., 2007) and Fos, a proto-oncogene that forms part of the activator protein 1 (AP-1) transcription factor complex (Okazaki and Sagata, 1995, Zhao et al., 2012, Kaiser et al., 2009), are downstream targets of the Tpl-2-MEK-ERK pathway and were significantly increased in *Bcl3*^{-/-} macrophages relative to wild type following LPS stimulation.

ERK activation following LPS stimulation is dependent on IKK activity and proteasomal degradation of p105 (Beinke et al., 2004, Waterfield et al., 2004). Consistent with previous reports (Beinke et al., 2004, Waterfield et al., 2004) pharmacological inhibition of IKK activation with BAY-11-7082 (Figure 5.3 A) and the proteasome with MG132 (Figure 5.3 B) inhibited LPS induced ERK phosphorylation. Although significantly more phosphorylated ERK1/2 was present in *Bcl3*^{-/-} macrophage following stimulation, it was also sensitive to inhibition by these compounds. This suggested that the hyper-phosphorylation of ERK1/2 in *Bcl3*^{-/-} macrophage was due to activation of the same signalling pathway as wild type macrophage. Taken together these data suggest a novel role for Bcl-3 as negative regulator of MAPK signalling and ERK-dependent gene expression.

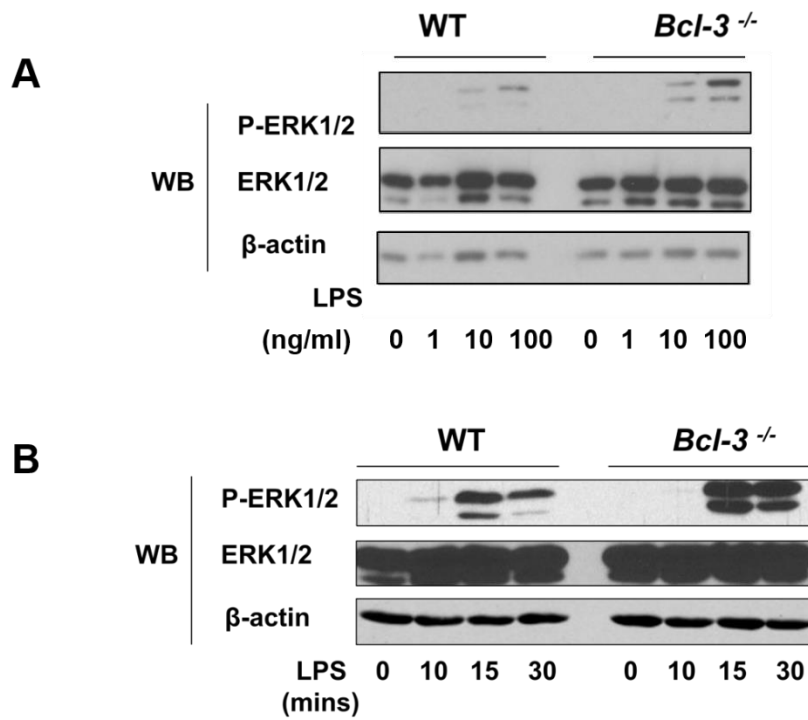


Figure 5.1 Increased ERK MAPK signalling in *Bcl-3*^{-/-} macrophage.

(A) Macrophages derived from wild-type (WT) and *Bcl3*^{-/-} bone marrow combined from three mice were stimulated for 15 minutes with 1ng/ml, 10ng/ml and 100ng/ml LPS. Whole cell extracts were analysed by WB for phosphorylated and total ERK1/2. (B) Macrophage derived from wild-type (WT) and *Bcl3*^{-/-} bone marrow combined from three mice were stimulated with 100ng/ml LPS for the indicated times. Whole cell extracts were analysed by WB for phosphorylated and total ERK1/2.

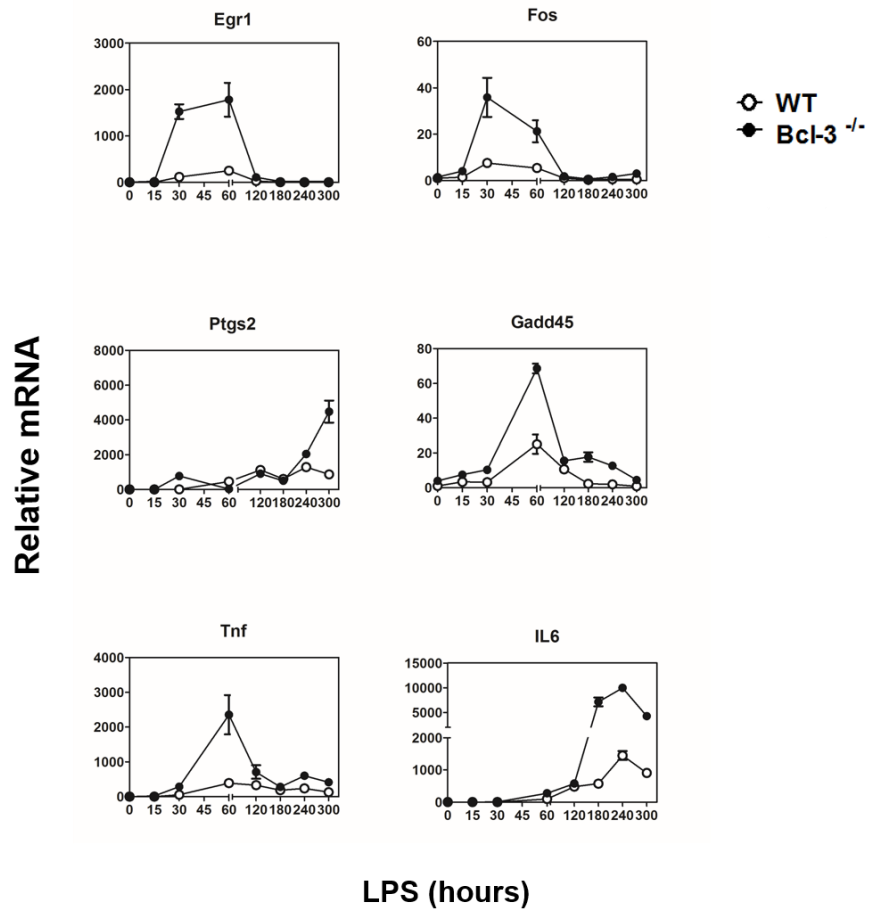


Figure 5.2 Increased ERK-dependent gene expression in *Bcl3*^{-/-} macrophage.

(A) Macrophages derived from wild-type (WT) (white circles) and *Bcl3*^{-/-} (black circles) bone marrow combined from two mice were stimulated with 10ng/ml LPS for the indicated time. Gene expression levels were determined by real-time PCR. Data shown are means \pm SEM of replicate samples and are representative of three independent experiments.

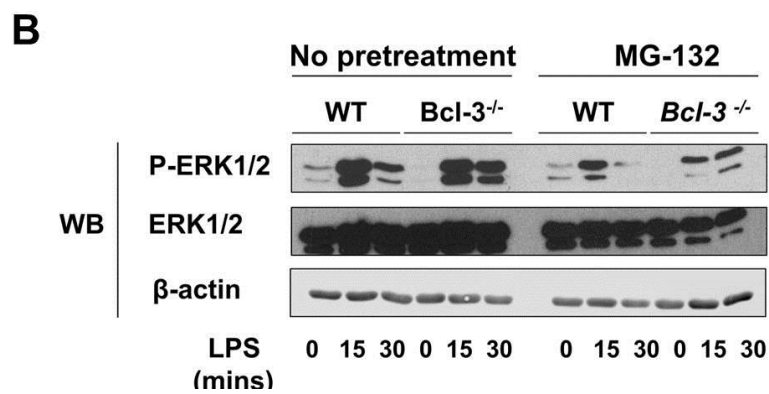
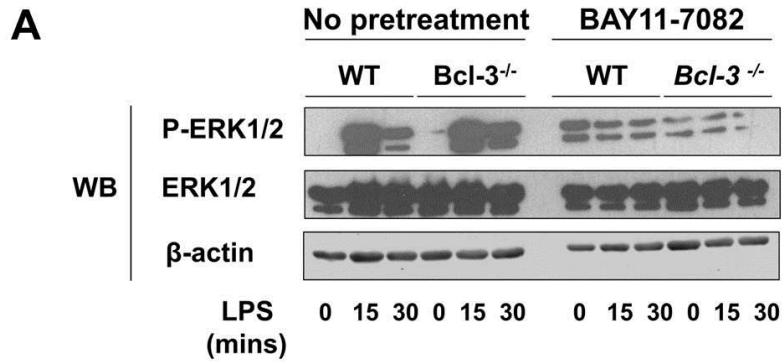


Figure 5.3 Proteasome and IKK activity is required for LPS activation of ERK1/2 in *Bcl3*^{-/-} macrophage .

Macrophages derived from wild-type (WT) and *Bcl3*^{-/-} bone marrow combined from three mice were left untreated or pre-treated for one hour with (A) 20µM BAY-11-7082 or (B) 20µM MG132 before stimulation with 100ng/ml LPS for the indicated times. Whole cell extracts were analysed by WB for phosphorylated and total ERK1/2.

5.3.2 Tpl-2 interacts with Bcl-3 independent of p105

As the specific target for Bcl-3 mediated inhibition of ERK1/2 signalling was unknown, individual tiers of the MAPK cascade were next investigated. LPS induced ERK activation in primary macrophage is dependent on Tpl-2. Tpl-2 interacts with p105, another I κ B family member, thus it's potential as a new binding partner of Bcl-3 was explored. The interaction of Tpl-2 with Bcl-3 was assessed by co-transfection in 293T cells (Figure 5.4 A). Tpl-2 is expressed in cells as a 58 and 52 kDa isoforms due to initiation of translation at alternative methionines, M1 and M30 respectively. Following immunoprecipitation with anti-FLAG, Tpl-2 was only detectable in immunoprecipitates co-transfected with Bcl-3-FLAG. This interaction was also dependent on the kinase activity of Tpl-2 (Figure 5.4 B). Tpl-2^{D270A} contains a mutation in the kinase domain activation loop of Tpl-2 rendering it catalytically inactive (Beinke et al., 2003). Tpl-2^{D270A} interacted with Bcl-3 at much reduced levels compared to wild type Tpl-2 and was only detectable after long exposure.

A critical step in the activation of the Tpl-2-ERK1/2 pathway is the IKK induced proteolysis of p105. Phosphorylation of p105 at S927 and S932 is essential for release of Tpl-2 from p105 and activation of the MAPK cascade (Beinke et al., 2004). Importantly, Bcl-3 did not block IKKB induced phosphorylation of p105 (Figure 5.5 A) suggesting Bcl-3 regulates MAPK signalling independently of p105. To explore the contribution of p105 in Tpl-2-Bcl-3 interaction, *Nfkb1*^{-/-} MEFs which do not contain either p105 or p50 were also co-transfected with Bcl-3 and Tpl-2 (Figure 5.5 B). As Tpl-2 is inherently unstable in the absence of p105 (Beinke et al., 2004, Waterfield et al., 2004), cells were treated with MG132 prior to immunoprecipitation. Tpl-2 was again detectable in immunoprecipitates of Bcl-3-FLAG suggesting that Bcl-3 does not require p105 for interaction with Tpl-2.

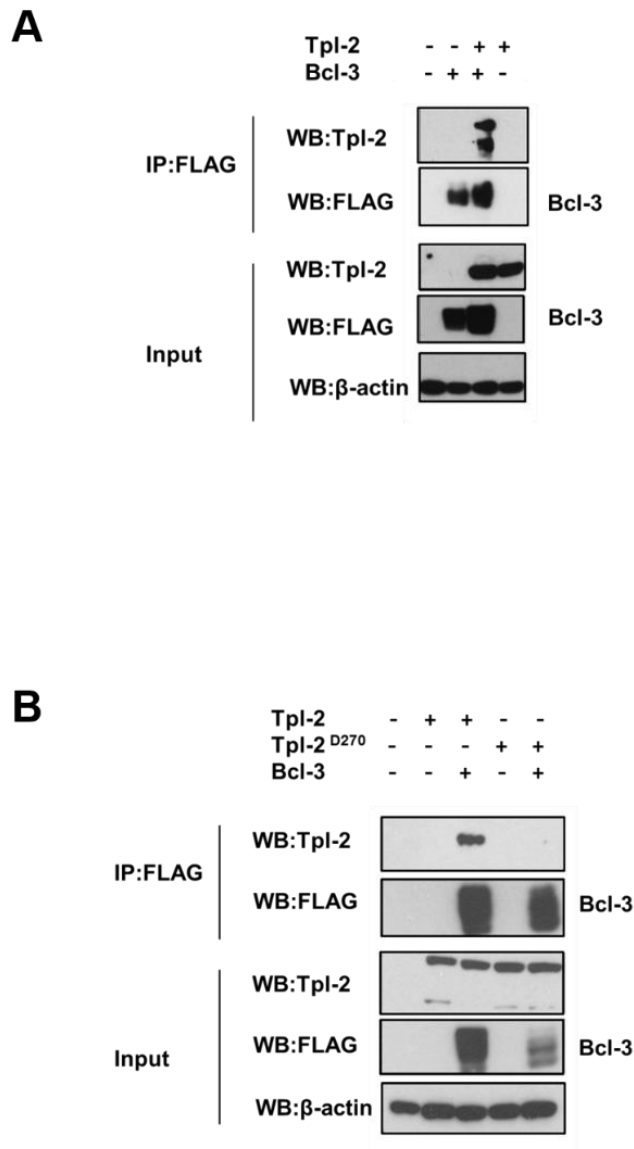


Figure 5.4 Bcl-3 interacts with Tpl-2.

(A) HEK293T cells were transfected with pRK5-Bcl-3-FLAG and pcDNA3-Tpl-2-MYC expression vectors as indicated. Whole cell lysates were immunoprecipitated (IP) with anti-FLAG and analysed by WB with anti-Tpl-2 for Tpl-2 and anti-FLAG for Bcl-3. (B) HEK293T cells were transfected with pRK5-Bcl-3-FLAG and pcDNA3-Tpl-2-MYC or a kinase dead Tpl-2^{D270A} mutant. Whole cell lysates were immunoprecipitated and analysed as in A.

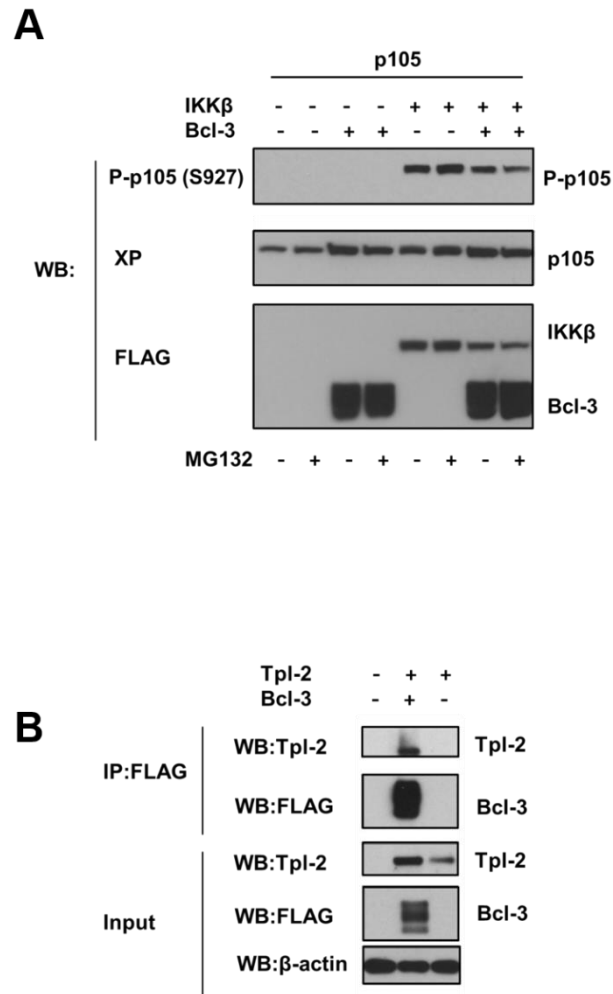


Figure 5.5 p105 independent Bcl-3-Tpl-2 interaction.

(A) Whole cell lysates were immunoprecipitated HEK293T cells were transfected with expression vectors for pEF4-105-Xpress, pRK5-Bcl-3-FLAG and pRK5-IKK β -FLAG as indicated. Cells were treated with 20 μ M MG132 for 2 hours prior to harvest. Whole cell lysates were analysed by WB for phosphorylated p105 with anti-phospho-p105 (S927). (B) *Nfkb1*^{-/-} MEFs were transfected with pRK5-Bcl-3-FLAG and pcDNA3.Tpl-2-MYC expression vectors as indicated. Cells were treated with 20 μ M MG132 for 2 hours prior to harvest. Whole cell lysates were immunoprecipitated (IP) with anti-FLAG and analysed by WB with the indicated antibodies.

5.3.3 Bcl-3 negatively regulates Tpl-2

5.3.3.1 Bcl-3 inhibits Tpl-2-MEK kinase activity

As Bcl-3 interacts with Tpl-2, the possibility that Tpl-2 kinase activity is regulated by association with Bcl-3 was next investigated. MYC tagged Tpl2 was immunoprecipitated from 293T cells transfected with or without Bcl-3. Tpl-2 kinase activity assay was assessed *in vitro* with inactive GST-MEK1 as a substrate. Immunoprecipitated Tpl-2 was incubated with inactive MEK1 in the presence of ATP and MEK phosphorylation was determined by Western blot with anti-phospho MEK1/2 antibody. Co-expression with Bcl-3 dramatically reduced *in vitro* Tpl-2 kinase activity (Figure 5.6 A). As only a fraction of overexpressed Tpl-2 is bound to p105 (Beinke et al., 2003), overexpression of Tpl-2 activates the MAPK pathway culminating in phosphorylation of ERK1/2. 293T cells were transfected with Tpl-2 on its own or with Bcl-3 and the phosphorylation of endogenous ERK1/2 was determined by Western blotting of cell lysates. Tpl-2 induced phosphorylation of ERK1/2 which was significantly inhibited by co-expression with Bcl-3 (Figure 5.6 B).

5.3.3.2 Bcl-3 inhibits Tpl-2 dependent AP1 reporter activity

AP-1 is a heterodimeric transcription factor composed of members of the Fos and Jun family that regulates a number of cellular processing including proliferation and cell survival (Angel and Karin, 1991). AP-1 activity is modulated by a variety of stimuli (extensively reviewed in (Shaulian and Karin, 2002)) that activate MAPK signalling (Karin, 1995). ERK1/2 activation can modulate AP-1 activity via *c-Fos* induction and thus increased synthesis of *c-Fos* (Karin et al., 1997, Herrera et al., 1990, Monje et al., 2003). To further investigate the role of Bcl-3 as a negative regulator of MAPK dependent transcription, a luciferase reporter assay incorporating the multiple copies of the AP1 enhancer AP1 gene promoter was employed. RAW 264.7 macrophage cells were transfected with p-AP1-Luc reporter plasmid and *Renilla* luciferase vectors and increasing amounts of Tpl-2. The total plasmid concentration was kept constant across all samples with an empty vector. Consistent with AP-1 activation in other cell lines (Li et al., 2010) Tpl-2 dose dependently induced AP-1 reporter activity in RAW 264.7 macrophage cells (Figure 5.7 A) which was significantly reduced by co-expression with Bcl-3 (Figure 5.7 B).

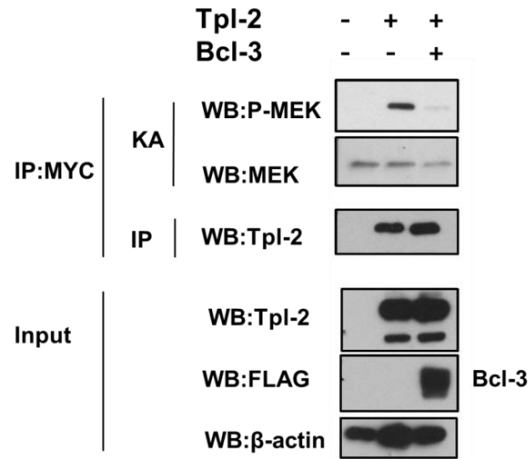
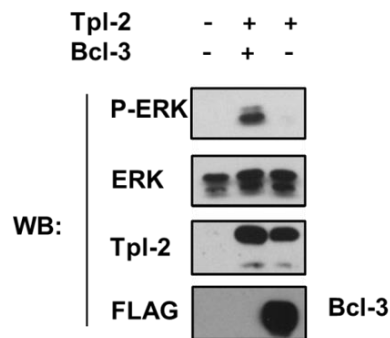
A**B**

Figure 5.6 Bcl-3 inhibits Tpl-2 MEK-kinase activity.

(A) HEK293T cells were transfected with pRK5-Bcl-3-FLAG and pcDNA3.Tpl-2-MYC expression vectors as indicated. Tpl-2 was immunoprecipitated (IP) from whole cell lysates with anti-MYC and *in vitro* MEK kinase assays (KA) were performed with inactive GST-MEK1 as a substrate. MEK phosphorylation was determined by WB of kinase assay reaction with anti-phospho MEK1/2 antibody. Immunoprecipitates were analysed for equal loading with anti-Tpl-2. (B) 293T cells were transfected with pRK5-Bcl-3-FLAG and pcDNA3. Tpl-3-MYC as indicated. Cytoplasmic extracts were analysed for endogenous ERK1/2 phosphorylation by WB with anti-phospho ERK1/2.

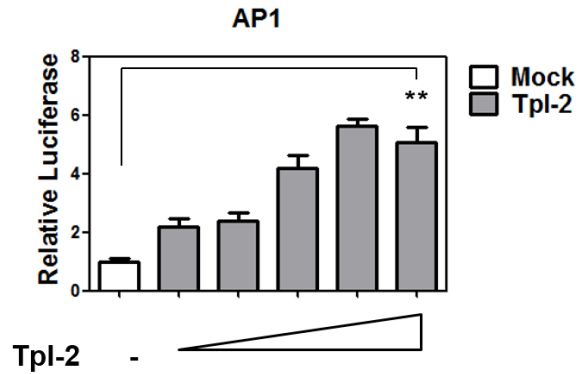
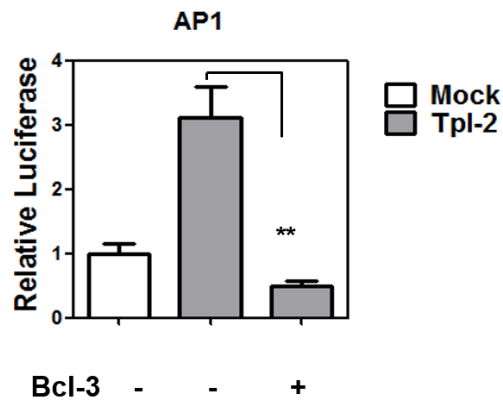
A**B**

Figure 5.7 Bcl-3 inhibits Tpl-2 induced AP-1 activation.

(A) RAW 264.7 cells were transiently transfected with 100ng pAP1-Luc luciferase and 10ng pRL-TK *Renella* luciferase expression vectors and increasing amounts (100,200,300,400 and 500ng) of Tpl-2-MYC (Tpl-2). The total amount of plasmid was kept constant across all samples by adjusting the amount of empty vector used. AP-1 reporter activity is represented as fold increase over cells transfected with empty vector (Mock). The *Renella* luciferase expression vector pRL-TK was used as an internal control to normalise the transfection efficiency across all samples. AP1 reporter activity is represented as fold increase over untreated cells transfected with pAP1-Luc plasmid and empty vector expression (mock). Statistical significance was determined by Student's t test; $P < 0.05$ (*), $P < 0.01$ (**), $P < 0.001$ (***). Data presented as +SEM of triplicate samples. (B) RAW 264.7 cells were transiently transfected with 100ng pAP1-Luc luciferase and 10ng pRL-TK *Renella* luciferase expression vectors and 300ng pcDNA3-Tpl-2-MYC (Tpl-2) with or without 150ng pRK5-Bcl-3-FLAG (Bcl-3). AP1 reporter activity was determined as A.

5.3.4 Accumulation of nuclear Tpl-2 with Bcl-3 co-expression

Tpl-2 is reported to be predominantly cytoplasmic in resting cells, however upon stimulation a number of other components of the ERK pathway can translocate to the nucleus. In order to determine the effect of Bcl-3 on subcellular localisation of Tpl-2, nuclear and cytoplasmic extracts were prepared from 293T transfected with Tpl-2 in the presence or absence of co-transfected Bcl-3 and analysed by western blot. In the absence of Bcl-3 the majority of Tpl-2 was contained in the cytoplasmic fraction, however when co-expressed with Bcl-3 the level of nuclear Tpl-2 increased dramatically (Figure 5.8 A). As Bcl-3 stabilises p50 protein levels through inhibition of p50 homodimer ubiquitination, we next investigated the ubiquitination status of Tpl-2 in the presence of Bcl-3. A ubiquitination assay in 293T cells transfected with HA-tagged ubiquitin and Tpl-2 with or without Bcl-3 was performed. Following denaturing lysis, Tpl-2 was immunoprecipitated with anti-MYC and immunoblotted with anti-HA antibody to detect ubiquitinated Tpl-2 species. Tpl-2 underwent ubiquitination however it was not sensitive to inhibition by Bcl-3 (Figure 5.8 B).

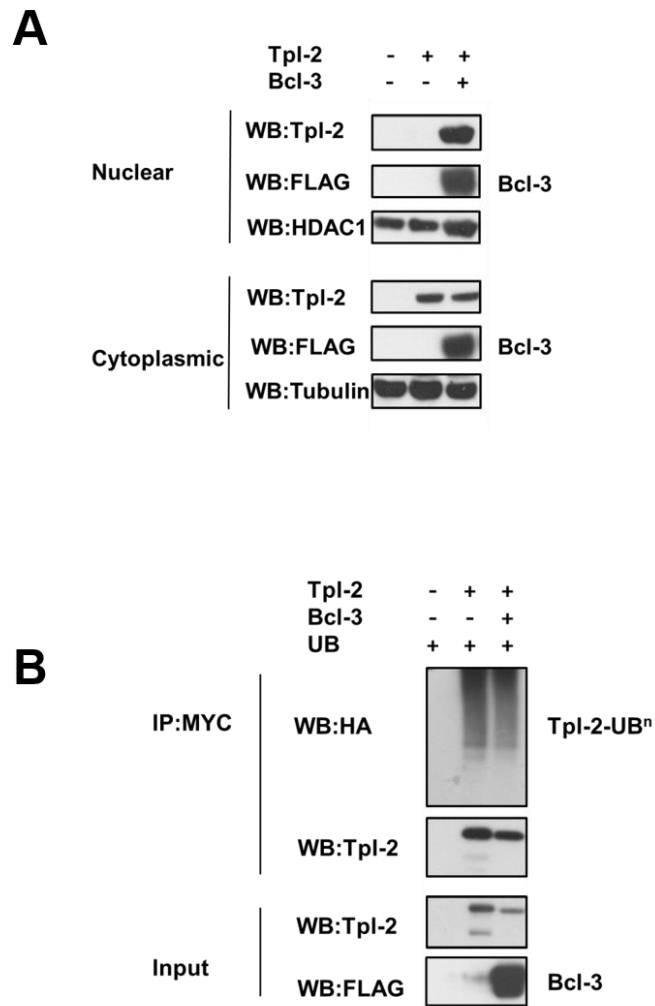


Figure 5.8 Bcl-3 overexpression increases nuclear Tpl-2.

(A) HEK293T cells were transfected with pRK5-Bcl-3-FLAG and pcDNA3.Tpl-2-MYC expression vectors as indicated. Nuclear and cytoplasmic extracts were analysed by WB with anti-FLAG and anti-Tpl-2 antibodies. Loading was assessed with antibodies for HDAC1 and tubulin. (B) HEK293T cells were transfected with pRK5-Bcl-3-FLAG and pcDNA3.Tpl-3-MYC and UB-HA vectors as indicated. Tpl-2 was immunoprecipitated from whole cell lysates with anti-MYC and immunoblotted with anti-HA to detect ubiquitinated Tpl-2.

5.4 DISCUSSION

TLR engagement leads to the production of pro-inflammatory cytokines and type I IFNs which are essential in mounting host defences during infection (Kondo et al., 2012). Although inflammation is a critical response required to eliminate specific pathogens and cellular debris, aberrant TLR activation may underlie the pathophysiology of a number of infectious and autoimmune diseases (Liew et al., 2005). Immune homeostasis is maintained by multiple negative regulatory mechanisms, which terminate TLR signalling to prevent harmful inflammatory responses. Bcl-3 was recently reported to act as an essential negative regulator of TLR signalling. Bcl-3 deficient mice and cells are hyper-responsive to TLR activation and hyper sensitive to septic shock (Carmody et al., 2007b). TLR stimulation initiates a number of signalling cascades which culminate in the activation of NF- κ B and various MAPK cascades. Investigation of Bcl-3's role in TLR signalling thus far has been restricted to the NF- κ B pathway, however data presented here suggest that Bcl-3 also regulates the MAPK pathway.

Following LPS stimulation, macrophages derived from *Bcl3*^{-/-} bone marrow exhibit increased phosphorylation of ERK1/2. Consequently, due to increased ERK1/2 activation, ERK dependent gene transcription is also upregulated. LPS induction of Egr-1 and c-Fos, two early response genes dependent on ERK activation (Waterfield et al., 2003), was significantly increased in *Bcl3*^{-/-} macrophages. ERK activation following LPS stimulation in macrophage is initiated by the MAP3K, Tpl-2. In the present study, we shown that Bcl-3 interacts with and dramatically inhibits Tpl-2. This presents a novel function of Bcl-3 as a negative regulator of MAPK signalling distinct from its previously identified role as an inhibitor of NF- κ B mediated transcription.

Although interaction with p50 is essential for Bcl-3 mediated inhibition of NF- κ B dependent gene expression, Bcl-3's role in regulating ERK appears to be independent of p50. p105 maintains Tpl-2 stability and is thus an critical component of the ERK cascade, however the p50 subunit is not required for ERK regulation (Yang et al., 2011). Reconstitution of *Nfk1b*^{-/-} macrophages with a version of p105 lacking the N-terminus i.e. p50, is sufficient to restore defective ERK activation in these cells (Zhao et al., 2012). Furthermore, Bcl-3 can interact with Tpl-2 in *Nfk1b*^{-/-} MEFs deficient in both p50 and p105. Nevertheless it would

be interesting to determine if the Tpl-2-Bcl-3 complex exists alone or as part of a larger complex containing p105.

ERK1/2 is activated following a number sequential phosphorylation steps, however Bcl-3 interaction with Tpl-2 suggests that Bcl-3 directly inhibits Tpl-2, upstream of both MEK1 and ERK1/2. Consistent with this theory, co-expression with Bcl-3 prevents Tpl-2 MEK kinase activity *in vitro*. Furthermore, Bcl-3 overexpression also inhibits Tpl-2 induced ERK1/2 phosphorylation and AP-1 transcriptional activity. It is also possible that Bcl-3 inhibits activation of Tpl-2, however basal ERK1/2 phosphorylation in *Bcl3*^{-/-} macrophages is unchanged and therefore it is more likely that Bcl-3 regulates Tpl-2 kinase activity following activation. Bcl-3 interacts with kinase domain mutant of Tpl-2 to a much lesser extent than wild type Tpl-2, suggesting that this domain may be important in facilitating this interaction. It is also possible that Bcl-3 preferentially interacts with an active form of Tpl-2, further supporting the idea that Bcl-3 regulates Tpl-2 activity following stimulation. p105 binds to and inhibits Tpl-2 in resting cells, however upon stimulation, p105 is degraded thus liberating Tpl-2. Bcl-3's role may be to inhibit this active form of Tpl-2, thereby attenuating ERK signaling following stimulation.

Signal strength and duration are critical factors in determining the specificity and outcome of the ERK cascade. ERK activation can elicit distinct biological responses and based on studies with PC12 cells. It was proposed that the duration of this activation controlled cell fate decisions [42]. Treatment of PC12 cells with nerve growth factor (NGF) which results in sustained ERK activation precedes cellular differentiation whereas transient activation with epidermal growth factor (EGF) promotes proliferation. This correlation between the duration of ERK signalling and distinct cell behaviours has also been documented in fibroblasts, T lymphocytes and myeloid cells (Murphy and Blenis, 2006). The expression kinetics of immediate early genes (IEGs) in response to specific stimuli are thought to regulate cell fate decisions (Sharrocks, 2006, Murphy and Blenis, 2006). Transient ERK activation triggers the expression of IEGs such as *c-fos*. *c-Fos* protein however is very unstable and is quickly degraded. C-terminal phosphorylation of *c-Fos* protects it from degradation and occurs only under sustained ERK activation. As *c-Fos* is an important factor of the AP-1 complex, this increased stability results in a second wave of transcription of late response genes (Sharrocks, 2006, Murphy and Blenis, 2006). LPS stimulation in wild type

macrophage results in transient ERK1/2 phosphorylation, with peak intensity at 15 minutes. In *Bcl3*^{-/-} macrophages however, a significant amount of phosphorylated ERK1/2 is still present at later time points. The current analysis is limited by a relatively short time course, further study of the activation dynamics *Bcl3*^{-/-} macrophages is needed to determine if ERK activation is sustained in the absence of Bcl-3.

The exact mechanism by which Bcl-3 inhibits Tpl-2 activity is yet to be elucidated. p105 inhibits Tpl-2 MEK kinase activity by physically preventing Tpl-2 access to MEK (Beinke et al., 2003), it is possible that Bcl-3 may also inhibit Tpl-2 activity by this method and is worth investigation. Previous reports suggest Tpl-2 is a cytoplasmic protein, however this raises the question as to how it interacts with Bcl-3, a predominantly nuclear protein, *in vivo*. It is important to note that the most available subcellular localization studies of Tpl-2 were conducted in resting cells (Belich et al., 1999). MEK1 and ERK1/2 which are also prominently localised to the cytoplasm in resting cells can translocate to the nucleus upon stimulation. ERK1/2 or MEK do not contain a classical nuclear localisation signal (NLS). Recent reports however, suggest a novel nuclear translocation signal (NTS) may be responsible for stimulus dependent nuclear import of these proteins via the nuclear translocating protein, importin 7 (Chuderland et al., 2008). MEK1 is exported from the nucleus by CRM1 dependent active transport facilitated by a classical NES located at its amino terminus, whereas nuclear export of ERK1/2 is thought to be mediated directly by MEK (Fukuda et al., 1996).

As substrates downstream of Tpl-2 can shuttle between the nucleus and the cytoplasm, the Tpl-2 sequence was analysed using NetNES prediction software (la Cour et al., 2004) to determine if Tpl-2 contained a putative NES (Figure 5.9 A) (full results Appendix 7.9). This analysis identified putative NES in the C-terminus of Tpl-2. The classical export pathway is dependent on CRM1, a member of the importin b superfamily of transport receptors and leucine-rich NESs (Lange et al., 2007). The consensus NES recognised by CRM1 is characterised as a short amino acid sequence of regularly spaced hydrophobic residues: $\Phi X_{2-3} \Phi X_{2-3} \Phi X \Phi$ where Φ =Leucine, isoleucine, valine, phenylalanine or methionine and X is any amino acid (Lange et al., 2007). Preliminary experiments using LMB, an inhibitor of CRM1-mediated nuclear export suggest that Tpl-2 may indeed shuttle to the nucleus (Figure 5.9 B). In untreated cells,

Tpl-2 was found to be predominantly cytoplasmic in localisation as assessed by immunofluorescence, however following treatment with LMB for 2 hours, Tpl-2 was also detected in the nucleus. Surprisingly, similar results were also obtained when cells were treated with MG132 alone, suggesting that nuclear Tpl-2 may be labile. These data suggest that, like other MAPK signalling proteins, Tpl-2 may also be capable of nucleocytoplasmic shuttling however, it does not rule out the possibility that Tpl-2 interacts with Bcl-3 in the cytoplasm. Further investigation into the localisation of Tpl-2:Bcl-3 complexes is necessary but the possibility that Bcl-3 acts as a novel negative regulator of Tpl-2 in the nucleus is exciting and merits further investigation.

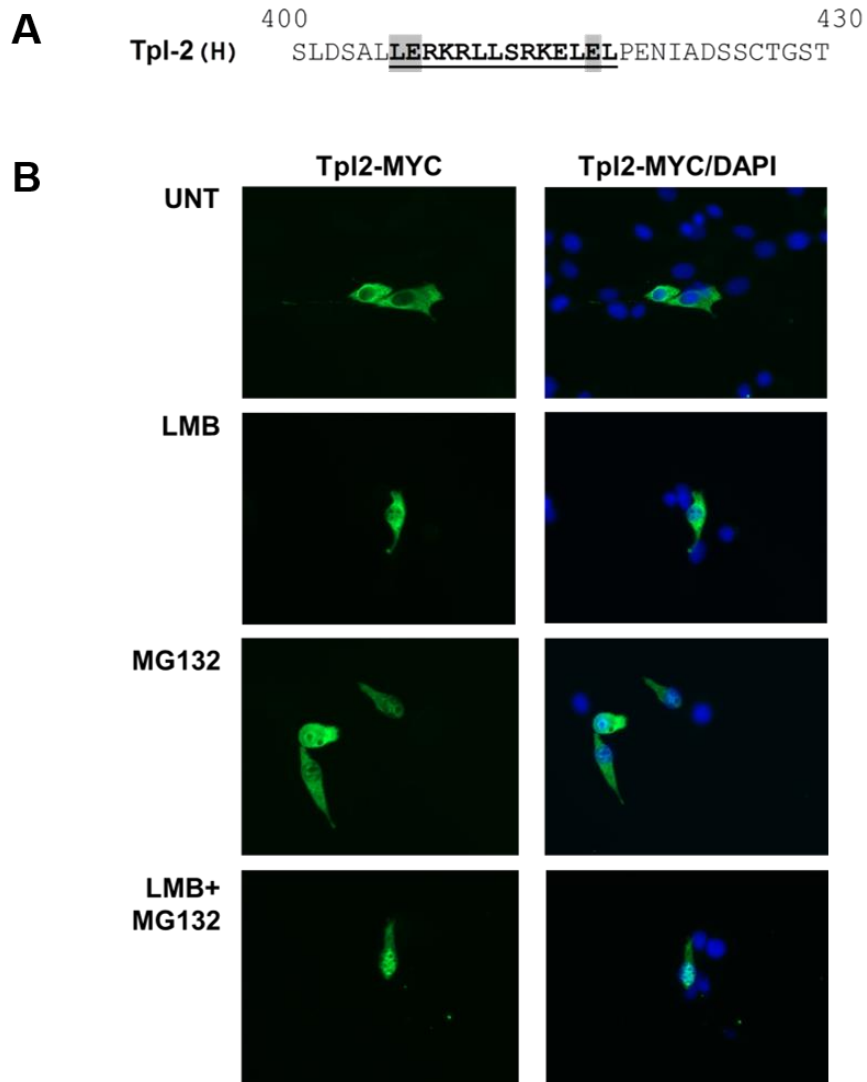


Figure 5.9 Potential nuclear export sequence in Tpl-2.

(A) NetNes nuclear export prediction tool was used to identify residues potentially involved in nuclear export (underlined). Human Tpl-2 sequence is shown and grey shading indicates non conserved rat and mouse Tpl-2 residues. (B) NIH 3T3s were transfected with pcDNA3-Tpl-2-MYC for 48 hours and were left untreated (UNT), treated with 20nM LMB for 2 hours (LMB), treated with 20 μ M MG132 for 30 minutes (MG132) or a combination of 20nM LMB for 2 hours with 20 μ M MG132 for the final 30 minutes. Cells were fixed cells and stained with anti-MYC and anti-Mouse-AF488. DMSO and ethanol were used as vehicle controls for MG132 and LMB respectively.

—— Chapter Six ——

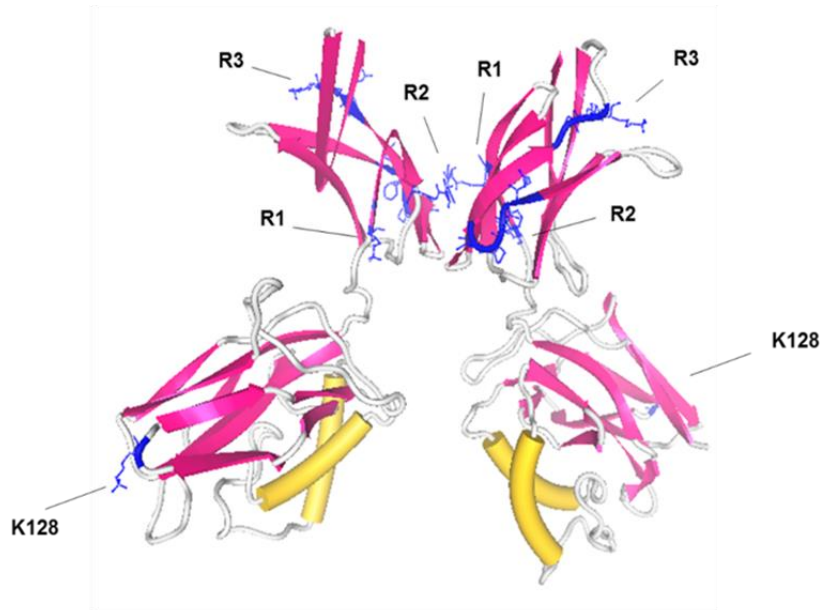
6 General Discussion

While TLR activation is an essential part of innate immunity and is also required to mount an effective adaptive immune response, tight regulation of TLR signalling is crucial. Aberrant TLR signalling can result in excessive production of potentially damaging pro-inflammatory cytokines which can have deleterious consequences for the host. Several members of the TLR family have been implicated in the pathogenesis of autoimmune, chronic inflammatory and infectious diseases (Liew et al., 2005). Uncontrolled or chronic TLR4 signalling in response to LPS, for example, can result in one of the most severe TLR-related diseases, sepsis, causing extreme inflammatory injuries to host tissues resulting in multiple organ dysfunction, shock, and eventual death (Van Amersfoort et al., 2003). The necessity for the strict control of TLR signalling is evident and a multiple negative regulators have evolved to prevent harmful inflammatory responses (Liew et al., 2005, Kondo et al., 2012).

The I κ B protein Bcl-3, regulates NF- κ B-dependent gene expression through interaction with homodimers of p50 and p52. p52 however, does not play a role in the classical NF- κ B pathway and p50 homodimers are thought to be the major target of Bcl-3 action in TLR signalling (Carmody et al., 2007b). Previous reports have shown that through the inhibition of p50 homodimer ubiquitination and subsequent degradation, Bcl-3 stabilises p50 homodimers, thus limiting NF- κ B mediated transcription of pro-inflammatory cytokines (Carmody et al., 2007b). *Bcl3*^{-/-} cells and mice are hyper-responsive to TLR signalling and are also defective in LPS tolerance. In addition to NF- κ B subunits, Bcl-3 has also been reported to interact with a number other regulators of transcription (Na et al., 1999, Jamaluddin et al., 2005, Yang et al., 2009, Viatour et al., 2004, Na et al., 1998, Weyrich et al., 1998, Zhao et al., 2005, Kabuta et al., 2010, Southern et al., 2012). Therefore, the possibility that Bcl-3 may also function through p50-independent mechanisms to regulate inflammatory gene transcription cannot be discounted in studies employing *Bcl3*^{-/-} mice and cells. Previous to this study, it was unclear whether interaction with p50 was essential for the inhibition of NF- κ B dependent cytokine expression or if other binding partners Bcl-3 are important. To further investigate this, we aimed to generate a p50 mutant incapable of binding to Bcl-3. We hypothesised that Bcl-3's inhibitory activity

was dependent on interaction with p50 and thus cells expressing a version of p50 that was unable to interact with Bcl-3 would be hyper responsive to stimulation, recapitulating the *Bcl3*^{-/-} phenotype.

Peptide arrays were employed to identify critical residues of both p50 and Bcl-3 required for this interaction. This method utilises a series of immobilised overlapping peptides encompassing the entire protein sequence being investigated. This approach presents a rapid method to identify specific regions of interest and is advantageous over traditional deletional mutagenic approaches, which for NF- κ B subunits can have severe consequences on DNA binding and dimerisation. Recombinant Bcl-3 bound with high affinity to a number p50 peptides representing regions in both DNA binding and dimerisation regions of the p50 RHD. Using alanine substitution peptide arrays, specific residues within these peptides that contributed to Bcl-3 binding were identified. While peptide array data is extremely informative, p50 is a large 400 amino acid protein and binds Bcl-3 as part of a homodimer complex. Evaluation of the role of these residues in Bcl-3 interaction in full-length p50 was therefore essential. Based on the peptide array data, we generated a number of p50 mutants but found that only one mutant, p50^{RKR}, was completely defective in Bcl-3 binding. Surprisingly however, all mutations tested affected the ubiquitination status of p50 (Figure 6.1).

A**B**

Region	Mutant	Mutation	Ubiquitination Status
R1	p50 ^{KRM}	Lys249, Arg252, Met253 to alanine	Increased
R2	p50 ^{DFSPT}	Asp297, Phe298, Ser299, Pro300, Thr301 to alanine	Increased
R3	p50 ^{K315A,K317A}	Lys315, Lys317 to alanine	Decreased
	p50 ^{Y316A}	Tyr316 to alanine	Increased
	p50 ^{Y316F}	Tyr316 to phenylalanine	Increased
	p50 ^{K315A,Y316A,K317A}	Tyr31, Tyr316, Lys317 to alanine	Increased
R4	p50 ^{RKR}	Arg359, Lys360 and Arg361 to alanine	Increased
-	p50 ^{K128R}	Lys128 to arginine	Decreased

Figure 6.1 Summary of p50 mutants generated.

(A) p50 homodimer crystal structure with specific regions mutated in this study highlighted in blue. (B) Table summarising the p50 mutants generated in this study with the associated ubiquitination status of each indicated.

The p50^{KRM} and p50^{DFSP} mutants had a very similar phenotype and it is likely that Lys249, Arg252, M253 and Asp297, Phe298, Ser299, Pro300 and Thr301 contribute to a shared protein interaction interface. Mutation of these residues resulted in a dramatic increase in p50 ubiquitination. While Bcl-3 interaction was reduced, Bcl-3 was able to bind to these mutants and also inhibit the ubiquitination, although not to the level seen with wild-type p50. It is possible that these residues contribute to interaction with Bcl-3, however, analysis of the crystal structure of the IκBα:NF-κB heterodimer complex revealed that Lys249, Arg252 and M253 of p50 also contact IκBα as part of a p65 heterodimer. Ser238, Phe239, Ser240, Gln341, and Ala342 of p65 which correspond to p50 residues 297-301 identified by the peptide array, also contact IκBα in this complex. In addition, *in silico* modelling predicted that some of these residues may also bind other IκB proteins such as IκBNS as part of a p50 homodimer complex. Collectively, these data suggest that p50 residues 249,252-253 and 297-301 may form as a general interface for interaction with IκB proteins. IκB proteins are highly conserved and it is not surprising that overlap with p50 interacting residues would occur. It would therefore be interesting to further test the p50^{KRM} and p50^{DFSP} mutant's ability to interact with other IκB family members apart from Bcl-3. NF-κB monomers are inherently unstable and require dimerisation to avoid degradation, it is also thought that IκB interaction with NF-κB contributes to the stability of these dimer complexes. Based on the available crystal structure and predicted IκB:p50 complexes it is highly likely that these mutants will be defective in binding to multiple IκB proteins, which may explain the instability of these mutants. We have also generated a *Nfkb1*^{-/-} MEF cell line reconstituted version of p105 containing the KRM mutation. While p105 and p105^{RKR} are equivalently expressed, p50^{KRM} is almost undetectable. Studies using *Nfkb1*^{-/-} cells investigating the role of p50 deficiency are limited, as in addition to p50, these cells are also deficient in p105 an important inhibitor of NF-κB. The p105^{KRM} cell line therefore may also be a useful tool in investigating p50 specific functions.

Binding to DNA triggers p50 ubiquitination, however the mechanisms preceding this event are unknown. The ubiquitination and degradation of p65 is regulated by a number of post translational modifications, such as acetylation, isomerisation and phosphorylation (Geng et al., 2009, Ryo et al., 2003, Li et al., 2012, Sacconi et al., 2004). TNF-induced phosphorylation on p65 Ser468 for example, regulates COMMD1-dependent ubiquitination of p65 (Geng et al.,

2009). Similar to p65, p50 ubiquitination is induced following TLR and TNFR stimulation and it is likely that these signalling events also trigger post translational modification of p50 (Geng et al., 2009, Collieran et al., 2013, Carmody et al., 2007b). The KYK motif (p50 315-317) identified by the peptide array may contain a novel p50 phosphorylation site and merits further investigation (Appendix 7.10). Mutation of Tyr316 to alanine dramatically increased p50 ubiquitination which is not rescued by mutation to phenylalanine, a structurally more similar amino acid. This suggests modification of this tyrosine, possibly phosphorylation, is required to negatively regulate p50 ubiquitination.

It is apparent from these mutational studies that p50 ubiquitination must be a tightly regulated process. Mutation of even a single amino acid can alter the ubiquitination status of p50 and have dramatic effects on p50-regulated NF- κ B inhibitory ability. Ubiquitination represents a critical regulatory step of NF- κ B-mediated transcription following TLR activation and we hypothesise that ubiquitination of p50 is required to remove inhibitory complexes from the promoters of NF- κ B target genes. Identification of Lys128 as a target for p50 ubiquitination will be valuable in investigating the role of p50 ubiquitination in regulating TLR-induced inflammatory gene expression and in innate immunity. NF- κ B turnover on active chromatin is a rapid process occurring in less than 30 seconds (Bosisio et al., 2006). We propose that a ubiquitination resistant version p50 would be highly stable therefore acting as super repressor of NF- κ B mediated transcription. Currently however, it is not clear whether this lysine residue is specific to p50 homodimers or if this residue is also targeted in p50:p65 complexes. We have generated a *Nfkb1*^{-/-} cell line stably expressing this ubiquitination defective version of p50 which will be beneficial in investigating this.

Previous studies have shown that Bcl-3 stabilises p50 homodimers through the inhibition of p50 ubiquitination however, the precise mechanism of this regulation was unknown. Our data demonstrates that Bcl-3-mediated repression of NF- κ B -dependent gene expression requires interaction with p50. p50 that cannot interact with Bcl-3 (p50^{RKR}) undergoes increased ubiquitination and degradation, even in the presence of over expressed Bcl-3. While Bcl-3 interacts with multiple regulators of transcription, our data suggests that p50 is the main target in the regulation of NF- κ B-dependent inflammatory gene expression by

Bcl-3. How Bcl-3 interaction with p50 inhibits its ubiquitination however is still unclear. Bcl-3 may physically prevent binding of components of the ubiquitination machinery, for example an ubiquitin ligase or perhaps blocks a post-translational modification such as phosphorylation that may trigger degradation. Identification of the p50 ubiquitin ligase and signalling events preceding ubiquitination will be essential in elucidating the exact mechanism of Bcl-3-mediated inhibition of p50 ubiquitination.

As elevated NF- κ B activity contributes to the pathology of several human diseases, there has been significant interest in developing methods to limit NF- κ B signalling (Gilmore and Herscovitch, 0000). Many NF- κ B inhibitors have entered clinical trials for the treatment of inflammatory diseases and as part of anti-cancer strategies (Gilmore and Garbati, 2011). The majority of inhibitors thus far act upstream of NF- κ B activation, blocking NF- κ B activity through the inhibition of receptors such as the TNF-R, and inhibition of IKK activity and I κ B degradation (Song et al., 2002, Swinney et al., 2002, May et al., 2000). Due to the large number of NF- κ B target genes, many involved in normal cell and tissue development, global inhibition of NF- κ B activation is problematic. Focus is instead turning to the development of gene selective inhibitors of NF- κ B. This is also proving a challenging task as many of the components involved in NF- κ B activation overlap with other signal transduction pathways. Modulation or inhibition of individual NF- κ B subunits therefore is an attractive approach and may provide a method to selectively block gene-specific events.

Based our finding that interaction with p50 is necessary to limit NF- κ B-mediated transcription, we explored the possibility of Bcl-3 mimetics as modulators as inhibitors of NF- κ B activity. Again a peptide array approach was employed to identify the minimal regions of Bcl-3 capable mediating its function and binding p50. Based on the peptide array data and I κ B multiple sequence alignment we identified a short, Bcl-3 specific peptide sequence that bound with high affinity to p50. The peptide sequence represented both α -helices of ANK1 and the first beta sheet of ANK2 and importantly was not well conserved among other I κ B proteins. By the addition of the HIV-TAT peptide to our sequence, we were able to generate a cell permeable Bcl-3 derived peptide. These peptides were able to mimic Bcl-3 function and effectively inhibit NF- κ B activity *in vitro*. While p50 ubiquitination is required for establishment of innate immunity, tight control of this regulatory step is essential. As illustrated in this study and in previous

studies using *Bcl3*^{-/-} cells (Carmody et al., 2007b), hyper ubiquitination of p50 reduces p50 half-life resulting in increased NF-κB dependent cytokine expression. Stabilising p50 homodimers and thus inhibiting NF-κB-mediated transcription through Bcl-3 derived peptides represents a novel therapeutic approach to regulate the inflammatory response in a gene specific manner. The sBDP developed during this study is currently being tested *in vivo* in a model of carrageenan-induced inflammation in collaboration with Dr. Gianluca Grassia and Prof. Armando Lalenti (University of Naples Federico II, Napoli, Italy) (Appendix 7.11). Preliminary data generated from this trial is very promising and indicates that Bcl-3 peptides are effective *in vivo*. These peptides not only provide proof of principle of Bcl-3 mimetics as inhibitors of NF-κB activity but also provide a basis for developing novel Bcl-3 based strategies for the treatment of inflammatory diseases.

Identification of Tpl-2 as a novel binding partner of Bcl-3 in this study reinforces the need to develop specific inhibitors of NF-κB in order to be therapeutically beneficial. Surprisingly we found that in addition to NF-κB, Bcl-3 also critically regulates TLR-induced MAPK signalling. *Bcl3* deficiency results in increased ERK1/2 activation and consequently increased ERK1/2-dependent gene expression. The dynamics of growth factor-induced ERK1/2 signalling through Raf have been extensively studied however ERK1/2 activation following TLR signalling is relatively unexplored. We have identified Bcl-3 as a novel negative regulator of this pathway, although the mechanism of this inhibition is as of yet unclear. LPS induced ERK1/2 activation is very transient, however in the absence of Bcl-3, the duration of ERK1/2 activity appears to be increased. Strong activation of ERK1/2 however generally leads to long term activity and so further investigation into the dynamics of ERK1/2 activation in the *Bcl3*^{-/-} cells is needed to discriminate between these effects (Ebisuya et al., 2005). A number of strength-controlling and temporal regulators of ERK1/2 activity exist which determine the duration and magnitude of the ERK1/2 response (Ebisuya et al., 2005). In many cell types ERK activation is not an all-or-none response and as shown by us and by others for EGF- and PMA- induced ERK signalling, the amplitude of ERK1/2 activation is proportional to the concentration of external stimulus (Whitehurst et al., 2004). *Bcl3* deficient macrophages are hypersensitive to TLR stimulation and produce a more robust ERK response at lower concentrations of LPS compared to wild type. *Bcl3* deficiency reduces the threshold for ERK activation but it is unclear from our current analysis whether

this is due to increased numbers of cells responding to activation or if the amplitude of activation in a fraction of the cells is increased. Further investigation using phospho-flow and single cell immunofluorescence based techniques will be necessary to clarify the role of Bcl-3 in regulating the amplitude of the ERK response.

Tpl-2 is the sole MAP3K responsible for activation of the ERK1/2 MAPK pathway following LPS stimulation in macrophages and we reason that Bcl-3 acts to regulate the ERK pathway at the level of Tpl-2. Based on our current data there are several possible mechanisms of Bcl-3 mediated ERK1/2 regulation which require further investigation (Figure 6.2). As other components of the ERK pathway MEK1/2 and ERK1/2 both translocate to the nucleus following activation, nucleocytoplasmic shuttling of active Tpl-2 is not unlikely. Nuclear localization of Tpl-2 in 293T cells has been reported following UVB radiation (Choi et al., 2008) and we have demonstrated accumulation of Tpl-2 in the nucleus following LMB treatment. As Bcl-3 is predominantly a nuclear protein, we postulate that Bcl-3 regulates nuclear Tpl-2, however, it is possible that Bcl-3 may also act in the cytoplasm. Free Tpl-2 is extremely unstable and following LPS stimulation, Tpl-2 is rapidly degraded (Waterfield et al., 2003). We found that in addition to treatment with LMB, blocking the proteasome also resulted in a build-up of nuclear Tpl-2. This suggests that the nuclear pool of Tpl-2 is extremely labile which may explain the very low steady state levels of Tpl-2 in *Nfkb1*^{-/-} cells. Without a cytoplasmic anchor, Tpl-2 may be free to constantly shuttle to the nucleus. Why nuclear Tpl-2 is unstable is yet to be determined but it is possible that Tpl-2 is modified in the nucleus in such a way that triggers its degradation and thus limits the ERK response.

There are several known spatial regulators of ERK activity and it is possible Tpl-2 is also regulated in a similar manner by Bcl-3. The golgi-localised scaffold protein Sef for example, binds to activated MEK and prevents ERK dissociation thereby targeting ERK activity to the cytoplasm (Torii et al., 2004). ERK activation can result in diverse cellular responses, which are influenced by the subcellular localisation of activated ERK and the subsequent phosphorylation of cytoplasmic and nuclear effectors. Nuclear localisation of active ERK, increases Elk-1 activity and induces the expression of a number of immediate early target genes such as *Fos*, *Jun* and *Egr1*, increasing proliferation in fibroblasts and epithelial cells. In contrast cytoplasmic retention of activated ERK can suppress

Fos expression and proliferation (Ebisuya et al., 2005). It is possible that interaction with Bcl-3 may prevent nuclear export of Tpl-2 simply by masking a NES or perhaps preventing interaction with other binding partners of Tpl-2. MEKs can interact with ERKs in the nucleus and actively export them back to the cytoplasm, nuclear export by MEK however is not restricted to ERKs and the nuclear receptor PPAR γ is also regulated in this manner following mitogen stimulation (Adachi et al., 2000, Burgermeister et al., 2007). It would be interesting to determine if Tpl-2:MEK complexes are restricted to the cytoplasm or if active Tpl-2 also interacts with MEK in the nucleus.

As mentioned the duration of the ERK response can determine the fate of certain cellular responses such as differentiation and proliferation. Subtle differences in the time course of activation can change the biological outcome of ERK activation. Sustained ERK activation in PC12 cells induced by NGF precedes cellular differentiation whereas EGF induced transient activation results in proliferation (Qiu and Green, 1992). These distinct biological outcomes are also dependent on the cell type however and sustained ERK activation by PDGF is required for quiescent fibroblasts to begin to proliferate. Macrophages have an essential role during the immune response and act as regulators of homeostasis, effector cells in inflammation and promoters of wound healing (Murray and Wynn, 2011). Macrophages are highly heterogeneous and in response to local environment can rapidly change function (Valledor et al., 2000). Tissue macrophages can either proliferate, further differentiate to more specialised resident macrophages such as Kupffer cells and osteoclasts or become activated (Murray and Wynn, 2011). Correct control of macrophage proliferation, differentiation and survival is paramount in regulating the duration and magnitude of the immune response (Xaus et al., 2001). The kinetics of ERK activation in macrophages have also been implicated in directing macrophage response to stimuli (Valledor et al., 2000). The MEK/ERK cascade is essential for macrophage proliferation in response to M-CSF, the major growth factor for these cells (Valledor et al., 2000, Stanley et al., 1997, Comalada et al., 2003). In contrast, macrophages cease proliferating in response to LPS and acquire effector functions such as the production of pro-inflammatory cytokines (Xaus et al., 2001). LPS activation of macrophages is also dependent on ERK activation but follows a delayed time course compared to that of M-CSF, which peaks at 5 minutes post stimulation and is directed through a Raf-1 dependent pathway (Comalada et al., 2003).

While activation of macrophages is critical for rapid elimination of invading microorganisms during the initial stages of inflammation, aberrant and chronic activation is associated with the pathogenesis of diseases including atherosclerosis, obesity-induced insulin resistance and LPS induced septic shock (Tabas, 2010, Valledor et al., 2010, Odegaard and Chawla, 2008). Thus maintaining the correct balance between macrophage activation and deactivation is crucial in the resolution of inflammation and preventing inappropriate inflammation-associated pathology. The mechanisms involved in regulation of the ERK cascade following LPS are poorly understood but the MAPK phosphatase, MKP-1 has been shown to be essential in macrophage deactivation through down regulation of MAPKs, p38 and JNK. *Mkp1*^{-/-} macrophages exhibit prolonged p38 and JNK activation following LPS and *Mkp1* deficiency renders mice hyper-responsive to LPS challenge and consequently more susceptible septic shock (Zhao et al., 2006, Hammer et al., 2006). This raises question as to the physiological role of Bcl-3 and if negative regulation of ERK activation by Bcl-3 controls cell fate to limit the inflammatory response. In a model of inflammatory lung injury, Bcl-3 was found to have an important role in regulating both the differentiation and proliferation of myeloid progenitors in emergency granulopoiesis and prevention of acute lung injury (Kreisel et al., 2011). *Bcl3* deficiency has also been recently shown to exacerbate insulinitis and intraislet infiltration by inflammatory cells in models of Type 1 diabetes (Ruan et al., 2010). Moreover, Bcl-3 was found to play a significant role in regulating proliferation of intestinal epithelial cells following dextran-sodium sulphate (DSS)-induced colitis (O'Carroll et al., 2013). The mechanisms associated with Bcl-3 function in these studies is unknown and it is possible that Bcl-3-mediated regulation of ERK activation may not be limited to macrophages, suggesting a greater role for Bcl-3 in the resolution of the immune response.

Collectively the findings of this thesis demonstrate that Bcl-3 is a multifaceted regulator of TLR-induced inflammatory responses. In addition to identification of a novel binding partner of Bcl-3 we have shown an essential role for Bcl-3 in limiting both NF- κ B and MAPK activity. Bcl-3 can no longer be simply thought of as an I κ B protein and the role of dysregulated ERK activation must now be carefully considered in interpretation of any studies using *Bcl3*^{-/-} cells and mice. Furthermore, the success in establishing functional Bcl-3 derived peptides provides an excellent basis for a gene-specific approach in the treatment of inflammatory diseases.

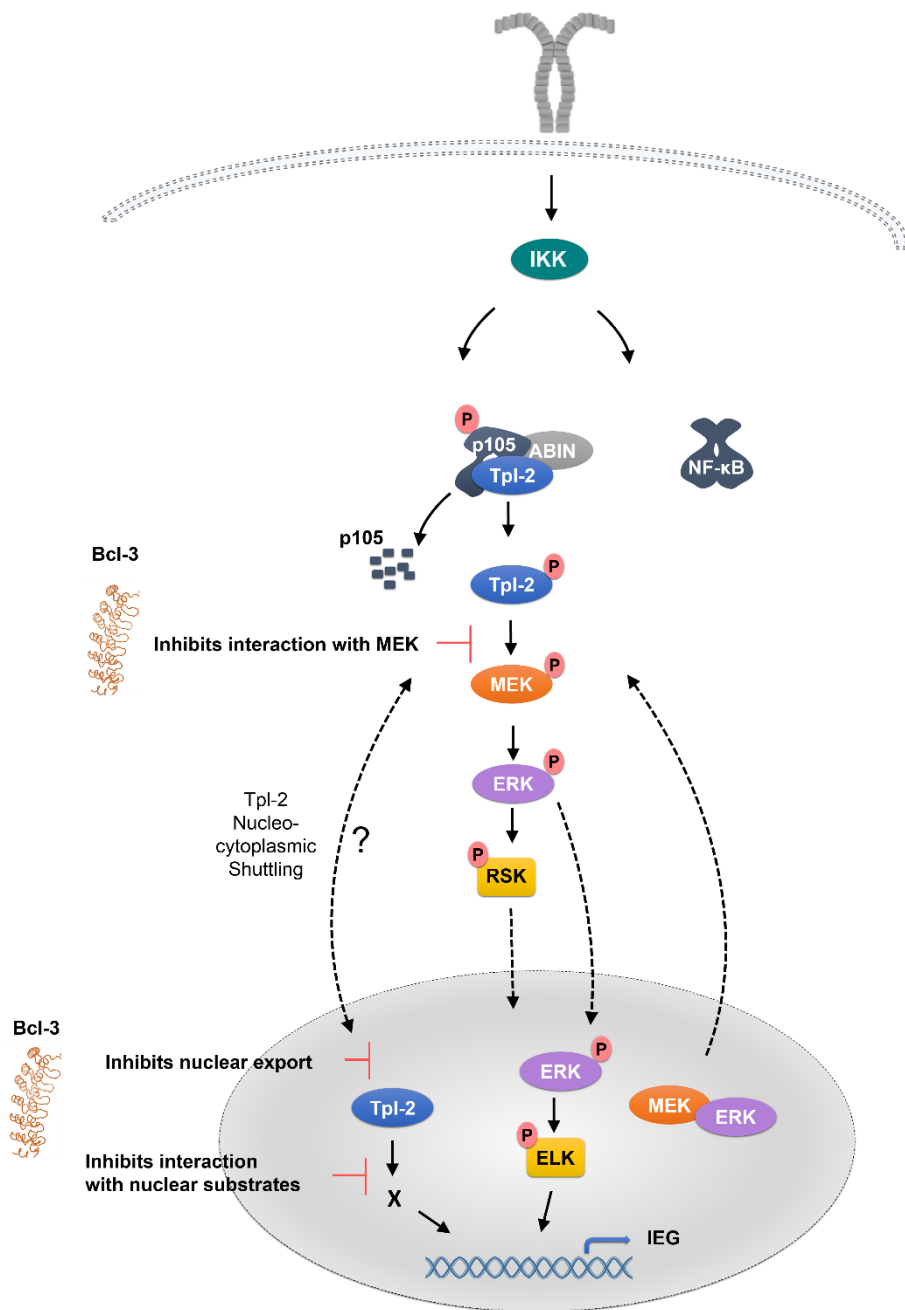


Figure 6.2 Schematic model of Bcl-3 mediated MAPK regulation

In resting cells, Tpl-2 is associated with an inhibitory cytoplasmic complex of p105 and ABIN2. Following LPS stimulation and IKK activation, p105 is phosphorylated and subsequently degraded. Liberated Tpl-2 initiates the ERK MAPK pathway by phosphorylation of MEK1/2, which in turn phosphorylates ERK1/2. Activated ERK dissociates from cytoplasmic anchors such as MEK and MAP kinase phosphatase (MKP) and phosphorylates a number of cytoplasmic targets such as RSK2. Activated ERK can also translocate to the nucleus phosphorylating several nuclear substrates such as Elk-1 resulting in distinct cellular responses. Cytoplasmic ERK substrates once activated can also translocate to the nucleus where they phosphorylate and activate transcription regulators such as E26 transformation-specific (Ets) and CREB to induce immediate early gens.

7 Appendix

7.1 p50 Peptide Array Sequences

Peptide Number	Amino Acid start #	Amino acid Sequence	Amino Acid end #
1	1	MADDDPYGTGQMFHLNTA	18
2	4	DDPYGTGQMFHLNTALHTH	21
3	7	YGTGQMFHLNTALHTHSIF	24
4	10	GQMFHLNTALHTHSIFNAE	27
5	13	FHLNTALHTHSIFNAELYS	30
6	16	NTALHTHSIFNAELYSPEI	33
7	19	LHTHSIFNAELYSPEIPLS	36
8	22	SIFNAELYSPEIPLSTDG	39
9	25	NAELYSPEIPLSTDGPYL	42
10	28	LYSPEIPLSTDGPYLQIL	45
11	31	PEIPLSTDGPYLQILEQP	48
12	34	PLSTDGPYLQILEQPKQR	51
13	37	TDGPYLQILEQPKQRGFR	54
14	40	PYLQILEQPKQRGFRFRY	57
15	43	QILEQPKQRGFRFRYVCE	60
16	46	EQPKQRGFRFRYVCEGPS	63
17	49	KQRGFRFRYVCEGPSHGG	66
18	52	GFRFRYVCEGPSHGGLPG	69
19	55	FRYVCEGPSHGGLPGASS	72
20	58	VCEGPSHGGLPGASSEKN	75
21	61	GPSHGGLPGASSEKNKKS	78
22	64	HGGLPGASSEKNKKSYPQ	81
23	67	LPGASSEKNKKSYPQVKI	84
24	70	ASSEKNKKSYPQVKICNY	87
25	73	EKNKKSYPQVKICNYVGP	90
26	76	KKSYPQVKICNYVGPAKV	93
27	79	YPQVKICNYVGPAKVIVQ	96
28	82	VKICNYVGPAKVIVQLVT	99
29	85	CNYVGPAKVIVQLVTNGK	102
30	88	VGPAKVIVQLVTNGKNIH	105
31	91	AKVIVQLVTNGKNIHLHA	108
32	94	IVQLVTNGKNIHLHAHSL	111
33	97	LVTNGKNIHLHAHSLVGK	114
34	100	NGKNIHLHAHSLVGKHCE	117
35	103	NIHLHAHSLVGKHCEDGV	120
36	106	LHAHSLVGKHCEDGVCTV	123
37	109	HSLVGKHCEDGVCTVTAG	126
38	112	VGKHCEDGVCTVTAGPKD	129
39	115	HCEDGVCTVTAGPKDMVV	132
40	118	DGVCTVTAGPKDMVVGFA	135
41	121	CTVTAGPKDMVVGFANLG	138
42	124	TAGPKDMVVGFANLGILH	141

43	127	PKDMVVG FANL GILHVTK	144
44	130	MVVG FANL GILHVTKKKV	147
45	133	GFANL GILHVTKKKVFET	150
46	136	NL GILHVTKKKVFETLEA	153
47	139	ILHVTKKKVFETLEARM T	156
48	142	VTKKKFETLEARMTEAC	159
49	145	KKVFETLEARMTEACIRG	162
50	148	FETLEARMTEACIRGYNP	165
51	151	LEARMTEACIRGYNPGLL	168
52	154	RMTEACIRGYNPGLLVHS	171
53	157	EACIRGYNPGLLVHSDLA	174
54	160	IRGYNPGLLVHSDLAYLQ	177
55	163	YNPGLLVHSDLAYLQAE G	180
56	166	GLLVHSDLAYLQAE GGD	183
57	169	VHSDLAYLQAE GGD RQL	186
58	172	DLAYLQAE GGD RQL TDR	189
59	175	YLQAE GGD RQL TDREKE	192
60	178	AEGGD RQL TDREKE I IR	195
61	181	GGDRQL TDREKE I IRQAA	198
62	184	RQL TDREKE I IRQAAVQQ	201
63	187	TDREKE I IRQAAVQQTKE	204
64	190	EKE I IRQAAVQQTKEMDL	207
65	193	I IRQAAVQQTKEMDLSVV	210
66	196	QAAVQQTKEMDLSVVRLM	213
67	199	VQQTKEMDLSVVRLMFTA	216
68	202	TKEMDLSVVRLMFTAFLP	219
69	205	MDLSVVRLMFTAFLPDST	222
70	208	SVVRLMFTAFLPDSTGSF	225
71	211	RLMFTAFLPDSTGSFTRR	228
72	214	FTAFLPDSTGSFTRRLEP	231
73	217	FLPDSTGSFTRRLEPVVS	234
74	220	DSTGSFTRRLEPVVSDAI	237
75	223	GSFTRRLEPVVSDAIYDS	240
76	226	TRRLEPVVSDAIYDSKAP	243
77	229	LEPVVSDAIYDSKAPNAS	246
78	232	VVSDAIYDSKAPNASNLK	249
79	235	DAIYDSKAPNASNLKIVR	252
80	238	YDSKAPNASNLKIVRMDR	255
81	241	KAPNASNLKIVRMDRTAG	258
82	244	NASNLKIVRMDRTAGCVT	261
83	247	NLKIVRMDRTAGCVTGGE	264
84	250	IVRMDRTAGCVTGGEIY	267
85	253	MDRTAGCVTGGEIYLLC	270
86	256	TAGCVTGGEIYLLCDKV	273
87	259	CVTGGEIYLLCDKVQKD	276
88	262	GGEEIYLLCDKVQKDDIQ	279
89	265	EIYLLCDKVQKDDIQIRF	282
90	268	LLCDKVQKDDIQIRFYEE	285
91	271	DKVQKDDIQIRFYEEEN	288
92	274	QKDDIQIRFYEEENGGV	291

93	277	DIQIRFYEEEEENGGVWEG	294
94	280	IRFYEEEEENGGVWEGFGD	297
95	283	YEEEEENGGVWEGFGDFSP	300
96	286	EENGGVWEGFGDFSPTDV	303
97	289	GGVWEGFGDFSPTDVHRQ	306
98	292	WEGFGDFSPTDVHRQFAI	309
99	295	FGDFSPTDVHRQFAIVFK	312
100	298	FSPTDVHRQFAIVFKTPK	315
101	301	TDVHRQFAIVFKTPKYKD	318
102	304	HRQFAIVFKTPKYKDVNI	321
103	307	FAIVFKTPKYKDVNITKP	324
104	310	VFKTPKYKDVNITKPASV	327
105	313	TPKYKDVNITKPASVQ	330
106	316	YKDVNITKPASVQVQLRR	333
107	319	VNITKPASVQVQLRRKSD	336
108	322	TKPASVQVQLRRKSDLET	339
109	325	ASVQVQLRRKSDLETSEP	342
110	328	FVQLRRKSDLETSEPKPF	345
111	331	LRRKSDLETSEPKPFLYY	348
112	334	KSDLETSEPKPFLYYPEI	351
113	337	LETSEPKPFLYYPEIKDK	354
114	340	SEPKPFLYYPEIKDKEEV	357
115	343	KPFLYYPEIKDKEEVQRK	360
116	346	LYYPEIKDKEEVQRKRQK	363
117	349	PEIKDKEEVQRKRQKLMP	366
118	352	KDKEEVQRKRQKLMPNFS	369
119	355	EEVQRKRQKLMPNFSDFS	372
120	358	QRKRQKLMPNFSDFSFGG	375
121	361	RQKLMPNFSDFSFGGSGA	378
122	364	LMPNFSDFSFGGSGAGAG	381
123	367	NFSDFSFGGSGAGAGGGG	384
124	370	DSFGGSGAGAGGGGMFG	387
125	373	GGGSGAGAGGGGMFGSGG	390
126	376	SGAGAGGGGMFGSGGGGG	393
127	379	GAGGGGMFGSGGGGGSTG	396
128	382	GGGMFGSGGGGGSTGSPG	399
129	385	GMFGSGGGGGSTGSPGPG	402

7.2 p50 Alanine Substitution Array Sequences

Original Peptide	Peptide Number	Amino acid Sequence
20	A1	V-C-E-G-P-S-H-G-G-L-P-G-A-S-S-E-K-N
	A2	A-C-E-G-P-S-H-G-G-L-P-G-A-S-S-E-K-N
	A3	V-A-E-G-P-S-H-G-G-L-P-G-A-S-S-E-K-N
	A4	V-C-A-G-P-S-H-G-G-L-P-G-A-S-S-E-K-N
	A5	V-C-E-A-P-S-H-G-G-L-P-G-A-S-S-E-K-N
	A6	V-C-E-G-A-S-H-G-G-L-P-G-A-S-S-E-K-N
	A7	V-C-E-G-P-A-H-G-G-L-P-G-A-S-S-E-K-N
	A8	V-C-E-G-P-S-A-G-G-L-P-G-A-S-S-E-K-N
	A9	V-C-E-G-P-S-H-A-G-L-P-G-A-S-S-E-K-N
	A10	V-C-E-G-P-S-H-G-A-L-P-G-A-S-S-E-K-N
	A11	V-C-E-G-P-S-H-G-G-A-P-G-A-S-S-E-K-N
	A12	V-C-E-G-P-S-H-G-G-L-A-G-A-S-S-E-K-N
	A13	V-C-E-G-P-S-H-G-G-L-P-A-A-S-S-E-K-N
	A14	V-C-E-G-P-S-H-G-G-L-P-G-A-S-S-E-K-N
	A15	V-C-E-G-P-S-H-G-G-L-P-G-A-A-S-E-K-N
	A16	V-C-E-G-P-S-H-G-G-L-P-G-A-S-A-E-K-N
	A17	V-C-E-G-P-S-H-G-G-L-P-G-A-S-S-A-K-N
	A18	V-C-E-G-P-S-H-G-G-L-P-G-A-S-S-E-A-N
	A19	V-C-E-G-P-S-H-G-G-L-P-G-A-S-S-E-K-A

Original Peptide	Peptide Number	Amino acid Sequence
22	A21	H-G-G-L-P-G-A-S-S-E-K-N-K-K-S-Y-P-Q
	A22	A-G-G-L-P-G-A-S-S-E-K-N-K-K-S-Y-P-Q
	A23	H-A-G-L-P-G-A-S-S-E-K-N-K-K-S-Y-P-Q
	A24	H-G-A-L-P-G-A-S-S-E-K-N-K-K-S-Y-P-Q
	A25	H-G-G-A-P-G-A-S-S-E-K-N-K-K-S-Y-P-Q
	A26	H-G-G-L-A-G-A-S-S-E-K-N-K-K-S-Y-P-Q
	A27	H-G-G-L-P-A-A-S-S-E-K-N-K-K-S-Y-P-Q
	A28	H-G-G-L-P-G-A-S-S-E-K-N-K-K-S-Y-P-Q
	A29	H-G-G-L-P-G-A-A-S-E-K-N-K-K-S-Y-P-Q
	A30	H-G-G-L-P-G-A-S-A-E-K-N-K-K-S-Y-P-Q
	B1	H-G-G-L-P-G-A-S-S-A-K-N-K-K-S-Y-P-Q
	B2	H-G-G-L-P-G-A-S-S-E-A-N-K-K-S-Y-P-Q
	B3	H-G-G-L-P-G-A-S-S-E-K-A-K-K-S-Y-P-Q
	B4	H-G-G-L-P-G-A-S-S-E-K-N-A-K-S-Y-P-Q
	B5	H-G-G-L-P-G-A-S-S-E-K-N-K-A-S-Y-P-Q
	B6	H-G-G-L-P-G-A-S-S-E-K-N-K-K-A-Y-P-Q
	B7	H-G-G-L-P-G-A-S-S-E-K-N-K-K-S-A-P-Q
	B8	H-G-G-L-P-G-A-S-S-E-K-N-K-K-S-Y-A-Q
	B9	H-G-G-L-P-G-A-S-S-E-K-N-K-K-S-Y-P-A

Original Peptide	Peptide Number	Amino acid Sequence
24	B11	A-S-S-E-K-N-K-K-S-Y-P-Q-V-K-I-C-N-Y
	B12	A-S-S-E-K-N-K-K-S-Y-P-Q-V-K-I-C-N-Y
	B13	A-A-S-E-K-N-K-K-S-Y-P-Q-V-K-I-C-N-Y
	B14	A-S-A-E-K-N-K-K-S-Y-P-Q-V-K-I-C-N-Y
	B15	A-S-S-A-K-N-K-K-S-Y-P-Q-V-K-I-C-N-Y
	B16	A-S-S-E-A-N-K-K-S-Y-P-Q-V-K-I-C-N-Y
	B17	A-S-S-E-K-A-K-K-S-Y-P-Q-V-K-I-C-N-Y
	B18	A-S-S-E-K-N-A-K-S-Y-P-Q-V-K-I-C-N-Y
	B19	A-S-S-E-K-N-K-A-S-Y-P-Q-V-K-I-C-N-Y
	B20	A-S-S-E-K-N-K-K-A-Y-P-Q-V-K-I-C-N-Y
	B21	A-S-S-E-K-N-K-K-S-A-P-Q-V-K-I-C-N-Y
	B22	A-S-S-E-K-N-K-K-S-Y-A-Q-V-K-I-C-N-Y
	B23	A-S-S-E-K-N-K-K-S-Y-P-A-V-K-I-C-N-Y
	B24	A-S-S-E-K-N-K-K-S-Y-P-Q-A-K-I-C-N-Y
	B25	A-S-S-E-K-N-K-K-S-Y-P-Q-V-A-I-C-N-Y
	B26	A-S-S-E-K-N-K-K-S-Y-P-Q-V-K-A-C-N-Y
	B27	A-S-S-E-K-N-K-K-S-Y-P-Q-V-K-I-A-N-Y
	B28	A-S-S-E-K-N-K-K-S-Y-P-Q-V-K-I-C-A-Y
	B29	A-S-S-E-K-N-K-K-S-Y-P-Q-V-K-I-C-N-A

Original Peptide	Peptide Number	Amino acid Sequence
26	C1	K-K-S-Y-P-Q-V-K-I-C-N-Y-V-G-P-A-K-V
	C2	A-K-S-Y-P-Q-V-K-I-C-N-Y-V-G-P-A-K-V
	C3	K-A-S-Y-P-Q-V-K-I-C-N-Y-V-G-P-A-K-V
	C4	K-K-A-Y-P-Q-V-K-I-C-N-Y-V-G-P-A-K-V
	C5	K-K-S-A-P-Q-V-K-I-C-N-Y-V-G-P-A-K-V
	C6	K-K-S-Y-A-Q-V-K-I-C-N-Y-V-G-P-A-K-V
	C7	K-K-S-Y-P-A-V-K-I-C-N-Y-V-G-P-A-K-V
	C8	K-K-S-Y-P-Q-A-K-I-C-N-Y-V-G-P-A-K-V
	C9	K-K-S-Y-P-Q-V-A-I-C-N-Y-V-G-P-A-K-V
	C10	K-K-S-Y-P-Q-V-K-A-C-N-Y-V-G-P-A-K-V
	C11	K-K-S-Y-P-Q-V-K-I-A-N-Y-V-G-P-A-K-V
	C12	K-K-S-Y-P-Q-V-K-I-C-A-Y-V-G-P-A-K-V
	C13	K-K-S-Y-P-Q-V-K-I-C-N-A-V-G-P-A-K-V
	C14	K-K-S-Y-P-Q-V-K-I-C-N-Y-A-G-P-A-K-V
	C15	K-K-S-Y-P-Q-V-K-I-C-N-Y-V-A-P-A-K-V
	C16	K-K-S-Y-P-Q-V-K-I-C-N-Y-V-G-A-A-K-V
	C17	K-K-S-Y-P-Q-V-K-I-C-N-Y-V-G-P-A-K-V
	C18	K-K-S-Y-P-Q-V-K-I-C-N-Y-V-G-P-A-A-V
	C19	K-K-S-Y-P-Q-V-K-I-C-N-Y-V-G-P-A-K-A

Original Peptide	Peptide Number	Amino acid Sequence
28	C21	V-K-I-C-N-Y-V-G-P-A-K-V-I-V-Q-L-V-T
	C22	A-K-I-C-N-Y-V-G-P-A-K-V-I-V-Q-L-V-T
	C23	V-A-I-C-N-Y-V-G-P-A-K-V-I-V-Q-L-V-T
	C24	V-K-A-C-N-Y-V-G-P-A-K-V-I-V-Q-L-V-T
	C25	V-K-I-A-N-Y-V-G-P-A-K-V-I-V-Q-L-V-T
	C26	V-K-I-C-A-Y-V-G-P-A-K-V-I-V-Q-L-V-T
	C27	V-K-I-C-N-A-V-G-P-A-K-V-I-V-Q-L-V-T
	C28	V-K-I-C-N-Y-A-G-P-A-K-V-I-V-Q-L-V-T
	C29	V-K-I-C-N-Y-V-A-P-A-K-V-I-V-Q-L-V-T
	C30	V-K-I-C-N-Y-V-G-A-A-K-V-I-V-Q-L-V-T
	D1	V-K-I-C-N-Y-V-G-P-A-K-V-I-V-Q-L-V-T
	D2	V-K-I-C-N-Y-V-G-P-A-A-V-I-V-Q-L-V-T
	D3	V-K-I-C-N-Y-V-G-P-A-K-A-I-V-Q-L-V-T
	D4	V-K-I-C-N-Y-V-G-P-A-K-V-A-V-Q-L-V-T
	D5	V-K-I-C-N-Y-V-G-P-A-K-V-I-A-Q-L-V-T
	D6	V-K-I-C-N-Y-V-G-P-A-K-V-I-V-A-L-V-T
	D7	V-K-I-C-N-Y-V-G-P-A-K-V-I-V-Q-A-V-T
	D8	V-K-I-C-N-Y-V-G-P-A-K-V-I-V-Q-L-A-T
	D9	V-K-I-C-N-Y-V-G-P-A-K-V-I-V-Q-L-V-A

Original Peptide	Peptide Number	Amino acid Sequence
30	D11	V-G-P-A-K-V-I-V-Q-L-V-T-N-G-K-N-I-H
	D12	A-G-P-A-K-V-I-V-Q-L-V-T-N-G-K-N-I-H
	D13	V-A-P-A-K-V-I-V-Q-L-V-T-N-G-K-N-I-H
	D14	V-G-A-A-K-V-I-V-Q-L-V-T-N-G-K-N-I-H
	D15	V-G-P-A-K-V-I-V-Q-L-V-T-N-G-K-N-I-H
	D16	V-G-P-A-A-V-I-V-Q-L-V-T-N-G-K-N-I-H
	D17	V-G-P-A-K-A-I-V-Q-L-V-T-N-G-K-N-I-H
	D18	V-G-P-A-K-V-A-V-Q-L-V-T-N-G-K-N-I-H
	D19	V-G-P-A-K-V-I-A-Q-L-V-T-N-G-K-N-I-H
	D20	V-G-P-A-K-V-I-V-A-L-V-T-N-G-K-N-I-H
	D21	V-G-P-A-K-V-I-V-Q-A-V-T-N-G-K-N-I-H
	D22	V-G-P-A-K-V-I-V-Q-L-A-T-N-G-K-N-I-H
	D23	V-G-P-A-K-V-I-V-Q-L-V-A-N-G-K-N-I-H
	D24	V-G-P-A-K-V-I-V-Q-L-V-T-A-G-K-N-I-H
	D25	V-G-P-A-K-V-I-V-Q-L-V-T-N-A-K-N-I-H
	D26	V-G-P-A-K-V-I-V-Q-L-V-T-N-G-A-N-I-H
	D27	V-G-P-A-K-V-I-V-Q-L-V-T-N-G-K-A-I-H
	D28	V-G-P-A-K-V-I-V-Q-L-V-T-N-G-K-N-A-H
	D29	V-G-P-A-K-V-I-V-Q-L-V-T-N-G-K-N-I-A

Original Peptide	Peptide Number	Amino acid Sequence
46	E1	N-L-G-I-L-H-V-T-K-K-K-V-F-E-T-L-E-A
	E2	A-L-G-I-L-H-V-T-K-K-K-V-F-E-T-L-E-A
	E3	N-A-G-I-L-H-V-T-K-K-K-V-F-E-T-L-E-A
	E4	N-L-A-I-L-H-V-T-K-K-K-V-F-E-T-L-E-A
	E5	N-L-G-A-L-H-V-T-K-K-K-V-F-E-T-L-E-A
	E6	N-L-G-I-A-H-V-T-K-K-K-V-F-E-T-L-E-A
	E7	N-L-G-I-L-A-V-T-K-K-K-V-F-E-T-L-E-A
	E8	N-L-G-I-L-H-A-T-K-K-K-V-F-E-T-L-E-A
	E9	N-L-G-I-L-H-V-A-K-K-K-V-F-E-T-L-E-A
	E10	N-L-G-I-L-H-V-T-A-K-K-V-F-E-T-L-E-A
	E11	N-L-G-I-L-H-V-T-K-A-K-V-F-E-T-L-E-A
	E12	N-L-G-I-L-H-V-T-K-K-A-V-F-E-T-L-E-A
	E13	N-L-G-I-L-H-V-T-K-K-K-A-F-E-T-L-E-A
	E14	N-L-G-I-L-H-V-T-K-K-K-V-A-E-T-L-E-A
	E15	N-L-G-I-L-H-V-T-K-K-K-V-F-A-T-L-E-A
	E16	N-L-G-I-L-H-V-T-K-K-K-V-F-E-A-L-E-A
	E17	N-L-G-I-L-H-V-T-K-K-K-V-F-E-T-A-E-A
	E18	N-L-G-I-L-H-V-T-K-K-K-V-F-E-T-L-A-A
	E19	N-L-G-I-L-H-V-T-K-K-K-V-F-E-T-L-E-A

Original Peptide	Peptide Number	Amino acid Sequence
60	E21	A-E-G-G-G-D-R-Q-L-T-D-R-E-K-E-I-I-R
	E22	A-E-G-G-G-D-R-Q-L-T-D-R-E-K-E-I-I-R
	E23	A-A-G-G-G-D-R-Q-L-T-D-R-E-K-E-I-I-R
	E24	A-E-A-G-G-D-R-Q-L-T-D-R-E-K-E-I-I-R
	E25	A-E-G-A-G-D-R-Q-L-T-D-R-E-K-E-I-I-R
	E26	A-E-G-G-A-D-R-Q-L-T-D-R-E-K-E-I-I-R
	E27	A-E-G-G-G-A-R-Q-L-T-D-R-E-K-E-I-I-R
	E28	A-E-G-G-G-D-A-Q-L-T-D-R-E-K-E-I-I-R
	E29	A-E-G-G-G-D-R-A-L-T-D-R-E-K-E-I-I-R
	E30	A-E-G-G-G-D-R-Q-A-T-D-R-E-K-E-I-I-R
	F1	A-E-G-G-G-D-R-Q-L-A-D-R-E-K-E-I-I-R
	F2	A-E-G-G-G-D-R-Q-L-T-A-R-E-K-E-I-I-R
	F3	A-E-G-G-G-D-R-Q-L-T-D-A-E-K-E-I-I-R
	F4	A-E-G-G-G-D-R-Q-L-T-D-R-A-K-E-I-I-R
	F5	A-E-G-G-G-D-R-Q-L-T-D-R-E-A-E-I-I-R
	F6	A-E-G-G-G-D-R-Q-L-T-D-R-E-K-A-I-I-R
	F7	A-E-G-G-G-D-R-Q-L-T-D-R-E-K-E-A-I-R
	F8	A-E-G-G-G-D-R-Q-L-T-D-R-E-K-E-I-A-R
	F9	A-E-G-G-G-D-R-Q-L-T-D-R-E-K-E-I-I-A

Original Peptide	Peptide Number	Amino acid Sequence
78	F11	V-V-S-D-A-I-Y-D-S-K-A-P-N-A-S-N-L-K
	F12	A-V-S-D-A-I-Y-D-S-K-A-P-N-A-S-N-L-K
	F13	V-A-S-D-A-I-Y-D-S-K-A-P-N-A-S-N-L-K
	F14	V-V-A-D-A-I-Y-D-S-K-A-P-N-A-S-N-L-K
	F15	V-V-S-A-A-I-Y-D-S-K-A-P-N-A-S-N-L-K
	F16	V-V-S-D-A-I-Y-D-S-K-A-P-N-A-S-N-L-K
	F17	V-V-S-D-A-A-Y-D-S-K-A-P-N-A-S-N-L-K
	F18	V-V-S-D-A-I-A-D-S-K-A-P-N-A-S-N-L-K
	F19	V-V-S-D-A-I-Y-A-S-K-A-P-N-A-S-N-L-K
	F20	V-V-S-D-A-I-Y-D-A-K-A-P-N-A-S-N-L-K
	F21	V-V-S-D-A-I-Y-D-S-A-A-P-N-A-S-N-L-K
	F22	V-V-S-D-A-I-Y-D-S-K-A-P-N-A-S-N-L-K
	F23	V-V-S-D-A-I-Y-D-S-K-A-A-N-A-S-N-L-K
	F24	V-V-S-D-A-I-Y-D-S-K-A-P-A-A-S-N-L-K
	F25	V-V-S-D-A-I-Y-D-S-K-A-P-N-A-S-N-L-K
	F26	V-V-S-D-A-I-Y-D-S-K-A-P-N-A-A-N-L-K
	F27	V-V-S-D-A-I-Y-D-S-K-A-P-N-A-S-A-L-K
	F28	V-V-S-D-A-I-Y-D-S-K-A-P-N-A-S-N-A-K
	F29	V-V-S-D-A-I-Y-D-S-K-A-P-N-A-S-N-L-A

Original Peptide	Peptide Number	Amino acid Sequence
80	G1	Y-D-S-K-A-P-N-A-S-N-L-K-I-V-R-M-D-R
	G2	A-D-S-K-A-P-N-A-S-N-L-K-I-V-R-M-D-R
	G3	Y-A-S-K-A-P-N-A-S-N-L-K-I-V-R-M-D-R
	G4	Y-D-A-K-A-P-N-A-S-N-L-K-I-V-R-M-D-R
	G5	Y-D-S-A-A-P-N-A-S-N-L-K-I-V-R-M-D-R
	G6	Y-D-S-K-A-P-N-A-S-N-L-K-I-V-R-M-D-R
	G7	Y-D-S-K-A-A-N-A-S-N-L-K-I-V-R-M-D-R
	G8	Y-D-S-K-A-P-A-A-S-N-L-K-I-V-R-M-D-R
	G9	Y-D-S-K-A-P-N-A-S-N-L-K-I-V-R-M-D-R
	G10	Y-D-S-K-A-P-N-A-A-N-L-K-I-V-R-M-D-R
	G11	Y-D-S-K-A-P-N-A-S-A-L-K-I-V-R-M-D-R
	G12	Y-D-S-K-A-P-N-A-S-N-A-K-I-V-R-M-D-R
	G13	Y-D-S-K-A-P-N-A-S-N-L-A-I-V-R-M-D-R
	G14	Y-D-S-K-A-P-N-A-S-N-L-K-A-V-R-M-D-R
	G15	Y-D-S-K-A-P-N-A-S-N-L-K-I-A-R-M-D-R
	G16	Y-D-S-K-A-P-N-A-S-N-L-K-I-V-A-M-D-R
	G17	Y-D-S-K-A-P-N-A-S-N-L-K-I-V-R-A-D-R
	G18	Y-D-S-K-A-P-N-A-S-N-L-K-I-V-R-M-A-R
	G19	Y-D-S-K-A-P-N-A-S-N-L-K-I-V-R-M-D-A

Original Peptide	Peptide Number	Amino acid Sequence
82	G21	N-A-S-N-L-K-I-V-R-M-D-R-T-A-G-C-V-T
	G22	A-A-S-N-L-K-I-V-R-M-D-R-T-A-G-C-V-T
	G23	N-A-S-N-L-K-I-V-R-M-D-R-T-A-G-C-V-T
	G24	N-A-A-N-L-K-I-V-R-M-D-R-T-A-G-C-V-T
	G25	N-A-S-A-L-K-I-V-R-M-D-R-T-A-G-C-V-T
	G26	N-A-S-N-A-K-I-V-R-M-D-R-T-A-G-C-V-T
	G27	N-A-S-N-L-A-I-V-R-M-D-R-T-A-G-C-V-T
	G28	N-A-S-N-L-K-A-V-R-M-D-R-T-A-G-C-V-T
	G29	N-A-S-N-L-K-I-A-R-M-D-R-T-A-G-C-V-T
	G30	N-A-S-N-L-K-I-V-A-M-D-R-T-A-G-C-V-T
	H1	N-A-S-N-L-K-I-V-R-A-D-R-T-A-G-C-V-T
	H2	N-A-S-N-L-K-I-V-R-M-A-R-T-A-G-C-V-T
	H3	N-A-S-N-L-K-I-V-R-M-D-A-T-A-G-C-V-T
	H4	N-A-S-N-L-K-I-V-R-M-D-R-A-A-G-C-V-T
	H5	N-A-S-N-L-K-I-V-R-M-D-R-T-A-G-C-V-T
	H6	N-A-S-N-L-K-I-V-R-M-D-R-T-A-A-C-V-T
	H7	N-A-S-N-L-K-I-V-R-M-D-R-T-A-G-A-V-T
	H8	N-A-S-N-L-K-I-V-R-M-D-R-T-A-G-C-A-T
	H9	N-A-S-N-L-K-I-V-R-M-D-R-T-A-G-C-V-A

Original Peptide	Peptide Number	Amino acid Sequence
91	H11	D-K-V-Q-K-D-D-I-Q-I-R-F-Y-E-E-E-E-N
	H12	A-K-V-Q-K-D-D-I-Q-I-R-F-Y-E-E-E-E-N
	H13	D-A-V-Q-K-D-D-I-Q-I-R-F-Y-E-E-E-E-N
	H14	D-K-A-Q-K-D-D-I-Q-I-R-F-Y-E-E-E-E-N
	H15	D-K-V-A-K-D-D-I-Q-I-R-F-Y-E-E-E-E-N
	H16	D-K-V-Q-A-D-D-I-Q-I-R-F-Y-E-E-E-E-N
	H17	D-K-V-Q-K-A-D-I-Q-I-R-F-Y-E-E-E-E-N
	H18	D-K-V-Q-K-D-A-I-Q-I-R-F-Y-E-E-E-E-N
	H19	D-K-V-Q-K-D-D-A-Q-I-R-F-Y-E-E-E-E-N
	H20	D-K-V-Q-K-D-D-I-A-I-R-F-Y-E-E-E-E-N
	H21	D-K-V-Q-K-D-D-I-Q-A-R-F-Y-E-E-E-E-N
	H22	D-K-V-Q-K-D-D-I-Q-I-A-F-Y-E-E-E-E-N
	H23	D-K-V-Q-K-D-D-I-Q-I-R-A-Y-E-E-E-E-N
	H24	D-K-V-Q-K-D-D-I-Q-I-R-F-A-E-E-E-E-N
	H25	D-K-V-Q-K-D-D-I-Q-I-R-F-Y-A-E-E-E-E-N
	H26	D-K-V-Q-K-D-D-I-Q-I-R-F-Y-E-A-E-E-E-N
	H27	D-K-V-Q-K-D-D-I-Q-I-R-F-Y-E-E-A-E-E-N
	H28	D-K-V-Q-K-D-D-I-Q-I-R-F-Y-E-E-E-A-N
	H29	D-K-V-Q-K-D-D-I-Q-I-R-F-Y-E-E-E-E-A

Original Peptide	Peptide Number	Amino acid Sequence
93	I1	D-I-Q-I-R-F-Y-E-E-E-E-N-G-G-V-W-E-G
	I2	A-I-Q-I-R-F-Y-E-E-E-E-N-G-G-V-W-E-G
	I3	D-A-Q-I-R-F-Y-E-E-E-E-N-G-G-V-W-E-G
	I4	D-I-A-I-R-F-Y-E-E-E-E-N-G-G-V-W-E-G
	I5	D-I-Q-A-R-F-Y-E-E-E-E-N-G-G-V-W-E-G
	I6	D-I-Q-I-A-F-Y-E-E-E-E-N-G-G-V-W-E-G
	I7	D-I-Q-I-R-A-Y-E-E-E-E-N-G-G-V-W-E-G
	I8	D-I-Q-I-R-F-A-E-E-E-E-N-G-G-V-W-E-G
	I9	D-I-Q-I-R-F-Y-A-E-E-E-N-G-G-V-W-E-G
	I10	D-I-Q-I-R-F-Y-E-A-E-E-N-G-G-V-W-E-G
	I11	D-I-Q-I-R-F-Y-E-E-A-E-N-G-G-V-W-E-G
	I12	D-I-Q-I-R-F-Y-E-E-E-A-N-G-G-V-W-E-G
	I13	D-I-Q-I-R-F-Y-E-E-E-E-A-G-G-V-W-E-G
	I14	D-I-Q-I-R-F-Y-E-E-E-E-N-A-G-V-W-E-G
	I15	D-I-Q-I-R-F-Y-E-E-E-E-N-G-A-V-W-E-G
	I16	D-I-Q-I-R-F-Y-E-E-E-E-N-G-G-A-W-E-G
	I17	D-I-Q-I-R-F-Y-E-E-E-E-N-G-G-V-A-E-G
	I18	D-I-Q-I-R-F-Y-E-E-E-E-N-G-G-V-W-A-G
	I19	D-I-Q-I-R-F-Y-E-E-E-E-N-G-G-V-W-E-A

Original Peptide	Peptide Number	Amino acid Sequence
95	I21	Y-E-E-E-E-N-G-G-V-W-E-G-F-G-D-F-S-P
	I22	A-E-E-E-E-N-G-G-V-W-E-G-F-G-D-F-S-P
	I23	Y-A-E-E-E-N-G-G-V-W-E-G-F-G-D-F-S-P
	I24	Y-E-A-E-E-N-G-G-V-W-E-G-F-G-D-F-S-P
	I25	Y-E-E-A-E-N-G-G-V-W-E-G-F-G-D-F-S-P
	I26	Y-E-E-E-A-N-G-G-V-W-E-G-F-G-D-F-S-P
	I27	Y-E-E-E-E-A-G-G-V-W-E-G-F-G-D-F-S-P
	I28	Y-E-E-E-E-N-A-G-V-W-E-G-F-G-D-F-S-P
	I29	Y-E-E-E-E-N-G-A-V-W-E-G-F-G-D-F-S-P
	I30	Y-E-E-E-E-N-G-G-A-W-E-G-F-G-D-F-S-P
	J1	Y-E-E-E-E-N-G-G-V-A-E-G-F-G-D-F-S-P
	J2	Y-E-E-E-E-N-G-G-V-W-A-G-F-G-D-F-S-P
	J3	Y-E-E-E-E-N-G-G-V-W-E-A-F-G-D-F-S-P
	J4	Y-E-E-E-E-N-G-G-V-W-E-G-A-G-D-F-S-P
	J5	Y-E-E-E-E-N-G-G-V-W-E-G-F-A-D-F-S-P
	J6	Y-E-E-E-E-N-G-G-V-W-E-G-F-G-A-F-S-P
	J7	Y-E-E-E-E-N-G-G-V-W-E-G-F-G-D-A-S-P
	J8	Y-E-E-E-E-N-G-G-V-W-E-G-F-G-D-F-A-P
	J9	Y-E-E-E-E-N-G-G-V-W-E-G-F-G-D-F-S-A

Original Peptide	Peptide Number	Amino acid Sequence
97	J11	G-G-V-W-E-G-F-G-D-F-S-P-T-D-V-H-R-Q
	J12	A-G-V-W-E-G-F-G-D-F-S-P-T-D-V-H-R-Q
	J13	G-A-V-W-E-G-F-G-D-F-S-P-T-D-V-H-R-Q
	J14	G-G-A-W-E-G-F-G-D-F-S-P-T-D-V-H-R-Q
	J15	G-G-V-A-E-G-F-G-D-F-S-P-T-D-V-H-R-Q
	J16	G-G-V-W-A-G-F-G-D-F-S-P-T-D-V-H-R-Q
	J17	G-G-V-W-E-A-F-G-D-F-S-P-T-D-V-H-R-Q
	J18	G-G-V-W-E-G-A-G-D-F-S-P-T-D-V-H-R-Q
	J19	G-G-V-W-E-G-F-A-D-F-S-P-T-D-V-H-R-Q
	J20	G-G-V-W-E-G-F-G-A-F-S-P-T-D-V-H-R-Q
	J21	G-G-V-W-E-G-F-G-D-A-S-P-T-D-V-H-R-Q
	J22	G-G-V-W-E-G-F-G-D-F-A-P-T-D-V-H-R-Q
	J23	G-G-V-W-E-G-F-G-D-F-S-A-T-D-V-H-R-Q
	J24	G-G-V-W-E-G-F-G-D-F-S-P-A-D-V-H-R-Q
	J25	G-G-V-W-E-G-F-G-D-F-S-P-T-A-V-H-R-Q
	J26	G-G-V-W-E-G-F-G-D-F-S-P-T-D-A-H-R-Q
	J27	G-G-V-W-E-G-F-G-D-F-S-P-T-D-V-A-R-Q
	J28	G-G-V-W-E-G-F-G-D-F-S-P-T-D-V-H-A-Q
	J29	G-G-V-W-E-G-F-G-D-F-S-P-T-D-V-H-R-A

Original Peptide	Peptide Number	Amino acid Sequence
99	K1	F-G-D-F-S-P-T-D-V-H-R-Q-F-A-I-V-F-K
	K2	A-G-D-F-S-P-T-D-V-H-R-Q-F-A-I-V-F-K
	K3	F-A-D-F-S-P-T-D-V-H-R-Q-F-A-I-V-F-K
	K4	F-G-A-F-S-P-T-D-V-H-R-Q-F-A-I-V-F-K
	K5	F-G-D-A-S-P-T-D-V-H-R-Q-F-A-I-V-F-K
	K6	F-G-D-F-A-P-T-D-V-H-R-Q-F-A-I-V-F-K
	K7	F-G-D-F-S-A-T-D-V-H-R-Q-F-A-I-V-F-K
	K8	F-G-D-F-S-P-A-D-V-H-R-Q-F-A-I-V-F-K
	K9	F-G-D-F-S-P-T-A-V-H-R-Q-F-A-I-V-F-K
	K10	F-G-D-F-S-P-T-D-A-H-R-Q-F-A-I-V-F-K
	K11	F-G-D-F-S-P-T-D-V-A-R-Q-F-A-I-V-F-K
	K12	F-G-D-F-S-P-T-D-V-H-A-Q-F-A-I-V-F-K
	K13	F-G-D-F-S-P-T-D-V-H-R-A-F-A-I-V-F-K
	K14	F-G-D-F-S-P-T-D-V-H-R-Q-A-A-I-V-F-K
	K15	F-G-D-F-S-P-T-D-V-H-R-Q-F-A-I-V-F-K
	K16	F-G-D-F-S-P-T-D-V-H-R-Q-F-A-A-V-F-K
	K17	F-G-D-F-S-P-T-D-V-H-R-Q-F-A-I-A-F-K
	K18	F-G-D-F-S-P-T-D-V-H-R-Q-F-A-I-V-A-K
	K19	F-G-D-F-S-P-T-D-V-H-R-Q-F-A-I-V-F-A

Original Peptide	Peptide Number	Amino acid Sequence
103	K21	F-A-I-V-F-K-T-P-K-Y-K-D-V-N-I-T-K-P
	K22	A-A-I-V-F-K-T-P-K-Y-K-D-V-N-I-T-K-P
	K23	F-A-I-V-F-K-T-P-K-Y-K-D-V-N-I-T-K-P
	K24	F-A-A-V-F-K-T-P-K-Y-K-D-V-N-I-T-K-P
	K25	F-A-I-A-F-K-T-P-K-Y-K-D-V-N-I-T-K-P
	K26	F-A-I-V-A-K-T-P-K-Y-K-D-V-N-I-T-K-P
	K27	F-A-I-V-F-A-T-P-K-Y-K-D-V-N-I-T-K-P
	K28	F-A-I-V-F-K-A-P-K-Y-K-D-V-N-I-T-K-P
	K29	F-A-I-V-F-K-T-A-K-Y-K-D-V-N-I-T-K-P
	K30	F-A-I-V-F-K-T-P-A-Y-K-D-V-N-I-T-K-P
	L1	F-A-I-V-F-K-T-P-K-A-K-D-V-N-I-T-K-P
	L2	F-A-I-V-F-K-T-P-K-Y-A-D-V-N-I-T-K-P
	L3	F-A-I-V-F-K-T-P-K-Y-K-A-V-N-I-T-K-P
	L4	F-A-I-V-F-K-T-P-K-Y-K-D-A-N-I-T-K-P
	L5	F-A-I-V-F-K-T-P-K-Y-K-D-V-A-I-T-K-P
	L6	F-A-I-V-F-K-T-P-K-Y-K-D-V-N-A-T-K-P
	L7	F-A-I-V-F-K-T-P-K-Y-K-D-V-N-I-A-K-P
	L8	F-A-I-V-F-K-T-P-K-Y-K-D-V-N-I-T-A-P
	L9	F-A-I-V-F-K-T-P-K-Y-K-D-V-N-I-T-K-A

Original Peptide	Peptide Number	Amino acid Sequence
105	L11	T-P-K-Y-K-D-V-N-I-T-K-P-A-S-V-F-V-Q
	L12	A-P-K-Y-K-D-V-N-I-T-K-P-A-S-V-F-V-Q
	L13	T-A-K-Y-K-D-V-N-I-T-K-P-A-S-V-F-V-Q
	L14	T-P-A-Y-K-D-V-N-I-T-K-P-A-S-V-F-V-Q
	L15	T-P-K-A-K-D-V-N-I-T-K-P-A-S-V-F-V-Q
	L16	T-P-K-Y-A-D-V-N-I-T-K-P-A-S-V-F-V-Q
	L17	T-P-K-Y-K-A-V-N-I-T-K-P-A-S-V-F-V-Q
	L18	T-P-K-Y-K-D-A-N-I-T-K-P-A-S-V-F-V-Q
	L19	T-P-K-Y-K-D-V-A-I-T-K-P-A-S-V-F-V-Q
	L20	T-P-K-Y-K-D-V-N-A-T-K-P-A-S-V-F-V-Q
	L21	T-P-K-Y-K-D-V-N-I-A-K-P-A-S-V-F-V-Q
	L22	T-P-K-Y-K-D-V-N-I-T-A-P-A-S-V-F-V-Q
	L23	T-P-K-Y-K-D-V-N-I-T-K-A-A-S-V-F-V-Q
	L24	T-P-K-Y-K-D-V-N-I-T-K-P-A-S-V-F-V-Q
	L25	T-P-K-Y-K-D-V-N-I-T-K-P-A-A-V-F-V-Q
	L26	T-P-K-Y-K-D-V-N-I-T-K-P-A-S-A-F-V-Q
	L27	T-P-K-Y-K-D-V-N-I-T-K-P-A-S-V-A-V-Q
	L28	T-P-K-Y-K-D-V-N-I-T-K-P-A-S-V-F-A-Q
	L29	T-P-K-Y-K-D-V-N-I-T-K-P-A-S-V-F-V-A

Original Peptide	Peptide Number	Amino acid Sequence
107	M1	V-N-I-T-K-P-A-S-V-F-V-Q-L-R-R-K-S-D
	M2	A-N-I-T-K-P-A-S-V-F-V-Q-L-R-R-K-S-D
	M3	V-A-I-T-K-P-A-S-V-F-V-Q-L-R-R-K-S-D
	M4	V-N-A-T-K-P-A-S-V-F-V-Q-L-R-R-K-S-D
	M5	V-N-I-A-K-P-A-S-V-F-V-Q-L-R-R-K-S-D
	M6	V-N-I-T-A-P-A-S-V-F-V-Q-L-R-R-K-S-D
	M7	V-N-I-T-K-P-A-S-V-F-V-Q-L-R-R-K-S-D
	M8	V-N-I-T-K-P-A-S-V-F-V-Q-L-R-R-K-S-D
	M9	V-N-I-T-K-P-A-S-V-F-V-Q-L-R-R-K-S-D
	M10	V-N-I-T-K-P-A-S-V-F-V-Q-L-R-R-K-S-D
	M11	V-N-I-T-K-P-A-S-V-F-V-Q-L-R-R-K-S-D
	M12	V-N-I-T-K-P-A-S-V-F-V-Q-L-R-R-K-S-D
	M13	V-N-I-T-K-P-A-S-V-F-V-Q-L-R-R-K-S-D
	M14	V-N-I-T-K-P-A-S-V-F-V-Q-L-R-R-K-S-D
	M15	V-N-I-T-K-P-A-S-V-F-V-Q-L-R-R-K-S-D
	M16	V-N-I-T-K-P-A-S-V-F-V-Q-L-R-R-K-S-D
	M17	V-N-I-T-K-P-A-S-V-F-V-Q-L-R-R-K-S-D
	M18	V-N-I-T-K-P-A-S-V-F-V-Q-L-R-R-K-S-D
	M19	V-N-I-T-K-P-A-S-V-F-V-Q-L-R-R-K-S-D

Original Peptide	Peptide Number	Amino acid Sequence
115	M21	K-P-F-L-Y-Y-P-E-I-K-D-K-E-E-V-Q-R-K
	M22	A-P-F-L-Y-Y-P-E-I-K-D-K-E-E-V-Q-R-K
	M23	K-A-F-L-Y-Y-P-E-I-K-D-K-E-E-V-Q-R-K
	M24	K-P-A-L-Y-Y-P-E-I-K-D-K-E-E-V-Q-R-K
	M25	K-P-F-A-Y-Y-P-E-I-K-D-K-E-E-V-Q-R-K
	M26	K-P-F-L-A-Y-P-E-I-K-D-K-E-E-V-Q-R-K
	M27	K-P-F-L-Y-A-P-E-I-K-D-K-E-E-V-Q-R-K
	M28	K-P-F-L-Y-Y-A-E-I-K-D-K-E-E-V-Q-R-K
	M29	K-P-F-L-Y-Y-P-A-I-K-D-K-E-E-V-Q-R-K
	M30	K-P-F-L-Y-Y-P-E-A-K-D-K-E-E-V-Q-R-K
	N1	K-P-F-L-Y-Y-P-E-I-A-D-K-E-E-V-Q-R-K
	N2	K-P-F-L-Y-Y-P-E-I-K-A-K-E-E-V-Q-R-K
	N3	K-P-F-L-Y-Y-P-E-I-K-D-A-E-E-V-Q-R-K
	N4	K-P-F-L-Y-Y-P-E-I-K-D-K-A-E-V-Q-R-K
	N5	K-P-F-L-Y-Y-P-E-I-K-D-K-E-A-V-Q-R-K
	N6	K-P-F-L-Y-Y-P-E-I-K-D-K-E-E-A-Q-R-K
	N7	K-P-F-L-Y-Y-P-E-I-K-D-K-E-E-V-A-R-K
	N8	K-P-F-L-Y-Y-P-E-I-K-D-K-E-E-V-Q-A-K
	N9	K-P-F-L-Y-Y-P-E-I-K-D-K-E-E-V-Q-R-A

Original Peptide	Peptide Number	Amino acid Sequence
117	N11	P-E-I-K-D-K-E-E-V-Q-R-K-R-Q-K-L-M-P
	N12	A-E-I-K-D-K-E-E-V-Q-R-K-R-Q-K-L-M-P
	N13	P-A-I-K-D-K-E-E-V-Q-R-K-R-Q-K-L-M-P
	N14	P-E-A-K-D-K-E-E-V-Q-R-K-R-Q-K-L-M-P
	N15	P-E-I-A-D-K-E-E-V-Q-R-K-R-Q-K-L-M-P
	N16	P-E-I-K-A-K-E-E-V-Q-R-K-R-Q-K-L-M-P
	N17	P-E-I-K-D-A-E-E-V-Q-R-K-R-Q-K-L-M-P
	N18	P-E-I-K-D-K-A-E-V-Q-R-K-R-Q-K-L-M-P
	N19	P-E-I-K-D-K-E-A-V-Q-R-K-R-Q-K-L-M-P
	N20	P-E-I-K-D-K-E-E-A-Q-R-K-R-Q-K-L-M-P
	N21	P-E-I-K-D-K-E-E-V-A-R-K-R-Q-K-L-M-P
	N22	P-E-I-K-D-K-E-E-V-Q-A-K-R-Q-K-L-M-P
	N23	P-E-I-K-D-K-E-E-V-Q-R-A-R-Q-K-L-M-P
	N24	P-E-I-K-D-K-E-E-V-Q-R-K-A-Q-K-L-M-P
	N25	P-E-I-K-D-K-E-E-V-Q-R-K-R-A-K-L-M-P
	N26	P-E-I-K-D-K-E-E-V-Q-R-K-R-Q-A-L-M-P
	N27	P-E-I-K-D-K-E-E-V-Q-R-K-R-Q-K-A-M-P
	N28	P-E-I-K-D-K-E-E-V-Q-R-K-R-Q-K-L-A-P
	N29	P-E-I-K-D-K-E-E-V-Q-R-K-R-Q-K-L-M-A

Original Peptide	Peptide Number	Amino acid Sequence
119	O1	E-E-V-Q-R-K-R-Q-K-L-M-P-N-F-S-D-S-F
	O2	A-E-V-Q-R-K-R-Q-K-L-M-P-N-F-S-D-S-F
	O3	E-A-V-Q-R-K-R-Q-K-L-M-P-N-F-S-D-S-F
	O4	E-E-A-Q-R-K-R-Q-K-L-M-P-N-F-S-D-S-F
	O5	E-E-V-A-R-K-R-Q-K-L-M-P-N-F-S-D-S-F
	O6	E-E-V-Q-A-K-R-Q-K-L-M-P-N-F-S-D-S-F
	O7	E-E-V-Q-R-A-R-Q-K-L-M-P-N-F-S-D-S-F
	O8	E-E-V-Q-R-K-A-Q-K-L-M-P-N-F-S-D-S-F
	O9	E-E-V-Q-R-K-R-A-K-L-M-P-N-F-S-D-S-F
	O10	E-E-V-Q-R-K-R-Q-A-L-M-P-N-F-S-D-S-F
	O11	E-E-V-Q-R-K-R-Q-K-A-M-P-N-F-S-D-S-F
	O12	E-E-V-Q-R-K-R-Q-K-L-A-P-N-F-S-D-S-F
	O13	E-E-V-Q-R-K-R-Q-K-L-M-A-N-F-S-D-S-F
	O14	E-E-V-Q-R-K-R-Q-K-L-M-P-A-F-S-D-S-F
	O15	E-E-V-Q-R-K-R-Q-K-L-M-P-N-A-S-D-S-F
	O16	E-E-V-Q-R-K-R-Q-K-L-M-P-N-F-A-D-S-F
	O17	E-E-V-Q-R-K-R-Q-K-L-M-P-N-F-S-A-S-F
	O18	E-E-V-Q-R-K-R-Q-K-L-M-P-N-F-S-D-A-F
	O19	E-E-V-Q-R-K-R-Q-K-L-M-P-N-F-S-D-S-A

Original Peptide	Peptide Number	Amino acid Sequence
121	O21	R-Q-K-L-M-P-N-F-S-D-S-F-G-G-G-S-G-A
	O22	A-Q-K-L-M-P-N-F-S-D-S-F-G-G-G-S-G-A
	O23	R-A-K-L-M-P-N-F-S-D-S-F-G-G-G-S-G-A
	O24	R-Q-A-L-M-P-N-F-S-D-S-F-G-G-G-S-G-A
	O25	R-Q-K-A-M-P-N-F-S-D-S-F-G-G-G-S-G-A
	O26	R-Q-K-L-A-P-N-F-S-D-S-F-G-G-G-S-G-A
	O27	R-Q-K-L-M-A-N-F-S-D-S-F-G-G-G-S-G-A
	O28	R-Q-K-L-M-P-A-F-S-D-S-F-G-G-G-S-G-A
	O29	R-Q-K-L-M-P-N-A-S-D-S-F-G-G-G-S-G-A
	O30	R-Q-K-L-M-P-N-F-A-D-S-F-G-G-G-S-G-A
	P1	R-Q-K-L-M-P-N-F-S-A-S-F-G-G-G-S-G-A
	P2	R-Q-K-L-M-P-N-F-S-D-A-F-G-G-G-S-G-A
	P3	R-Q-K-L-M-P-N-F-S-D-S-A-G-G-G-S-G-A
	P4	R-Q-K-L-M-P-N-F-S-D-S-F-A-G-G-S-G-A
	P5	R-Q-K-L-M-P-N-F-S-D-S-F-G-A-G-S-G-A
	P6	R-Q-K-L-M-P-N-F-S-D-S-F-G-G-A-S-G-A
	P7	R-Q-K-L-M-P-N-F-S-D-S-F-G-G-G-A-G-A
	P8	R-Q-K-L-M-P-N-F-S-D-S-F-G-G-G-S-A-A
	P9	R-Q-K-L-M-P-N-F-S-D-S-F-G-G-G-S-G-A

7.3 p50 Alanine Substitution Peptide Array Data

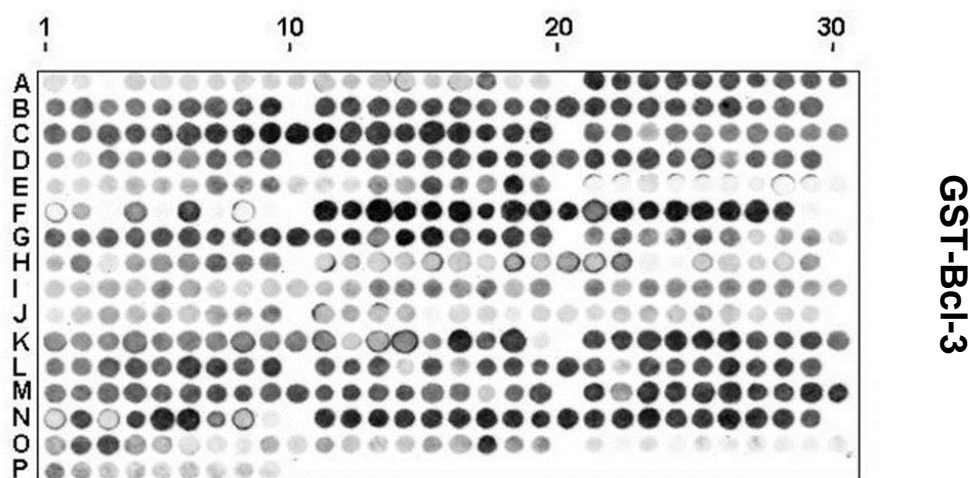


Figure 7.1 Full p50 alanine substitution peptide array.

The 18 amino acids of the p50-derived peptides 20, 22, 24, 26, 28, 30, 46, 60, 78, 80,82, 91, 93, 95, 97, 99, 103,105, 107, 115, 117, 119 and 121 were sequentially substituted with alanine. See Appendix 7.2 for peptide locations on array. Arrays were probed with GST-Bcl-3 and detected by immunoblotting with anti-GST antibody. GST-Bcl-3 binding was quantified by densitometry and represented as a percentage binding of the control control parent peptide peptides (see below).

Peptide 20 Intensity	Percent Binding	A.A Sub
9.3	100.0	—
7.1	75.7	V
2.7	29.1	C
12.5	134.1	E
10.0	107.2	G
9.6	102.4	P
10.1	107.8	S
10.5	112.3	H
10.3	110.6	G
10.9	117.1	G
17.1	183.2	L
12.8	137.0	P
13.5	145.0	G
19.4	208.0	A
11.3	120.9	S
16.0	170.9	S
38.0	407.2	E
7.5	80.4	K
10.1	108.2	N

Peptide 22 Intensity	Percent Binding	A.A Sub
70.1	100.0	—
52.2	74.5	H
56.6	80.8	G
54.1	77.2	G
48.9	69.8	L
48.7	69.5	P
38.1	54.4	G
42.1	60.1	A
40.8	58.2	S
34.9	49.8	S
31.9	45.6	E
43.0	61.4	K
25.3	36.1	N
32.3	46.2	K
34.4	49.1	K
48.7	69.5	S
49.3	70.3	Y
45.8	65.3	P
62.8	89.6	Q

Peptide 24 Intensity	Percent Binding	A.A Sub
55.8	100.0	_
52.8	94.5	A
56.5	101.2	S
50.9	91.1	S
51.6	92.4	E
59.9	107.3	K
43.3	77.6	N
42.4	75.9	K
46.3	83.0	K
64.5	115.5	S
58.6	105.0	Y
54.4	97.4	P
55.5	99.4	Q
50.8	91.0	V
49.2	88.2	K
66.7	119.5	I
35.1	62.9	C
41.5	74.4	N
47.2	84.5	Y

Peptide 26 Intensity	Percent Binding	A.A Sub
43.4	100.0	_
34.8	80.2	K
51.9	119.5	K
46.7	107.6	S
53.3	122.7	Y
64.0	147.5	P
67.0	154.2	Q
72.8	167.6	V
88.4	203.7	K
91.5	210.8	I
85.2	196.2	C
65.3	150.4	N
74.3	171.2	Y
59.0	135.9	V
85.4	196.8	G
79.6	183.3	P
56.0	129.0	A
60.3	138.9	K
67.9	156.4	V

Peptide 28 Intensity	Percent Binding	A.A Sub
42.5	100.0	_
40.6	95.5	V
18.3	43.1	K
39.3	92.5	I
31.0	73.0	C
30.6	72.0	N
34.9	82.3	Y
28.8	67.8	V
28.1	66.0	G
29.6	69.8	P
19.9	46.8	A
10.2	24.1	K
37.3	87.8	V
27.6	65.0	I
35.4	83.4	V
29.8	70.1	Q
45.8	107.8	L
34.4	81.1	V
42.3	99.7	T

Peptide 30 Intensity	Percent Binding	A.A Sub
54.7	100.0	_
45.0	82.2	V
55.7	101.8	G
45.3	82.7	P
50.0	91.3	A
60.4	110.3	K
56.7	103.6	V
51.5	94.0	I
57.7	105.4	V
47.6	87.0	Q
58.2	106.3	L
48.5	88.5	V
60.7	110.9	T
38.8	70.9	N
53.0	96.9	G
22.0	40.2	K
39.5	72.1	N
40.0	73.0	I
42.9	78.4	H

Peptide 46 Intensity	Percent Binding	A.A Sub
9.1	100.0	_
8.0	87.8	N
11.2	122.6	L
16.1	176.5	G
15.1	165.4	I
13.3	145.9	L
35.8	392.8	H
22.7	249.3	V
29.9	327.7	T
10.4	114.4	K
9.1	100.2	K
7.2	79.1	K
28.4	310.7	V
18.7	205.0	F
49.7	544.9	E
28.1	308.4	T
26.5	290.6	L
68.3	748.0	E
29.0	317.4	A

Peptide 60 Intensity	Percent Binding	A.A Sub
7.9	100.0	_
6.1	77.3	A
8.5	108.3	E
5.8	74.2	G
6.6	84.3	G
5.9	74.3	G
4.7	59.4	D
8.7	110.4	R
7.2	91.9	Q
3.8	48.3	L
12.5	158.5	T
17.4	221.4	D
3.0	37.8	R
39.6	503.3	E
3.4	43.2	K
68.4	868.3	E
3.4	43.6	I
13.7	174.5	I
3.2	40.2	R

Peptide 78 Intensity	Percent Binding	A.A Sub
92.1	100.0	
73.1	79.4	V
116.1	126.1	V
93.4	101.4	S
79.8	86.6	D
101.8	110.5	A
52.0	56.4	I
86.1	93.5	Y
82.7	89.8	D
66.3	72.0	S
57.1	62.0	K
90.3	98.1	A
72.1	78.2	P
92.4	100.3	N
82.1	89.1	A
79.1	85.9	S
83.2	90.3	N
59.7	64.8	L
3.6	3.9	K

Peptide 80 Intensity	Percent Binding	A.A Sub
40.5	100.0	Y
35.5	87.6	D
46.7	115.4	S
43.5	107.4	K
51.3	126.7	A
56.2	138.8	P
41.5	102.5	N
52.2	128.9	A
55.7	137.7	S
67.7	167.3	N
51.9	128.1	L
59.3	146.4	K
37.4	92.3	I
71.3	176.1	V
79.5	196.4	R
44.9	110.9	M
52.1	128.7	D
63.6	157.1	R
51.1	126.3	Y

Peptide 82 Intensity	Percent Binding	A.A Sub
28.6	100.0	_
38.7	135.4	N
28.7	100.5	A
31.4	109.6	S
38.3	134.0	N
33.8	118.2	L
9.5	33.1	K
18.3	63.8	I
24.1	84.1	V
6.0	21.0	R
14.0	49.0	M
34.3	120.0	D
7.9	27.6	R
22.3	77.8	T
28.8	100.7	A
31.0	108.5	G
43.7	152.9	C
34.3	119.7	V
32.5	113.6	T

Peptide 91 Intensity	Percent Binding	A.A Sub
21.0	100.0	_
18.0	85.8	D
15.6	74.5	K
15.6	74.4	V
26.7	127.6	Q
17.3	82.4	K
10.3	49.2	D
36.8	175.7	D
18.1	86.4	I
38.4	183.2	Q
31.0	148.0	I
41.7	199.0	R
4.8	23.0	F
3.3	15.7	Y
17.3	82.4	E
14.0	66.8	E
9.4	44.8	E
13.0	62.2	E
23.7	113.3	N

Peptide 93 Intensity	Percent Binding	A.A Sub
12.3	100.0	_
12.8	104.4	D
20.8	169.4	I
16.1	131.4	Q
31.5	256.5	I
22.0	179.7	R
11.2	91.6	F
9.3	75.6	Y
12.5	101.7	E
14.4	117.8	E
13.5	109.7	E
17.8	145.1	E
31.8	259.6	N
31.6	257.8	G
32.5	265.0	G
26.4	215.3	V
36.1	294.2	W
16.7	136.3	E
30.2	246.5	G

Peptide 95 Intensity	Percent Binding	A.A Sub
30.2	100.0	_
16.0	53.0	Y
29.8	98.7	E
27.8	92.0	E
28.6	94.6	E
30.4	100.7	E
25.3	83.7	N
28.0	92.7	G
19.9	65.9	G
15.7	52.0	V
6.0	19.7	W
13.1	43.4	E
21.4	70.7	G
16.0	53.0	F
20.2	66.9	G
14.8	49.0	D
23.6	78.2	F
21.5	71.3	S
31.7	104.8	P

Peptide 97 Intensity	Percent Binding	A.A Sub
24.0	100.0	_
17.8	74.4	G
17.5	73.0	G
16.2	67.4	V
3.5	14.8	W
10.1	42.2	E
10.0	41.9	G
5.6	23.3	F
9.9	41.5	G
9.6	39.9	D
8.0	33.3	F
12.2	50.8	S
15.4	64.3	P
13.5	56.4	T
19.4	81.0	D
14.3	59.6	V
8.9	36.9	H
10.1	42.1	R
9.4	39.1	Q

Peptide 99 Intensity	Percent Binding	A.A Sub
32.3	100.0	_
26.8	82.8	F
30.2	93.5	G
44.5	137.6	D
33.9	104.7	F
39.3	121.4	S
35.1	108.7	P
45.0	139.2	T
35.6	110.2	D
39.4	122.0	V
46.0	142.2	H
12.6	38.9	R
34.2	105.8	Q
51.5	159.2	F
25.7	79.5	A
95.3	295.0	I
43.0	133.2	V
79.2	245.0	F
6.6	20.5	K

Peptide 103 Intensity	Percent Binding	A.A Sub
53.9	100.0	_
55.6	103.1	F
65.3	121.1	A
77.2	143.2	I
67.3	124.8	V
78.2	144.9	F
48.0	88.9	K
45.4	84.2	T
51.9	96.3	P
38.7	71.8	K
27.9	51.8	Y
29.8	55.2	K
46.2	85.7	D
51.8	96.1	V
39.8	73.7	N
69.9	129.7	I
55.8	103.5	T
44.5	82.5	K
54.2	100.5	P

Peptide 105 Intensity	Percent Binding	A.A Sub
42.6	100.0	_
36.3	85.2	T
47.8	112.0	P
9.2	21.5	K
45.2	106.0	Y
14.6	34.4	K
42.2	99.0	D
48.8	114.4	V
31.4	73.8	N
58.5	137.3	I
46.3	108.6	T
10.5	24.7	K
49.7	116.5	P
42.4	99.5	A
46.0	108.0	S
62.4	146.3	V
46.6	109.4	F
53.1	124.5	V
43.1	101.2	Q

Peptide 107 Intensity	Percent Binding	A.A Sub
34.0	100.0	_
32.1	94.5	V
44.0	129.5	N
49.3	145.2	I
40.2	118.3	T
46.9	138.0	K
48.1	141.7	P
40.2	118.4	A
43.3	127.3	S
55.2	162.6	V
36.3	106.9	F
43.9	129.2	V
42.0	123.5	Q
38.1	112.1	L
40.2	118.2	R
37.0	108.9	R
11.9	35.0	K
33.5	98.7	S
55.1	162.2	D

Peptide 115 Intensity	Percent Binding	A.A Sub
58.9	100.0	_
27.4	46.5	K
71.8	122.0	P
63.0	107.0	F
65.4	111.2	L
77.4	131.5	Y
50.9	86.5	Y
50.6	85.9	P
70.1	119.1	E
55.7	94.7	I
18.5	31.4	K
51.4	87.3	D
18.1	30.7	K
47.4	80.5	E
83.5	141.8	E
86.0	146.1	V
31.9	54.1	Q
32.5	55.2	R
5.4	9.2	K

Peptide 117 Intensity	Percent Binding	A.A Sub
62.8	100.0	_
65.6	104.5	P
65.9	105.0	E
60.5	96.4	I
62.3	99.2	K
67.7	107.9	D
76.8	122.3	K
64.4	102.6	E
53.9	85.8	E
71.5	113.9	V
61.6	98.2	Q
67.1	106.9	R
83.6	133.3	K
58.9	93.9	R
63.4	101.1	Q
83.9	133.7	K
69.8	111.3	L
62.5	99.6	M
42.8	68.3	P

Peptide 119 Intensity	Percent Binding	A.A Sub
22.0	100.0	_
43.1	195.8	E
57.1	259.2	E
27.2	123.8	V
18.4	83.4	Q
10.5	47.7	R
7.8	35.5	K
6.4	29.0	R
17.6	79.8	Q
10.1	45.8	K
18.7	85.1	L
12.8	58.3	M
12.2	55.6	P
12.1	55.1	N
19.6	89.1	F
19.7	89.5	S
56.6	257.0	D
22.0	99.9	S
20.1	91.3	F

Peptide 121 Intensity	Percent Binding	A.A Sub
6.8	100.0	_
3.3	48.3	R
7.0	102.6	Q
3.7	54.4	K
7.3	107.0	L
5.3	78.4	M
7.4	108.1	P
5.0	73.1	N
4.2	62.0	F
6.0	88.6	S
29.4	431.8	D
19.4	285.0	S
13.6	199.9	F
13.5	197.9	G
10.7	156.6	G
14.2	207.9	G
11.1	162.5	S
11.9	175.3	G
8.5	124.4	A

7.4 Additional p50 Ubiquitination Data

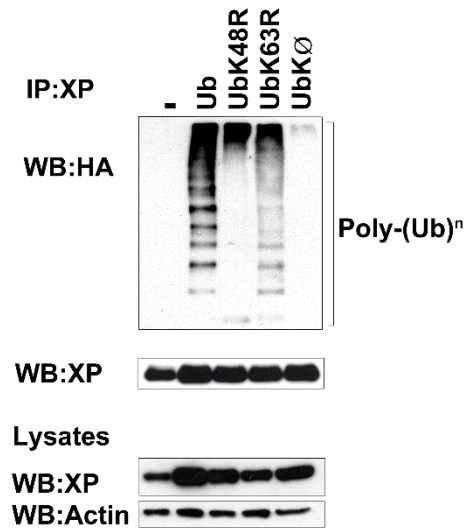


Figure 7.2. p50 is ubiquitinated via K48 linked ubiquitination

Work carried out by Dr. Ruaidhrí.J.Carmody

HEK293T cells were transfected with XPRESS (XP) tagged p50 and ubiquitin wild-type and ubiquitin mutants constructs as indicated. p50 ubiquitination was determined by IP from whole cell lysates with anti-XPRESS and WB with anti-HA for HA-ubiquitin.

7.5 Bcl-3 Peptide Array Sequences

Peptide Number	Amino Acid start #	Amino acid Sequence	Amino Acid end #
1	1	MPRCPAGAMDEGPVDLRT	18
2	5	PAGAMDEGPVDLRTTRPKG	22
3	9	MDEGPVDLRTTRPKGTPGA	26
4	13	PVDLRTTRPKGTPGAALPL	30
5	17	RTRPKGTPGAALPLRKR	34
6	21	KGTPGAALPLRKRPLRPA	38
7	25	GAALPLRKRPLRPASPEP	42
8	29	PLRKRPLRPASPEPATTR	46
9	33	RPLRPASPEPATTRSPAG	50
10	37	PASPEPATTRSPAGPLDA	54
11	41	EPATTRSPAGPLDALRSG	58
12	45	TRSPAGPLDALRSGCDVP	62
13	49	AGPLDALRSGCDVPVVG	66
14	53	DALRSGCDVPVVGPPHC	70
15	57	SGCDVPVVGPPHCVARP	74
16	61	VPVVGPPHCVARPEALY	78
17	65	PGPPHCVARPEALYYQGP	82
18	69	HCVARPEALYYQGPLMPI	86
19	73	RPEALYYQGPLMPIYSTP	90
20	77	LYYQGPLMPIYSTPTMAP	94
21	81	GPLMPIYSTPTMAPHFPL	98
22	85	PIYSTPTMAPHFPLLNLP	102
23	89	TPTMAPHFPLLNLPHPY	106
24	93	APHFPLLNLPHPYSMIC	110
25	97	PLLNLPHPYSMICPMEH	114
26	101	LHPYSMICPMEHPLSA	118
27	105	PYSMICPMEHPLSADIAM	122
28	109	ICPMEHPLSADIAMATRV	126
29	113	EHPLSADIAMATRVDEDG	130
30	117	SADIAMATRVDEDGDTPL	134
31	121	AMATRVDEDGDTPLHIAV	138
32	125	RVDEDGDTPLHIAVVQNN	142
33	129	DGDTPLHIAVVQNNIAAV	146
34	133	PLHIAVVQNNIAAVYRIL	150
35	137	AVVQNNIAAVYRILSLFK	154
36	141	NNIAAVYRILSLFKLGSR	158
37	145	AVYRILSLFKLGSREVDV	162
38	149	IILSLFKLGSREVDVHNNL	166
39	153	FKLGSREVDVHNNLRQTP	170
40	157	SREVDVHNNLRQTPLHLA	174
41	161	DVHNNLRQTPLHLAVITT	178

42	165	NLRQTPHLHAVITTLPDM	182
43	169	TPHLHAVITTLPDMVRL	186
44	173	LAVITTLPDMVRLVLTAG	190
45	177	TLPDMVRLVLTAGASPM	194
46	181	DMVRLVLTAGASPMALDR	198
47	185	LLVLTAGASPMALDRHGQT	202
48	189	AGASPMALDRHGQTAIHL	206
49	193	PMALDRHGQTAIHLACEH	210
50	197	DRHGQTAIHLACEHRSPS	214
51	201	QTAIHLACEHRSPSCLQA	218
52	205	HLACEHRSPSCLQALLDS	222
53	209	EHRSPSCLQALLDSATSG	226
54	213	PSCLQALLDSATSGSVDL	230
55	217	QALLDSATSGSVDLEVRN	234
56	221	DSATSGSVDLEVRNYEGL	238
57	225	SGSVDLEVRNYEGLTALH	242
58	229	DLEVRNYEGLTALHVAVN	246
59	233	RNYEGLTALHVAVNTGCQ	250
60	237	GLTALHVAVNTGCQEAVL	254
61	241	LHVAVNTGCQEAVLLLLLE	258
62	245	VNTGCQEAVLLLLLARGAD	262
63	249	CQEAVLLLLLARGADIDAV	266
64	253	VLLLLLARGADIDAVDIKS	270
65	257	LERGADIDAVDIKSGRSP	274
66	261	ADIDAVDIKSGRSPLIHA	278
67	265	AVDIKSGRSPLIHAVENN	282
68	269	KSGRSPLIHAVENNSLNM	286
69	273	SPLIHAVENNSLNMVQLL	290
70	277	HAVENNSLNMVQLLLLLHG	294
71	281	NNSLNMVQLLLLLHGAVN	298
72	285	NMVQLLLLLHGAVNAQMY	302
73	289	LLLLHGAVNAQMYSGSS	306
74	293	HGANVNAQMYSGSSALHS	310
75	297	VNAQMYSGSSALHSASGR	314
76	301	MYSGSSALHSASGRGLLP	318
77	305	SSALHSASGRGLLPVVRT	322
78	309	HSASGRGLLPVVRTLVRS	326
79	313	GRGLLPVVRTLVRS GADS	330
80	317	LPLVRTLVRS GADSGLKN	334
81	321	RTLVRSGADSGLKNCHND	338
82	325	RSGADSGLKNCHNDTPLM	342
83	329	DSGLKNCHNDTPLMVAR	346
84	333	KNCHNDTPLMVARSRVI	350
85	337	NDTPLMVARSRVIDILR	354
86	341	LMVARSRVIDILRGKAS	358
87	345	RSRRVIDILRGKASRAAS	362
88	349	VIDILRGKASRAASGSQT	366
89	353	LRGKASRAASGSQPEPSP	370

90	357	ASRAASGSQPEPSPDQSA	374
91	361	ASGSQPEPSPDQSATNSP	378
92	365	QPEPSPDQSATNSPESSS	382
93	369	SPDQSATNSPESSSRLSS	386
94	373	SATNSPESSSRLSSNGLQ	390
95	377	SPESSSRLSSNGLQSSPS	394
96	381	SSRLSSNGLQSSPSSPS	398
97	385	SSNGLQSSPSSPSLSPP	402
98	389	LQSSPSSPSLSPPKDAP	406
99	393	PSSSPSLSPPKDAPGFPA	410
100	397	PSLSPPKDAPGFPATPQN	414
101	401	PPKDAPGFPATPQNFFLP	418
102	405	APGFPATPQNFFLPTTST	422
103	409	PATPQNFFLPTTSTPAFL	426
104	413	QNFFLPTTSTPAFLPFG	430
105	417	LPTTSTPAFLPFGVLRG	434
106	421	STPAFLPFGVLRGPGRP	438
107	425	FLPFGVLRGPGRVPPS	442
108	429	PGVLRGPGRVPPSPAPG	446
109	431	VLRGPGRVPPSPAPGSS	448

7.6 Bcl-3 Alanine Substitution Peptide Array Sequences

Original Peptide	Peptide Number	Amino acid Sequence
2	A1	PAGAMDEGPVDLRTRPKG
	A2	AAGAMDEGPVDLRTRPKG
	A3	PDGAMDEGPVDLRTRPKG
	A4	PAAAMDEGPVDLRTRPKG
	A5	PAGDMDEGPVDLRTRPKG
	A6	PAGAADEGPVDLRTRPKG
	A7	PAGAMAEGPVDLRTRPKG
	A8	PAGAMDAGPVDLRTRPKG
	A9	PAGAMDEAPVDLRTRPKG
	A10	PAGAMDEGAVDLRTRPKG
	A11	PAGAMDEGPADLRTRPKG
	A12	PAGAMDEGPVALRTRPKG
	A13	PAGAMDEGPVDARTRPKG
	A14	PAGAMDEGPVDLATRPKG
	A15	PAGAMDEGPVDLRARPKG
	A16	PAGAMDEGPVDLRTAPKG
	A17	PAGAMDEGPVDLRTRAKG
	A18	PAGAMDEGPVDLRTRPAG
	A19	PAGAMDEGPVDLRTRPKA

Original Peptide	Peptide Number	Amino acid Sequence
5	A21	RTRPKGTPGAALPLRKR
	A22	ATRPKGTPGAALPLRKR
	A23	RARPKGTPGAALPLRKR
	A24	RTAPKGTPGAALPLRKR
	A25	RTRAKGTPGAALPLRKR
	A26	RTRPAGTPGAALPLRKR
	A27	RTRPKATPGAALPLRKR
	A28	RTRPKGAPGAALPLRKR
	A29	RTRPKGTAGAALPLRKR
	A30	RTRPKGTPAAALPLRKR
	B1	RTRPKGTPGDALPLRKR
	B2	RTRPKGTPGADLPLRKR
	B3	RTRPKGTPGAAAPLRKR
	B4	RTRPKGTPGAALALRKR
	B5	RTRPKGTPGAALPARKR
	B6	RTRPKGTPGAALPLAKR
	B7	RTRPKGTPGAALPLRARP
	B8	RTRPKGTPGAALPLRKAP
	B9	RTRPKGTPGAALPLRKRA

Original Peptide	Peptide Number	Amino acid Sequence
6	B11	KGTPGAALPLRKRPLRPA
	B12	AGTPGAALPLRKRPLRPA
	B13	KATPGAALPLRKRPLRPA
	B14	KGAPGAALPLRKRPLRPA
	B15	KGTAGAALPLRKRPLRPA
	B16	KGTPAAALPLRKRPLRPA
	B17	KGTPGDALPLRKRPLRPA
	B18	KGTPGADLPLRKRPLRPA
	B19	KGTPGAAAPLRKRPLRPA
	B20	KGTPGAALALRKRPLRPA
	B21	KGTPGAALPARKRPLRPA
	B22	KGTPGAALPLAKRPLRPA
	B23	KGTPGAALPLRARPLRPA
	B24	KGTPGAALPLRKAPLRPA
	B25	KGTPGAALPLRKRALRPA
	B26	KGTPGAALPLRKRPARPA
	B27	KGTPGAALPLRKRPLAPA
	B28	KGTPGAALPLRKRPLRAA
	B29	KGTPGAALPLRKRPLRPD

Original Peptide	Peptide Number	Amino acid Sequence
8	C1	PLRKRPLRPASPEPATTR
	C2	ALRKRPLRPASPEPATTR
	C3	PARKRPLRPASPEPATTR
	C4	PLAKRPLRPASPEPATTR
	C5	PLRARPLRPASPEPATTR
	C6	PLRKAPLRPASPEPATTR
	C7	PLRKRALRPASPEPATTR
	C8	PLRKRPARPASPEPATTR
	C9	PLRKRPLAPASPEPATTR
	C10	PLRKRPLRAASPEPATTR
	C11	PLRKRPLRPDSPEPATTR
	C12	PLRKRPLRPAAPEPATTR
	C13	PLRKRPLRPASAEPATTR
	C14	PLRKRPLRPASPAPATTR
	C15	PLRKRPLRPASPEAATTR
	C16	PLRKRPLRPASPEPDTR
	C17	PLRKRPLRPASPEPAATR
	C18	PLRKRPLRPASPEPATAR
	C19	PLRKRPLRPASPEPATTA

Original Peptide	Peptide Number	Amino acid Sequence
35	C21	AVVQNNIAAVYRILSLFK
	C22	DVVQNNIAAVYRILSLFK
	C23	AAVQNNIAAVYRILSLFK
	C24	AVAQNNIAAVYRILSLFK
	C25	AVVANNIAAVYRILSLFK
	C26	AVVQANIAAVYRILSLFK
	C27	AVVQNAIAAVYRILSLFK
	C28	AVVQNNAAAVYRILSLFK
	C29	AVVQNNIDAVYRILSLFK
	C30	AVVQNNIADVYRILSLFK
	D1	AVVQNNIAAAVYRILSLFK
	D2	AVVQNNIAAVDRILSLFK
	D3	AVVQNNIAAVYAILSLFK
	D4	AVVQNNIAAVYRALSLFK
	D5	AVVQNNIAAVYRIASLFK
	D6	AVVQNNIAAVYRILALFK
	D7	AVVQNNIAAVYRILSAFK
	D8	AVVQNNIAAVYRILSLAK
	D9	AVVQNNIAAVYRILSLFA

Original Peptide	Peptide Number	Amino acid Sequence
36	D11	NNIAAVYRILSLFKLGSR
	D12	ANIAAVYRILSLFKLGSR
	D13	NAIAAVYRILSLFKLGSR
	D14	NNAAAVYRILSLFKLGSR
	D15	NNIDAVYRILSLFKLGSR
	D16	NNIAAVYRILSLFKLGSR
	D17	NNIAAAVYRILSLFKLGSR
	D18	NNIAAVARILSLFKLGSR
	D19	NNIAAVYAILSLFKLGSR
	D20	NNIAAVYRALSLFKLGSR
	D21	NNIAAVYRIASLFKLGSR
	D22	NNIAAVYRILALFKLGSR
	D23	NNIAAVYRILSAFKLGSR
	D24	NNIAAVYRILSLAKLGSR
	D25	NNIAAVYRILSLFALGSR
	D26	NNIAAVYRILSLFKAGSR
	D27	NNIAAVYRILSLFKLASR
	D28	NNIAAVYRILSLFKLGAR
	D29	NNIAAVYRILSLFKLGSA

Original Peptide	Peptide Number	Amino acid Sequence
46	E1	DMVRLLVTAGASPMALDR
	E2	AMVRLLVTAGASPMALDR
	E3	DAVRLLVTAGASPMALDR
	E4	DMARLLVTAGASPMALDR
	E5	DMVALLVTAGASPMALDR
	E6	DMVRALVTAGASPMALDR
	E7	DMVRLAVTAGASPMALDR
	E8	DMVRLLATAGASPMALDR
	E9	DMVRLLVAAAGASPMALDR
	E10	DMVRLLVTDGASPMALDR
	E11	DMVRLLVTAASPALDR
	E12	DMVRLLVTAGDSPALDR
	E13	DMVRLLVTAGAAPALDR
	E14	DMVRLLVTAGASAMALDR
	E15	DMVRLLVTAGASPADLDR
	E16	DMVRLLVTAGASPMALDR
	E17	DMVRLLVTAGASPMAADR
	E18	DMVRLLVTAGASPMALAR
	E19	DMVRLLVTAGASPMALDA

Original Peptide	Peptide Number	Amino acid Sequence
75	E21	VNAQMYSGSSALHSASGR
	E22	ANAQMYSGSSALHSASGR
	E23	VAAQMYSGSSALHSASGR
	E24	VNDQMYSGSSALHSASGR
	E25	VNAAMYSGSSALHSASGR
	E26	VNAQAYSGSSALHSASGR
	E27	VNAQMASGSSALHSASGR
	E28	VNAQMYAGSSALHSASGR
	E29	VNAQMYSAASSALHSASGR
	E30	VNAQMYSGASALHSASGR
	F1	VNAQMYSGSAALHSASGR
	F2	VNAQMYSGSSDLHSASGR
	F3	VNAQMYSGSSAAHSASGR
	F4	VNAQMYSGSSALASASGR
	F5	VNAQMYSGSSALHAASGR
	F6	VNAQMYSGSSALHSDSGR
	F7	VNAQMYSGSSALHSAAGR
	F8	VNAQMYSGSSALHSASAR
	F9	VNAQMYSGSSALHSASGA

Original Peptide	Peptide Number	Amino acid Sequence
78	F11	HSASGRGLLPLVRTLVR
	F12	ASASGRGLLPLVRTLVR
	F13	HAASGRGLLPLVRTLVR
	F14	HSDSGRGLLPLVRTLVR
	F15	HSAAGRGLLPLVRTLVR
	F16	HSASARGLLPLVRTLVR
	F17	HSASGAGLLPLVRTLVR
	F18	HSASGRALLPLVRTLVR
	F19	HSASGRGALPLVRTLVR
	F20	HSASGRGLAPLVRTLVR
	F21	HSASGRGLLALVRTLVR
	F22	HSASGRGLLPAVRTLVR
	F23	HSASGRGLLPLARTLVR
	F24	HSASGRGLLPLVATLVR
	F25	HSASGRGLLPLVRALVR
	F26	HSASGRGLLPLVRTAVR
	F27	HSASGRGLLPLVRTLAR
	F28	HSASGRGLLPLVRTLVA
	F29	HSASGRGLLPLVRTLVAA

Original Peptide	Peptide Number	Amino acid Sequence
80	G1	LPLVRTLVRSGADSGLKN
	G2	APLVRTLVRSGADSGLKN
	G3	LALVRTLVRSGADSGLKN
	G4	LPAVRTLVRSGADSGLKN
	G5	LPLARTLVRSGADSGLKN
	G6	LPLVATLVRSGADSGLKN
	G7	LPLVRALVRSGADSGLKN
	G8	LPLVRTAVRSGADSGLKN
	G9	LPLVRTLARSGADSGLKN
	G10	LPLVRTLVASGADSGLKN
	G11	LPLVRTLVRAGADSGLKN
	G12	LPLVRTLVRSAADSGLKN
	G13	LPLVRTLVRSGDDSGLKN
	G14	LPLVRTLVRSGAASGLKN
	G15	LPLVRTLVRSGADAGLKN
	G16	LPLVRTLVRSGADSALKN
	G17	LPLVRTLVRSGADSGAKN
	G18	LPLVRTLVRSGADSGLAN
	G19	LPLVRTLVRSGADSGLKA

Original Peptide	Peptide Number	Amino acid Sequence
85	G21	NDTPLMVARSRVIDILR
	G22	ADTPLMVARSRVIDILR
	G23	NATPLMVARSRVIDILR
	G24	NDAPLMVARSRVIDILR
	G25	NDTALMVARSRVIDILR
	G26	NDTPAMVARSRVIDILR
	G27	NDTPLAVARSRVIDILR
	G28	NDTPLMAARSRRVIDILR
	G29	NDTPLMVDRSRRVIDILR
	G30	NDTPLMVAASRRVIDILR
	H1	NDTPLMVARARRVIDILR
	H2	NDTPLMVARARVIDILR
	H3	NDTPLMVARRAVIDILR
	H4	NDTPLMVARSRRAIDILR
	H5	NDTPLMVARSRVADILR
	H6	NDTPLMVARSRVIAILR
	H7	NDTPLMVARSRVIDALR
	H8	NDTPLMVARSRVIDIAR
	H9	NDTPLMVARSRVIDILA

Original Peptide	Peptide Number	Amino acid Sequence
87	H11	RSRRVIDILRGKASRAAS
	H12	ASRRVIDILRGKASRAAS
	H13	RARRVIDILRGKASRAAS
	H14	RSARVIDILRGKASRAAS
	H15	RSRAVIDILRGKASRAAS
	H16	RSRRAIDILRGKASRAAS
	H17	RSRRVADILRGKASRAAS
	H18	RSRRVIAILRGKASRAAS
	H19	RSRRVIDALRGKASRAAS
	H20	RSRRVIDIARGKASRAAS
	H21	RSRRVIDILAGKASRAAS
	H22	RSRRVIDILRAKASRAAS
	H23	RSRRVIDILRGAASRAAS
	H24	RSRRVIDILRGKDSRAAS
	H25	RSRRVIDILRGKAARAAS
	H26	RSRRVIDILRGKASAAAS
	H27	RSRRVIDILRGKASRDAS
	H28	RSRRVIDILRGKASRADS
	H29	RSRRVIDILRGKASRAAA

Original Peptide	Peptide Number	Amino acid Sequence
	I1	LRGKASRAASGSQPEPSP
89	I2	ARGKASRAASGSQPEPSP
	I3	LAGKASRAASGSQPEPSP
	I4	LRAKASRAASGSQPEPSP
	I5	LRGAASRAASGSQPEPSP
	I6	LRGKDSRAASGSQPEPSP
	I7	LRGKAARAASGSQPEPSP
	I8	LRGKASAAASGSQPEPSP
	I9	LRGKASRDASGSQPEPSP
	I10	LRGKASRADSGSQPEPSP
	I11	LRGKASRAAAGSQPEPSP
	I12	LRGKASRAASASQPEPSP
	I13	LRGKASRAASGAQPEPSP
	I14	LRGKASRAASGSAPEPSP
	I15	LRGKASRAASGSQAEPSP
	I16	LRGKASRAASGSQPAPSP
	I17	LRGKASRAASGSQPEASP
	I18	LRGKASRAASGSQPEPAP
	I19	LRGKASRAASGSQPEPSA

Original Peptide	Peptide Number	Amino acid Sequence
109	I21	VLRGPGRPVPPSPAPGSS
	I22	ALRGPGRPVPPSPAPGSS
	I23	VARGPGRPVPPSPAPGSS
	I24	VLAGPGRPVPPSPAPGSS
	I25	VLRAPGRPVPPSPAPGSS
	I26	VLRGAGRPVPPSPAPGSS
	I27	VLRGPARPVPPSPAPGSS
	I28	VLRGPGAPVPPSPAPGSS
	I29	VLRGPGRAVPPSPAPGSS
	I30	VLRGPGRPAPPSPAPGSS
	J1	VLRGPGRPVAPSPAPGSS
	J2	VLRGPGRPVPASPAPGSS
	J3	VLRGPGRPVPPAPAPGSS
	J4	VLRGPGRPVPPSAAPGSS
	J5	VLRGPGRPVPPSPDPGSS
	J6	VLRGPGRPVPPSPAAGSS
	J7	VLRGPGRPVPPSPAPASS
	J8	VLRGPGRPVPPSPAPGAS
	J9	VLRGPGRPVPPSPAPGSA

7.7 Bcl-3 Alanine Substitution Peptide Array Data

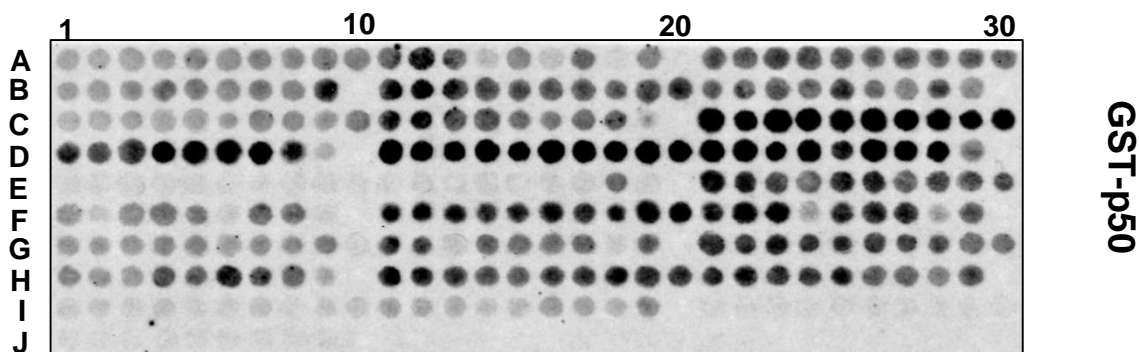


Figure 7.3 Full Bcl-3 alanine substitution peptide array.

The 18 amino acids of the Bcl-3 derived peptides 2, 5, 6, 8, 35, 36, 46, 75, 78, 80, 85, 87, 89 and 109 were sequentially substituted with alanine. See Appendix 7.6 for peptide locations on array. Arrays were probed with GST-p50 and detected by immunoblotting with anti-GST antibody. GST-p50 binding was quantified by densitometry and represented as a percentage binding of the control parent peptide peptides (see below).

Peptide 2 Intensity	Percent Binding	A.A Sub
0.268	100	—
0.228	85.07463	P
0.328	122.3881	A
0.308	114.9254	G
0.438	163.4328	A
0.428	159.7015	M
0.438	163.4328	D
0.408	152.2388	E
0.528	197.0149	G
0.498	185.8209	P
0.638	238.0597	V
1.038	387.3134	D
0.618	230.597	L
0.158	58.95522	R
0.448	167.1642	T
0.148	55.22388	R
0.578	215.6716	P
0.058	21.64179	K
0.458	170.8955	G

Peptide 5 Intensity	Percent Binding	A.A Sub
0.648	100	—
0.638	98.45679	R
0.768	118.5185	T
0.738	113.8889	R
0.628	96.91358	P
0.548	84.5679	K
0.648	100	G
0.488	75.30864	T
0.608	93.82716	P
0.548	84.5679	G
0.258	39.81481	A
0.298	45.98765	A
0.358	55.24691	L
0.558	86.11111	P
0.488	75.30864	L
0.438	67.59259	R
0.498	76.85185	K
0.438	67.59259	R
1.348	208.0247	P

Peptide 6 Intensity	Percent Binding	A.A Sub
0.948	100	_
1.028	108.4388	K
0.918	96.83544	G
0.778	82.06751	T
0.648	68.35443	P
0.678	71.51899	G
0.668	70.46414	A
0.538	56.75105	A
0.828	87.34177	L
0.878	92.61603	P
0.488	51.47679	L
0.548	57.80591	R
0.678	71.51899	K
0.538	56.75105	R
0.778	82.06751	P
0.458	48.31224	L
0.448	47.25738	R
0.598	63.08017	P
0.408	43.03797	A

Peptide 8 Intensity	Percent Binding	A.A Sub
0.188	100	_
0.218	115.9574	P
0.258	137.234	L
0.288	153.1915	R
0.318	169.1489	K
0.238	126.5957	R
0.498	264.8936	P
0.388	206.383	L
0.328	174.4681	R
0.528	280.8511	P
0.798	424.4681	A
0.888	472.3404	S
0.748	397.8723	P
0.788	419.1489	E
0.488	259.5745	P
0.398	211.7021	A
0.568	302.1277	T
0.618	328.7234	T
0.198	105.3191	D

Peptide 35 Intensity	Percent Binding	A.A Sub
1.858	100	_
1.308	70.39828	A
1.908	102.6911	V
1.498	80.62433	V
1.428	76.85684	Q
1.828	98.38536	N
1.598	86.00646	N
1.418	76.31862	I
1.038	55.86652	A
1.118	60.17223	A
0.778	41.87298	V
0.668	35.95264	Y
0.988	53.17546	R
1.468	79.00969	I
1.508	81.16254	L
1.418	76.31862	S
1.458	78.47147	L
0.908	48.86975	F
0.168	9.041981	K

Peptide 36 Intensity	Percent Binding	A.A Sub
1.818	100	_
1.428	78.54785	N
1.308	71.94719	N
1.588	87.34873	I
1.168	64.24642	A
1.708	93.94939	A
1.758	96.69967	V
1.588	87.34873	Y
1.788	98.34983	R
1.898	104.4004	I
1.738	95.59956	L
1.478	81.29813	S
1.218	66.9967	L
1.378	75.79758	F
0.798	43.89439	K
1.578	86.79868	L
1.378	75.79758	G
1.188	65.34653	S
0.518	28.49285	R

Peptide 46 Intensity	Percent Binding	A.A Sub
0.048	100	_
0.038	79.16667	D
0.068	141.6667	M
0.068	141.6667	V
0.068	141.6667	R
0.038	79.16667	L
0.038	79.16667	L
0.078	162.5	V
0.068	141.6667	T
0.048	100	A
0.048	100	G
0.098	204.1667	A
0.068	141.6667	S
0.108	225	P
0.068	141.6667	M
0.098	204.1667	A
0.108	225	L
0.518	1079.167	D
0.098	204.1667	R

Peptide 75 Intensity	Percent Binding	A.A Sub
1.098	100	_
0.888	80.87432	V
0.738	67.21311	N
0.638	58.10565	A
0.898	81.78506	Q
0.888	80.87432	M
0.628	57.1949	Y
0.708	64.48087	S
0.648	59.01639	G
0.528	48.08743	S
0.378	34.42623	S
0.078	7.103825	A
0.438	39.89071	L
0.608	55.37341	H
0.438	39.89071	S
0.078	7.103825	A
0.598	54.46266	S
0.568	51.73042	G
0.068	6.193078	R

Peptide 78 Intensity	Percent Binding	A.A Sub
0.778	100	_
0.838	107.7121	H
0.818	105.1414	S
0.698	89.71722	A
0.728	93.57326	S
0.958	123.1362	G
0.768	98.71465	R
0.678	87.14653	G
1.188	152.6992	L
1.118	143.7018	L
0.798	102.5707	P
1.178	151.4139	L
1.148	147.5578	V
0.258	33.16195	R
0.818	105.1414	T
0.918	117.9949	L
0.868	111.5681	V
0.218	28.02057	R
0.648	83.29049	S

Peptide 80 Intensity	Percent Binding	A.A Sub
0.298	100	_
0.238	79.86577	L
0.308	103.3557	P
0.378	126.8456	L
0.408	136.9128	V
0.318	106.7114	R
0.348	116.7785	T
0.318	106.7114	L
0.428	143.6242	V
0.068	22.81879	R
0.668	224.1611	S
0.528	177.1812	G
0.138	46.30872	A
0.558	187.2483	D
0.538	180.5369	S
0.548	183.8926	G
0.558	187.2483	L
0.088	29.5302	K
0.558	187.2483	N

Peptide 85 Intensity	Percent Binding	A.A Sub
0.928	100	_
0.688	74.13793	N
0.858	92.4569	D
0.638	68.75	T
0.618	66.59483	P
0.718	77.37069	L
0.568	61.2069	M
0.568	61.2069	V
0.578	62.28448	A
0.508	54.74138	R
0.398	42.88793	S
0.298	32.11207	R
0.298	32.11207	R
0.648	69.82759	V
0.538	57.97414	I
0.958	103.2328	D
0.628	67.67241	I
0.628	67.67241	L
0.198	21.33621	R

Peptide 87 Intensity	Percent Binding	A.A Sub
0.928	100	_
0.778	83.83621	R
0.728	78.44828	S
0.618	66.59483	R
0.538	57.97414	R
0.708	76.2931	V
0.708	76.2931	I
0.888	95.68966	D
0.848	91.37931	I
0.768	82.75862	L
0.668	71.98276	R
0.878	94.61207	G
0.758	81.68103	K
0.678	73.06034	A
0.748	80.60345	S
0.608	65.51724	R
0.588	63.36207	A
0.408	43.96552	A
0.698	75.21552	S

Peptide 89 Intensity	Percent Binding	A.A Sub
0.078	100	_
0.098	125.641	L
0.078	100	R
0.138	176.9231	G
0.088	112.8205	K
0.078	100	A
0.128	164.1026	S
0.058	74.35897	R
0.098	125.641	A
0.118	151.2821	A
0.248	317.9487	S
0.218	279.4872	G
0.208	266.6667	S
0.118	151.2821	Q
0.148	189.7436	P
0.318	407.6923	E
0.248	317.9487	P
0.168	215.3846	S
0.388	497.4359	P

Peptide109 Intensity	Percent Binding	A.A Sub
0.048	100	_
0.048	100	V
0.058	120.8333	L
0.048	100	R
0.068	141.6667	G
0.078	162.5	P
0.058	120.8333	G
0.048	100	R
0.038	79.16667	P
0.028	58.33333	V
0.028	58.33333	P
0.028	58.33333	P
0.028	58.33333	S
0.068	141.6667	P
0.058	120.8333	A
0.048	100	P
0.048	100	G
0.058	120.8333	S
0.058	120.8333	S

7.8 Murine IκB Protein Alignment

		1	50
Bcl-3	(127)	DEDGDTPLHFAVQNNIAAYRILSLFK--LGSREVDVHNNLRQTPLHLA	
IκBα	(92)	TEDGDSFLHLAIIHEEKPITMEVIQQVK--GDLAFINLQNNLQQTPLHLA	
IκBβ	(55)	TEDGDTALHLAVIHQHEPFLDFLLGFSA---GTEYLDLQNDLQQTALHLA	
IκBε	(120)	SEDGDTLHLAVIHEAPSVLFCCLAFLP---QEVLDIQNNLYQTALHLA	
IKBNS	(60)	DEEGDTLHLIFAARGLRWAAIAAAEVLQ---MYRQLDIREHKGKTPLLVAA	
IκBζ	(451)	DGDGDTFLHFAVQGRRAISVVLARKMN---ALHMLDIKEHNGQSFAQVA	
p100	(485)	DENGDTPHLAIIHQGTGVIEQLAHVIYHAQYLGVINLTNHLHQTPHLA	
p105	(536)	DENGDVSLHLAIIHLHAQLVRLDLEVTSGLISDDLINMRNDLYQTPLHLA	
		51	100
Bcl-3	(175)	VITTLFDMVRLIVTAGASFMALDRHGQTALHLACEHR--SPSCLQALLDS	
IκBα	(140)	VITNPGIAEALLKAGCDPELRFRCNTPLHLACEQG--CLASVAVITQT	
IκBβ	(102)	AILGEASTVEKLYAAGAGVLAERGGHTALHLACRVR--AHTCACVLLQP	
IκBε	(166)	VHLDQPDVVRALVILKASRIIQDQHGDALHLVACRQ--NLACACCLLEE	
IKBNS	(107)	AAANQPLIVEDLISLGAEPNATDHQGRSVLHVAAATYG--LPGVLSAVFKS	
IκBζ	(498)	VAANOHLIVQDLVNLGAQVNTTDCWGRTPLEHCAEKG--HSQVQLAIQKG	
p100	(535)	VITGQTRVVSFLLIQVADPTLLDRHGDSALHLALFAGAAPELQALLRS	
p105	(586)	VITKQEDVVEDLIRVGDLSLLDRWGNVSLHLAAKEG--HDRLLISILLKS	
		101	150
Bcl-3	(223)	AT-----SLS-----VD	
IκBα	(188)	CT-----PQHLH-----SV	
IκBβ	(150)	RPSHPRDASDTYLTQSQDCTPDTSHAPAAVDSQPNPENEEEEPRDEDWRLQ	
IκBε	(214)	QP-----EGRQLSHP-----LD	
IKBNS	(155)	GI-----Q-----VD	
IκBζ	(546)	AV-----RSNQF-----VD	
p100	(585)	GA-----HAVP-----QI	
p105	(634)	RK-----AA-----PL	
		151	200
Bcl-3	(230)	LEVRNYEGLTALHVAVNTGC-----QEAA	
IκBα	(197)	LQATNYNGHTCLHLASTHGY-----LAI	
IκBβ	(200)	LEAENYDGHFTPLHVAVIHKD-----AEM	
IκBε	(227)	LQLKNWQGLACLHATLQRN-----QPL	
IKBNS	(160)	LEARDFEGLTPLHTAVLALNAAM-----LPASVCPRMQNSQARDRLITC	
IκBζ	(555)	LEATNYDGLTPLHCAVVAHNAVVELQRNRQSHSPEVQDLLLRNKSLVDT	
p100	(593)	LHMPDFEGTYPVHIAVHARS-----PEC	
p105	(640)	LHNPNGEGLNATHIAVMSNS-----LPC	
		201	250
Bcl-3	(253)	VLLILLERGADIDAVDIKSGRSPLIHAVENNSLNMVQ-LLLHLG-----AN	
IκBα	(220)	VEHLVTLGADVNAQEPNCNGRTALHLAVDLQNPDLVS-LLLKCG-----AD	
IκBβ	(223)	VRLLRDAGADLNKPEPTCGRTPLHLAVEAQAASVLE-LLLKAG-----AD	
IκBε	(250)	LELLQNAGADILVQEGTSGKTAHLAVETQERSLVQ-FLLQAG-----AR	
IKBNS	(203)	VQMLLQMGASHTSQEIKSNKTIHLAVQAANPTLVQ-LLGLPRGDLRAF	
IκBζ	(605)	LKCLIQMGAAVEAKDRKSGRTALHLAAEEANLELIR-LFLELP--SCLSF	
p100	(616)	LDLLVDCGAEVEAPERQGGRTALHLATEMEEGLVTHLVTKLH-----AN	
p105	(663)	LLLVAAAGAEVNAQEQKSGRTALHLAVEYDNLISLAGCLLLEGD-----AH	

		251		300															
Bcl-3	(297)	VNAQ	MYSGS	SALH	ASGRG	----	LLP	LVRT	VRS	GADSG	--	LK	CHND	--					
IκBα	(264)	VNRVT	YQGY	SFYQ	TWGRP	----	STR	IQQL	GQLT	LENL	QMT	PES	FDE	--					
IκBβ	(267)	PTA	RMYG	CR	TPL	GS	ALL	RP	----	NPI	LAR	LRA	HGA	PEP	--	EDED	KL	--	
IκBε	(294)	VDA	RMLN	GC	TP	LH	LA	AGRG	----	LNS	ISST	CE	AG	ADSL	--	LI	NV	FDE	--
IKBNS	(252)	VNMKA	H	GN	TAL	HMA	AAAL	PPGPP	QEA	IVR	H	LA	AG	ADPT	--	LR	NLE	NE	--
IκBζ	(652)	VNAKA	YNG	NT	AL	HVA	ASL	QYRVT	QLDAV	RLL	MRK	GAD	PS	--	TR	NLE	NE	--	
p100	(661)	VNART	FAG	NT	PL	H	LA	AGLG	---	SPTL	TRL	LI	KAG	ADIHA	--	ENE	EPL	CPL	
p105	(708)	VDS	TTY	DGT	TP	LH	LA	AGRG	---	STR	LAAL	L	KAG	ADPLV	--	ENE	FPLY	DLD	

		301		328												
Bcl-3	(339)	-----	T	PLM	VARS	RRVI	D	I	L							
IκBα	(308)	-----	E	SYD	TES	F	T	E	E	--						
IκBβ	(309)	-----	S	PCSS	SGS	DSDS	---									
IκBε	(336)	-----	T	PQD	LAE	L	L	S	Y	L	P	F				
IKBNS	(297)	-----	Q	PVH	L	L	R	P	G	P	G	E	G	L		
IκBζ	(698)	-----	Q	PVH	L	V	P	G	P	V	G	E	Q	L		
p100	(706)	PSPST	SGSDS	DSE	-----											
p105	(753)	DDSWE	KAGE	DEGVV	P	G	T	P	L	M	A	A	N	W	Q	V

Colour coding:

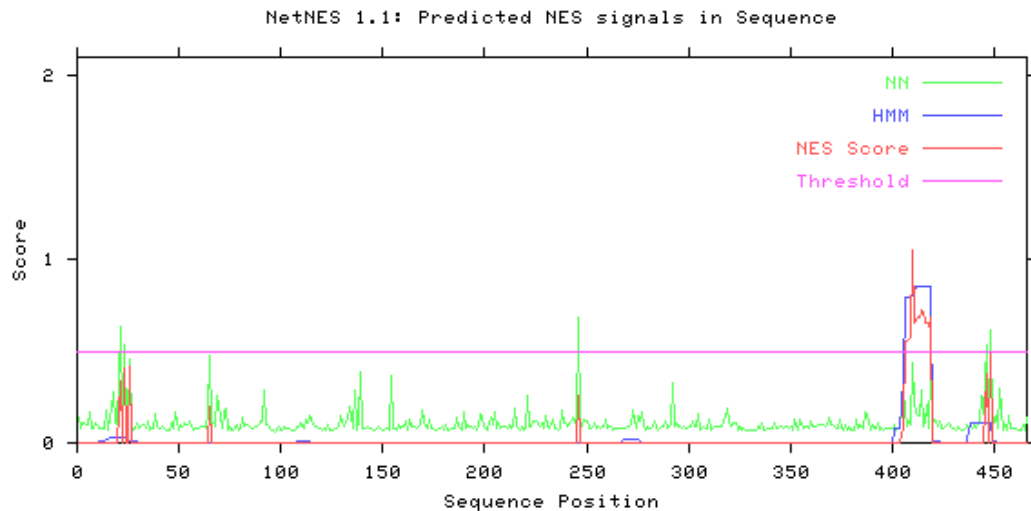
- non similar amino acids black on white background
- identical amino acids red on yellow background
- conservative amino acids black on green background
- block of similar amino acids black on blue background
- weakly similar amino acids green on white background

Only identical and similar amino acids used in consensus calculation.

7.9 NetNES Prediction Results

Analyzed using NetNES 1.1 (la Cour et al., 2004)

Tpl2(human): NCBI Reference Sequence: NP_001231063.



Nes Prediction

#Seq-Pos-Residue	ANN	HMM	NES	Predicted
Sequence-406-L	0.180	0.790	0.552	Yes
Sequence-407-E	0.092	0.790	0.550	Yes
Sequence-408-R	0.121	0.790	0.560	Yes
Sequence-409-K	0.098	0.804	0.577	Yes
Sequence-410-R	0.431	0.804	1.047	Yes
Sequence-411-L	0.224	0.825	0.654	Yes
Sequence-412-L	0.160	0.850	0.675	Yes
Sequence-413-S	0.144	0.850	0.686	Yes
Sequence-414-R	0.286	0.850	0.719	Yes
Sequence-415-K	0.092	0.850	0.717	Yes
Sequence-416-E	0.120	0.850	0.655	Yes
Sequence-417-L	0.211	0.852	0.654	Yes
Sequence-418-E	0.079	0.851	0.638	Yes
Sequence-419-L	0.398	0.851	0.688	Yes

Artificial Neural Network (ANN)

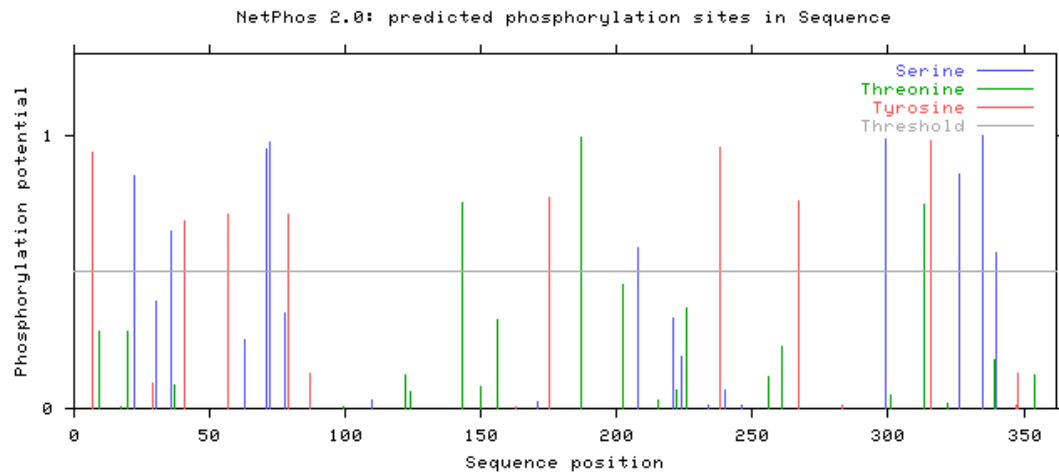
Hidden Markov models (HMM)

Nuclear Export Sequence (NES)

7.10 NetPhos Prediction Results

Analyzed using NetPhos 2.0 (Blom et al., 1999)

p50 (mouse): NCBI Reference Sequence AAH50841.1



Tyrosine predictions

Name	Pos	Context	Score	Pred
v				
Sequence	7	DDDPYGTGQ	0.941	*Y*
Sequence	29	NAELYSPEI	0.089	.
Sequence	41	TDGPYLQIL	0.687	*Y*
Sequence	57	FRFRYVCEG	0.711	*Y*
Sequence	79	NKKSYPQVK	0.709	*Y*
Sequence	87	KICNYVGPA	0.126	.
Sequence	163	CIRGYNPGL	0.009	.
Sequence	175	SDLAYLQAE	0.774	*Y*
Sequence	238	SDAIYDSKA	0.959	*Y*
Sequence	267	GEEIYLLCD	0.761	*Y*
Sequence	283	QIRFYEEEE	0.013	.
Sequence	316	KTPKYKDVN	0.984	*Y*
Sequence	347	KPFLYYPEI	0.010	.
Sequence	348	PFLYYPEIK	0.131	.

7.11 Bcl-3 Derived Peptide *in vivo* trial

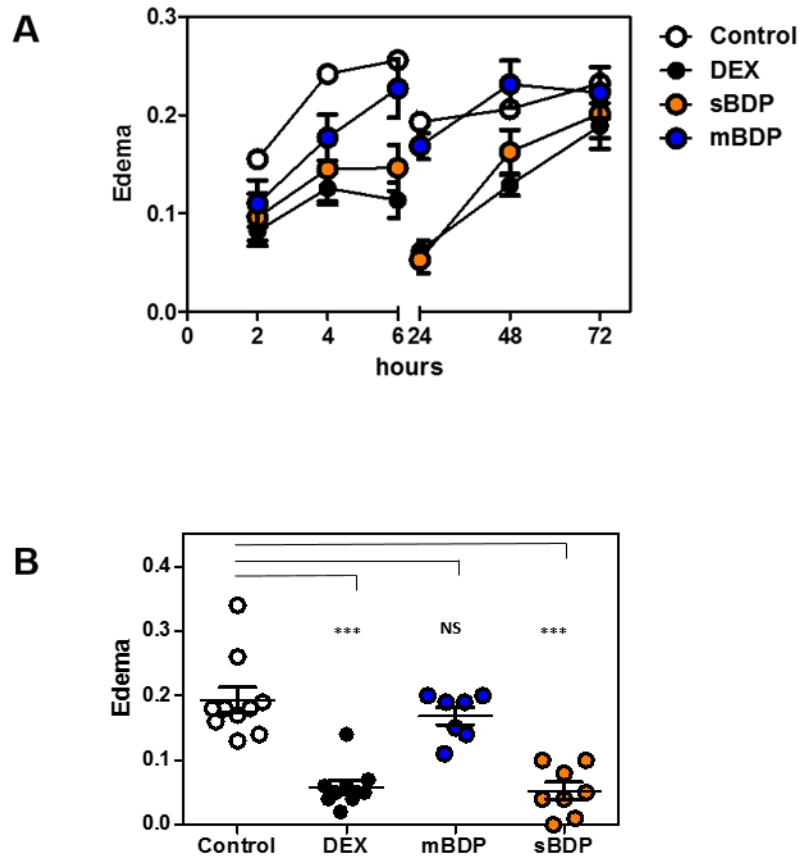


Figure 7. 4 Bcl-3 derived peptide inhibits carrageenan-induced inflammation

Work carried out in coleraboation with Dr. Gianluca Grassia and Prof. Armando Lalenti (University of Naples Federico II, Napoli, Italy).

(A) Paw edema was induced by subplantar injection of 50 μ l of sterile saline containing 2% λ -carrageenin (Sigma Aldrich, Italy) into the right hind paw. Paw volumes were measured by a plethysmometer (Ugo Basile, Milan, Italy) at varying time intervals. Edema was evaluated as difference between the paw volume measured at each time point and the basal paw volume measured immediately before carrageenin injection. 1hr before edema induction, mice were pretreated with PBS (Control), 1 mg/kg Dexamethasone (DEX), 10mg/kg sBDP or 10mg/kg mBDP. (B) 24 hour post edema induction time point from A. Statistical significance was determined by one way anova and Tukey's multiple comparison test; P<0.05 (*), P<0.01 (**), P<0.001(***)

7.12 Supplementary Figures

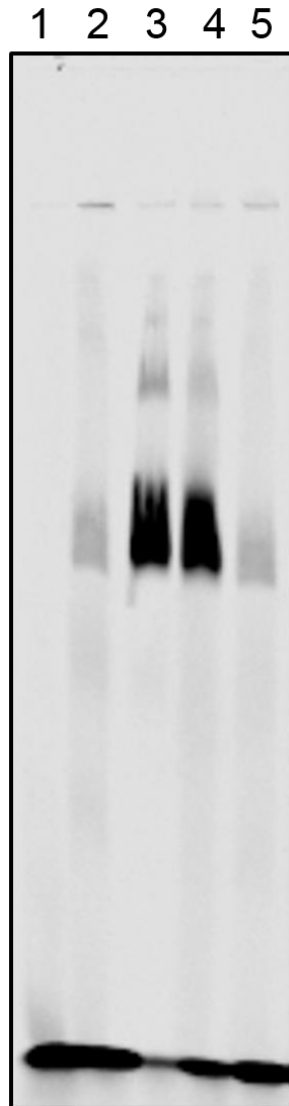


Figure 7.5 EMSA.

HEK293T cells were transfected with empty vector (lane2), pRK5-p50-FLAG (lane3) or pRK5-p50-FLAG in which Lys249, Arg252 and Met253 of p50 are mutated to alanine (p50KRM)) (lane4). 5ug of Nuclear extracts were prepared from the transfected cells and tested in an Electrophoretic Mobility Shift Assay (EMSA) using the consensus NF- κ B binding nucleotide. As a negative control, in addition to the KRM mutation, residues critical for DNA binding, Y57 and D60 were mutated to alanine and aspartic acid respectively (p50 KRM,DBM) to produce a DNA binding deficient mutant (lane5). Binding reactions were resolved on a 5% non-denaturing polyacrylamide gel at 300V at 4°C. The gel was visualised using LI-COR Odyssey, scanned on the 800nm channel. The EMSA reaction mixture minus nuclear extract was loaded in lane 1 and free probe is apparent at the bottom of the gel.

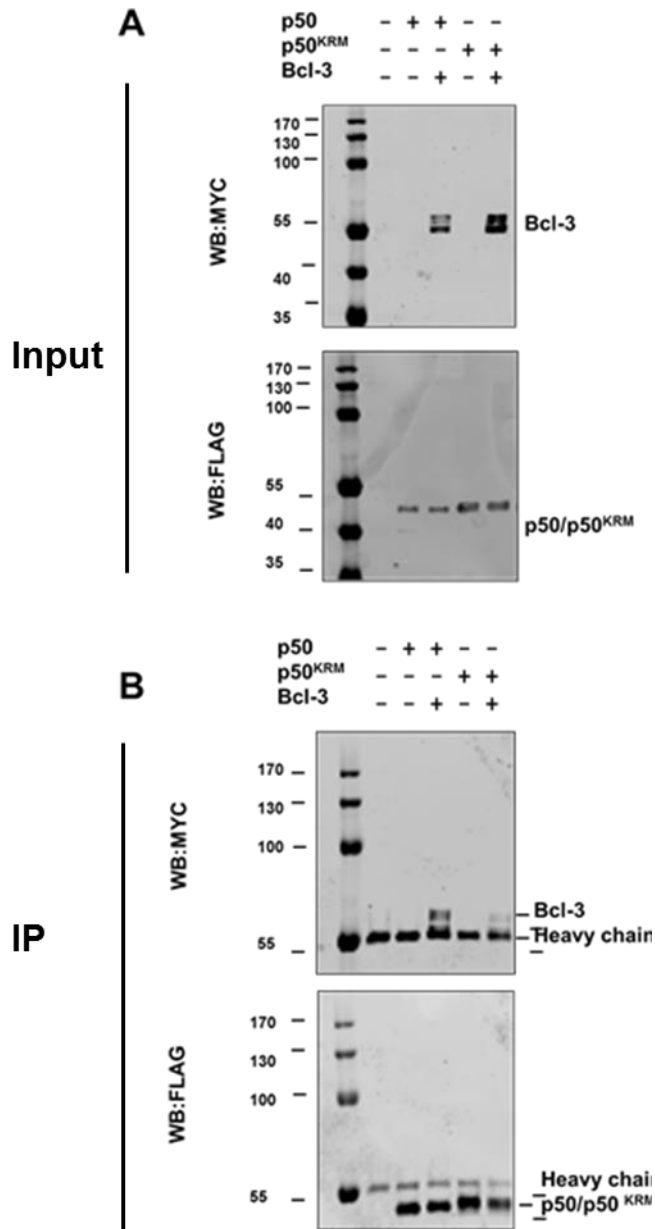


Figure 7.6 p50 and Bcl-3 co-immunoprecipitation.

HEK293T cells were transfected with pRK5-p50-FLAG (p50) or pRK5-p50-FLAG in which Lys249, Arg252 and Met253 of p50 are mutated to alanine (p50^{KRM}) with or without pcDNA3.1-Bcl-3-MYC (Bcl-3). Whole cell lysates were immunoprecipitated (IP) with anti-FLAG and analysed by Western blot (WB) with anti-FLAG and anti-MYC for p50 and Bcl-3 respectively. Western Blots were visualised using LI-COR Odyssey scanned on the 800nm channel following incubation with DyLight 800 conjugated anti-mouse antibody. For A (input) and B (IP) the images shown represent the same membrane probed with different antibodies as indicated. The heavy chain from the immunoprecipitating antibody is also indicated.

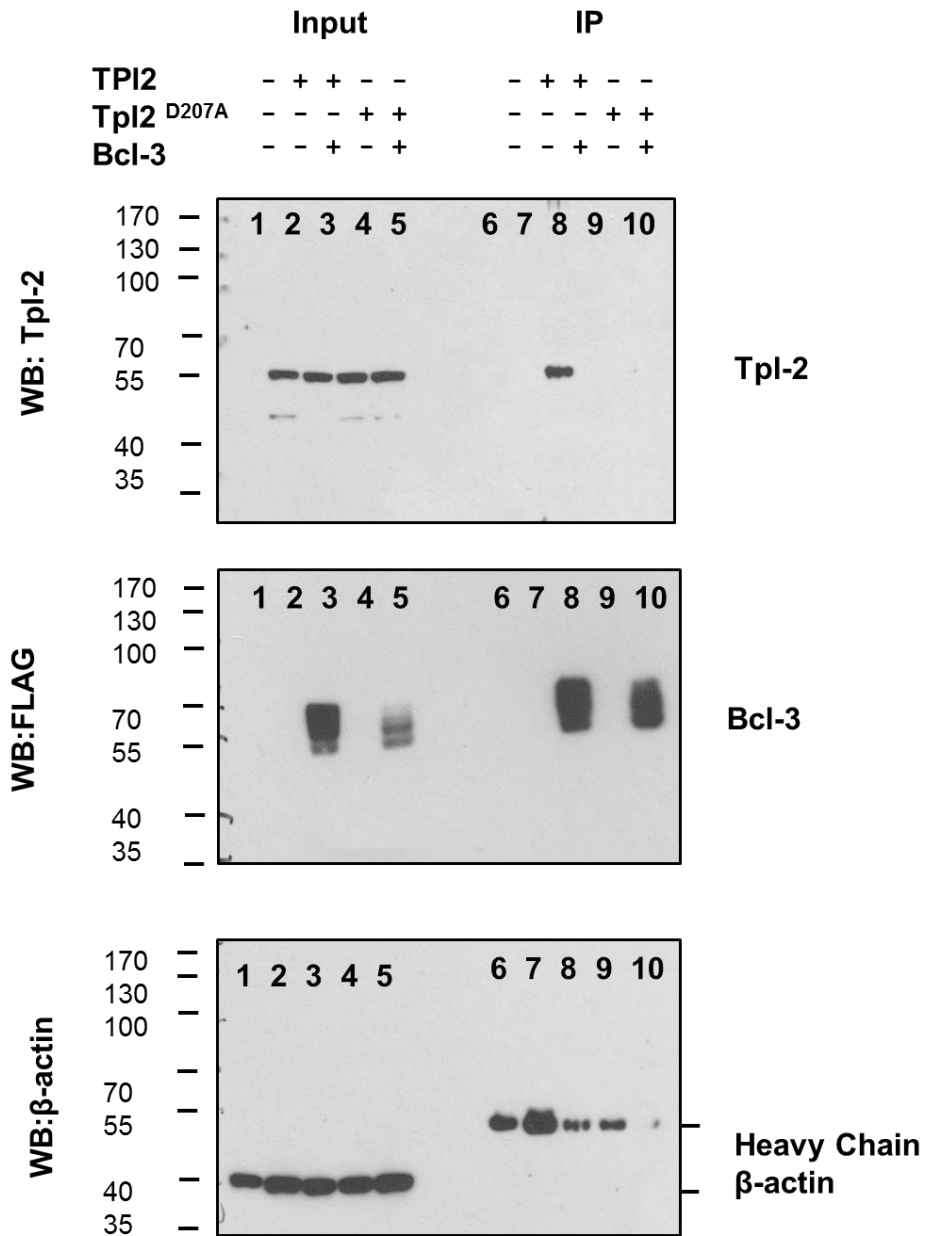


Figure 7. 7 Tpl-2 and Bcl-3 co-immunoprecipitation.

HEK293T cells were transfected with pRK5-Bcl-3-FLAG and pcDNA3-Tpl-2-MYC expression vectors as indicated. Whole cell lysates were immunoprecipitated (IP) with anti-FLAG and analysed by WB with anti-Tpl-2 for Tpl-2 and anti-FLAG for Bcl-3. Bound protein was detected with HRP-conjugated secondary antibodies and WesternBright ECL chemiluminescent HRP substrate. The images shown represent the same membrane probed with different antibodies as indicated. The heavy chain from the immunoprecipitating antibody is also indicated

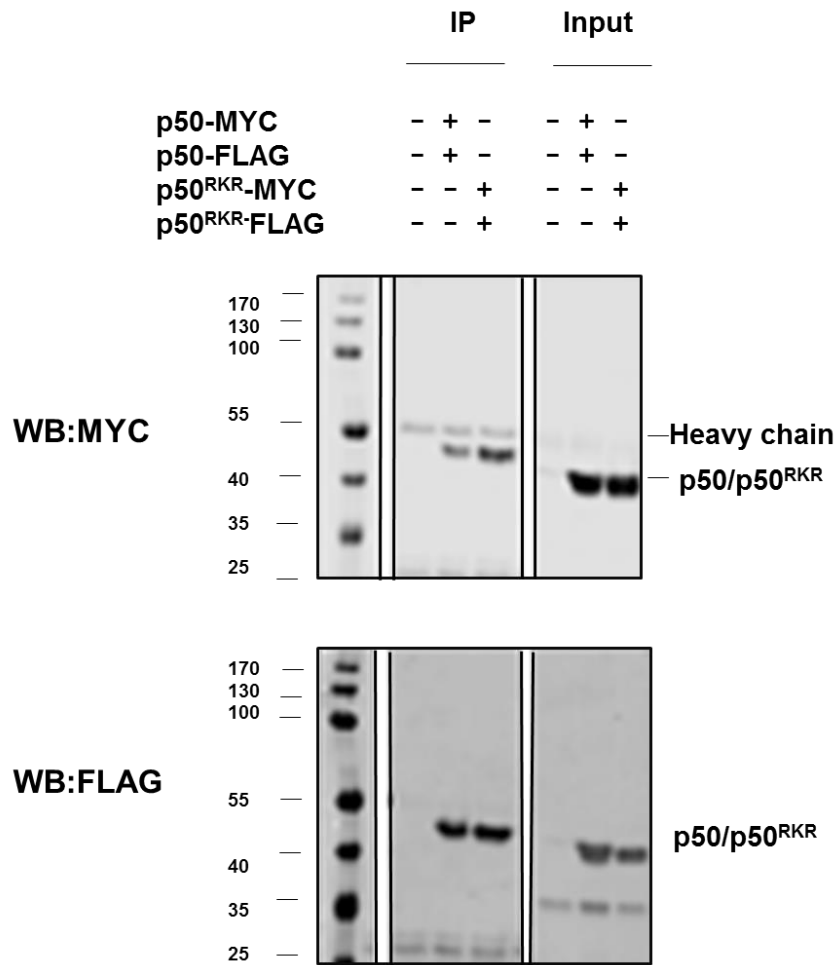


Figure 7.8 p50 homodimer co-immunoprecipitation.

HEK293T cells were transfected as indicated with pRK5-p50-FLAG and pEF4a-p50-MYC (p50) or pRK5-p50-FLAG and pEF4a-p50-MYC in which Arg359, Lys360 and Arg361 of p50 were mutated to alanine (p50^{RKR}). FLAG-p50 or FLAG-p50^{RKR} were immunoprecipitated (IP) from whole cell lysates with anti-FLAG(mouse) and analysed by western blot (WB) with anti-MYC (mouse) and DyLight 800 conjugated anti-mouse antibody for MYC-p50 and p50^{RKR}. FLAG-p50 and p50^{RKR} were visualised with anti-FLAG (rabbit) and DyLight 680 conjugated anti-rabbit antibody. Western Blots were visualised using LI-COR Odyssey scanned separately on the 800nm and 700nm channels for DyLight 800 and DyLight 680 conjugated antibodies respectively. The heavy chain from the immunoprecipitating antibody is also indicated.

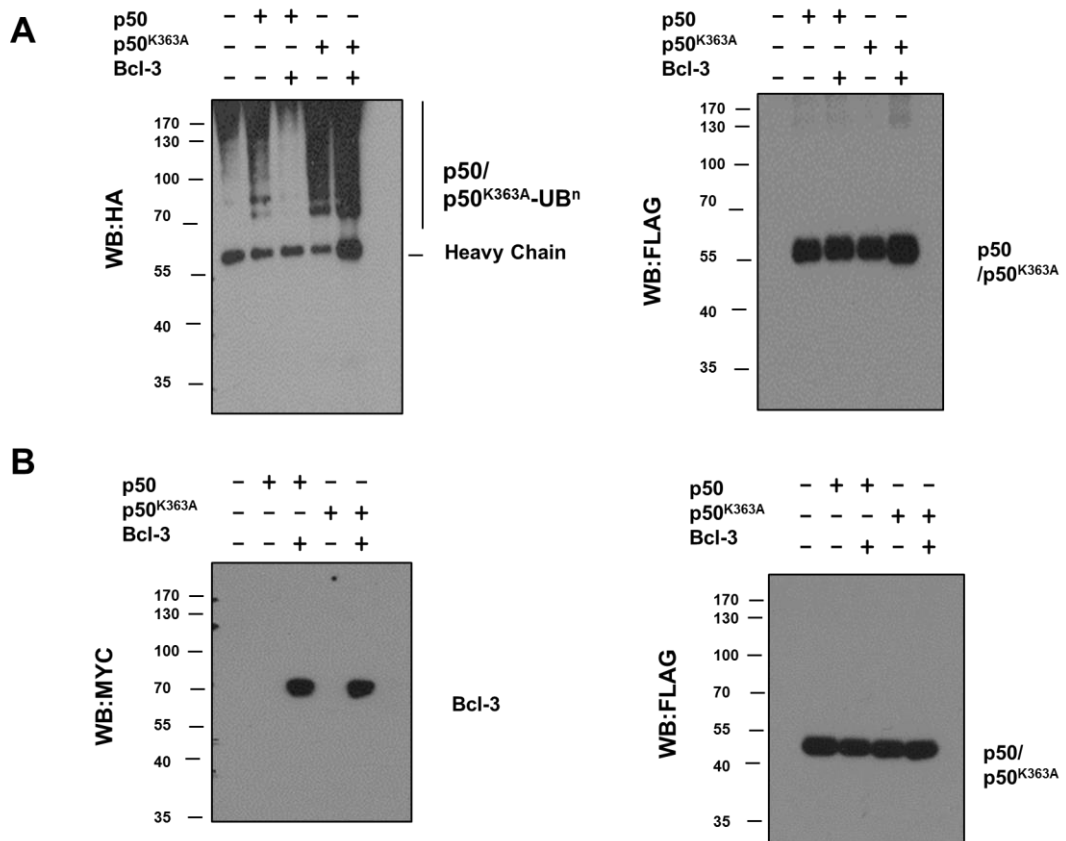


Figure 7. 9 p50 ubiquitination assay.

HEK293T cells were transfected as indicated with pRK5-p50-FLAG or pRK5-p50-FLAG in which Lys363 of p50 was mutated to alanine (p50^{K363A}) with or without pcDNA3.1-Bcl-3-MYC (Bcl-3). All samples were also transfected with ubiquitin-HA, the total concentration of plasmid was maintained constant with the addition of empty expression vector. p50/p50^{K363A} ubiquitination was determined by immunoprecipitation (IP) from whole cell lysates with anti-FLAG and Western blot (WB) with anti-HA for HA-ubiquitin. For A (IP) and B(input) the images shown represent the same membrane probed with different antibodies as indicated. Bound protein was detected with HRP-conjugated secondary antibodies and WesternBright ECL chemiluminescent HRP substrate. The heavy chain from the immunoprecipitating antibody is also indicated.

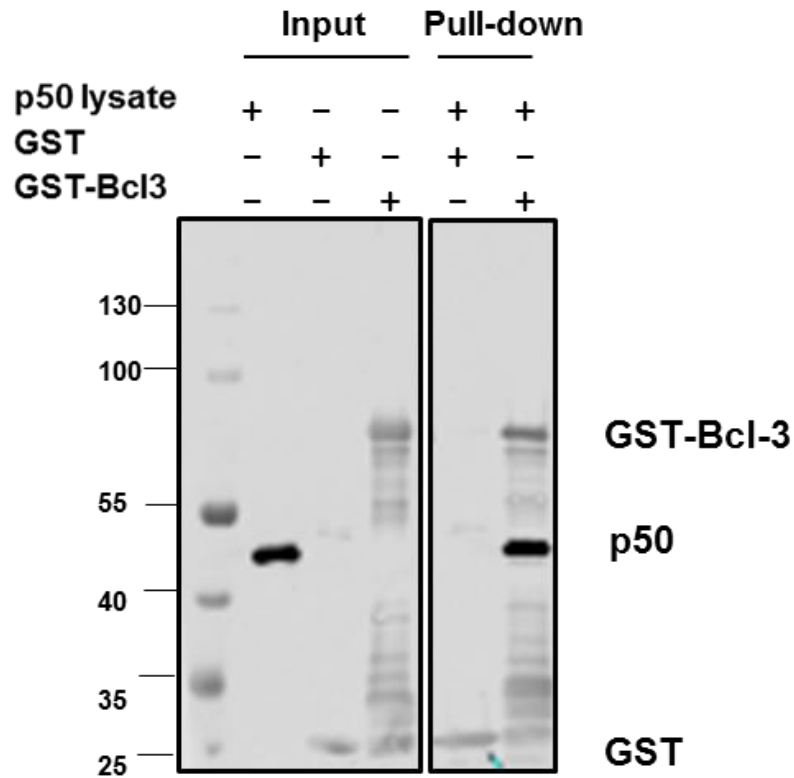


Figure 7.10 GST Pull down assay.

Purified bacterial recombinant GST or GST-Bcl-3 was incubated with a HEK293 whole cell lysate overexpressing FLAG-p50. GST recombinant proteins were affinity purified with GSH agarose. Pull down complexes were resolved by SDS-PAGE and immunoblotted with anti-FLAG(mouse) and DyLight 800 conjugated anti-mouse antibody for FLAG-p50 and anti-GST(rabbit) and DyLight 680 conjugated anti-rabbit antibody for GST and GST-Bcl-3. Western Blots were visualised using LI-COR Odyssey scanned separately on the 800nm and 700nm channels for DyLight 800 and DyLight 680 conjugated antibodies respectively .The image shown is an overlay of both channels.

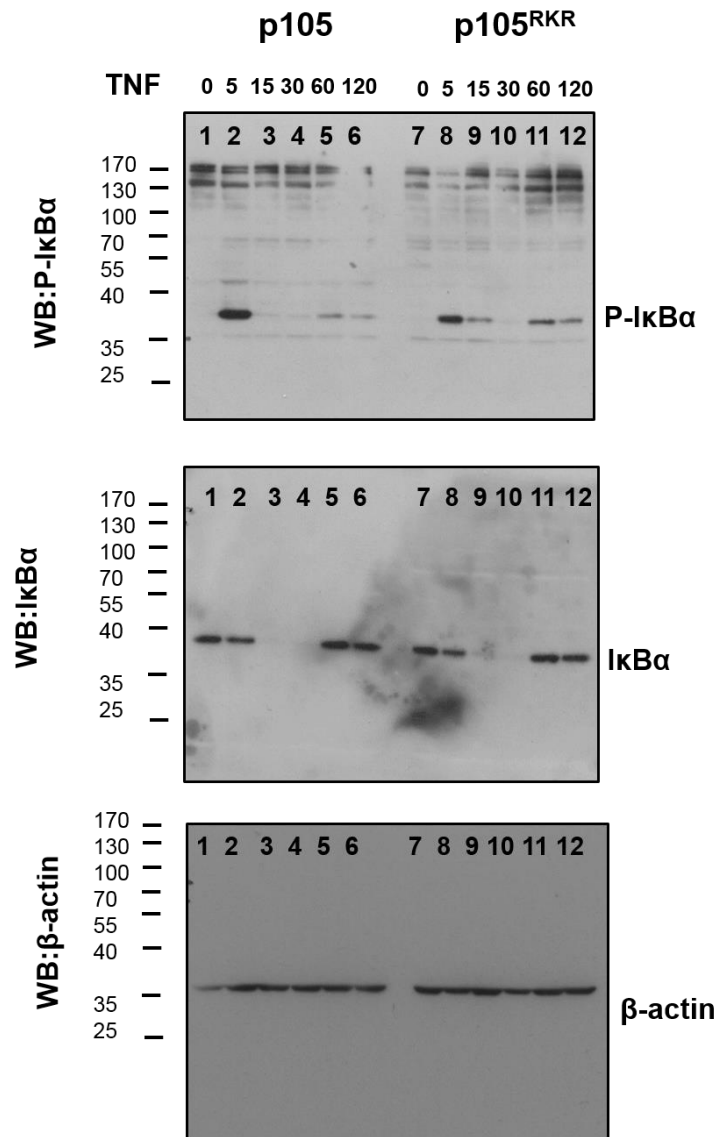
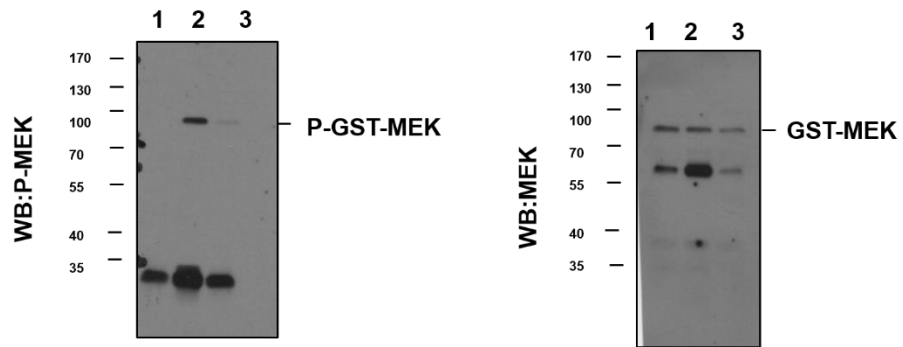


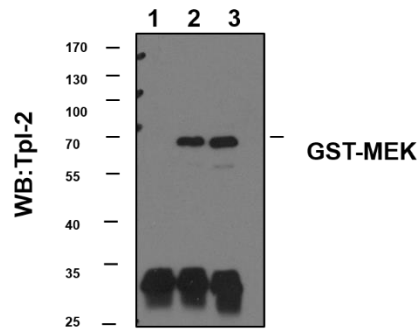
Figure 7.11 TNF induced Iκ α phosphorylation in p105 stable cell lines.

Nfkb1^{-/-} MEF cells were stably transfected with expression vectors encoding p105^{WT} or p105^{RKR}. p105^{WT} or p105^{RKR} MEFs were stimulated with 20ng/ml TNF for the indicated times prior to lysis. Whole cell extracts were analysed by Western blotting for phosphorylated Iκ α and total Iκ α . The images shown represent the same membrane probed with different antibodies as indicated.

A Kinase Assay



B Immunoprecipitation



C Input

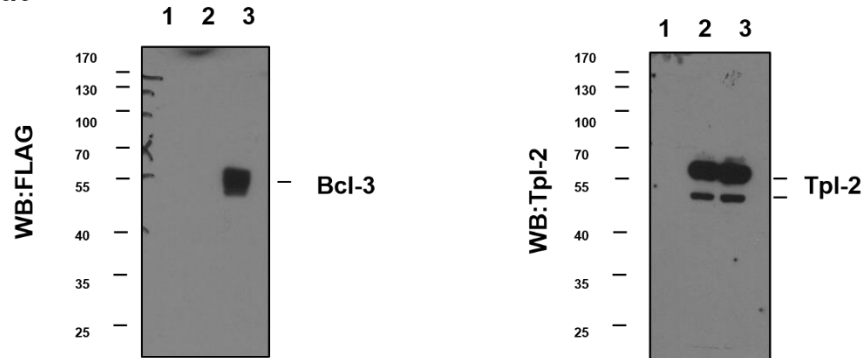


Figure 7.12 MEK-Kinase assay.

HEK293T cells were transfected with pRK5-Bcl-3-FLAG(Bcl-3) and pcDNA3.Tpl-2-MYC(Tpl-2) expression vectors as follows lane 1 mock transfection, lane 2 Tpl-2 and lane 3 Tpl-2 and Bcl-3. Tpl-2 was immunoprecipitated (IP) from whole cell lysates with anti-MYC and used in an *in vitro* MEK kinase assay with unactive GST-MEK1 as a substrate. MEK phosphorylation was determined by WB of kinase assay reaction (A) with anti-phospho MEK1/2 antibody. Immunoprecipitates (B) and inputs (C) were also analysed by Western blot.

8 References

- ADACHI, M., FUKUDA, M. & NISHIDA, E. 2000. Nuclear Export of Map Kinase (ERK) Involves a Map Kinase Kinase (Mek-Dependent) Active Transport Mechanism. *The Journal of Cell Biology*, 148, 849-856.
- ADHIKARI, A., XU, M. & CHEN, Z. J. 0000. Ubiquitin-mediated activation of TAK1 and IKK. *Oncogene*, 26, 3214-3226.
- AGUILERA, C., HOYA-ARIAS, R., HAEGEMAN, G., ESPINOSA, L. & BIGAS, A. 2004. Recruitment of I κ B α to the hes1 promoter is associated with transcriptional repression. *Proceedings of the National Academy of Sciences of the United States of America*, 101, 16537-16542.
- ALAGBALA AJIBADE, A., WANG, Q., CUI, J., ZOU, J., XIA, X., WANG, M., TONG, Y., HUI, W., LIU, D., SU, B., WANG, HELEN Y. & WANG, R.-F. 2012. TAK1 Negatively Regulates NF- κ B and p38 MAP Kinase Activation in Gr-1+CD11b+ Neutrophils. *Immunity*, 36, 43-54.
- ALKALAY, I., YARON, A., HATZUBAI, A., JUNG, S., AVRAHAM, A., GERLITZ, O., PASHUT-LAVON, I. & BEN-NERIAH, Y. 1995a. In vivo stimulation of I kappa B phosphorylation is not sufficient to activate NF-kappa B. *Molecular and Cellular Biology*, 15, 1294-301.
- ALKALAY, I., YARON, A., HATZUBAI, A., ORIAN, A., CIECHANOVER, A. & BEN-NERIAH, Y. 1995b. Stimulation-dependent I kappa B alpha phosphorylation marks the NF-kappa B inhibitor for degradation via the ubiquitin-proteasome pathway. *Proceedings of the National Academy of Sciences*, 92, 10599-10603.
- ANDERSON, K. V., JÜRGENS, G. & NÜSSLEIN-VOLHARD, C. 1985. Establishment of dorsal-ventral polarity in the Drosophila embryo: Genetic studies on the role of the Toll gene product. *Cell*, 42, 779-789.
- ANGEL, P. & KARIN, M. 1991. The role of Jun, Fos and the AP-1 complex in cell-proliferation and transformation. *Biochimica et Biophysica Acta (BBA) - Reviews on Cancer*, 1072, 129-157.
- ANRATHER, J., RACCHUMI, G. & IADECOLA, C. 2005. cis-Acting Element-specific Transcriptional Activity of Differentially Phosphorylated Nuclear Factor- κ B. *Journal of Biological Chemistry*, 280, 244-252.
- ARTHUR, J. S. C. & LEY, S. C. 2013. Mitogen-activated protein kinases in innate immunity. *Nat Rev Immunol*, 13, 679-692.
- BAEUEERLE, P. & BALTIMORE, D. 1988a. I kappa B: a specific inhibitor of the NF-kappa B transcription factor. *Science*, 242, 540-546.
- BAEUEERLE, P. A. & BALTIMORE, D. 1988b. Activation of DNA-binding activity in an apparently cytoplasmic precursor of the NF- κ B transcription factor. *Cell*, 53, 211-217.
- BANERJEE, A., GUGASYAN, R., MCMAHON, M. & GERONDAKIS, S. 2006. Diverse Toll-like receptors utilize Tpl2 to activate extracellular signal-regulated kinase (ERK) in hemopoietic cells. *Proceedings of the National Academy of Sciences of the United States of America*, 103, 3274-3279.
- BARRÉ, B. & PERKINS, N. D. 2010. The Skp2 Promoter Integrates Signaling through the NF- κ B, p53, and Akt/GSK3B Pathways to Regulate Autophagy and Apoptosis. *Molecular Cell*, 38, 524-538.
- BARTON, G. M. & MEDZHITOV, R. 2003. Toll-Like Receptor Signaling Pathways. *Science*, 300, 1524-1525.
- BASAK, S., KIM, H., KEARNS, J. D., TERGAONKAR, V., O'DEA, E., WERNER, S. L., BENEDICT, C. A., WARE, C. F., GHOSH, G., VERMA, I. M. & HOFFMANN, A.

2007. A Fourth I κ B Protein within the NF- κ B Signaling Module. *Cell*, 128, 369-381.
- BASITH, S., MANAVALAN, B., GOSU, V. & CHOI, S. 2013. Evolutionary, Structural and Functional Interplay of the I κ B Family Members. *PLoS ONE*, 8, e54178.
- BEESON, P. B. & ROBERTS, W. T. T. A. O. E. 1947. TOLERANCE TO BACTERIAL PYROGENS: I. FACTORS INFLUENCING ITS DEVELOPMENT. *The Journal of Experimental Medicine*, 86, 29-38.
- BEG, A. A., FINCO, T. S., NANTERMET, P. V. & BALDWIN, A. S. 1993. Tumor necrosis factor and interleukin-1 lead to phosphorylation and loss of I kappa B alpha: a mechanism for NF-kappa B activation. *Molecular and Cellular Biology*, 13, 3301-3310.
- BEG, A. A., RUBEN, S. M., SCHEINMAN, R. I., HASKILL, S., ROSEN, C. A. & BALDWIN, A. S. 1992. I kappa B interacts with the nuclear localization sequences of the subunits of NF-kappa B: a mechanism for cytoplasmic retention. *Genes & Development*, 6, 1899-1913.
- BEG, A. A., SHA, W. C., BRONSON, R. T., GHOSH, S. & BALTIMORE, D. 1995. Embryonic lethality and liver degeneration in mice lacking the RelA component of NF-[kappa]B. *Nature*, 376, 167-170.
- BEINKE, S., DEKA, J., LANG, V., BELICH, M. P., WALKER, P. A., HOWELL, S., SMERDON, S. J., GAMBLIN, S. J. & LEY, S. C. 2003. NF- κ B1 p105 Negatively Regulates TPL-2 MEK Kinase Activity. *Molecular and Cellular Biology*, 23, 4739-4752.
- BEINKE, S. & LEY, S. C. 2004. Functions of NF-kappaB1 and NF-kappaB2 in immune cell biology. *Biochem. J.*, 382, 393-409.
- BEINKE, S., ROBINSON, M. J., HUGUNIN, M. & LEY, S. C. 2004. Lipopolysaccharide Activation of the TPL-2/MEK/Extracellular Signal-Regulated Kinase Mitogen-Activated Protein Kinase Cascade Is Regulated by I κ B Kinase-Induced Proteolysis of NF- κ B1 p105. *Molecular and Cellular Biology*, 24, 9658-9667.
- BELICH, M. P., SALMERON, A., JOHNSTON, L. H. & LEY, S. C. 1999. TPL-2 kinase regulates the proteolysis of the NF-[kappa]B-inhibitory protein NF-[kappa]B1 p105. *Nature*, 397, 363-368.
- BEN-ADDI, A., MAMBOLE-DEMA, A., BRENDER, C., MARTIN, S. R., JANZEN, J., KJAER, S., SMERDON, S. J. & LEY, S. C. 2014. I κ B kinase-induced interaction of TPL-2 kinase with 14-3-3 is essential for Toll-like receptor activation of ERK-1 and -2 MAP kinases. *Proceedings of the National Academy of Sciences*, 111, E2394-E2403.
- BISWAS, S. K. & LOPEZ-COLLAZO, E. 2009. Endotoxin tolerance: new mechanisms, molecules and clinical significance. *Trends in immunology*, 30, 475-487.
- BLOM, N., GAMMELTOFT, S. & BRUNAK, S. 1999. Sequence and structure-based prediction of eukaryotic protein phosphorylation sites. *Journal of Molecular Biology*, 294, 1351-1362.
- BOHUSLAV, J., KRAVCHENKO, V. V., PARRY, G. C., ERLICH, J. H., GERONDAKIS, S., MACKMAN, N. & ULEVITCH, R. J. 1998. Regulation of an essential innate immune response by the p50 subunit of NF-kappaB. *The Journal of Clinical Investigation*, 102, 1645-1652.
- BOSISIO, D., MARAZZI, I., AGRETI, A., SHIMIZU, N., BIANCHI, M. E. & NATOLI, G. 2006. A hyper-dynamic equilibrium between promoter-bound and nucleoplasmic dimers controls NF-kappaB-dependent gene activity. *Embo J*, 25, 798-810.
- BOTOS, I., SEGAL, DAVID M. & DAVIES, DAVID R. 2011. The Structural Biology of Toll-like Receptors. *Structure*, 19, 447-459.
- BOULTON, T., YANCOPOULOS, G., GREGORY, J., SLAUGHTER, C., MOOMAW, C., HSU, J. & COBB, M. 1990. An insulin-stimulated protein kinase similar to yeast kinases involved in cell cycle control. *Science*, 249, 64-67.

- BOULTON, T. G., NYE, S. H., ROBBINS, D. J., IP, N. Y., RADZLEJEWSKA, E., MORGENBESSER, S. D., DEPINHO, R. A., PANAYOTATOS, N., COBB, M. H. & YANCOPOULOS, G. D. 1991. ERKs: A family of protein-serine/threonine kinases that are activated and tyrosine phosphorylated in response to insulin and NGF. *Cell*, 65, 663-675.
- BOURS, V., FRANZOSO, G., AZARENKO, V., PARK, S., KANNO, T., BROWN, K. & SIEBENLIST, U. 1993. The oncoprotein Bcl-3 directly transactivates through κ B motifs via association with DNA-binding p50B homodimers. *Cell*, 72, 729-739.
- BREEDEN, L. & NASMYTH, K. 1987. Similarity between cell-cycle genes of budding yeast and fission yeast and the Notch gene of *Drosophila*. *Nature*, 329, 651-654.
- BROCKMAN, J. A., SCHERER, D. C., MCKINSEY, T. A., HALL, S. M., QI, X., LEE, W. Y. & BALLARD, D. W. 1995. Coupling of a signal response domain in I kappa B alpha to multiple pathways for NF-kappa B activation. *Molecular and Cellular Biology*, 15, 2809-18.
- BROWN, K., GERSTBERGER, S., CARLSON, L., FRANZOSO, G. & SIEBENLIST, U. 1995. Control of I kappa B-alpha proteolysis by site-specific, signal-induced phosphorylation. *Science*, 267, 1485-1488.
- BROWN, K., PARK, S., KANNO, T., FRANZOSO, G. & SIEBENLIST, U. 1993. Mutual regulation of the transcriptional activator NF-kappa B and its inhibitor, I kappa B-alpha. *Proceedings of the National Academy of Sciences*, 90, 2532-2536.
- BROWNELL, J. E., SINTCHAK, M. D., GAVIN, J. M., LIAO, H., BRUZZESE, F. J., BUMP, N. J., SOUCY, T. A., MILHOLLEN, M. A., YANG, X., BURKHARDT, A. L., MA, J., LOKE, H.-K., LINGARAJ, T., WU, D., HAMMAN, K. B., SPELMAN, J. J., CULLIS, C. A., LANGSTON, S. P., VYSKOCIL, S., SELLS, T. B., MALLENDER, W. D., VISIERS, I., LI, P., CLAIBORNE, C. F., ROLFE, M., BOLEN, J. B. & DICK, L. R. 2010. Substrate-Assisted Inhibition of Ubiquitin-like Protein-Activating Enzymes: The NEDD8 E1 Inhibitor MLN4924 Forms a NEDD8-AMP Mimetic In Situ. *Molecular cell*, 37, 102-111.
- BURGERMEISTER, E., CHUDERLAND, D., HANOCH, T., MEYER, M., LISCOVITCH, M. & SEGER, R. 2007. Interaction with MEK Causes Nuclear Export and Downregulation of Peroxisome Proliferator-Activated Receptor γ . *Molecular and Cellular Biology*, 27, 803-817.
- CAAMAÑO, J. H., PEREZ, P., LIRA, S. A. & BRAVO, R. 1996. Constitutive expression of Bcl-3 in thymocytes increases the DNA binding of NF-kappaB1 (p50) homodimers in vivo. *Molecular and Cellular Biology*, 16, 1342-8.
- CAI, S.-R., XU, G., BECKER-HAPAK, M., MA, M., DOWDY, S. F. & MCLEOD, H. L. 2006. The kinetics and tissue distribution of protein transduction in mice. *European Journal of Pharmaceutical Sciences*, 27, 311-319.
- CAO, S., ZHANG, X., EDWARDS, J. P. & MOSSER, D. M. 2006. NF- κ B1 (p50) Homodimers Differentially Regulate Pro- and Anti-inflammatory Cytokines in Macrophages. *Journal of Biological Chemistry*, 281, 26041-26050.
- CARGNELLO, M. & ROUX, P. P. 2011. Activation and Function of the MAPKs and Their Substrates, the MAPK-Activated Protein Kinases. *Microbiology and Molecular Biology Reviews*, 75, 50-83.
- CARMODY, R. J. & CHEN, Y. H. 2007. Nuclear factor-kappaB: activation and regulation during toll-like receptor signaling. *Cell Mol Immunol*, 4, 31-41.
- CARMODY, R. J., RUAN, Q., LIOU, H. C. & CHEN, Y. H. 2007a. Essential roles of c-Rel in TLR-induced IL-23 p19 gene expression in dendritic cells. *J Immunol*, 178, 186-91.

- CARMODY, R. J., RUAN, Q., PALMER, S., HILLIARD, B. & CHEN, Y. H. 2007b. Negative regulation of toll-like receptor signaling by NF-kappaB p50 ubiquitination blockade. *Science*, 317, 675-8.
- CARPINO, L. A. & HAN, G. Y. 1972. 9-Fluorenylmethoxycarbonyl amino-protecting group. *The Journal of Organic Chemistry*, 37, 3404-3409.
- CECCARELLI, DEREK F., TANG, X., PELLETIER, B., ORLICKY, S., XIE, W., PLANTEVIN, V., NECULAI, D., CHOU, Y.-C., OGUNJIMI, A., AL-HAKIM, A., VARELAS, X., KOSZELA, J., WASNEY, GREGORY A., VEDADI, M., DHE-PAGANON, S., COX, S., XU, S., LOPEZ-GIRONA, A., MERCURIO, F., WRANA, J., DUROCHER, D., MELOCHE, S., WEBB, DAVID R., TYERS, M. & SICHERI, F. 2011. An Allosteric Inhibitor of the Human Cdc34 Ubiquitin-Conjugating Enzyme. *Cell*, 145, 1075-1087.
- CECI, J. D., PATRIOTIS, C. P., TSATSANIS, C., MAKRIS, A. M., KOVATCH, R., SWING, D. A., JENKINS, N. A., TSICHLIS, P. N. & COPELAND, N. G. 1997. Tpl-2 is an oncogenic kinase that is activated by carboxy-terminal truncation. *Genes & Development*, 11, 688-700.
- CHEN, F., BHATIA, D., CHANG, Q. & CASTRANOVA, V. 2006. Finding NEMO by K63-linked polyubiquitin chain. *Cell Death Differ*, 13, 1835-1838.
- CHEN, L.-F., MU, Y. & GREENE, W. C. 2002. Acetylation of RelA at discrete sites regulates distinct nuclear functions of NF-[kappa]B. *EMBO J*, 21, 6539-6548.
- CHEN, Y., WU, J. & GHOSH, G. 2003. κ B-Ras Binds to the Unique Insert within the Ankyrin Repeat Domain of I κ BB and Regulates Cytoplasmic Retention of I κ BB-NF- κ B Complexes. *Journal of Biological Chemistry*, 278, 23101-23106.
- CHEN, Z., GIBSON, T. B., ROBINSON, F., SILVESTRO, L., PEARSON, G., XU, B.-E., WRIGHT, A., VANDERBILT, C. & COBB, M. H. 2001. MAP Kinases. *Chemical Reviews*, 101, 2449-2476.
- CHEN, Z., HAGLER, J., PALOMBELLA, V. J., MELANDRI, F., SCHERER, D., BALLARD, D. & MANIATIS, T. 1995. Signal-induced site-specific phosphorylation targets I kappa B alpha to the ubiquitin-proteasome pathway. *Genes & Development*, 9, 1586-1597.
- CHEN, Z. J. 2005. Ubiquitin signalling in the NF-[kappa]B pathway. *Nat Cell Biol*, 7, 758-765.
- CHENG, C. S., FELDMAN, K. E., LEE, J., VERMA, S., HUANG, D. B., HUYNH, K., CHANG, M., PONOMARENKO, J. V., SUN, S. C., BENEDICT, C. A., GHOSH, G. & HOFFMANN, A. 2011. The specificity of innate immune responses is enforced by repression of interferon response elements by NF-kappaB p50. *Sci Signal*, 4, ra11.
- CHIARIELLO, M., MARINISSEN, M. J. & GUTKIND, J. S. 2000. Multiple Mitogen-Activated Protein Kinase Signaling Pathways Connect the Cot Oncoprotein to the c-junPromoter and to Cellular Transformation. *Molecular and Cellular Biology*, 20, 1747-1758.
- CHIARIELLO, M., VAQUÉ, J., CRESPO, P. & GUTKIND, J. S. 2010. Activation of Ras and Rho GTPases and MAP Kinases by G-Protein-Coupled Receptors. In: SEGER, R. (ed.) *MAP Kinase Signaling Protocols*. Humana Press.
- CHIN, C. & BEACHY, P. A. 1994. Expression of a novel Toll-like gene spans the parasegment boundary and contributes to hedgehog function in the adult eye of Drosophila. *Mechanisms of Development*, 47, 225-239.
- CHO, J., MELNICK, M., SOLIDAKIS, G. P. & TSICHLIS, P. N. 2005. Tpl2 (Tumor Progression Locus 2) Phosphorylation at Thr290 Is Induced by Lipopolysaccharide via an I κ -B Kinase- β -dependent Pathway and Is Required for Tpl2 Activation by External Signals. *Journal of Biological Chemistry*, 280, 20442-20448.
- CHOI, H. S., KANG, B. S., SHIM, J.-H., CHO, Y.-Y., CHOI, B. Y., BODE, A. M. & DONG, Z. 2008. Cot, a novel kinase of histone H3, induces cellular transformation

- through up-regulation of c-fos transcriptional activity. *The FASEB Journal*, 22, 113-126.
- CHUDERLAND, D., KONSON, A. & SEGER, R. 2008. Identification and Characterization of a General Nuclear Translocation Signal in Signaling Proteins. *Molecular Cell*, 31, 850-861.
- CLACKSON T, W. J. 1995. A hot spot of binding energy in a hormone-receptor interface. *Science*, 267, 383-386.
- COHEN, P. & TCHERPAKOV, M. 2010. Will the Ubiquitin System Furnish as Many Drug Targets as Protein Kinases? *Cell*, 143, 686-693.
- COHEN, S., ACHBERT-WEINER, H. & CIECHANOVER, A. 2004. Dual Effects of I κ B Kinase β -Mediated Phosphorylation on p105 Fate: SCF β -TrCP-Dependent Degradation and SCF β -TrCP-Independent Processing. *Molecular and Cellular Biology*, 24, 475-486.
- COLLAND, F., FORMSTECHE, E., JACQ, X., REVERDY, C., PLANQUETTE, C., CONRATH, S., TROUPLIN, V., BIANCHI, J., AUSHEV, V. N., CAMONIS, J., CALABRESE, A., BORG-CAPRA, C., SIPPL, W., COLLURA, V., BOISSY, G., RAIN, J.-C., GUEDAT, P., DELANSORNE, R. & DAVIET, L. 2009. Small-molecule inhibitor of USP7/HAUSP ubiquitin protease stabilizes and activates p53 in cells. *Molecular Cancer Therapeutics*, 8, 2286-2295.
- COLLERAN, A., COLLINS, P. E., O'CARROLL, C., AHMED, A., MAO, X., MCMANUS, B., KIELY, P. A., BURSTEIN, E. & CARMODY, R. J. 2013. Deubiquitination of NF- κ B by Ubiquitin-Specific Protease-7 promotes transcription. *Proc Natl Acad Sci U S A*, 110, 618-23.
- COMALADA, M., VALLEDOR, A. F., SANCHEZ-TILLÓ, E., UMBERT, I., XAUS, J. & CELADA, A. 2003. Macrophage colony-stimulating factor-dependent macrophage proliferation is mediated through a calcineurin-independent but immunophilin-dependent mechanism that mediates the activation of external regulated kinases. *European Journal of Immunology*, 33, 3091-3100.
- COURTIES, G., SEIFFART, V., PRESUMEY, J., ESCRIOU, V., SCHERMAN, D., ZWERINA, J., RUIZ, G., ZIETARA, N., JABLONSKA, J., WEISS, S., HOFFMANN, A., JORGENSEN, C., APPARAILLY, F. & GROSS, G. 2010. In vivo RNAi-mediated silencing of TAK1 decreases inflammatory Th1 and Th17 cells through targeting of myeloid cells. *Blood*, 116, 3505-3516.
- COWAN, R. & WHITTAKER, R. G. 1990. Hydrophobicity indices for amino acid residues as determined by high-performance liquid chromatography. *Peptide research*, 3, 75-80.
- CRAIG, E. A., STEVENS, M. V., VAILLANCOURT, R. R. & CAMENISCH, T. D. 2008. MAP3Ks as central regulators of cell fate during development. *Developmental Dynamics*, 237, 3102-3114.
- DAS, S., CHO, J., LAMBERTZ, I., KELLIHER, M. A., ELIOPOULOS, A. G., DU, K. & TSICHLIS, P. N. 2005. Tpl2/Cot Signals Activate ERK, JNK, and NF- κ B in a Cell-type and Stimulus-specific Manner. *Journal of Biological Chemistry*, 280, 23748-23757.
- DELHASE, M., HAYAKAWA, M., CHEN, Y. & KARIN, M. 1999. Positive and Negative Regulation of I κ B Kinase Activity Through IKK β Subunit Phosphorylation. *Science*, 284, 309-313.
- DENG, L., WANG, C., SPENCER, E., YANG, L., BRAUN, A., YOU, J., SLAUGHTER, C., PICKART, C. & CHEN, Z. J. 2000. Activation of the I κ B Kinase Complex by TRAF6 Requires a Dimeric Ubiquitin-Conjugating Enzyme Complex and a Unique Polyubiquitin Chain. *Cell*, 103, 351-361.
- DENNIS, A., KUDO, T., KRUIDENIER, L., GIRARD, F., CREPIN, V. F., MACDONALD, T. T., FRANKEL, G. & WILES, S. 2008. The p50 Subunit of NF- κ B Is Critical for

- In Vivo Clearance of the Noninvasive Enteric Pathogen *Citrobacter rodentium*. *Infection and Immunity*, 76, 4978-4988.
- DIDONATO, J. A., HAYAKAWA, M., ROTHWARF, D. M., ZANDI, E. & KARIN, M. 1997. A cytokine-responsive I[κ]B kinase that activates the transcription factor NF-[κ]B. *Nature*, 388, 548-554.
- DIDONATO, J. A., MERCURIO, F. & KARIN, M. 1995. Phosphorylation of I kappa B alpha precedes but is not sufficient for its dissociation from NF-kappa B. *Molecular and Cellular Biology*, 15, 1302-11.
- DIDONATO, J. A., MERCURIO, F. & KARIN, M. 2012. NF- κ B and the link between inflammation and cancer. *Immunological Reviews*, 246, 379-400.
- DUMITRU, C. D., CECI, J. D., TSATSANIS, C., KONTOYIANNIS, D., STAMATAKIS, K., LIN, J.-H., PATRIOTIS, C., JENKINS, N. A., COPELAND, N. G., KOLLIAS, G. & TSICHLIS, P. N. 2000. TNF- \pm Induction by LPS Is Regulated Posttranscriptionally via a Tpl2/ERK-Dependent Pathway. *Cell*, 103, 1071-1083.
- DYER, B. W., FERRER, F. A., KLINEDINST, D. K. & RODRIGUEZ, R. 2000. A noncommercial dual luciferase enzyme assay system for reporter gene analysis. *Anal Biochem*, 282, 158-61.
- EBISUYA, M., KONDOH, K. & NISHIDA, E. 2005. The duration, magnitude and compartmentalization of ERK MAP kinase activity: mechanisms for providing signaling specificity. *Journal of Cell Science*, 118, 2997-3002.
- ELIOPOULOS, A. G., DUMITRU, C. D., WANG, C.-C., CHO, J. & TSICHLIS, P. N. 2002. Induction of COX-2 by LPS in macrophages is regulated by Tpl2-dependent CREB activation signals. *EMBO J*, 21, 4831-4840.
- ELIOPOULOS, A. G., WANG, C.-C., DUMITRU, C. D. & TSICHLIS, P. N. 2003. Tpl2 transduces CD40 and TNF signals that activate ERK and regulates IgE induction by CD40. *EMBO J*, 22, 3855-3864.
- ELSHARKAWY, A. M., OAKLEY, F., LIN, F., PACKHAM, G., MANN, D. A. & MANN, J. 2010. The NF- κ B p50:p50:HDAC-1 repressor complex orchestrates transcriptional inhibition of multiple pro-inflammatory genes. *Journal of hepatology*, 53, 519-527.
- ERNST, M. K., DUNN, L. L. & RICE, N. R. 1995. The PEST-like sequence of I kappa B alpha is responsible for inhibition of DNA binding but not for cytoplasmic retention of c-Rel or RelA homodimers. *Molecular and Cellular Biology*, 15, 872-82.
- ESPINOSA, L., BIGAS, A. & MULERO, M. C. 2011. Alternative nuclear functions for NF-kappaB family members. *Am J Cancer Res*, 1, 446-59.
- FAWELL, S., SEERY, J., DAIKH, Y., MOORE, C., CHEN, L. L., PEPINSKY, B. & BARSOU, J. 1994. Tat-mediated delivery of heterologous proteins into cells. *Proceedings of the National Academy of Sciences*, 91, 664-668.
- FERRELL, J. E. & BHATT, R. R. 1997. Mechanistic Studies of the Dual Phosphorylation of Mitogen-activated Protein Kinase. *Journal of Biological Chemistry*, 272, 19008-19016.
- FINCO, T. S., BEG, A. A. & BALDWIN, A. S. 1994. Inducible phosphorylation of I kappa B alpha is not sufficient for its dissociation from NF-kappa B and is inhibited by protease inhibitors. *Proceedings of the National Academy of Sciences*, 91, 11884-11888.
- FIORINI, E., SCHMITZ, I., MARISSSEN, W. E., OSBORN, S. L., TOUMA, M., SASADA, T., RECHE, P. A., TIBALDI, E. V., HUSSEY, R. E., KRUISBEEK, A. M., REINHERZ, E. L. & CLAYTON, L. K. 2002. Peptide-Induced Negative Selection of Thymocytes Activates Transcription of an NF- κ B Inhibitor. *Molecular Cell*, 9, 637-648.
- FITZGERALD, K. A., PALSSON-MCDERMOTT, E. M., BOWIE, A. G., JEFFERIES, C. A., MANSELL, A. S., BRADY, G., BRINT, E., DUNNE, A., GRAY, P., HARTE, M. T.,

- MCMURRAY, D., SMITH, D. E., SIMS, J. E., BIRD, T. A. & O'NEILL, L. A. J. 2001. Mal (MyD88-adaptor-like) is required for Toll-like receptor-4 signal transduction. *Nature*, 413, 78-83.
- FITZGERALD, K. A., ROWE, D. C., BARNES, B. J., CAFFREY, D. R., VISINTIN, A., LATZ, E., MONKS, B., PITHA, P. M. & GOLENBOCK, D. T. 2003. LPS-TLR4 Signaling to IRF-3/7 and NF- κ B Involves the Toll Adapters TRAM and TRIF. *The Journal of Experimental Medicine*, 198, 1043-1055.
- FOSTER, S. L., HARGREAVES, D. C. & MEDZHITOV, R. 2007. Gene-specific control of inflammation by TLR-induced chromatin modifications. *Nature*, 447, 972-978.
- FRANK, R. 1992. Spot-synthesis: an easy technique for the positionally addressable, parallel chemical synthesis on a membrane support. *Tetrahedron*, 48, 9217-9232.
- FRANK, R. 2002. The SPOT-synthesis technique: Synthetic peptide arrays on membrane supports—principles and applications. *Journal of Immunological Methods*, 267, 13-26.
- FRANK, R., HEIKENS, W., HEISTERBERG-MOUTSIS, G. & BLÖCKER, H. 1983. A new general approach for the simultaneous chemical synthesis of large numbers of oligonucleotides: Segmental solid supports. *Nucleic Acids Research*, 11, 4365-4377.
- FRANK, R. & OVERWIN, H. 1996. SPOT synthesis. Epitope analysis with arrays of synthetic peptides prepared on cellulose membranes. *Methods in molecular biology (Clifton, N.J.)*, 66, 149-169.
- FRANKEL, A. D. & PABO, C. O. 1988. Cellular uptake of the tat protein from human immunodeficiency virus. *Cell*, 55, 1189-1193.
- FRANZOSO, B., AZARENKO, PARK, TOMITA-YAMAGUCHI, KANNO, BROWN, AND SIEBENLIST 1993. The oncoprotein Bcl-3 can facilitate NF-kappa B-mediated transactivation by removing inhibiting p50 homodimers from select kappa B sites. *The EMBO journal*, 12, 3893-3901.
- FRANZOSO, G., BOURS, V., PARK, S., TOMFTA-YAMAGUCHI, M., KELLY, K. & SIEBENLIST, U. 1992. The candidate oncoprotein Bcl-3 is an antagonist of p50/NF-[kappa]B-mediated inhibition. *Nature*, 359, 339-342.
- FRANZOSO, G., CARLSON, L., SCHARTON-KERSTEN, T., SHORES, E. W., EPSTEIN, S., GRINBERG, A., TRAN, T., SHACTER, E., LEONARDI, A., ANVER, M., LOVE, P., SHER, A. & SIEBENLIST, U. 1997. Critical Roles for the Bcl-3 Oncoprotein in T Cell Mediated Immunity, Splenic Microarchitecture, and Germinal Center Reactions. *Immunity*, 6, 479-490.
- FUCHS, S. Y., SPIEGELMAN, V. S. & SURESH KUMAR, K. G. 0000. The many faces of [beta]-TrCP E3 ubiquitin ligases: reflections in the magic mirror of cancer. *Oncogene*, 23, 2028-2036.
- FUJITA, T., NOLAN, G. P., LIOU, H. C., SCOTT, M. L. & BALTIMORE, D. 1993. The candidate proto-oncogene bcl-3 encodes a transcriptional coactivator that activates through NF-kappa B p50 homodimers. *Genes & Development*, 7, 1354-1363.
- FUKUDA, M., GOTOH, I., GOTOH, Y. & NISHIDA, E. 1996. Cytoplasmic Localization of Mitogen-activated Protein Kinase Kinase Directed by Its NH2-terminal, Leucine-rich Short Amino Acid Sequence, Which Acts as a Nuclear Export Signal. *Journal of Biological Chemistry*, 271, 20024-20028.
- GANTKE, T., SRISKANTHARAJAH, S. & LEY, S. C. 2011. Regulation and function of TPL-2, an I[kappa]B kinase-regulated MAP kinase kinase kinase. *Cell Res*, 21, 131-145.
- GANTKE, T., SRISKANTHARAJAH, S., SADOWSKI, M. & LEY, S. C. 2012. I κ B kinase regulation of the TPL-2/ERK MAPK pathway. *Immunological Reviews*, 246, 168-182.

- GAY, N. J. & KEITH, F. J. 1991. Drosophila Toll and IL-1 receptor. *Nature*, 351, 355-356.
- GENG, F., WENZEL, S. & TANSEY, W. P. 2012. Ubiquitin and Proteasomes in Transcription. *Annual Review of Biochemistry*, 81, 177-201.
- GENG, H., WITTEWERT, T., DITTRICH-BREIHZOLZ, O., KRACHT, M. & SCHMITZ, M. L. 2009. Phosphorylation of NF- κ B p65 at Ser468 controls its COMMD1-dependent ubiquitination and target gene-specific proteasomal elimination. *EMBO reports*, 10, 381-386.
- GERONDAKIS, S., GRUMONT, R., GUGASYAN, R., WONG, L., ISOMURA, I., HO, W. & BANERJEE, A. 2000. Unravelling the complexities of the NF- κ B signalling pathway using mouse knockout and transgenic models. *Oncogene*, 25, 6781-6799.
- GEYSEN, H. M., RODDA, S. J., MASON, T. J., TRIBBICK, G. & SCHOOF, P. G. 1987. Strategies for epitope analysis using peptide synthesis. *Journal of Immunological Methods*, 102, 259-274.
- GHOSH, G., DUYNE, G. V., GHOSH, S. & SIGLER, P. B. 1995. Structure of NF- κ B p50 homodimer bound to a κ B site. *Nature*, 373, 303-310.
- GHOSH, S. & BALTIMORE, D. 1990. Activation in vitro of NF- κ B" by phosphorylation of its inhibitor I κ B". *Nature*, 344, 678-682.
- GHOSH, S., GIFFORD, A. M., RIVIERE, L. R., TEMPST, P., NOLAN, G. P. & BALTIMORE, D. 1990. Cloning of the p50 DNA binding subunit of NF- κ B: Homology to rel and dorsal. *Cell*, 62, 1019-1029.
- GHOSH, S. & HAYDEN, M. S. 2008. New regulators of NF- κ B in inflammation. *Nat Rev Immunol*, 8, 837-848.
- GHOSH, S. & KARIN, M. 2002. Missing Pieces in the NF- κ B Puzzle. *Cell*, 109, S81-S96.
- GILMORE, T. & GARBATI, M. 2011. Inhibition of NF- κ B Signaling as a Strategy in Disease Therapy. In: KARIN, M. (ed.) *NF- κ B in Health and Disease*. Springer Berlin Heidelberg.
- GILMORE, T. D. & HERSCOVITCH, M. 2000. Inhibitors of NF- κ B signaling: 785 and counting. *Oncogene*, 25, 6887-6899.
- GLICKMAN, M. H. & CIECHANOVER, A. 2002. The Ubiquitin-Proteasome Proteolytic Pathway: Destruction for the Sake of Construction. *Physiological Reviews*, 82, 373-428.
- GUAN, H., HOU, S. & RICCIARDI, R. P. 2005. DNA Binding of Repressor Nuclear Factor- κ B p50/p50 Depends on Phosphorylation of Ser337 by the Protein Kinase A Catalytic Subunit. *Journal of Biological Chemistry*, 280, 9957-9962.
- GUHA, M., O'CONNELL, M. A., PAWLINSKI, R., HOLLIS, A., MCGOVERN, P., YAN, S.-F., STERN, D. & MACKMAN, N. 2001. Lipopolysaccharide activation of the MEK-ERK1/2 pathway in human monocytic cells mediates tissue factor and tumor necrosis factor α expression by inducing Elk-1 phosphorylation and Egr-1 expression: Presented in abstract form at the 42nd annual meeting of the American Society of Hematology, December 1-5, 2000, San Francisco, CA. *Blood*, 98, 1429-1439.
- HAMMER, M., MAGES, J., DIETRICH, H., SERVATIUS, A., HOWELLS, N., CATO, A. C. B. & LANG, R. 2006. Dual specificity phosphatase 1 (DUSP1) regulates a subset of LPS-induced genes and protects mice from lethal endotoxin shock. *The Journal of Experimental Medicine*, 203, 15-20.
- HASHIMOTO, C., GERTTULA, S. & ANDERSON, K. V. 1991. Plasma membrane localization of the Toll protein in the syncytial Drosophila embryo: importance of transmembrane signaling for dorsal-ventral pattern formation. *Development*, 111, 1021-1028.

- HASHIMOTO, C., HUDSON, K. L. & ANDERSON, K. V. 1988. The Toll gene of drosophila, required for dorsal-ventral embryonic polarity, appears to encode a transmembrane protein. *Cell*, 52, 269-279.
- HASKILL, S., BEG, A. A., TOMPKINS, S. M., MORRIS, J. S., YUROCHKO, A. D., SAMPSON-JOHANNES, A., MONDAL, K., RALPH, P. & BALDWIN JR, A. S. 1991. Characterization of an immediate-early gene induced in adherent monocytes that encodes I κ B-like activity. *Cell*, 65, 1281-1289.
- HAYDEN, M. S. & GHOSH, S. 2004. Signaling to NF- κ B. *Genes & Development*, 18, 2195-2224.
- HAYDEN, M. S. & GHOSH, S. 2012. NF- κ B, the first quarter-century: remarkable progress and outstanding questions. *Genes & Development*, 26, 203-234.
- HEISSMEYER, V., KRAPPMANN, D., HATADA, E. N. & SCHEIDEREIT, C. 2001. Shared Pathways of I κ B Kinase-Induced SCFBTrCP-Mediated Ubiquitination and Degradation for the NF- κ B Precursor p105 and I κ B α . *Molecular and Cellular Biology*, 21, 1024-1035.
- HERRERA, R., AGARWAL, S., WALTON, K., SATTERBERG, B., DISTEL, R., GOODMAN, R., SPIEGELMAN, B. & ROBERTS, T. 1990. A direct role for c-fos in AP-1-dependent gene transcription. *Cell Growth Differ*, 1, 483-490.
- HERSHKO, A., HELLER, H., ELIAS, S. & CIECHANOVER, A. 1983. Components of ubiquitin-protein ligase system. Resolution, affinity purification, and role in protein breakdown. *Journal of Biological Chemistry*, 258, 8206-14.
- HINZ, M., ARSLAN, S. Ç. & SCHEIDEREIT, C. 2012. It takes two to tango: I κ Bs, the multifunctional partners of NF- κ B. *Immunological Reviews*, 246, 59-76.
- HISHIKI, T., OHSHIMA, T., EGO, T. & SHIMOTOHNO, K. 2007. BCL3 acts as a negative regulator of transcription from the human T-cell leukemia virus type 1 long terminal repeat through interactions with TORC3. *J Biol Chem*, 282, 28335-43.
- HOFFMANN, A., LEUNG, T. H. & BALTIMORE, D. 2003. Genetic analysis of NF- κ B/Rel transcription factors defines functional specificities. *The EMBO Journal*, 22, 5530-5539.
- HOFFMANN, A., LEVCHENKO, A., SCOTT, M. L. & BALTIMORE, D. 2002. The I κ B-NF- κ B Signaling Module: Temporal Control and Selective Gene Activation. *Science*, 298, 1241-1245.
- HOFFMANN, A., NATOLI, G. & GHOSH, G. 2006. Transcriptional regulation via the NF- κ B signaling module. *Oncogene*, 25, 6706-6716.
- HORNBECK, P. V., KORNHAUSER, J. M., TKACHEV, S., ZHANG, B., SKRZYPEK, E., MURRAY, B., LATHAM, V. & SULLIVAN, M. 2012. PhosphoSitePlus: a comprehensive resource for investigating the structure and function of experimentally determined post-translational modifications in man and mouse. *Nucleic Acids Res*, 40, D261-70.
- HORNG, T., BARTON, G. M. & MEDZHITOV, R. 2001. TIRAP: an adapter molecule in the Toll signaling pathway. *Nat Immunol*, 2, 835-841.
- HOSHINO, K., TAKEUCHI, O., KAWAI, T., SANJO, H., OGAWA, T., TAKEDA, Y., TAKEDA, K. & AKIRA, S. 1999. Cutting Edge: Toll-Like Receptor 4 (TLR4)-Deficient Mice Are Hyporesponsive to Lipopolysaccharide: Evidence for TLR4 as the Lps Gene Product. *The Journal of Immunology*, 162, 3749-3752.
- HOU, S., GUAN, H. & RICCIARDI, R. P. 2003. Phosphorylation of Serine 337 of NF- κ B p50 Is Critical for DNA Binding. *Journal of Biological Chemistry*, 278, 45994-45998.
- HUANG, D.-B., CHEN, Y.-Q., RUETSCHKE, M., PHELPS, C. B. & GHOSH, G. 2001. X-Ray Crystal Structure of Proto-Oncogene Product c-Rel Bound to the CD28 Response Element of IL-2. *Structure*, 9, 669-678.
- HUANG, T. T., KUDO, N., YOSHIDA, M. & MIYAMOTO, S. 2000. A nuclear export signal in the N-terminal regulatory domain of I κ B α controls cytoplasmic

- localization of inactive NF- κ B/I κ B α complexes. *Proceedings of the National Academy of Sciences*, 97, 1014-1019.
- HUXFORD, T. & GHOSH, G. 2009. A Structural Guide to Proteins of the NF- κ B Signaling Module. *Cold Spring Harbor Perspectives in Biology*, 1.
- HUXFORD, T., HUANG, D.-B., MALEK, S. & GHOSH, G. 1998. The Crystal Structure of the I κ B \pm /NF- κ B Complex Reveals Mechanisms of NF- κ B Inactivation. *Cell*, 95, 759-770.
- IKEDA, F. & DIKIC, I. 2008. Atypical ubiquitin chains: new molecular signals. *EMBO Rep*, 9, 536-542.
- IMBERT, V., RUPEC, R. A., LIVOLSI, A., PAHL, H. L., TRAENCKNER, E. B.-M., MUELLER-DIECKMANN, C., FARAHIFAR, D., ROSSI, B., AUBERGER, P., BAEUERLE, P. A. & PEYRON, J.-F. 1996. Tyrosine Phosphorylation of I κ B \pm Activates NF- κ B without Proteolytic Degradation of I κ B \pm . *Cell*, 86, 787-798.
- ISRAËL, A. 2010. The IKK Complex, a Central Regulator of NF- κ B Activation. *Cold Spring Harbor Perspectives in Biology*, 2.
- ISSAEVA, N., BOZKO, P., ENGE, M., PROTOPOPOVA, M., VERHOEF, L. G. G. C., MASUCCI, M., PRAMANIK, A. & SELIVANOVA, G. 2004. Small molecule RITA binds to p53, blocks p53-HDM-2 interaction and activates p53 function in tumors. *Nat Med*, 10, 1321-1328.
- JACOBS, M. D. & HARRISON, S. C. 1998. Structure of an I κ B \pm /NF- κ B Complex. *Cell*, 95, 749-758.
- JAMALUDDIN, M., CHOUDHARY, S., WANG, S., CASOLA, A., HUDA, R., GAROFALO, R. P., RAY, S. & BRASIER, A. R. 2005. Respiratory syncytial virus-inducible BCL-3 expression antagonizes the STAT/IRF and NF-kappaB signaling pathways by inducing histone deacetylase 1 recruitment to the interleukin-8 promoter. *J Virol*, 79, 15302-13.
- JANEWAY, C. A. 1989. Approaching the Asymptote? Evolution and Revolution in Immunology. *Cold Spring Harbor Symposia on Quantitative Biology*, 54, 1-13.
- JÄRVER, P. & LANGEL, Ü. 2006. Cell-penetrating peptides—A brief introduction. *Biochimica et Biophysica Acta (BBA) - Biomembranes*, 1758, 260-263.
- JOHNSON, C., VAN ANTWERP, D. & HOPE, T. J. 1999. An N-terminal nuclear export signal is required for the nucleocytoplasmic shuttling of I κ B α . *EMBO J*, 18, 6682-6693.
- KABUTA, T., HAKUNO, F., CHO, Y., YAMANAKA, D., CHIDA, K., ASANO, T., WADA, K. & TAKAHASHI, S. 2010. Insulin receptor substrate-3, interacting with Bcl-3, enhances p50 NF-kappaB activity. *Biochem Biophys Res Commun*, 394, 697-702.
- KAISER, F., COOK, D., PAPOUTSOPOULOU, S., RAJSBAUM, R., WU, X., YANG, H.-T., GRANT, S., RICCIARDI-CASTAGNOLI, P., TSICHLIS, P. N., LEY, S. C. & O'GARRA, A. 2009. TPL-2 negatively regulates interferon- β production in macrophages and myeloid dendritic cells. *The Journal of Experimental Medicine*, 206, 1863-1871.
- KAKIMOTO, K., MUSIKACHAROEN, T., CHIBA, N., BANDOW, K., OHNISHI, T. & MATSUGUCHI, T. 2010. Cot/Tpl2 regulates IL-23 p19 expression in LPS-stimulated macrophages through ERK activation. *Journal of Physiology and Biochemistry*, 66, 47-53.
- KANAREK, N. & BEN-NERIAH, Y. 2012. Regulation of NF- κ B by ubiquitination and degradation of the I κ Bs. *Immunological Reviews*, 246, 77-94.
- KANAREK, N., LONDON, N., SCHUELER-FURMAN, O. & BEN-NERIAH, Y. 2010. Ubiquitination and Degradation of the Inhibitors of NF- κ B. *Cold Spring Harbor Perspectives in Biology*, 2.
- KARIN, M. 1995. The Regulation of AP-1 Activity by Mitogen-activated Protein Kinases. *Journal of Biological Chemistry*, 270, 16483-16486.

- KARIN, M., LIU, Z.-G. & ZANDI, E. 1997. AP-1 function and regulation. *Current Opinion in Cell Biology*, 9, 240-246.
- KASTENBAUER, S. & ZIEGLER-HEITBROCK, H. W. L. 1999. NF- κ B1 (p50) Is Upregulated in Lipopolysaccharide Tolerance and Can Block Tumor Necrosis Factor Gene Expression. *Infection and Immunity*, 67, 1553-1559.
- KAWAI, T., ADACHI, O., OGAWA, T., TAKEDA, K. & AKIRA, S. 1999. Unresponsiveness of MyD88-Deficient Mice to Endotoxin. *Immunity*, 11, 115-122.
- KAWAI, T. & AKIRA, S. 2007. Signaling to NF- κ B by Toll-like receptors. *Trends in Molecular Medicine*, 13, 460-469.
- KAWAI, T., TAKEUCHI, O., FUJITA, T., INOUE, J.-I., MÜHLRADT, P. F., SATO, S., HOSHINO, K. & AKIRA, S. 2001. Lipopolysaccharide Stimulates the MyD88-Independent Pathway and Results in Activation of IFN-Regulatory Factor 3 and the Expression of a Subset of Lipopolysaccharide-Inducible Genes. *The Journal of Immunology*, 167, 5887-5894.
- KELLEY, L. A. & STERNBERG, M. J. E. 2009. Protein structure prediction on the Web: a case study using the Phyre server. *Nat. Protocols*, 4, 363-371.
- KERR, L. D., DUCKETT, C. S., WAMSLEY, P., ZHANG, Q., CHIAO, P., NABEL, G., MCKEITHAN, T. W., BAEUERLE, P. A. & VERMA, I. M. 1992. The proto-oncogene bcl-3 encodes an I kappa B protein. *Genes & Development*, 6, 2352-2363.
- KESHET, Y. & SEGER, R. 2010. The MAP Kinase Signaling Cascades: A System of Hundreds of Components Regulates a Diverse Array of Physiological Functions. In: SEGER, R. (ed.) *MAP Kinase Signaling Protocols*. Humana Press.
- KESKIN, O., MA, B. & NUSSINOV, R. 2005. Hot Regions in Protein-Protein Interactions: The Organization and Contribution of Structurally Conserved Hot Spot Residues. *Journal of Molecular Biology*, 345, 1281-1294.
- KIELY, P. A., BAILLIE, G. S., BARRETT, R., BUCKLEY, D. A., ADAMS, D. R., HOUSLAY, M. D. & O'CONNOR, R. 2009. Phosphorylation of RACK1 on tyrosine 52 by c-Abl is required for insulin-like growth factor I-mediated regulation of focal adhesion kinase. *J Biol Chem*, 284, 20263-74.
- KIERNAN, R., BRÉS, V., NG, R. W. M., COUDART, M.-P., EL MESSAOUDI, S., SARDET, C., JIN, D.-Y., EMILIANI, S. & BENKIRANE, M. 2003. Post-activation Turn-off of NF- κ B-dependent Transcription Is Regulated by Acetylation of p65. *Journal of Biological Chemistry*, 278, 2758-2766.
- KOMANDER, D., CLAGUE, M. J. & URBE, S. 2009. Breaking the chains: structure and function of the deubiquitinases. *Nat Rev Mol Cell Biol*, 10, 550-563.
- KONDO, T., KAWAI, T. & AKIRA, S. 2012. Dissecting negative regulation of Toll-like receptor signaling. *Trends in immunology*, 33, 449-458.
- KONTOYIANNIS, D., BOULOUGOURIS, G., MANOLOUKOS, M., ARMAKA, M., APOSTOLAKI, M., PIZARRO, T., KOTLYAROV, A., FORSTER, I., FLAVELL, R., GAESTEL, M., TSICHLIS, P., COMINELLI, F. & KOLLIAS, G. 2002. Genetic Dissection of the Cellular Pathways and Signaling Mechanisms in Modeled Tumor Necrosis Factor-induced Crohn's-like Inflammatory Bowel Disease. *The Journal of Experimental Medicine*, 196, 1563-1574.
- KRAMER, A. & SCHNEIDER-MERGENER, J. 1998. Synthesis and screening of peptide libraries on continuous cellulose membrane supports. *Methods Mol Biol*, 87, 25-39.
- KREISEL, D., SUGIMOTO, S., TIETJENS, J., ZHU, J., YAMAMOTO, S., KRUPNICK, A. S., CARMODY, R. J. & GELMAN, A. E. 2011. Bcl3 prevents acute inflammatory lung injury in mice by restraining emergency granulopoiesis. *The Journal of Clinical Investigation*, 121, 265-276.

- KULATHU, Y. & KOMANDER, D. 2012. Atypical ubiquitylation – the unexplored world of polyubiquitin beyond Lys48 and Lys63 linkages. *Nat Rev Mol Cell Biol*, 13, 508-523.
- LA COUR, T., KIEMER, L., MOLGAARD, A., GUPTA, R., SKRIVER, K. & BRUNAK, S. 2004. Analysis and prediction of leucine-rich nuclear export signals. *Protein Eng Des Sel*, 17, 527-36.
- LANG, V., JANZEN, J., FISCHER, G. Z., SONEJI, Y., BEINKE, S., SALMERON, A., ALLEN, H., HAY, R. T., BEN-NERIAH, Y. & LEY, S. C. 2003. BTrCP-Mediated Proteolysis of NF- κ B1 p105 Requires Phosphorylation of p105 Serines 927 and 932. *Molecular and Cellular Biology*, 23, 402-413.
- LANG, V., SYMONS, A., WATTON, S. J., JANZEN, J., SONEJI, Y., BEINKE, S., HOWELL, S. & LEY, S. C. 2004. ABIN-2 Forms a Ternary Complex with TPL-2 and NF- κ B1 p105 and Is Essential for TPL-2 Protein Stability. *Molecular and Cellular Biology*, 24, 5235-5248.
- LANGE, A., MILLS, R. E., LANGE, C. J., STEWART, M., DEVINE, S. E. & CORBETT, A. H. 2007. Classical Nuclear Localization Signals: Definition, Function, and Interaction with Importin α . *Journal of Biological Chemistry*, 282, 5101-5105.
- LANGEL, U. 2006. Preface. In: LANGEL, U. (ed.) *Handbook of Cell Penetrating Peptides*. CRC press.
- LATIMER, M., ERNST, M. K., DUNN, L. L., DRUTSKAYA, M. & RICE, N. R. 1998. The N-terminal domain of I κ B α masks the nuclear localization signal(s) of p50 and c-Rel homodimers. *Mol Cell Biol*, 18, 2640-9.
- LATRES, E., CHIAUR, D. S. & PAGANO, M. 1999. The human F box protein beta-Trcp associates with the Cul1/Skp1 complex and regulates the stability of beta-catenin. *Oncogene*, 18, 849-854.
- LEE, C. C., AVALOS, A. M. & PLOEGH, H. L. 2012. Accessory molecules for Toll-like receptors and their function. *Nat Rev Immunol*, 12, 168-179.
- LEE, J., MIRA-ARBIBE, L. & ULEVITCH, R. J. 2000. TAK1 regulates multiple protein kinase cascades activated by bacterial lipopolysaccharide. *Journal of Leukocyte Biology*, 68, 909-915.
- LETUNIC, I., DOERKS, T. & BORK, P. 2012. SMART 7: recent updates to the protein domain annotation resource. *Nucleic Acids Research*, 40, D302-D305.
- LI, H., WITTEWER, T., WEBER, A., SCHNEIDER, H., MORENO, R., MAINE, G. N., KRACHT, M., SCHMITZ, M. L. & BURSTEIN, E. 2012. Regulation of NF- κ B activity by competition between RelA acetylation and ubiquitination. *Oncogene*, 31, 611-623.
- LI, J., MAHAJAN, A. & TSAI, M.-D. 2006. Ankyrin Repeat: A Unique Motif Mediating Protein-Protein Interactions. *Biochemistry*, 45, 15168-15178.
- LI, X., FENG, J., CHEN, S., PENG, L., HE, W.-W., QI, J., DENG, H. & SUN, R. 2010. Tpl2/AP-1 Enhances Murine Gammaherpesvirus 68 Lytic Replication. *Journal of Virology*, 84, 1881-1890.
- LI, Z. & NABEL, G. J. 1997. A new member of the I κ B protein family, I κ B ϵ , inhibits RelA (p65)-mediated NF- κ B transcription. *Molecular and Cellular Biology*, 17, 6184-90.
- LIEW, F. Y., XU, D., BRINT, E. K. & O'NEILL, L. A. J. 2005. Negative regulation of Toll-like receptor-mediated immune responses. *Nat Rev Immunol*, 5, 446-458.
- LIN, L., DEMARTINO, G. N. & GREENE, W. C. 1998. Cotranslational Biogenesis of NF- κ B p50 by the 26S Proteasome. *Cell*, 92, 819-828.
- LIN, L., DEMARTINO, G. N. & GREENE, W. C. 2000. Cotranslational dimerization of the Rel homology domain of NF- κ B1 generates p50-p105 heterodimers and is required for effective p50 production.

- LIN, L. & GHOSH, S. 1996. A glycine-rich region in NF-kappaB p105 functions as a processing signal for the generation of the p50 subunit. *Molecular and Cellular Biology*, 16, 2248-54.
- LIN, R., GEWERT, D. & HISCOTT, J. 1995. Differential Transcriptional Activation in Vitro by NF-B/Rel Proteins. *Journal of Biological Chemistry*, 270, 3123-3131.
- LUCIANO, B. S., HSU, S., CHANNAVAJHALA, P. L., LIN, L.-L. & CUOZZO, J. W. 2004. Phosphorylation of Threonine 290 in the Activation Loop of Tpl2/Cot Is Necessary but Not Sufficient for Kinase Activity. *Journal of Biological Chemistry*, 279, 52117-52123.
- LUX, S. E., JOHN, K. M. & BENNETT, V. 1990. Analysis of cDNA for human erythrocyte ankyrin indicates a repeated structure with homology to tissue-differentiation and cell-cycle control proteins. *Nature*, 344, 36 - 42.
- MADANI, F., LINDBERG, S., LANGEL, #220, LO, FUTAKI, S., GR, #228 & SLUND, A. 2011. Mechanisms of Cellular Uptake of Cell-Penetrating Peptides. *Journal of Biophysics*, 2011.
- MAINE, G. N., MAO, X., KOMARCK, C. M. & BURSTEIN, E. 2007. COMMD1 promotes the ubiquitination of NF-kB subunits through a cullin-containing ubiquitin ligase. *The EMBO Journal*, 26, 436-447.
- MALEK, S., CHEN, Y., HUXFORD, T. & GHOSH, G. 2001. IkbB, but Not Ikb α , Functions as a Classical Cytoplasmic Inhibitor of NF-kB Dimers by Masking Both NF-kB Nuclear Localization Sequences in Resting Cells. *Journal of Biological Chemistry*, 276, 45225-45235.
- MALEK, S., HUANG, D.-B., HUXFORD, T., GHOSH, S. & GHOSH, G. 2003. X-ray Crystal Structure of an IkbB-NF-kB p65 Homodimer Complex. *Journal of Biological Chemistry*, 278, 23094-23100.
- MANAVALAN, B., BASITH, S., CHOI, Y.-M., LEE, G. & CHOI, S. 2010. Structure-Function Relationship of Cytoplasmic and Nuclear Ikb Proteins: An In Silico Analysis. *PLoS ONE*, 5, e15782.
- MAY, M. J., D'ACQUISTO, F., MADGE, L. A., GLÖCKNER, J., POBER, J. S. & GHOSH, S. 2000. Selective Inhibition of NF-kB Activation by a Peptide That Blocks the Interaction of NEMO with the Ikb Kinase Complex. *Science*, 289, 1550-1554.
- MCKEITHAN, T. W., ROWLEY, J. D., SHOWS, T. B. & DIAZ, M. O. 1987. Cloning of the chromosome translocation breakpoint junction of the t(14;19) in chronic lymphocytic leukemia. *Proceedings of the National Academy of Sciences*, 84, 9257-9260.
- MEDVEDEV, A. E., KOPYDLOWSKI, K. M. & VOGEL, S. N. 2000. Inhibition of Lipopolysaccharide-Induced Signal Transduction in Endotoxin-Tolerized Mouse Macrophages: Dysregulation of Cytokine, Chemokine, and Toll-Like Receptor 2 and 4 Gene Expression. *The Journal of Immunology*, 164, 5564-5574.
- MEDZHITOV, R., PRESTON-HURLBURT, P. & JANEWAY, C. A. 1997. A human homologue of the Drosophila Toll protein signals activation of adaptive immunity. *Nature*, 388, 394-397.
- MEDZHITOV, R., PRESTON-HURLBURT, P., KOPP, E., STADLEN, A., CHEN, C., GHOSH, S. & JANEWAY JR, C. A. 1998. MyD88 Is an Adaptor Protein in the hToll/IL-1 Receptor Family Signaling Pathways. *Molecular Cell*, 2, 253-258.
- MERCURIO, F., ZHU, H., MURRAY, B. W., SHEVCHENKO, A., BENNETT, B. L., LI, J. W., YOUNG, D. B., BARBOSA, M., MANN, M., MANNING, A. & RAO, A. 1997. IKK-1 and IKK-2: Cytokine-Activated Ikb Kinases Essential for NF-kB Activation. *Science*, 278, 860-866.
- MEYLAN, E. & TSCHOPP, J. 2008. IRAK2 takes its place in TLR signaling. *Nat Immunol*, 9, 581-582.

- MICHEL ESPINOZA-FONSECA, L. 2005. Targeting MDM2 by the small molecule RITA: towards the development of new multi-target drugs against cancer. *Theoretical Biology and Medical Modelling*, 2, 1-6.
- MICHEL, F., SOLER-LOPEZ, M., PETOSA, C., CRAMER, P., SIEBENLIST, U. & MULLER, C. W. 2001. Crystal structure of the ankyrin repeat domain of Bcl-3: a unique member of the I[κ]B protein family. *EMBO J*, 20, 6180-6190.
- MIELKE, L. A., ELKINS, K. L., WEI, L., STARR, R., TSICHLIS, P. N., O'SHEA, J. J. & WATFORD, W. T. 2009. Tumor Progression Locus 2 (Map3k8) Is Critical for Host Defense against *Listeria monocytogenes* and IL-1 β Production. *The Journal of Immunology*, 183, 7984-7993.
- MILLETTI, F. 2012. Cell-penetrating peptides: classes, origin, and current landscape. *Drug Discovery Today*, 17, 850-860.
- MITCHELL, T. C., THOMPSON, B. S., TRENT, J. O. & CASELLA, C. R. 2002. A Short Domain within Bcl-3 Is Responsible for Its Lymphocyte Survival Activity. *Annals of the New York Academy of Sciences*, 975, 132-147.
- MIYAMOTO, S., MAKI, M., SCHMITT, M. J., HATANAKA, M. & VERMA, I. M. 1994. Tumor necrosis factor alpha-induced phosphorylation of I kappa B alpha is a signal for its degradation but not dissociation from NF-kappa B. *Proceedings of the National Academy of Sciences*, 91, 12740-12744.
- MIYOSHI, J., HIGASHI, T., MUKAI, H., OHUCHI, T. & KAKUNAGA, T. 1991. Structure and transforming potential of the human cot oncogene encoding a putative protein kinase. *Molecular and Cellular Biology*, 11, 4088-4096.
- MONJE, P., MARINISSEN, M. J. & GUTKIND, J. S. 2003. Phosphorylation of the Carboxyl-Terminal Transactivation Domain of c-Fos by Extracellular Signal-Regulated Kinase Mediates the Transcriptional Activation of AP-1 and Cellular Transformation Induced by Platelet-Derived Growth Factor. *Molecular and Cellular Biology*, 23, 7030-7043.
- MOORTHY, A. K., HUXFORD, T. & GHOSH, G. 2010. Structural aspects of NF- κ B and I κ B proteins. In: GHOSH, S. (ed.) *Handbook of Transcription Factor NF-kappa B*. CRC Press.
- MOREIRA, I. S., FERNANDES, P. A. & RAMOS, M. J. 2007. Hot spots—A review of the protein-protein interface determinant amino-acid residues. *Proteins: Structure, Function, and Bioinformatics*, 68, 803-812.
- MORENO, R., SOBOTZIK, J.-M., SCHULTZ, C. & SCHMITZ, M. L. 2010. Specification of the NF- κ B transcriptional response by p65 phosphorylation and TNF-induced nuclear translocation of IKK ϵ . *Nucleic Acids Research*, 38, 6029-6044.
- MOSAVI, L. K., CAMMETT, T. J., DESROSIERS, D. C. & PENG, Z.-Y. 2004. The ankyrin repeat as molecular architecture for protein recognition. *Protein Science*, 13, 1435-1448.
- MOSAVI, L. K., MINOR, D. L. & PENG, Z.-Y. 2002. Consensus-derived structural determinants of the ankyrin repeat motif. *Proceedings of the National Academy of Sciences*, 99, 16029-16034.
- MUHLBAUER, M., CHILTON, P. M., MITCHELL, T. C. & JOBIN, C. 2008. Impaired Bcl3 up-regulation leads to enhanced lipopolysaccharide-induced interleukin (IL)-23P19 gene expression in IL-10(-/-) mice. *J Biol Chem*, 283, 14182-9.
- MULERO, MARÍA C., FERRER-MARCO, D., ISLAM, A., MARGALEF, P., PECORARO, M., TOLL, A., DRECHSEL, N., CHARNECO, C., DAVIS, S., BELLORA, N., GALLARDO, F., LÓPEZ-ARRIBILLAGA, E., ASENSIO-JUAN, E., RODILLA, V., GONZÁLEZ, J., IGLESIAS, M., SHIH, V., MAR ALBÀ, M., DI CROCE, L., HOFFMANN, A., MIYAMOTO, S., VILLÀ-FREIXA, J., LÓPEZ-BIGAS, N., KEYES, WILLIAM M., DOMÍNGUEZ, M., BIGAS, A. & ESPINOSA, L. 2013. Chromatin-Bound I κ B α Regulates a Subset of Polycomb Target Genes in Differentiation and Cancer. *Cancer Cell*, 24, 151-166.

- MÜLLER, C. W. & HARRISON, S. C. 1995. The structure of the NF- κ B p50:DNA-complex a starting point for analyzing the Rel family. *FEBS Letters*, 369, 113-117.
- MÜLLER, C. W., REY, F. A. & HARRISON, S. C. 1996. Comparison of two different DNA-binding modes of the NF-kappa B p50 homodimer. *Nature structural biology*, 3, 224-227.
- MULLER, C. W., REY, F. A., SODEOKA, M., VERDINE, G. L. & HARRISON, S. C. 1995. Structure of the NF-[kappa]B p50 homodimer bound to DNA. *Nature*, 373, 311-317.
- MURPHY, L. O. & BLENIS, J. 2006. MAPK signal specificity: the right place at the right time. *Trends in biochemical sciences*, 31, 268-275.
- MURRAY, P. J. & WYNN, T. A. 2011. Protective and pathogenic functions of macrophage subsets. *Nat Rev Immunol*, 11, 723-737.
- NA, S. Y., CHOI, H. S., KIM, J. W., NA, D. S. & LEE, J. W. 1998. Bcl3, an IkappaB protein, as a novel transcription coactivator of the retinoid X receptor. *J Biol Chem*, 273, 30933-8.
- NA, S. Y., CHOI, J. E., KIM, H. J., JHUN, B. H., LEE, Y. C. & LEE, J. W. 1999. Bcl3, an IkappaB protein, stimulates activating protein-1 transactivation and cellular proliferation. *J Biol Chem*, 274, 28491-6.
- NATOLI, G., SACCANI, S., BOSISIO, D. & MARAZZI, I. 2005. Interactions of NF-[kappa]B with chromatin: the art of being at the right place at the right time. *Nat Immunol*, 6, 439-445.
- NAUMANN, M. & SCHEIDEREIT, C. 1994. Activation of NF-kappa B in vivo is regulated by multiple phosphorylations. *The EMBO journal*, 13, 11.
- NEWTON, K. & DIXIT, V. M. 2012. Signaling in Innate Immunity and Inflammation. *Cold Spring Harbor Perspectives in Biology*, 4.
- NOLAN, G. P., FUJITA, T., BHATIA, K., HUPPI, C., LIU, H. C., SCOTT, M. L. & BALTIMORE, D. 1993. The bcl-3 proto-oncogene encodes a nuclear I kappa B-like molecule that preferentially interacts with NF-kappa B p50 and p52 in a phosphorylation-dependent manner. *Molecular and Cellular Biology*, 13, 3557-3566.
- O'CARROLL, C., MOLONEY, G., HURLEY, G., MELGAR, S., BRINT, E., NALLY, K., NIBBS, R. J., SHANAHAN, F. & CARMODY, R. J. 2013. Bcl-3 deficiency protects against dextran-sodium sulphate-induced colitis in the mouse. *Clinical & Experimental Immunology*, 173, 332-342.
- O'DEA, E. & HOFFMANN, A. 2010. The Regulatory Logic of the NF- κ B Signaling System. *Cold Spring Harbor Perspectives in Biology*, 2.
- O'NEILL, L. A. J. & BOWIE, A. G. 2007. The family of five: TIR-domain-containing adaptors in Toll-like receptor signalling. *Nat Rev Immunol*, 7, 353-364.
- O'NEILL, L. A. J., GOLENBOCK, D. & BOWIE, A. G. 2013. The history of Toll-like receptors [mdash] redefining innate immunity. *Nat Rev Immunol*, 13, 453-460.
- OAKLEY, F., MANN, J., NAILARD, S., SMART, D. E., MUNGALSINGH, N., CONSTANDINOU, C., ALI, S., WILSON, S. J., MILLWARD-SADLER, H., IREDALE, J. P. & MANN, D. A. 2005. Nuclear Factor- κ B1 (p50) Limits the Inflammatory and Fibrogenic Responses to Chronic Injury. *The American journal of pathology*, 166, 695-708.
- ODEGAARD, J. I. & CHAWLA, A. 2008. Mechanisms of macrophage activation in obesity-induced insulin resistance. *Nat Clin Pract End Met*, 4, 619-626.
- OECKINGHAUS, A. & GHOSH, S. 2009. The NF- κ B Family of Transcription Factors and Its Regulation. *Cold Spring Harbor Perspectives in Biology*, 1.
- OHNO, H., TAKIMOTO, G. & MCKEITHAN, T. W. 1990. The candidate proto-oncogene bcl-3 is related to genes implicated in cell lineage determination and cell cycle control. *Cell*, 60, 991-997.

- OKAZAKI, K. & SAGATA, N. 1995. The Mos/MAP kinase pathway stabilizes c-Fos by phosphorylation and augments its transforming activity in NIH 3T3 cells. *The EMBO journal*, 14, 5048-5059.
- ORANGE, J. S. & MAY, M. J. 2008. Cell penetrating peptide inhibitors of Nuclear Factor-kappa B. *Cellular and Molecular Life Sciences*, 65, 3564-3591.
- ORIAN, A., GONEN, H., BERCOVICH, B., FAJERMAN, I., EYTAN, E., ISRAEL, A., MERCURIO, F., IWAI, K., SCHWARTZ, A. L. & CIECHANOVER, A. 2000. SCF[beta]-TrCP ubiquitin ligase-mediated processing of NF-[kappa]B p 105 requires phosphorylation of its C-terminus by I[kappa]B kinase. *EMBO J*, 19, 2580-2591.
- ORIAN, A., SCHWARTZ, A. L., ISRAËL, A., WHITESIDE, S., KAHANA, C. & CIECHANOVER, A. 1999. Structural Motifs Involved in Ubiquitin-Mediated Processing of the NF- κ B Precursor p105: Roles of the Glycine-Rich Region and a Downstream Ubiquitination Domain. *Molecular and Cellular Biology*, 19, 3664-3673.
- ORIAN, A., WHITESIDE, S., ISRAËL, A., STANCOVSKI, I., SCHWARTZ, A. L. & CIECHANOVER, A. 1995. Ubiquitin-mediated Processing of NF- κ B Transcriptional Activator Precursor p105: RECONSTITUTION OF A CELL-FREE SYSTEM AND IDENTIFICATION OF THE UBIQUITIN-CARRIER PROTEIN, E2, AND A NOVEL UBIQUITIN-PROTEIN LIGASE, E3, INVOLVED IN CONJUGATION. *Journal of Biological Chemistry*, 270, 21707-21714.
- OSHIUMI, H., MATSUMOTO, M., FUNAMI, K., AKAZAWA, T. & SEYA, T. 2003a. TICAM-1, an adaptor molecule that participates in Toll-like receptor 3-mediated interferon-[beta] induction. *Nat Immunol*, 4, 161-167.
- OSHIUMI, H., SASAI, M., SHIDA, K., FUJITA, T., MATSUMOTO, M. & SEYA, T. 2003b. TIR-containing Adapter Molecule (TICAM)-2, a Bridging Adapter Recruiting to Toll-like Receptor 4 TICAM-1 That Induces Interferon- β . *Journal of Biological Chemistry*, 278, 49751-49762.
- PANZER, U., STEINMETZ, O. M., TURNER, J. E., MEYER-SCHWESINGER, C., VON RUFFER, C., MEYER, T. N., ZAHNER, G., GÓMEZ-GUERRERO, C., SCHMID, R. M., HELMCHEN, U., MOECKEL, G. W., WOLF, G., STAHL, R. A. K. & THAISS, F. 2009. Resolution of renal inflammation: A new role for NF- κ B1 (p50) in inflammatory kidney diseases. *American Journal of Physiology - Renal Physiology*, 297, F429-F439.
- PARK, S. W., HUQ, M. D. M., HU, X. & WEI, L.-N. 2005. Tyrosine Nitration on p65: A Novel Mechanism to Rapidly Inactivate Nuclear Factor- κ B. *Molecular & Cellular Proteomics*, 4, 300-309.
- PATRIOTIS, C., MAKRIS, A., BEAR, S. E. & TSICHLIS, P. N. 1993. Tumor progression locus 2 (Tpl-2) encodes a protein kinase involved in the progression of rodent T-cell lymphomas and in T-cell activation. *Proceedings of the National Academy of Sciences*, 90, 2251-2255.
- PATRIOTIS, C., MAKRIS, A., CHERNOFF, J. & TSICHLIS, P. N. 1994. Tpl-2 acts in concert with Ras and Raf-1 to activate mitogen-activated protein kinase. *Proceedings of the National Academy of Sciences*, 91, 9755-9759.
- PAXIAN*, S., MERKLE*, H., RIEMANN*, M., WILDA†, M., ADLER*, G., HAMEISTER‡, H., LIPTAY§, S., PFEFFER||, K. & SCHMID*, R. M. 2002. Abnormal organogenesis of Peyer's patches in mice deficient for NF- κ B1, NF- κ B2, and Bcl-3. *Gastroenterology*, 122, 1853-1868.
- PÈNE, F., PAUN, A., SØNDER, S. U., RIKHI, N., WANG, H., CLAUDIO, E. & SIEBENLIST, U. 2011. The I κ B Family Member Bcl-3 Coordinates the Pulmonary Defense against *Klebsiella pneumoniae* Infection. *The Journal of Immunology*, 186, 2412-2421.
- PERKINS, N. D. 2000. Post-translational modifications regulating the activity and function of the nuclear factor kappa B pathway. *Oncogene*, 25, 6717-6730.

- PERKINS, N. D. 2007. Integrating cell-signalling pathways with NF- κ B and IKK function. *Nat Rev Mol Cell Biol*, 8, 49-62.
- PETERSEN, B., PETERSEN, T., ANDERSEN, P., NIELSEN, M. & LUNDEGAARD, C. 2009. A generic method for assignment of reliability scores applied to solvent accessibility predictions. *BMC Structural Biology*, 9, 51.
- PHELPS, C. B., SENGCHANTHALANGSY, L. L., MALEK, S. & GHOSH, G. 2000. Mechanism of κ B DNA binding by Rel/NF- κ B dimers. *Journal of Biological Chemistry*, 275, 24392-24399.
- POLTORAK, A., HE, X., SMIRNOVA, I., LIU, M.-Y. & ET AL. 1998. Defective LPS signaling in C3H/HeJ and C57BL10ScCr mice: Mutations in Tlr4 gene. *Science*, 282, 2085-8.
- QIU, M.-S. & GREEN, S. H. 1992. PC12 cell neuronal differentiation is associated with prolonged p21ras activity and consequent prolonged ERK activity. *Neuron*, 9, 705-717.
- RAO, P., HAYDEN, M. S., LONG, M., SCOTT, M. L., WEST, A. P., ZHANG, D., OECKINGHAUS, A., LYNCH, C., HOFFMANN, A., BALTIMORE, D. & GHOSH, S. 2010. I κ B acts to inhibit and activate gene expression during the inflammatory response. *Nature*, 466, 1115-1119.
- RAPE, M. & JENTSCH, S. 2002. Taking a bite: proteasomal protein processing. *Nat Cell Biol*, 4, E113-E116.
- REINEKE, U., VOLKMER-ENGERT, R. & SCHNEIDER-MERGENER, J. 2001. Applications of peptide arrays prepared by the SPOT-technology. *Current Opinion in Biotechnology*, 12, 59-64.
- RICHARD, J. P., MELIKOV, K., VIVES, E., RAMOS, C., VERBEURE, B., GAIT, M. J., CHERNOMORDIK, L. V. & LEBLEU, B. 2003. Cell-penetrating Peptides: A REEVALUATION OF THE MECHANISM OF CELLULAR UPTAKE. *Journal of Biological Chemistry*, 278, 585-590.
- RICHARD, M., LOUAHED, J., DEMOULIN, J.-B. & RENAULD, J.-C. 1999. Interleukin-9 Regulates NF- κ B Activity Through BCL3 Gene Induction. *Blood*, 93, 4318-4327.
- RIEMANN, M., ENDRES, R., LIPTAY, S., PFEFFER, K. & SCHMID, R. M. 2005. The I κ B Protein Bcl-3 Negatively Regulates Transcription of the IL-10 Gene in Macrophages. *The Journal of Immunology*, 175, 3560-3568.
- ROBINSON, M. J., BEINKE, S., KOUROUMALIS, A., TSICHLIS, P. N. & LEY, S. C. 2007. Phosphorylation of TPL-2 on Serine 400 Is Essential for Lipopolysaccharide Activation of Extracellular Signal-Regulated Kinase in Macrophages. *Molecular and Cellular Biology*, 27, 7355-7364.
- ROCK, F. L., HARDIMAN, G., TIMANS, J. C., KASTELEIN, R. A. & BAZAN, J. F. 1998. A family of human receptors structurally related to Drosophila Toll. *Proceedings of the National Academy of Sciences*, 95, 588-593.
- RODRIGUEZ, M. S., MICHALOPOULOS, I., ARENZANA-SEISDEDOS, F. & HAY, R. T. 1995. Inducible degradation of I κ B α in vitro and in vivo requires the acidic C-terminal domain of the protein. *Molecular and Cellular Biology*, 15, 2413-9.
- RODRIGUEZ, M. S., THOMPSON, J., HAY, R. T. & DARGEMONT, C. 1999. Nuclear Retention of I κ B α Protects It from Signal-induced Degradation and Inhibits Nuclear Factor κ B Transcriptional Activation. *Journal of Biological Chemistry*, 274, 9108-9115.
- ROGERS, S., WELLS, R. & RECHSTEINER, M. 1986. Amino acid sequences common to rapidly degraded proteins: the PEST hypothesis. *Science*, 234, 364-368.
- ROGET, K., BEN-ADDI, A., MAMBOLE-DEMA, A., GANTKE, T., YANG, H.-T., JANZEN, J., MORRICE, N., ABBOTT, D. & LEY, S. C. 2012. I κ B Kinase 2 Regulates TPL-2 Activation of Extracellular Signal-Regulated Kinases 1 and 2 by Direct

- Phosphorylation of TPL-2 Serine 400. *Molecular and Cellular Biology*, 32, 4684-4690.
- ROST, B., YACHDAV, G. & LIU, J. 2004. The PredictProtein server. *Nucleic Acids Research*, 32, W321-W326.
- ROTHWARF, D. M., ZANDI, E., NATOLI, G. & KARIN, M. 1998. IKK- γ is an essential regulatory subunit of the I κ B kinase complex. *Nature*, 395, 297-300.
- ROUX, P. P. & BLENIS, J. 2004. ERK and p38 MAPK-Activated Protein Kinases: a Family of Protein Kinases with Diverse Biological Functions. *Microbiology and Molecular Biology Reviews*, 68, 320-344.
- RUAN, Q., ZHENG, S.-J., PALMER, S., CARMODY, R. J. & CHEN, Y. H. 2010. Roles of Bcl-3 in the Pathogenesis of Murine Type 1 Diabetes. *Diabetes*, 59, 2549-2557.
- RUSHLOW, C. & WARRIOR, R. 1992. The rel family of proteins. *BioEssays*, 14, 89-95.
- RYO, A., SUIZU, F., YOSHIDA, Y., PERREM, K., LIOU, Y.-C., WULF, G., ROTTAPPEL, R., YAMAOKA, S. & LU, K. P. 2003. Regulation of NF- κ B Signaling by Pin1-Dependent Prolyl Isomerization and Ubiquitin-Mediated Proteolysis of p65/RelA. *Molecular Cell*, 12, 1413-1426.
- SACCANI, S., MARAZZI, I., BEG, A. A. & NATOLI, G. 2004. Degradation of promoter-bound p65/RelA is essential for the prompt termination of the nuclear factor κ B response. *J Exp Med*, 200, 107-113.
- SACCANI, S., PANTANO, S. & NATOLI, G. 2003. Modulation of NF- κ B Activity by Exchange of Dimers. *Molecular Cell*, 11, 1563-1574.
- SALMERON, A., AHMAD, T. B., CARLILE, G. W., PAPPIN, D., NARSIMHAN, R. P. & LEY, S. C. 1996. Activation of MEK-1 and SEK-1 by Tpl-2 proto-oncoprotein, a novel MAP kinase kinase kinase. *The EMBO journal*, 15, 817-826.
- SAMBROOK, J. & RUSSELL, D. W. *Molecular Cloning: A Laboratory Manual*, Cold Spring Harbor Laboratory Press.
- SATO, S., SANJO, H., TAKEDA, K., NINOMIYA-TSUJI, J., YAMAMOTO, M., KAWAI, T., MATSUMOTO, K., TAKEUCHI, O. & AKIRA, S. 2005. Essential function for the kinase TAK1 in innate and adaptive immune responses. *Nat Immunol*, 6, 1087-1095.
- SAVINOVA, O. V., HOFFMANN, A. & GHOSH, G. 2009. The Nfkb1 and Nfkb2 Proteins p105 and p100 Function as the Core of High-Molecular-Weight Heterogeneous Complexes. *Molecular Cell*, 34, 591-602.
- SCHEIBEL, M., KLEIN, B., MERKLE, H., SCHULZ, M., FRITSCH, R., GRETEN, F. R., ARKAN, M. C., SCHNEIDER, G. & SCHMID, R. M. 2010. I κ B β is an essential co-activator for LPS-induced IL-1 β transcription in vivo. *The Journal of Experimental Medicine*, 207, 2621-2630.
- SCHNEIDER, D. S., HUDSON, K. L., LIN, T. Y. & ANDERSON, K. V. 1991. Dominant and recessive mutations define functional domains of Toll, a transmembrane protein required for dorsal-ventral polarity in the Drosophila embryo. *Genes & Development*, 5, 797-807.
- SCHULTZ, J., MILPETZ, F., BORK, P. & PONTING, C. P. 1998. SMART, a simple modular architecture research tool: Identification of signaling domains. *Proceedings of the National Academy of Sciences*, 95, 5857-5864.
- SCHWARZ, E. M., KRIMPENFORT, P., BERNS, A. & VERMA, I. M. 1997. Immunological defects in mice with a targeted disruption in Bcl-3. *Genes & Development*, 11, 187-197.
- SEN, R. 2011. The origins of NF- κ B. *Nat Immunol*, 12, 686-688.
- SEN, R. & BALTIMORE, D. 1986a. Inducibility of κ immunoglobulin enhancer-binding protein NF- κ B by a posttranslational mechanism. *Cell*, 47, 921-928.
- SEN, R. & BALTIMORE, D. 1986b. Multiple nuclear factors interact with the immunoglobulin enhancer sequences. *Cell*, 46, 705-716.

- SENGCHANTHALANGSY, L. L., DATTA, S., HUANG, D.-B., ANDERSON, E., BRASWELL, E. H. & GHOSH, G. 1999. Characterization of the Dimer Interface of Transcription Factor NF κ B p50 Homodimer. *Journal of Molecular Biology*, 289, 1029-1040.
- SHA, W. C., LIU, H.-C., TUOMANEN, E. I. & BALTIMORE, D. 1995. Targeted disruption of the p50 subunit of NF- κ B leads to multifocal defects in immune responses. *Cell*, 80, 321-330.
- SHARROCKS, A. D. 2006. Cell Cycle: Sustained ERK Signalling Represses the Inhibitors. *Current Biology*, 16, R540-R542.
- SHAULIAN, E. & KARIN, M. 2002. AP-1 as a regulator of cell life and death. *Nat Cell Biol*, 4, E131-E136.
- SHIM, J.-H., XIAO, C., PASCHAL, A. E., BAILEY, S. T., RAO, P., HAYDEN, M. S., LEE, K.-Y., BUSSEY, C., STECKEL, M., TANAKA, N., YAMADA, G., AKIRA, S., MATSUMOTO, K. & GHOSH, S. 2005. TAK1, but not TAB1 or TAB2, plays an essential role in multiple signaling pathways in vivo. *Genes & Development*, 19, 2668-2681.
- SONG, X. Y., TORPHY, T. J., GRISWOLD, D. E. & SHEALY, D. 2002. Coming of age: anti-cytokine therapies. *Mol Interv*, 2, 36-46.
- SOUTHERN, S. L., COLLARD, T. J., URBAN, B. C., SKEEN, V. R., SMARTT, H. J., HAGUE, A., OAKLEY, F., TOWNSEND, P. A., PERKINS, N. D., PARASKEVA, C. & WILLIAMS, A. C. 2012. BAG-1 interacts with the p50-p50 homodimeric NF-kappa B complex: implications for colorectal carcinogenesis. *Oncogene*, 31, 2761-2772.
- SPENCER, E., JIANG, J. & CHEN, Z. J. 1999. Signal-induced ubiquitination of I κ B α by the F-box protein Slimb/ β -TrCP. *Genes & Development*, 13, 284-294.
- STAFFORD, M. J., MORRICE, N. A., PEGGIE, M. W. & COHEN, P. 2006. Interleukin-1 stimulated activation of the COT catalytic subunit through the phosphorylation of Thr290 and Ser62. *FEBS Letters*, 580, 4010-4014.
- STANLEY, E. R., BERG, K. L., EINSTEIN, D. B., LEE, P. S. W., PIXLEY, F. J., WANG, Y. & YEUNG, Y.-G. 1997. Biology and action of colony-stimulating factor-1. *Molecular Reproduction and Development*, 46, 4-10.
- STERGHIOS MOSCHOS, A. W., MARK A LINDSAY 2006. In vivo applications of cell-penetrating peptides. In: LANGEL, U. (ed.) *Handbook of Cell Penetrating Peptides*. Second ed.: CRC Press.
- STEWART, R. 1989. Relocalization of the dorsal protein from the cytoplasm to the nucleus correlates with its function. *Cell*, 59, 1179-1188.
- SUN, S.-C. 2012. The noncanonical NF- κ B pathway. *Immunological Reviews*, 246, 125-140.
- SUZUKI, H., CHIBA, T., KOBAYASHI, M., TAKEUCHI, M., SUZUKI, T., ICHIYAMA, A., IKENOUE, T., OMATA, M., FURUICHI, K. & TANAKA, K. 1999. I κ B α Ubiquitination Is Catalyzed by an SCF-like Complex Containing Skp1, Cullin-1, and Two F-Box/WD40-Repeat Proteins, β TrCP1 and β TrCP2. *Biochemical and Biophysical Research Communications*, 256, 127-132.
- SWINNEY, D. C., XU, Y.-Z., SCARAFIA, L. E., LEE, I., MAK, A. Y., GAN, Q.-F., RAMESHA, C. S., MULKINS, M. A., DUNN, J., SO, O.-Y., BIEGEL, T., DINH, M., VOLKEL, P., BARNETT, J., DALRYMPLE, S. A., LEE, S. & HUBER, M. 2002. A Small Molecule Ubiquitination Inhibitor Blocks NF- κ B-dependent Cytokine Expression in Cells and Rats. *Journal of Biological Chemistry*, 277, 23573-23581.
- TABAS, I. 2010. Macrophage death and defective inflammation resolution in atherosclerosis. *Nature Reviews Immunology*, 10, 36-46.
- TAM, W. F., LEE, L. H., DAVIS, L. & SEN, R. 2000. Cytoplasmic sequestration of Rel proteins by I κ B α requires CRM1- dependent nuclear export. *Molecular and Cellular Biology*, 20, 2269-2284.

- TANAKA, T., GRUSBY, M. J. & KAISHO, T. 2007. PDLIM2-mediated termination of transcription factor NF- κ B activation by intranuclear sequestration and degradation of the p65 subunit. *Nat Immunol*, 8, 584-591.
- TARCIĆ, G. & YARDEN, Y. 2010. MAP Kinase Activation by Receptor Tyrosine Kinases: In Control of Cell Migration. In: SEGER, R. (ed.) *MAP Kinase Signaling Protocols*. Humana Press.
- TAS, S. W., DE JONG, E. C., HAJJI, N., MAY, M. J., GHOSH, S., VERVOORDELDONK, M. J. & TAK, P. P. 2005. Selective inhibition of NF- κ B in dendritic cells by the NEMO-binding domain peptide blocks maturation and prevents T cell proliferation and polarization. *European Journal of Immunology*, 35, 1164-1174.
- TERGAONKAR, V., CORREA, R. G., IKAWA, M. & VERMA, I. M. 2005. Distinct roles of I κ B proteins in regulating constitutive NF- κ B activity. *Nat Cell Biol*, 7, 921-923.
- THOMPSON, J. E., PHILLIPS, R. J., ERDJUMENT-BROMAGE, H., TEMPST, P. & GHOSH, S. 1995. I κ B- β regulates the persistent response in a biphasic activation of NF- κ B. *Cell*, 80, 573-582.
- THORN, K. S. & BOGAN, A. A. 2001. ASEdb: a database of alanine mutations and their effects on the free energy of binding in protein interactions. *Bioinformatics*, 17, 284-285.
- TORII, S., KUSAKABE, M., YAMAMOTO, T., MAEKAWA, M. & NISHIDA, E. 2004. Sef Is a Spatial Regulator for Ras/MAP Kinase Signaling. *Developmental Cell*, 7, 33-44.
- TÜNNEMANN, G., MARTIN, R. M., HAUPT, S., PATSCH, C., EDENHOFER, F. & CARDOSO, M. C. 2006. Cargo-dependent mode of uptake and bioavailability of TAT-containing proteins and peptides in living cells. *The FASEB Journal*, 20, 1775-1784.
- UDALOVA, I. A., MOTT, R., FIELD, D. & KWIATKOWSKI, D. 2002. Quantitative prediction of NF- κ B DNA- protein interactions. *Proceedings of the National Academy of Sciences*, 99, 8167-8172.
- UEMATSU, S. & AKIRA, S. 2007. Toll-like Receptors and Type I Interferons. *Journal of Biological Chemistry*, 282, 15319-15323.
- VALLEDOR, A. F., COMALADA, M., SANTAMARÍA-BABI, L. F., LLOBERAS, J. & CELADA, A. 2010. Chapter 1 - Macrophage Proinflammatory Activation and Deactivation: A Question of Balance. In: FREDERICK W. ALT, K. F. A. T. H. F. M. J. W. U. & EMIL, R. U. (eds.) *Advances in Immunology*. Academic Press.
- VALLEDOR, A. F., COMALADA, M., XAUS, J. & CELADA, A. 2000. The Differential Time-course of Extracellular-regulated Kinase Activity Correlates with the Macrophage Response toward Proliferation or Activation. *Journal of Biological Chemistry*, 275, 7403-7409.
- VAN AMERSFOORT, E. S., VAN BERKEL, T. J. C. & KUIPER, J. 2003. Receptors, Mediators, and Mechanisms Involved in Bacterial Sepsis and Septic Shock. *Clinical Microbiology Reviews*, 16, 379-414.
- VASSILEV, L. T., VU, B. T., GRAVES, B., CARVAJAL, D., PODLASKI, F., FILIPOVIC, Z., KONG, N., KAMMLOTT, U., LUKACS, C., KLEIN, C., FOTOUHI, N. & LIU, E. A. 2004. In Vivo Activation of the p53 Pathway by Small-Molecule Antagonists of MDM2. *Science*, 303, 844-848.
- VENDEVILLE, A., RAYNE, F., BONHOURE, A., BETTACHE, N., MONTCOURRIER, P. & BEAUMELLE, B. 2004. HIV-1 Tat Enters T Cells Using Coated Pits before Translocating from Acidified Endosomes and Eliciting Biological Responses. *Molecular Biology of the Cell*, 15, 2347-2360.
- VIATOUR, P., BENTIREZ-ALJ, M., CHARIOT, A., DEREGOWSKI, V., DE LEVAL, L., MERVILLE, M. P. & BOURS, V. 2000. NF- κ B2/p100 induces Bcl-2 expression. *Leukemia*, 17, 1349-1356.

- VIATOUR, P., DEJARDIN, E., WARNIER, M., LAIR, F., CLAUDIO, E., BUREAU, F., MARINE, J. C., MERVILLE, M. P., MAURER, U., GREEN, D., PIETTE, J., SIEBENLIST, U., BOURS, V. & CHARIOT, A. 2004. GSK3-Mediated BCL-3 phosphorylation modulates its degradation and its oncogenicity. *Molecular Cell*, 16, 35-45.
- VIVÈS, E., BRODIN, P. & LEBLEU, B. 1997. A Truncated HIV-1 Tat Protein Basic Domain Rapidly Translocates through the Plasma Membrane and Accumulates in the Cell Nucleus. *Journal of Biological Chemistry*, 272, 16010-16017.
- VOGES, D., ZWICKL, P. & BAUMEISTER, W. 1999. THE 26S PROTEASOME: A Molecular Machine Designed for Controlled Proteolysis. *Annual Review of Biochemistry*, 68, 1015-1068.
- WANG, C., DENG, L., HONG, M., AKKARAJU, G. R., INOUE, J.-I. & CHEN, Z. J. 2001. TAK1 is a ubiquitin-dependent kinase of MKK and IKK. *Nature*, 412, 346-351.
- WANG, Y. F., XU, X., FAN, X., ZHANG, C., WEI, Q., WANG, X., GUO, W., XING, W., YU, J., YAN, J.-L. & LIANG, H.-P. 2011. A Cell-penetrating Peptide Suppresses Inflammation by Inhibiting NF- κ B Signaling. *Mol Ther*, 19, 1849-1857.
- WASSERMAN, S. A. 1993. A conserved signal transduction pathway regulating the activity of the rel-like proteins dorsal and NF-kappa B. *Molecular Biology of the Cell*, 4, 767-771.
- WATERFIELD, M., JIN, W., REILEY, W., ZHANG, M. & SUN, S.-C. 2004. I κ B Kinase Is an Essential Component of the Tpl2 Signaling Pathway. *Molecular and Cellular Biology*, 24, 6040-6048.
- WATERFIELD, M. R., ZHANG, M., NORMAN, L. P. & SUN, S.-C. 2003. NF- κ B1/p105 Regulates Lipopolysaccharide-Stimulated MAP Kinase Signaling by Governing the Stability and Function of the Tpl2 Kinase. *Molecular Cell*, 11, 685-694.
- WERTZ, I. E. & DIXIT, V. M. 2010. Signaling to NF- κ B: Regulation by Ubiquitination. *Cold Spring Harbor Perspectives in Biology*, 2.
- WESSELLS, J., BAER, M., YOUNG, H. A., CLAUDIO, E., BROWN, K., SIEBENLIST, U. & JOHNSON, P. F. 2004. BCL-3 and NF- κ B p50 Attenuate Lipopolysaccharide-induced Inflammatory Responses in Macrophages. *Journal of Biological Chemistry*, 279, 49995-50003.
- WEYRICH, A. S., DIXON, D. A., PABLA, R., ELSTAD, M. R., MCINTYRE, T. M., PRESCOTT, S. M. & ZIMMERMAN, G. A. 1998. Signal-dependent translation of a regulatory protein, Bcl-3, in activated human platelets. *Proc Natl Acad Sci U S A*, 95, 5556-61.
- WHITEHURST, A., COBB, M. H. & WHITE, M. A. 2004. Stimulus-Coupled Spatial Restriction of Extracellular Signal-Regulated Kinase 1/2 Activity Contributes to the Specificity of Signal-Response Pathways. *Molecular and Cellular Biology*, 24, 10145-10150.
- WHITESIDE, S. T., EPINAT, J.-C., RICE, N. R. & ISRAEL, A. 1997. I kappa B epsilon, a novel member of the I[kappa]B family, controls RelA and cRel NF-[kappa]B activity. *EMBO J*, 16, 1413-1426.
- WHITHAM, S., DINESH-KUMAR, S. P., CHOI, D., HEHL, R., CORR, C. & BAKER, B. 1994. The product of the tobacco mosaic virus resistance gene N: Similarity to toll and the interleukin-1 receptor. *Cell*, 78, 1101-1115.
- WINSTON, J. T., STRACK, P., BEER-ROMERO, P., CHU, C. Y., ELLEDGE, S. J. & HARPER, J. W. 1999. The SCFB-TRCP-ubiquitin ligase complex associates specifically with phosphorylated destruction motifs in I κ B α and β -catenin and stimulates I κ B α ubiquitination in vitro. *Genes & Development*, 13, 270-283.
- WU, G., XU, G., SCHULMAN, B. A., JEFFREY, P. D., HARPER, J. W. & PAVLETICH, N. P. 2003. Structure of a β -TrCP1-Skp1- β -Catenin Complex: Destruction Motif

- Binding and Lysine Specificity of the SCF^B-TrCP1 Ubiquitin Ligase. *Molecular Cell*, 11, 1445-1456.
- WULCZYN, F. G., NAUMANN, M. & SCHEIDEREIT, C. 1992. Candidate proto-oncogene bcl-3 encodes a subunit-specific inhibitor of transcription factor NF- κ B. *Nature*, 358, 597-599.
- XAUS, J., COMALADA, M., VALLEDOR, A. F., CARDÓ, M., HERRERO, C., SOLER, C., LLOBERAS, J. & CELADA, A. 2001. Molecular Mechanisms Involved in Macrophage Survival, Proliferation, Activation or Apoptosis. *Immunobiology*, 204, 543-550.
- YAMADA, T., CHRISTOV, K., SHILKAITIS, A., BRATESCU, L., GREEN, A., SANTINI, S., BIZZARRI, A. R., CANNISTRARO, S., GUPTA, T. K. D. & BEATTIE, C. W. 2013. p28, A first in class peptide inhibitor of cop1 binding to p53. *Br J Cancer*, 108, 2495-2504.
- YAMAMOTO, M., SATO, S., HEMMI, H., HOSHINO, K., KAISHO, T., SANJO, H., TAKEUCHI, O., SUGIYAMA, M., OKABE, M., TAKEDA, K. & AKIRA, S. 2003a. Role of Adaptor TRIF in the MyD88-Independent Toll-Like Receptor Signaling Pathway. *Science*, 301, 640-643.
- YAMAMOTO, M., SATO, S., HEMMI, H., UEMATSU, S., HOSHINO, K., KAISHO, T., TAKEUCHI, O., TAKEDA, K. & AKIRA, S. 2003b. TRAM is specifically involved in the Toll-like receptor 4-mediated MyD88-independent signaling pathway. *Nat Immunol*, 4, 1144-1150.
- YAMAMOTO, M., YAMAZAKI, S., UEMATSU, S., SATO, S., HEMMI, H., HOSHINO, K., KAISHO, T., KUWATA, H., TAKEUCHI, O., TAKESHIGE, K., SAITOH, T., YAMAOKA, S., YAMAMOTO, N., YAMAMOTO, S., MUTA, T., TAKEDA, K. & AKIRA, S. 2004. Regulation of Toll/IL-1-receptor-mediated gene expression by the inducible nuclear protein I κ B ζ . *Nature*, 430, 218-222.
- YAMAUCHI, S., ITO, H. & MIYAJIMA, A. 2010. I κ B η , a nuclear I κ B protein, positively regulates the NF- κ B-mediated expression of proinflammatory cytokines. *Proceedings of the National Academy of Sciences*, 107, 11924-11929.
- YAMAZAKI, S., MUTA, T. & TAKESHIGE, K. 2001. A Novel I κ B Protein, I κ B- ζ , Induced by Proinflammatory Stimuli, Negatively Regulates Nuclear Factor- κ B in the Nuclei. *Journal of Biological Chemistry*, 276, 27657-27662.
- YAN, Q., CARMODY, R. J., QU, Z., RUAN, Q., JAGER, J., MULLICAN, S. E., LAZAR, M. A. & CHEN, Y. H. 2012. Nuclear factor- κ B binding motifs specify Toll-like receptor-induced gene repression through an inducible repressosome. *Proc Natl Acad Sci U S A*, 109, 14140-5.
- YANG, H.-T., WANG, Y., ZHAO, X., DEMISSIE, E., PAPOUTSOPOULOU, S., MAMBOLE, A., O'GARRA, A., TOMCZAK, M. F., ERDMAN, S. E., FOX, J. G., LEY, S. C. & HORWITZ, B. H. 2011. NF- κ B1 Inhibits TLR-Induced IFN- β Production in Macrophages through TPL-2-Dependent ERK Activation. *The Journal of Immunology*.
- YANG, J., WILLIAMS, R. S. & KELLY, D. P. 2009. Bcl3 interacts cooperatively with peroxisome proliferator-activated receptor gamma (PPAR γ) coactivator 1 α to coactivate nuclear receptors estrogen-related receptor alpha and PPAR α . *Mol Cell Biol*, 29, 4091-102.
- YANG, Y., KITAGAKI, J., DAI, R.-M., TSAI, Y. C., LORICK, K. L., LUDWIG, R. L., PIERRE, S. A., JENSEN, J. P., DAVYDOV, I. V., OBEROI, P., LI, C.-C. H., KENTEN, J. H., BEUTLER, J. A., VOUSDEN, K. H. & WEISSMAN, A. M. 2007. Inhibitors of Ubiquitin-Activating Enzyme (E1), a New Class of Potential Cancer Therapeutics. *Cancer Research*, 67, 9472-9481.
- YARON, A., HATZUBAI, A., DAVIS, M., LAVON, I., AMIT, S., MANNING, A. M., ANDERSEN, J. S., MANN, M., MERCURIO, F. & BEN-NERIAH, Y. 1998. Identification of the receptor component of the I κ B α -ubiquitin ligase. *Nature*, 396, 590-594.

- YE, Y. & RAPE, M. 2009. Building ubiquitin chains: E2 enzymes at work. *Nat Rev Mol Cell Biol*, 10, 755-764.
- ZABEL, U. & BAEUERLE, P. A. 1990. Purified human I[°]B can rapidly dissociate the complex of the NF-[°]B transcription factor with its cognate DNA. *Cell*, 61, 255-265.
- ZHAO, Q., WANG, X., NELIN, L. D., YAO, Y., MATTA, R., MANSON, M. E., BALIGA, R. S., MENG, X., SMITH, C. V., BAUER, J. A., CHANG, C.-H. & LIU, Y. 2006. MAP kinase phosphatase 1 controls innate immune responses and suppresses endotoxic shock. *The Journal of Experimental Medicine*, 203, 131-140.
- ZHAO, X., ROSS, E. J., WANG, Y. & HORWITZ, B. H. 2012. *Nfkb1* Inhibits LPS-Induced IFN- β and IL-12 p40 Production in Macrophages by Distinct Mechanisms. *PLoS ONE*, 7, e32811.
- ZHAO, Y., RAMAKRISHNAN, A., KIM, K. E. & RABSON, A. B. 2005. Regulation of Bcl-3 through interaction with the Lck tyrosine kinase. *Biochem Biophys Res Commun*, 335, 865-73.

9 Publications

This work has been presented in the following formats.

Journal Articles

Collins, P.E., P.A. Kiely, and R.J. Carmody, Inhibition of transcription by B Cell Leukaemia 3 (Bcl-3) requires interaction with Nuclear Factor (NF)- κ B p50. *Journal of Biological Chemistry*, 2014.

Poster Presentations

3rd UK & Ireland NF κ B Workshop, (Maynooth 2011).

Investigation of the molecular determinants of NF- κ B p50 ubiquitination

Patricia Collins, Patrick Kiely and Ruaidhrí Carmody

Keystone Symposia meeting on NF- κ B Signaling and Biology: From Bench to Bedside, (Whistler, 2012).

Identification of the molecular determinants of NF- κ B p50 homodimer ubiquitination and inhibition of inflammatory gene expression

Patricia Collins, Patrick Kiely and Ruaidhrí Carmody

IRUN Workshop 'Immune Integrity', (Nijmegen, 2013).

Bcl-3 regulates Toll-like Receptor-induced MAP kinase signalling by inhibiting Tpl-2 function

Patricia Collins and Ruaidhrí Carmody

4th UK & Ireland NF κ B Workshop, (Liverpool 2013).

Bcl-3 regulates Toll-like Receptor-induced MAP kinase signalling by inhibiting Tpl-2 function

Patricia Collins and Ruaidhrí Carmody

